Title

Investigating Macrophage Phenotype and Arterial Heterogeneity in Antibody-Mediated Rejection and Cardiac Allograft Vasculopathy

Author

Nevarez-Mejia, Jessica

Publication Date

2023

Peer reviewed|Thesis/dissertation

UNIVERSITY OF CALIFORNIA

Los Angeles

Investigating Macrophage Phenotype and Arterial Heterogeneity in Antibody-Mediated Rejection and Cardiac Allograft Vasculopathy

A dissertation submitted in partial satisfaction of the requirements for the degree Doctor of Philosophy in Molecular, Cellular, and Integrative Physiology

by

Jessica Nevarez-Mejia

2023

ABSTRACT OF THE DISSERTATION

Investigating Macrophage Phenotype and Arterial Heterogeneity in Antibody-Mediated Rejection and Cardiac Allograft Vasculopathy

by

Jessica Nevarez-Mejia

Doctor of Philosophy in Molecular, Cellular, and Integrative Physiology

University of California, Los Angeles, 2023

Professor Elaine F. Reed, Chair

Solid organ transplantation is a lifesaving therapy for patients with end-stage organ failure. Although modern immunosuppressive strategies have allowed organ survival one-year post-transplants, chronic allograft rejection remains a main clinical challenge. Approximately 20% of recipients lose their graft within 5 years, and 50% within 10 years. Antibody-mediated rejection (AMR) described by the recipient production of donor-specific antibodies (DSA) remains the main risk factor contributing to late graft loss. DSA target human leukocyte antigen (HLA) class I and class II molecules present of the donor graft endothelium. DSA triggers strong alloimmune responses against allograft endothelial cells (ECs) leading to vascular injury and inflammation. Chronic inflammation induces vascular remodeling processes consisting of EC, smooth muscle cell (SMC), and myofibroblast proliferation leading to thickening of the intimal layer of vessels (neointima). This process ultimately leads to vessel occlusion, a condition termed transplant vasculopathy (TV) and specifically in heart transplant, cardiac allograft vasculopathy (CAV). Although macrophages remain a distinguishing feature of graft pathology in both AMR and CAV

lesions, their precise phenotype and function in the context of HLA class I DSA remain poorly understood. Furthermore, there is a lack of research exploring the vascular characteristics of CAV-affected vessels in patients with DSA.

In this dissertation, we utilized both *in vitro* and *in vivo* approaches to investigate the mechanisms by which HLA class I DSA activate EC signaling and the impact on monocyte-to-macrophage polarization and functions. Our findings revealed that crosslinking of anti-HLA I (IgG and $F(ab')_2$) antibodies with HLA class I molecules (HLA I) forms a complex with TLR4. Signaling through TLR4 and the adaptor protein MyD88 triggers the release of Weibel-Palade bodies (WPbs) containing P-selectin. P-selectin surface expression mediates the capture of monocytes to ECs via interactions with monocyte P-selectin glycoprotein ligand-1 (PSGL-1). Second, we identified that anti-HLA I antibodies (IgG and $F(ab')_2$) antibody-activated ECs induced the polarization of M2-like macrophages with distinct cytokine/chemokine secretion and transcriptomic expression. We further delineated that M2-macrophage polarization was enhanced via Fc-gamma receptor (FcγR) interactions. For example, monocytes co-cultured with HLA I IgG-stimulated ECs differentiated into CD68+CD206+CD163+ macrophages, while monocytes co-cultured with HLA I $F(ab')_2$ only upregulated CD206. Thirdly, by inhibiting TLR4 signaling and PSGL-1-P-selectin interaction during monocyte transmigration across HLA I (IgG or $F(ab')_2$) antibody-activated ECs, we discovered that macrophage expression of CD206 and the secretion of matrix metalloproteinase-9 (MMP9) is regulated by P-selectin. We validated the expression of CD68+CD206+CD163+MMP9+ M2-like macrophages within CAV affected lesions of DSA+ rejected cardiac explants.

Finally, using innovative spatial multi-omics techniques, we examined protein and transcriptomic expression in arterial regions of DSA+ CAV+ human rejected cardiac allografts. Our analysis revealed distinct profiles in regions with low and high neointima, encompassing differentially expressed proteins, transcripts, gene modules, and gene regulatory networks. Notably, low neointimal regions exhibited elevated inflammatory profiles, while high neointima regions

demonstrated features associated with fibrotic and remodeling processes. These results suggested a speculative sequential time-frame of the arterial changes that may occur during CAV progression.

This dissertation provides valuable insights into the immunological mechanisms driving AMR and CAV progression. The study highlights the role of HLA I DSA-activated ECs in regulating macrophage functions and uncovers molecular signatures of different arterial regions from DSA+ CAV+ rejected cardiac allografts. These findings offer a deeper understanding of AMR and CAV pathogenesis, suggesting potential therapeutic targets to prevent leukocyte infiltration and EC activation in rejecting grafts. Finally, this research contributes to the development of interventions for improved long-term graft survival in transplantation.

The dissertation of Jessica Nevarez-Mejia is approved.

Gregory A. Fishbein

Mario C. Deng

Tomas Ganz

Kristina Bostrom

Elaine F. Reed, Committee Chair

University of California, Los Angeles

2023

Dedication

To my mother, Nydia Nevarez, who always told me to take things one step at a time.

To my father, Ezequiel Nevarez, who during my childhood, always mentioned that “If you are going to do something, you should always aim to do it right.”

To my brother, Ezequiel Nevarez-Mejia, for encouraging me to seize every opportunity.

To my partner, Dr. Michael R. Emami, for being my unwavering pillar of support and bringing joy to challenging moments.

Table of Contents

List of Figures

List of Tables

Acknowledgements

I would like to personally thank my mentor, Dr. Elaine Reed, for her unwavering support and guidance throughout my graduate journey. I am grateful for her belief in my abilities, especially during moments of self-doubt, and for continuously pushing me to excel and grow as an independent and confident scientist. I also wish to thank the current and former members of the research laboratory and clinical team for their camaraderie, optimism, and guidance. Specially, I am grateful to Dr. Yiping Jin for his exceptional support with experiments. Thank you for patiently training me, providing valuable feedback, and offering guidance whenever I encountered challenges in the lab. I extend my gratitude to my dissertation committee members: Drs. Gregory A. Fishbein, Mario C. Deng, Tomas Ganz, and Kristina Bostrom for their feedback and insightful comments. I am also appreciative of my previous mentors who provided me with valuable training and inspired me to pursue a graduate degree in science: Drs. Luis Mota-Bravo, Marlene de la Cruz, Simon M. Hughes, and Dr. Alexander D. Boiko.

I would like to express my heartfelt gratitude to my extended family and friends for their support throughout my academic and personal life. I am particularly thankful for the unwavering support, kindness, and generosity of the Emami family, who were always there for me, ready to lend a helping hand whenever needed. Moreover, I am deeply grateful to my remarkable partner, Dr. Michael Emami, who accompanied me throughout my journey in graduate school. Your encouragement and guidance played an invaluable role in my success, and I am truly fortunate to have you by my side. I am also thankful to the support of my brother, Ezequiel Nevarez-Mejia who has been there for me in every possible way. Lastly, I am profoundly grateful to my parents, Ezequiel and Nydia Nevarez, for instilling in me the fundamental values of perseverance and commitment. They have not only exemplified hard work and dedication themselves, but have also surpassed their own boundaries to ensure that my brother and I are afforded opportunities they never had.

Chapter 2 is adapted from Jin YP, Nevarez-Mejia J, Terry AQ, Sosa RA, Heidt S, Valenzuela NM, Rozengurt E, Reed EF. Cross-Talk between HLA Class I and TLR4 Mediates P-Selectin Surface Expression and Monocyte Capture to Human Endothelial Cells. J Immunol. 2022 Oct 1;209(7):1359-1369. doi: 10.4049/jimmunol.2200284. Epub 2022 Sep 2. PMID: 36165200; PMCID: PMC9635437. Link to article in J Immunol: https://journals.aai.org/jimmunol/article-abstract/209/7/1359/234639/Cross-Talk-between-HLA-Class-I-and-TLR4-Mediates-P?redirectedFrom=fulltext

Chapter 3 is adapted from Wei X, Valenzuela NM, Rossetti M, Sosa RA, Nevarez-Mejia J, Fishbein GA, Mulder A, Dhar J, Keslar KS, Baldwin WM 3rd, Fairchild RL, Hou J, Reed EF. Antibody-induced vascular inflammation skews infiltrating macrophages to a novel remodeling phenotype in a model of transplant rejection. Am J Transplant. 2020 Oct;20(10):2686-2702. doi: 10.1111/ajt.15934. Epub 2020 May 22. PMID: 32320528; PMCID: PMC7529968. Link to article in AJT: https://www.amjtransplant.org/article/S1600-6135(22)22459-9/fulltext

Chapter 4 is a version of Nevarez-Mejia J, Jin YP, Pickering H, Parmar R, Valenzuela NM, Sosa RA, Heidt S, Fishbein GA, Rozengurt E, Baldwin WM 3rd, Fairchild RL, Reed EF. HLA I Antibody-activated endothelium mediates monocyte polarization into CD206+ M2-macrophages with MMP9 secretion via TLR4 signaling and P-selectin. Manuscript *in preparation.* The authors would like to acknowledge Dr. Yunfeng Li at the UCLA Translation Pathology Core Lab (TPLC) for her expertise on multiplex-immunofluorescence staining. This research was supported by the National Institutes of Health (NIH) Grant R01AI135201 (EFR, NMV, and RLF), NIH Grant R21AI156592 (EFR, ER, and RLF), the NIH Ruth L. Kirschstein National Research Service Award (NRSA) T32HL069766 (JNM), and the UCLA Eugene V. Cota Robles Fellowship (JNM). Author contributions: JNM, EFR, and NMV designed the research study. JNM and YPJ performed experiments and data analysis. JNM, HCP, and RP analyzed transcriptomic data. RAS and GAF identified patient allografts. SH provided HLA I antibodies. ER, WMB and RLF provided feedback

and contributed to the design of the study. All authors reviewed the manuscript and provided feedback.

Chapter 5 is a version of Nevarez-Mejia J, Pickering H, Sosa RA, Valenzuela NM, Fishbein GA, Baldwin WM 3rd, Fairchild RL, Reed EF. Spatial Multi-omics of Arterial Regions from Cardiac Allograft Vasculopathy Rejected Grafts Reveal Mechanistic Insights into the Pathogenesis of Chronic Antibody-Mediated Rejection. Manuscript *pre-print* in BioRxiv (DOI: 10.1101/2023.04.12.536667) and *submitted for review to AJT.* The authors would like to thank the NanoString Technology Access Program (TAP) for the opportunity to utilize the innovative GeoMx digital spatial profiling (DSP) platform. We would also like to extend our appreciation to the UCLA TPCL for their valuable resources and support. Finally, the authors express their gratitude to the organ donors and their families for their generous gifts of life and knowledge. This study was funded by the NIH Grant R01AI135201 (EFR, NMV, and RLF), NIH Grant R21AI156592 (EFR and RLF), the NIH Ruth L. Kirschstein National Research Service Award (NRSA) T32HL069766 (JNM), and the UCLA Eugene V. Cota Robles Fellowship (JNM). Author contributions: JNM and EFR designed research study. JNM and HCP performed data analysis. RAS, GAF, and WMB identified patient tissue, region selection, and grading. WMB and RLF contributed to the design of the study. JNM and EFR wrote the manuscript. All authors read and approved the manuscript.

VITA

Education

- University of California, Los Angeles (UCLA) Sept 2017 – *[In progress]*
  Ph.D., Molecular, Cellular, and Integrative Physiology (GPA: 3.935)
- University of California, Irvine (UCI) Sept 2013 – June 2017
  B.S., in Biological Sciences (GPA: 3.51)

Research Experience

- University of California, Los Angeles (UCLA) Sept 2017 – Present
  Graduate Student Researcher, Dr. Elaine F. Reed laboratory
  Dissertation: Investigating macrophage polarization in antibody-mediated rejection and vascular heterogeneities in cardiac allograft vasculopathy
- University of California, Los Angeles (UCLA) Aug 2017 – Sept 2017
  UCLA Competitive Edge summer research program, Dr. James G. Tidball's laboratory. Examined the role of CTLA-4 in preventing macrophage transmigration into peripheral tissue using primary isolated and polarized mouse macrophages.
- University of California, Irvine (UCI) Sept 2016 – June 2017
  Undergraduate research funded by NIH-MARC, Dr. Alexander D. Boiko laboratory
  Focused on targeting the Wnt and MAPK signaling pathways as a therapeutic approach to prevent cell proliferation and metastasis of human melanoma.
- King's College London, United Kingdom June 2016 – Aug 2016
  Summer internship funded by NIH-MHIRT, Dr. Simon M. Hughes laboratory
  Studied the role of LARP6 protein in myogenesis via gene editing (TALENS and CRISPR) and phenotypic analysis in a zebrafish model.
- University of California, Irvine (UCI) March 2014 – June 2016
  Undergraduate research funded by NIH-MBRS, Dr. Luis Mota-Bravo Laboratory
  Research the transmission of mobile elements (plasmids) carrying antibiotic resistance genes in environmental Acinetobacter sp. using molecular tools.

Selected Awards and Fellowships

- President's Choice Poster Award 2022
  ASHI: The American Society for Histocompatibility and Immunogenetics under the category of Immunogenetics and Disease association
- ASHI Travel Award 2022
- NanoString's Immunology 2022 Grand Prize Travel Grant Winner 2022
- Ruth L. Kirschtein National Research Service Award T32HL069766 2018 – 2021
- Ford Foundation Predoctoral Fellowship Honorable Mention 2019
- Jennifer S. Buchwald Graduate Fellowship in Physiology 2018 – 2019
- UCLA Eugene V. Cota Robles Fellowship 2017 – 2018/2022 – 2023
- UCLA Competitive Edge Summer Program Fellowship Aug 2017 – Sept 2017
- ABRCMS poster presenter awardee in Molecular and Computational Biology 2015

Selected Presentations

1. Nevarez-Mejia J, Pickering HC, Parmar R, Sosa RA, Lau RP, Fishbein GA, Baldwin WM, Fairchild RL, Reed EF. "Characterizing Macrophage Function in Human Cardiac Allograft Vasculopathy Rejected Grafts using GeoMx Spatial Multi-omics". 2022 American Society for Histocompatibility and Immunogenetics (ASHI), Las Vegas NV, October 2022, poster presentation.
2. Nevarez-Mejia J, Pickering HC, Sosa RA, Lau RP, Fishbein GA, Baldwin WM, Fairchild RL, Reed EF. "Protein and Transcriptomic Differences Between High and Low Neointimal Arteries

in Human Cardiac allograft Vasculopathy Rejected Grafts". 2022 American Transplant Congress (ATC), Boston MA, June 2022, poster presentation.

3. Nevarez-Mejia J, Pickering HC, Sosa RA, Lau RP, Fishbein GA, Baldwin WM, Fairchild RL, Reed EF. "Characterizing Arterial Lesions in Cardiac Allograft Vasculopathy Rejected Grafts using NanoString GeoMx Spatial Profiling." 2022 Immunology, The American Association of Immunologist (AAI), Portland OR, May 2022, poster presentation
4. Nevarez-Mejia J, Pickering HC, Sosa RA, Lau RP, Fishbein GA, Baldwin WM, Fairchild RL, Reed EF. "GeoMx Digital Spatial Profiling of Vessels from Human Cardiac Allograft Vasculopathy Rejected Grafts." 2021 American Society for Histocompatibility and Immunogenetics (ASHI), Virtual Meeting, October 2021, poster presentation
5. Nevarez-Mejia J, Wei X, Valenzuela NM, Rossetti M, Pickering HP, Fishbein GA, Mulder A, Reed EF. "HLA I Antibody-activated Endothelium Polarized M2-like Macrophages with Increased Efferocytic and Phagocytic Capacity". 2021 American Transplant Congress (ATC), Virtual Meeting, June 2021, poster presentation.
6. Nevarez-Mejia J, Wei X, Valenzuela NM, Rossetti M, Pickering HP, Fishbein GA, Mulder A, Baldwin WM, Fairchild RL, Reed EF. "Macrophage Polarization Induced by HLA I Antibody-activated Endothelium during Antibody-mediated Rejection". 2020 American Society of Histocompatibility and Immunogenetics (ASHI), Virtual Meeting, October 2020, poster presentation.

Publications

1. **Nevarez-Mejia J**, Pickering H, Sosa RA, Valenzuela NM, Fishbein GA, Baldwin WM 3rd, Fairchild RL, Reed EF. Spatial Multi-omics of Arterial Regions from Cardiac Allograft Vasculopathy Rejected Grafts Reveal Mechanistic Insights into the Pathogenesis of Chronic Antibody-Mediated Rejection. Manuscript *pre-print* in BioRxiv (DOI: 10.1101/2023.04.12.536667) and *submitted for review to AJT.*
2. Jin YP, **Nevarez-Mejia J**, Terry AQ, Sosa RA, Heidt S, Valenzuela NM, Rozengurt E, Reed EF. Cross-Talk between HLA Class I and TLR4 Mediates P-Selectin Surface Expression and Monocyte Capture to Human Endothelial Cells. J Immunol. 2022 Oct 1;209(7):1359-1369. doi: 10.4049/jimmunol.2200284. Epub 2022 Sep 2. PMID: 36165200; PMCID: PMC9635437.
3. Tsuda H, Dvorina N, Keslar KS, **Nevarez-Mejia J**, Valenzuela NM, Reed EF, Fairchild RL, Baldwin WM 3rd. Molecular Signature of Antibody-Mediated Chronic Vasculopathy in Heart Allografts in a Novel Mouse Model. Am J Pathol. 2022 Jul;192(7):1053-1065. doi: 10.1016/j.ajpath.2022.04.003. Epub 2022 Apr 29. PMID: 35490714; PMCID: PMC9253905.
4. Sosa RA, Terry AQ, Kaldas FM, Jin YP, Rossetti M, Ito T, Li F, Ahn RS, Naini BV, Groysberg VM, Zheng Y, Aziz A, **Nevarez-Mejia J**, Zarrinpar A, Busuttil RW, Gjertson DW, Kupiec-Weglinski JW, Reed EF. Disulfide High-Mobility Group Box 1 Drives Ischemia-Reperfusion Injury in Human Liver Transplantation. Hepatology. 2021 Mar;73(3):1158-1175. doi: 10.1002/hep.31324. Epub 2020 Oct 30. PMID: 32426849; PMCID: PMC8722704.
5. Wei X, Valenzuela NM, Rossetti M, Sosa RA, **Nevarez-Mejia J**, Fishbein GA, Mulder A, Dhar J, Keslar KS, Baldwin WM 3rd, Fairchild RL, Hou J, Reed EF. Antibody-induced vascular inflammation skews infiltrating macrophages to a novel remodeling phenotype in a model of transplant rejection. Am J Transplant. 2020 Oct;20(10):2686-2702. doi: 10.1111/ajt.15934. Epub 2020 May 22. PMID: 32320528; PMCID: PMC7529968.
6. Hau HTA, Ogundele O, Hibbert AH, Monfries CAL, Exelby K, Wood NJ, **Nevarez-Mejia J**, Carbajal MA, Fleck RA, Dermit M, Mardakheh FK, Williams-Ward VC, Pipalia TG, Conte MR, Hughes SM. Maternal Larp6 controls oocyte development, chorion formation and elevation. Development. 2020 Feb 26;147(4):dev187385. doi: 10.1242/dev.187385. PMID: 32054660; PMCID: PMC7055395

Chapter 1 – Introduction

Mechanisms of Antibody-mediated Rejection (AMR)

Solid-organ transplantation is a lifesaving procedure for patients with end-stage heart, lung, liver, kidney, pancreas, and intestinal organ failure[1,2]. According to the United Network for Organ Sharing (UNOS), a total of 41,355 organ transplants were performed from both deceased and living donors during 2021 in the United States[3]. Modern immunosuppressive regimens have allowed organ survival one-year post-transplant; nonetheless, due to the lack of improvements in long-term graft survival, 20% of recipients will lose their graft within 5 years, and 50% within 10 years[1,2]. Antibody-mediated rejection (AMR) remains the major risk factor contributing to late graft loss. AMR is characterized by the production of donor-specific antibodies (DSA) to polymorphic human leukocyte antigens (HLA class I and HLA class II) found on the surface of graft endothelial cells (ECs)[4]. HLA I and HLA II DSA drive strong alloimmune responses against the graft vasculature mediating vascular inflammation and graft injury[5,6]. DSA play a crucial role in activating multiple pathological mechanisms, which mediate vascular injury. Specifically, DSA and inflammatory stimuli (e.g., TNF-α) increase EC surface expression of adhesion molecules and chemokines, which facilitates the recruitment of graft-infiltrating immune cells. Here, CD4+ T-lymphocytes recognize allograft HLA antigens (via direct or indirect allo-recognition) and activate B-cells to differentiate into plasma cells, which are mainly responsible for producing HLA DSA[7]. Moreover, both cytotoxic CD8+ T-cells and NK-cells secrete inflammatory cytokines and granules targeting graft ECs[7,8]. Graft-infiltrating monocytes differentiate into macrophages, which can secrete inflammatory cytokines (M1 subtype) or growth factors and vascular remodeling proteins (M2 subtype)[9]. Lastly, HLA DSA can directly activate the classical complement cascade on the surface of ECs leading to MAC complex formation and cell injury and the generation of anaphylatoxins[4-6]. Across most solid organs, AMR is diagnosed by the presence of microvascular

inflammation (subendothelial mononuclear cell infiltration), EC swelling, C4d complement deposition, and by the presence of CD68+ macrophages[5,10]. Overall, AMR represents a disease spectrum characterized by varying degrees of severity that can initiate at any point following transplantation. Its progression, with varying levels of intensity, contributes to the development of chronic rejection. Specifically, around 50% of heart transplants recipients who reject after >7 years post-transplants have evidence of AMR[11].

Endothelial cell activation by HLA Donor-Specific Antibodies (DSA)

Our group has conducted multiple studies to uncover the mechanisms by which HLA DSA trigger outside-in signaling in ECs and lead to functional alterations that contribute to chronic rejection (**Figure 1**). Specifically, anti-HLA I IgG crosslinking to HLA I molecules expressed on ECs promotes the formation of molecular complex between HLA I and integrin-β4 (ITGB4). Signaling via ITGB4 triggers the phosphorylation and activation of Src/PI3K/Akt/mTOR pathway inducing EC migration and proliferation[12]. HLA I DSA induced signaling via PI3K/Akt also increases EC expression of survival proteins (e.g., BCL-2 and BCL-XL)[13]. Moreover, HLA I antibody-induced activation of mTOR complex 1 (MTORC1) and mTOR complex 2 (mTORC2) leads to downstream activation of RhoA/ROCK proteins which phosphorylate ERM (ezrin-radixin-moesin) proteins leading to cytoskeletal rearrangements and intercellular adhesion molecule 1 (ICAM-1) clustering at the cell surface[14]. Clustering of ICAM-1 enhances the tethering of monocytes at the EC surface, facilitating their infiltration into the allograft[14]. Activation of ECs by HLA II DSA triggers similar signaling cascades (e.g., FAK, PI3K, EKR, mTOR) inducing cell proliferation and migration[15].

In addition, recent studies in our lab have indicated that anti-HLA I IgG crosslinking to HLA I molecules can also induce the formation of a separate molecular complex between HLA I and toll-like receptor 4 (TLR4)[16]. Signaling via TLR4 adaptor proteins (e.g., MyD88) and elevation of intracellular Ca^{2+} induce the rapid exocytosis of Weibel-Palade bodies (WPb) that store von Willebrand Factor (vWF) and P-selectin[17,18]. P-selectin surface expression promotes monocyte

tethering to EC surface via monocyte P-selectin glycoprotein-1 (PSGL-1)[16-18]. Here, monocyte can also undergo interactions with Fc-portion of IgG via Fc-receptors (FcyRs)[19]. The findings from these studies collectively underscore the significant role played by HLA DSA in promoting

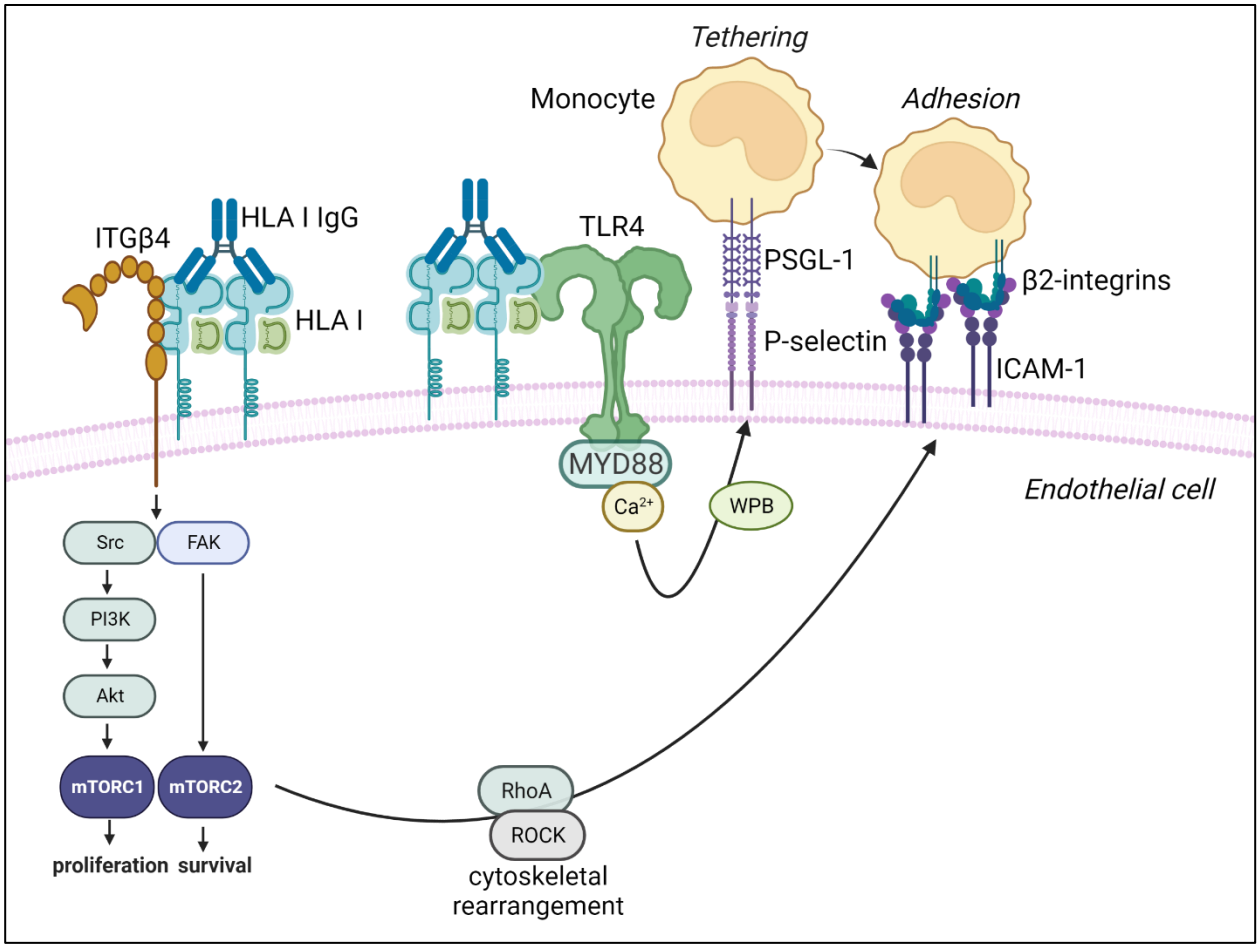

vascular inflammation and remodeling, which in turn contribute to AMR and chronic rejection.

Figure 1-1: Mechanisms of HLA I IgG antibody-activation of allograft endothelial cells.

Anti-HLA I IgG crosslinking to HLA I molecules present on the surface of endothelial cells (ECs) induces the formation of a molecular complex between HLA I and integrin-β4 (ITGB4). This triggers activation of signaling cascades (e.g., Src/PI3K/Akt/mTOR and FAK), which induce EC migration, proliferation, and expression of survival proteins[12,13]. Activation of mTOR complexes triggers downstream activation of RhoA/ROCK proteins which regulate cytoskeletal rearrangements resulting in ICAM-1 clustering at the cell surface[14]. Anti-HLA I IgG crosslinking

also induces the formation of a separate molecular complex between HLA I and Toll-like Receptor-4 (TLR4)[16]. TLR4-MyD88 and intracellular Ca^{2+} signaling induce the exocytosis of Weibel-Palade bodies (WPbs) containing P-selectin. P-selectin surface expression mediates monocyte tethering via P-selectin glycoprotein-1 (PSGL-1) to the surface of ECs[16-18]. Figure created using BioRender.com.

Mechanisms of Cardiac Allograft Vasculopathy (CAV)

Recurrent episodes of AMR in heart transplant recipients, marked by vascular inflammation and the activation of ECs and smooth muscle cells (SMCs) contribute to the progressive thickening of the inner layer of vessels (neointima). This process ultimately leads to the development of the occlusive vascular disease known as cardiac allograft vasculopathy (CAV)[20]. CAV remains the primary cause of long-term mortality, responsible for approximately 1 in 8 deaths beyond one-year post-transplant[21]. CAV lesions are mainly composed of actively dividing myofibroblast and infiltrating immune cells[20]. CAV impacts arteries of varying sizes, including large and small epicardial and intramyocardial arteries, as well as veins. It affects both males and females, adults, and children in a similar manner[22]. The exact mechanisms underlying CAV development are complex and involve immune responses, chronic inflammation, EC dysfunction, and vascular remodeling processes. Specifically, the presence of circulating HLA DSA has been associated with increased risk of developing CAV[23]. Additional risks factors for CAV include metabolic disorders (e.g., obesity, hyperglycemia, and hyperlipidemia), older donor and recipient age, ischemic-reperfusion injury (IRI), organ presentation, chronic T-cell mediated injury, and cytomegalovirus (CMV) infection[24,25]. Furthermore, endothelial-to-mesenchymal transition (EndoMT) is recognized as a pivotal process underlying the development of CAV[26]. EndoMT is a phenomenon in which sustained EC activation by inflammatory stimuli (e.g., IL-6, TNF-α, IL-1β, and pathogens) induce EC dysfunction and the downregulation of EC markers (e.g., CD31 and VE-cadherin). Concurrently, ECs upregulate the expression of specific EndoMT transcription

factors (e.g., SNAIL/SLUG and ZEB) which suppress the expression of EC markers and upregulate the expression of mesenchymal cell markers (e.g., N-cadherin, a-SMA, and Vimentin). This process ultimately results in the differentiation of ECs into highly proliferative and migratory mesenchymal cells[26]. This phenomenon contributes to neointimal formation and progression of vascular occlusion.

Today, CAV is monitored using invasive techniques such as angiography or intravascular ultrasound (IVUS), which are both inefficient for early detection[27]. Moreover, these techniques do not display the exact composition of the vessel wall. For now, vessel composition can only be visualized in explanted hearts or autopsy hearts from transplant patients. While current treatments, including mTOR inhibitors (mTORi), statins, vasodilators, and revascularization, have shown some efficacy in slowing down the progression of CAV, they are unable to completely prevent its development[24]. Unfortunately, once CAV is established, it becomes an irreversible often requiring re-transplantation as the sole viable option.

In this study, we focused on analyzing both the proteomic and transcriptomic expression of arterial CAV affected lesions from DSA+ CAV+ rejected cardiac allografts using digital spatial profiling. The dataset generated from this research will serve as a fundamental resource for future investigations into the mechanisms underlying CAV.

Macrophages in AMR and CAV

Macrophages are a distinguishing feature in graft pathology in both acute and chronic AMR lesions as well as in CAV[10]. In cardiac allograft endomyocardial biopsies (EMBs), intravascular graft macrophages accumulate in capillaries and venules that distend and fill vascular lumens[10]. This leads to widespread alterations of the microvasculature and endothelial cells lining the vessel[10]. Precisely, the presence of CD68+ graft infiltrating macrophages is highly associated with worse graft function and survival[28-32]. Following organ procurement, cold storage, and surgical

anastomosis, IRI increases vascular permeability and promotes EC apoptosis[33,34]. Moreover, cellular and acute AMR increase microvasculature damage[35]. Activated ECs secrete chemokines (e.g., MCP-1 and fractalkine) and upregulate adhesion molecules (e.g., P-selectin, ICAM-1 and VCAM-1) which recruit recipient circulating monocytes[36]. During transmigration, monocyte and EC interactions activate outside-in signaling that induce functional changes and alter gene expression in both cell types[37]. For example, binding of monocyte integrins (LFA-1, MAC-1, and VLA-4) to EC intracellular adhesion molecules (ICAM-1 and VCAM-1) activates monocyte signaling cascades involved with cell migration, actin cytoskeleton and focal adhesions to drive efficient chemotaxis[38,39]. Moreover, engagement of EC ICAM-1/VCAM-1 with monocyte integrins mediate intracellular signaling, which results in loss of tight cell-to-cell junctions (e.g.VE-cadherin) to mediate monocyte diapedesis[40]. Although the cell interactions and intracellular signaling cascades that mediate extravasation have been studied, it remains unknown how these interactions may have the potential to guide monocyte-macrophage phenotype and function in rejecting allografts.

Historically, canonical environmental cues have been described to drive monocyte-macrophage differentiation into two major phenotypes: “Classically activated” or **M1**, pro-inflammatory macrophages and “alternatively activated” or **M2** profibrotic macrophages[41] (**Figure 2**). M1 are activated by IFN-y or by engagement of pathogen-associated patterns via toll-like receptors (TLRs)[41,42]. M1 promote a Th1-type response producing pro-inflammatory cytokines (e.g., IL-1, IL-6, and TNF-α) that can activate cytotoxic T cells and induce the production of EC chemokines (e.g., CSF-1 and MCP-1)[42]. Moreover, M1 generate harmful reactive oxygens species (ROS), and iNOS-derived nitric oxide[42]. M1 also express high levels of co-stimulatory molecules (e.g., CD80/CD86), which amplify T cell-mediated activation. On the other hand, “Alternatively activated” or M2 macrophages are known to mediate tissue healing, angiogenesis, and fibrosis[41,43]. Depending on their activating stimuli, M2 are subdivide into M2a (IL-4), M2b (via

FcγRs and TLRs e.g., IgG+LPS), and M2c (IL-10) subtypes[43]. M2 promote a Th2-type response by secreting regulatory cytokines (e.g., IL-10) and decreasing pro-inflammatory cytokine production. Moreover, M2 secrete pro-angiogenic growth factors such as TGF-b, endothelial cell growth factor (VEGF), platelet-derived growth factor (PDGF), matrix metalloproteinases (MMPs) and tissue inhibitors of metalloproteinases (TIMPs) that alter matrix turnover and composition[43,44]. M2 express phagocytosis receptors (e.g., CD163, CD206, CD209, and Dectin-1) which enable removal of microbes, debris, and dead cells[45,46].

Based on the M1/M2 paradigm, M1 have been associated with acute rejection while M2 with chronic rejection[9,47,48]. Nonetheless, recent studies have highlighted the oversimplification of the M1/M2 paradigm in transplantation. For instance, kidney allografts with acute tubular necrosis have identified M2 transcripts (e.g., Arg1 and Mrc1)[49]. Further, while M2-like macrophages are identified in chronically rejecting grafts, the development of vasculopathy and induction of vascular damage also points to the production of M1 secreted factors (e.g., ROS and IFN-y)[50]. Due to the dynamic heterogeneity of macrophage polarization, it has become very difficult to identify the phenotype and function of macrophages present in allografts. Some studies suggest that macrophages may undergo a phenotype switch or that at a certain point in the development of chronic rejection, macrophages may display dual characteristics. Thus, the exact phenotype and function of macrophages found in acute and chronically rejecting grafts remains unknown.

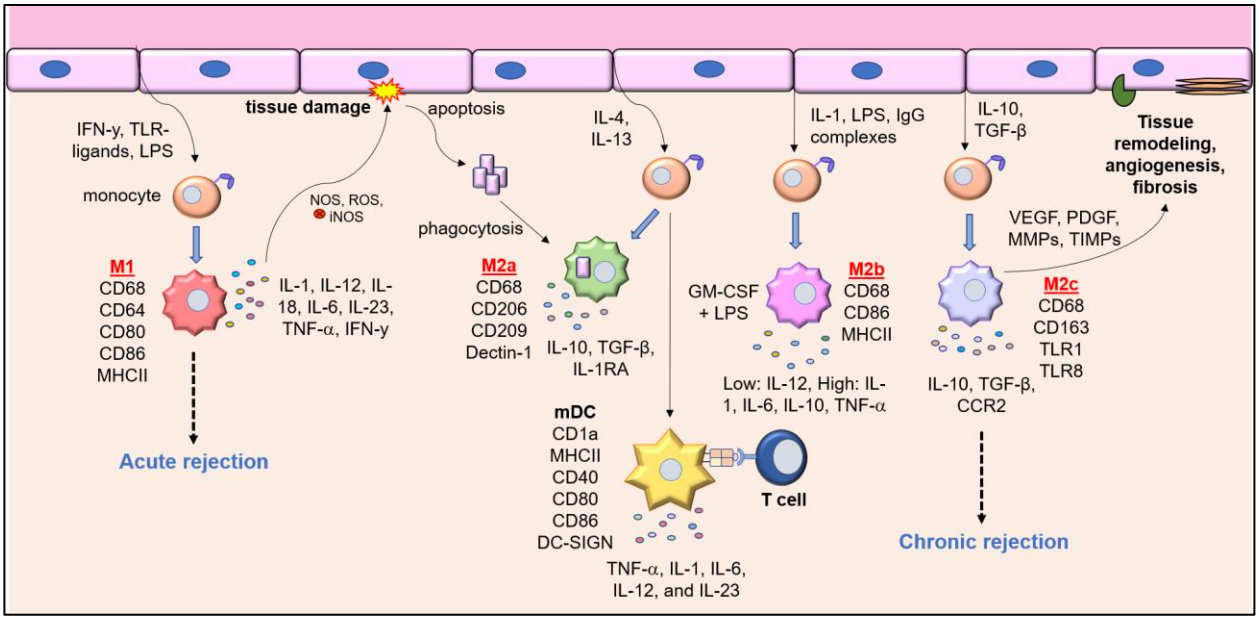

Figure 1-2: Monocytes differentiate into distinct macrophage subtypes depending on the activating stimuli upon transmigrating across the vascular endothelium.

Macrophages are typically classified into pro-inflammatory (M1) or anti-inflammatory/resolving (M2) subtypes, characterized by their distinct marker expression and specialized functions. M1 macrophages are primarily implicated in acute rejection as they activate T-cells, as well as secrete pro-inflammatory cytokines and generate reactive oxygen species (ROS), contributing to endothelial cell (EC) damage. On the other hand, M2a macrophages specialize in phagocytosing apoptotic ECs and cellular debris. M2b macrophages are known for their production of regulatory cytokines. Finally, M2c macrophages contribute to vascular remodeling by synthesizing proteins like VEGF and MMPs. Generally, M2 macrophages secrete anti-inflammatory cytokines and are associated with chronic rejection. However, the precise role of macrophages in rejection is still not fully understood due to the overlapping and distinct marker expression as well as diverse functions exhibited by each subtype.

Monocyte recruitment and activation by Fc-gamma receptors (FcγRs)

A few studies have highlighted humoral activation via Fc-gamma receptors (FcγR) signaling in mediating monocyte-macrophage polarization and functional activity during AMR[51]. The majority of circulating monocytes (80-95%) co-express the high affinity FcγRI (CD64) and intermediate affinity FcγRII (CD32), and a subpopulation (2-11%) co-expresses FcγRIII (CD16)[52]. Monocyte FcγR-IgG interactions have been shown to elicit distinct monocyte functions such as production of cytokines/chemokines, cell migration, phagocytosis, and differentiation. This occurs via both activating (FcγRI and FcγRIII), and inhibitory (FcγRII) signals following crosslinking with IgG and/or IgG-complexes[51-54]. Similarly, macrophages can differentially co-express all FcγRs on their surface activating antibody-dependent cellular phagocytosis (ADPC) and antibody-dependent cellular cytotoxicity (ADCC)[55]. FcγR-IgG affinity is highly dependent on IgG subclass (IgG1, IgG2, IgG3, and IgG4), Fc-glycosylation state, and FcγR polymorphisms[56]. In general, IgG1/3 have higher affinity for most FcγRs, while IgG2 only binds FcγRII, and IgG4 binds most FcγRs moderately[5]. Polymorphism in recipient FcγRIIa (H131/R131) and FcγRIIIa (V158/F158) have been shown to differentially affect clinical transplant outcomes in kidney, heart, and lung transplants[57-59]. This is as polymorphic differences can alter the affinity of Fc-IgG binding and/or functionality of activating FcγRs. For example, FcγRIIa-H131 has higher affinity to IgG2 than FcγRIIa-R131 and FcγRIIIa-V158 has higher affinity for IgG1/3 than FcγRIIIa-F158[56]. Thus, variability in recipient production of specific IgG subclasses and FcγR genotype may impact the degree of cell recruitment, activation, and transplant outcome. However, it remains unclear how different FcγR-IgG interactions may be able to modulate distinct cell fates and effector functions in AMR. Recent studies utilize IgG-degrading enzyme of *Streptococcus pyogenes* (IdeS) and an endoglycosidase (EndoS) produced by *S. pyogenes* to prevent FcγR-dependent functions and immune-cell recruitment[60]. Particularly, IdeS cleaves IgG into an intact Fc region and $F(ab')_2$

fragments, while EndoS hydrolyzes the N-linked carbohydrate from the Fc region of IgG[61]. Yet, the efficacy of IdeS/EndoS as therapeutics to treat AMR is currently being explored.

By generating chimeric pan-HLA I human IgG1 and IgG2 Abs (carrying the variable regions of murine pan HLA I mAb W6/32), we have shown that IgG subclass and FcγRIIa polymorphisms influence monocyte binding to HLA I antibody-activated ECs[19]. For instance, monocytes perfused over HLA I antibody-activated ECs under shear stress exhibit slower rolling and increased arrest on ECs treated with IgG1 compared with IgG2[19]. Moreover, monocytes from donors expressing high-affinity FcγRIIa-H131 alleles exhibited greater adhesion to ECs stimulated with HLA I antibodies. These studies suggest that transplant recipients carrying specific FcγR polymorphisms and production of specific IgGs influence macrophage accumulation in the graft.

Significance of study

Despite the active role of macrophages in mediating poorer graft outcomes, their exact phenotype and function in the context of HLA I antibody-mediated injury remains unexplored. This gap in knowledge hinders effective therapeutic targeting of DSA effector functions to prevent CAV development. Moreover, although prior studies have shown that immunosuppressive drugs (e.g., mTOR inhibitors) can be effective in inhibiting monocyte/macrophage functions (e.g., migration) targeting all macrophages indiscriminately could be disadvantageous[62-64]. This is since effector or 'regulatory macrophages' (Mregs) also have beneficial roles including the control of infections and induction of regulatory cells (e.g. Tregs)[64]. Thus, it remains critical to identify the exact cellular mechanisms guiding macrophage polarization and function by DSA activated endothelium during AMR.

Summary of Study

In this study, we aimed to further investigate the molecular mechanism underlying the signaling between HLA I and TLR4 complex in HLA I DSA activated ECs. We revealed that TLR4/MyD88

signaling upregulates P-selectin surface expression on ECs, facilitating monocyte capture. Moreover, we identified that HLA I antibody-activated ECs guide monocyte-to-macrophage polarization into distinct M2-macrophage phenotypes characterized by the co-expression of CD68, CD206, and CD163 markers. These M2-macrophage subtypes exhibit unique cytokine secretion patterns and transcriptomic profiles. Furthermore, our findings illustrated that increased M2-macrophage expression of CD206 and matrix metalloproteinase-9 (MMP9) are regulated by P-selectin which is expressed on the surface of HLA I DSA-activated ECs. Finally, employing a multi-omics approach, we explored the differences between arterial regions containing low and high neointima in DSA+ CAV+ human rejected cardiac allografts. Our results identified potential immune proteins, enriched transcripts, and pathways involved in neointima progression.

Overall, our study sheds light on the intricate molecular mechanisms involved in the interplay between HLA I DSA, ECs, monocytes, and macrophages, as well as provides insights into neointimal development during CAV progression. The findings of this study contribute to the crucial goal of identifying molecular targets aimed at reducing vessel and graft immunogenicity in AMR and CAV across diverse solid organ transplantations.

Chapter 2 – Cross-Talk between HLA Class I and TLR4 Mediates P-selectin Surface Expression and Monocyte Capture to Human Endothelial Cells

The Journal of Immunology

Cross-Talk between HLA Class I and TLR4 Mediates P-Selectin Surface Expression and Monocyte Capture to Human Endothelial Cells

Yi-Ping Jin, Jessica Nevarez-Mejia, Allyson Q. Terry, Rebecca A. Sosa, Sebastiaan Heidt, Nicole M. Valenzuela, Enrique Rozengurt and Elaine F. Reed

J Immunol published online 2 September 2022
http://www.jimmunol.org/content/early/2022/09/02/jimmunol.2200284

Supplementary Material http://www.jimmunol.org/content/suppl/2022/09/02/jimmunol.2200284.DCSupplemental

The Journal of Immunology is published twice each month by The American Association of Immunologists, Inc., 1451 Rockville Pike, Suite 650, Rockville, MD 20852

Print ISSN: 0022-1767 Online ISSN: 1550-6606.

Published September 2, 2022, doi:10.4049/jimmunol.2200284

Cross-Talk between HLA Class I and TLR4 Mediates P-Selectin Surface Expression and Monocyte Capture to Human Endothelial Cells

Yi-Ping Jin,* Jessica Nevarez-Mejia,* Allyson Q. Terry,* Rebecca A. Sosa,* Sebastiaan Heidt,† Nicole M. Valenzuela,* Enrique Rozengurt,‡ and Elaine F. Reed*

Donor-specific HLA Abs contribute to Ab-mediated rejection (AMR) by binding to HLA molecules on endothelial cells (ECs) and triggering intracellular signaling, leading to EC activation and leukocyte recruitment. The molecular mechanisms involving donor-specific HLA Ab–mediated EC activation and leukocyte recruitment remain incompletely understood. In this study, we determined whether TLRs act as coreceptors for HLA class I (HLA I) in ECs. We found that human aortic ECs express TLR3, TLR4, TLR6, and TLR10, but only TLR4 was detected on the EC surface. Consequently, we performed coimmunoprecipitation experiments to examine complex formation between HLA I and TLR4. Stimulation of human ECs with HLA Ab increased the amount of complex formation between HLA I and TLR4. Reciprocal coimmunoprecipitation with a TLR4 Ab confirmed that the crosslinking of HLA I increased complex formation between TLR4 and HLA I. Knockdown of TLR4 or MyD88 with small interfering RNAs inhibited HLA I Ab–stimulated P-selectin expression, von Willebrand factor release, and monocyte recruitment on ECs. Our results show that TLR4 is a novel coreceptor for HLA I to stimulate monocyte recruitment on activated ECs. Taken together with our previous published results, we propose that HLA I molecules form two separate signaling complexes at the EC surface, that is, with TLR4 to upregulate P-selectin surface expression and capture of monocytes to human ECs and integrin β_4 to induce mTOR-dependent firm monocyte adhesion via ICAM-1 clustering on ECs, two processes implicated in Ab-mediated rejection. ***The Journal of Immunology*****, 2022, 209: 1–11.**

Ab-mediated rejection (AMR) is a major obstacle for long-term survival of allograft transplants and is estimated to affect 10–20% of allografts (1–3). The production of anti-donor HLA class I (HLA I) and class II (HLA II) Abs is a risk factor for development of chronic rejection, which manifests as transplant vasculopathy (4–6). Although the development of posttransplant anti-HLA Ab is linked to transplant vasculopathy, the physiologic and pathologic effects of their binding to the endothelium of the transplanted organ have only recently been explored. Donor-specific HLA Abs contribute to the process of AMR by binding to the HLA molecules on endothelial cells (ECs) and triggering intracellular signaling networks, leading to EC activation and leukocyte recruitment. In previous studies, we showed that Ab crosslinking of HLA I molecules on ECs stimulates intracellular signaling, including FAK/Src, ERK, PI3K, and mTORC1 (7–11). HLA I triggers these signaling pathways by physically associating with integrin β_4 in ECs, an interaction that is required for HLA I Ab–induced signaling, leading to cytoskeletal remodeling, proliferation, and migration (12). Thus, integrin β_4 functions as a coreceptor for HLA I in signal transduction in ECs.

ECs contain specialized secretory granules, termed Weibel–Palade bodies (WPBs), that store von Willebrand factor (vWF) and P-selectin (13, 14), which are the best characterized constituents of WPBs. The trafficking of vWF and P-selectin to the EC surface in response to a variety of stimuli plays a critical role in converting the nonadhesive surface of ECs into a highly adhesive surface that captures blood cells, including monocytes, which are crucial in the pathogenesis of vascular inflammation in AMR (15). Indeed, vWF knockout mice display defective leukocyte attachment, in line with the involvement of P-selectin externalization in monocyte adherence (16). Our studies demonstrated that HLA I engagement with Abs directed against monomorphic or polymorphic residues on HLA I promotes P-selectin expression on the EC surface and consequent monocyte recruitment (17–19). Collectively, these results imply that these changes in the adhesive properties of the EC surface initiated by HLA I Ab play a critical role in AMR. However, the specific mechanisms by which Ab binding to HLA I induces P-selectin expression and subsequent monocyte capture by ECs remain poorly understood, and the role of integrin β_4 in these processes has not been investigated.

*Department of Pathology and Laboratory Medicine, David Geffen School of Medicine, University of California, Los Angeles, Los Angeles, CA; †Department of Immunology, Leiden University Medical Center, Leiden, the Netherlands; and ‡Department of Medicine, David Geffen School of Medicine, University of California, Los Angeles, Los Angeles, CA

ORCIDs: 0000-0001-6620-4274 (Y.-P.J.), 0000-0003-3390-4818 (J.N.-M.), 0000-0002-4156-991X (A.Q.T.), 0000-0002-9860-6830 (R.A.S.), 0000-0002-6700-188X (S.H.), 0000-0003-2024-5382 (N.M.V.), 0000-0002-7838-9170 (E.R.), 0000-0002-3524-545X (E.F.R.).

Received for publication April 18, 2022. Accepted for publication July 22, 2022.

This work was supported by National Institute of Allergy and Infectious Diseases Grant R01AI135201 (to E.F.R., N.M.V., and E.R.). E.F.R. was also supported by National Institute of Allergy and Infectious Diseases Grants R21AI156592, U19AI128913, and P01AI120944 and National Institute of Allergy and Infectious Diseases Contract 75N93019C00052. E.R. was also supported by National Cancer Institute Grant P01CA236585, National Institute of Allergy and Infectious Diseases Grant R21AI156592, and by Department of Veterans Affairs Merit Award 1I01BX003801. In addition, this work was supported by the Norman E. Shumway Career Development Award from the International Society of Heart and Lung Transplantation and Enduring Hearts (to N.M.V., 2017–2019) and the UCLA Faculty Development Award (to N.M.V., 2019–2020). J.N.-M. was supported by the Ruth L. Kirschstein National Research Service Award T32HL069766.

Address correspondence and reprint requests to Prof. Elaine F. Reed, UCLA Immunogenetics Center, Department of Pathology and Laboratory Medicine, David Geffen School of Medicine, University of California, Los Angeles, 1000 Veteran Avenue, Los Angeles, CA 90095. E-mail address: ereed@mednet.ucla.edu

The online version of this article contains supplemental material.

Abbreviations used in this article: AMR, Ab-mediated rejection; EC, endothelial cell; HLA I, HLA class I; HLA II, HLA class II; PFA, paraformaldehyde; siRNA, small interfering RNA; TRIF, Toll/IL-1R domain–containing adaptor inducing IFN-β; WPB, Weibel–Palade body; vWF, von Willebrand factor.

www.jimmunol.org/cgi/doi/10.4049/jimmunol.2200284

In the current study, we demonstrate that HLA I Abs induce P-selectin externalization and monocyte binding to ECs through an integrin β_4–independent mechanism. Given that HLA molecules lack signal motifs and kinase activity in their short cytoplasmic tail, we postulated that HLA I triggers these changes in the properties of EC surface by forming a signaling complex with other molecules. TLR4 is known to regulate P-selectin expression and vWF release on ECs in response to its ligand, LPS (20, 21). We found that TLR4 is the only TLR expressed on the EC surface and accordingly hypothesized that HLA I molecules associate with TLR4 to transduce signals that lead to P-selectin externalization and monocyte recruitment.

Pursuing this hypothesis, we found that Ab ligation of HLA I molecules on ECs stimulated the formation of a molecular complex between HLA I and TLR4. These results support the notion that HLA I molecules physically associate with TLR4 together with the adaptor proteins MyD88 and TIRAP. Our data also show that HLA I Ab–stimulated P-selectin expression on the surface of ECs is abrogated by knocking down TLR4 or MyD88 with small interfering RNAs (siRNAs). Reciprocally, our results also imply that HLA I functions as a coreceptor for TLR4-mediated P-selectin externalization and monocyte adhesion. We conclude that HLA I forms two separate molecular complexes at the cell surface, that is, with integrin β_4 or TLR4, each of which plays a critical role to elicit signals that regulate fundamental functions in ECs that are implicated in the pathogenesis of AMR.

Materials and Methods

Abs and chemicals

Cell culture reagents were from Invitrogen. Purified allele-specific human mAbs HLA-A2/A28 (clone SN607D8, IgG1), HLA-A3/A11/A24 (clone MUL2C6, IgG1), and HLA-B12 (clone DK7C11, IgG1) were gifts from Dr. Sebastiaan Heidt. Purified mouse mAbs against HLA-A2/A28 (clone H0037, IgG) were provided by Dr. Jar-how Lee (One Lambda, Canoga Park, CA). Anti–HLA I mAb W6/32 (mouse IgG2a), recognizing a conformational epitope on all HLA-A, HLA-B, and HLA-C H chains when they are in association with β_2-microglobulin (22), was purified from cultured supernatants of the hybridoma HB-95 (American Type Culture Collection, Manassas, VA). The F(ab′)$_2$ fragments of mAbs were generated by using IdeZ protease (Promega, Madison, WI) according to the manufacturer's protocol. The mouse mAb EMR8-5, recognizing the denatured H chain of HLA-A, HLA-B, and HLA-C, and anti–HLA-A2 mAb for Western blot were obtained from Medical & Biological Laboratories. The mouse mAb TLR4 (HTA125, mouse IgG2a) for immunoprecipitation was from eBioscience. Ab against integrin β_4 was purchased from BD Biosciences (San Diego, CA). Sheep anti-human P-selectin Ab and donkey anti-sheep IgG HRP-conjugated Ab were purchased from R&D Systems (Minneapolis, MN). Rabbit polyclonal Abs against TLR1, TLR2, TLR3, TLR4, TLR6, TLR7, TLR8, TLR9, MyD88, and β-actin were purchased from Cell Signaling Technology (Beverly, MA). The rabbit polyclonal Ab against β-tubulin (H-235), mAbs against TLR4, TLR5, and TLR10, MD2 (J-12B), GAPDH, goat anti-rabbit HRP, goat anti-mouse HRP IgG, and Protein A/G Plus agarose beads were purchased from Santa Cruz Biotechnology (Santa Cruz, CA). The rabbit polyclonal Ab against TIRAP was from Novus (Centennial, CO). The monoclonal anti-vinculin (clone Hvin-1) and mouse isotype control were from Sigma-Aldrich (St. Louis, MO). PE-conjugated Abs against TLR2, TLR3, TLR4, TLR5, and TLR10, as well as mouse IgG2a, were purchased from BioLegend. PE-conjugated Ab against TLR1 and a Vybrant CFDA SE cell tracer kit (V-12883) were purchased from Molecular Probes (Eugene, OR). Mouse mAb against TLR4 (76B357.1) for immunohistochemistry and rabbit polyclonal against TRIF (Toll/IL-1R domain–containing adaptor inducing IFN-β) were purchased from Abcam (Cambridge, MA). FITC-conjugated donkey anti-rabbit IgG was purchased from Jackson ImmunoResearch Laboratories (West Grove, PA).

Cell culture

Human aortic ECs were isolated from the aortic rings of explanted donor hearts, as described previously (9), or obtained from Lonza/Clonetics (Walkersville, MD). ECs were cultured in M199 medium (Mediatech, Manassas, VA) supplemented with 20% (v/v) FBS (HyClone), penicillin-streptomycin (100 U/ml and 100 μg/ml, respectively; both from Invitrogen), sodium pyruvate (1 mmol/l), heparin (90 μg/ml, Sigma-Aldrich), and EC growth supplement (20 μg/ml, BD Biosciences). Cells were used for experiments from passage 3 to 8. Prior to use in experiments, cells were grown for 6 h in medium M199 containing 0.2% FBS.

The human monocytic cell line Mono Mac 6 (23, 24) (a gift of Dr. Judith Berliner, Department of Pathology and Laboratory Medicine, University of California, Los Angeles) was cultured in RPMI 1640 supplemented with 10% FBS, 10 mg/ml insulin, sodium pyruvate, penicillin-streptomycin, and nonessential amino acids (Life Technologies).

Human peripheral blood monocytes were isolated from healthy donors as previously reported (18). Briefly, PBMCs were isolated using Ficoll-Paque density centrifugation (Eppendorf centrifuge 5810; Eppendorf, Hauppauge, NY). Total monocytes were then enriched from PBMCs using a MACS negative selection Pan Monocyte Isolation Kit (Miltenyi Biotec, Bergisch Gladbach, Germany) according to the manufacturer's protocol. The purity of monocytes was > 90% as determined by flow cytometric analysis with CD14 Ab.

Coimmunoprecipitation

ECs (4×10^6 to 5×10^6) were treated with W6/32 F(ab′)$_2$ for 20 min, giving results comparable to those in cells treated with whole IgG of W6/32 (7); mouse IgG2a F(ab′)$_2$ was used as a negative control. The W6/32 F(ab′)$_2$ fragments were used instead of the whole IgG to prevent the Fc parts from interfering with immunoprecipitation with protein A/G agarose beads. Cells were lysed in ice-cold buffer containing 1% CHAPS, 150 mM NaCl, 50 mM Tris-HCl (pH 7.4), 50 mM NaF, 1.5 mM Na_3VO_4, 0.5 mM PMSF, 0.2 μg/ml aprotinin, and 0.5 μg/ml leupeptin, and cell lysates were collected after spinning down at 10,000 × *g* for 10 min. Precleared cell lysates were immunoprecipitated with anti–HLA I mAb W6/32, murine anti–HLA-A2, or TLR4 mAb (HAT125) at 4°C on a rotator overnight. Then, samples were incubated with Protein A/G Plus agarose beads for 4 h. Immunoprecipitates were washed three times with immunoprecipitation wash buffer (40 mM HEPES [pH 7.5], 10 mM β-glycerophosphate, 120 mM NaCl, 1 mM EDTA, 50 mM NaF, 1.5 mM Na_3VO_4, 0.3% CHAPS, 0.2 μg/ml aprotinin, 0.5 μg/ml leupeptin), and samples were resolved using SDS-PAGE. Five percent of the total amount of protein used in the immunoprecipitation was loaded onto the gel as an input control.

Western blot

Cell lysates for Western blot were prepared as previously described (9). Briefly, cells cultured in a low-serum concentration for 6 h, stimulated with human or murine anti–HLA I mAb or control IgG at 37°C, and lysed in buffer (containing 20 mM Tris [pH 7.9], 137 mM NaCl, 5 mM EDTA, 1 mM EGTA, 10% glycerol, 1% Triton X-100, 10 mM NaF, 1 mM PMSF, 1 mM Na_3VO_4, 10 μg/ml aprotinin, and 10 μg/ml leupeptin) for 10 min on ice. The cell lysates were resolved by SDS-PAGE and proteins were transferred overnight onto polyvinylidene difluoride membranes (Millipore). The membranes were blocked using 5% nonfat dry milk in TBS (pH 7.4) containing 0.05% Tween 20 (TBST) for 1 h at room temperature and incubated overnight with appropriate primary Abs. The blots were incubated with HRP-conjugated secondary Abs and developed with ECL (Amersham). The phosphorylated protein bands were scanned using the Epson Perfection V700 photo scanner (Epson) and were quantified using the ImageJ program (http://rsb.info.nih.gov/ij/; National Institutes of Health, Bethesda, MD).

siRNA transfection

The human integrin β_4 siRNA (target sequence, 5′-CAG AAG AUG UGG AUG AGU UUU-3′), the siRNAs against the HLA I H chain targeting the HLA-A and HLA-B alleles (5′-GCA GAG AUA CAC CUG CCA U-3′ and 5′-GAG CUC AGA UAG AAA AGG A-3′), TLR4, MyD88, TLR3, and TRIF smart pool siRNA, and control nontargeting siRNA duplexes (5′-UAG CGA CUA AAC ACA UCA AUU-3′ and 5′-AAU UGA UGU GUU UAG UCG CUA-3′) were synthesized by Dharmacon (Lafayette, CO). ECs were plated at a density of 70% confluence and transfected with siRNA using Mirus TransIT-TKO transfection reagents (Mirus Bio, Madison, WI) according to the manufacturer's protocol. Experiments were conducted 48 h after transfection (8).

Flow cytometry determination

ECs were grown in 2 ml of complete medium in 35-mm dishes coated with 0.1% gelatin until confluent and detached by trypsin-EDTA (Life Technologies) and incubated with HLA I Ab (1 μg/ml) in 0.1 ml of paraformaldehyde (PFA) (PBS with 2.5% FBS and 0.1% sodium azide) for 30 min on ice. Cells were washed twice with PFA and incubated with FITC-conjugated anti-mouse secondary Ab at 1:100 (Jackson ImmunoResearch Laboratories) used to detect HLA I molecule expression. Alternatively, ECs or monocytes were incubated with PE-conjugated TLR1, TLR2, TLR3, TLR4, TLR5, or

TLR10 Abs. Cell fluorescence was measured by flow cytometry on a LSRFortessa cytometer, calculated with the BD FACSDiva program (Becton Dickinson, Mountain View, CA), and analyzed with FlowJo v10 software.

Cell surface P-selectin expression

Cell surface P-selectin expression on ECs was detected by cell-based ELISA as described previously (18). Briefly, ECs were cultured in 35-mm dishes to 70% confluence and transfected with siRNA for 24 h. Transfected cells were detached with Accutase, seeded in a 96-well plate to confluence for 48 h, and treated with Ab against HLA I or mouse IgG2a as an isotype control for 30 min. Cells were fixed with freshly prepared 2.5% PFA in PBS for 5 min at room temperature. Unpermeabilized cells were blocked with 5% BSA in PBS and incubated with sheep anti–P-selectin Ab (1 μg/ml) for 2 h followed by incubation with anti-sheep HRP secondary Ab at 1:1000 for 2 h at room temperature. After washing three times, tetramethylbenzidine substrate was added into wells and OD was read at 650 nm on a SpectraMax plate reader (Molecular Devices).

Blockade of FcγRs

FcγRs were blocked as previously described (18). Briefly, in monocyte adhesion experiments, monocytes or Mono Mac 6 cells were incubated with 10 μg/ml purified human IgG in PBS for 15 min to block the FcγRs from binding HLA I IgG on the surface of ECs.

Monocyte adhesion assay

Monocyte adhesion on ECs was described previously (25, 26). Briefly, ECs were cultured in 24-well plates coated with 0.1% gelatin and were transfected with siRNA and treated with Abs against HLA I, or HLA-A2, HLA-A3, or HLA-B12. CFSE (Invitrogen)-labeled primary monocytes or Mono Mac 6 were added onto EC monolayers at a ratio of approximately three monocytes per EC for 20 min at 37°C. After washing three times, adherent monocytes were imaged by fluorescence microscopy (Nikon Eclipse Ti) with magnification ×4 and analyzed with software CellProfiler or ImageJ. Results are expressed for each condition as fold change in mean of adhesion monocytes per field normalized to control cells ± SEM.

Immunofluorescence staining

Indirect immunofluorescence analysis of cell surface molecules was previously described (12). For P-selectin expression and vWF release, ECs were transfected with TLR3, TRIF, TLR4, MyD88, or control siRNA (100 nM each) for 48 h, or pretreated with TLR4 inhibitor TAK242, and cells were stimulated with an anti–HLA I Ab $F(ab')_2$ fragment or a mouse IgG2a $F(ab')_2$ fragment (1 μg/ml) for 30 min. Cells were fixed with freshly prepared 4% PFA, and surface P-selectin was stained on unpermeabilized cells with mouse anti-human P-selectin mAb and rabbit anti-human vWF Ab followed by Alexa Fluor 488 rabbit anti-mouse IgG1, Alexa Fluor 594 goat anti-rabbit IgG (H+L), and DAPI. Images were obtained with a Zeiss LSM 880 fluorescence microscope using a ×40 objective lens.

Statistical analysis

Data are presented as mean ± SEM. Differences were calculated using a one-way ANOVA with Tukey's multiple comparison test, or a Student *t* test. A p value <0.05 was considered significant.

Results

Ligation of HLA I by Abs induces P-selectin externalization through an integrin β_4–independent pathway

We previously reported that HLA I molecules physically associate with integrin β_4 in ECs, an interaction that is required for HLA I Ab–induced signaling, leading to EC proliferation and migration (12). Given that HLA I Abs also trigger WPB exocytosis and adherence of monocytes (18, 25), we asked whether integrin β_4 was similarly required for eliciting this effect. To answer this question, we knocked down integrin β_4 with siRNA in primary ECs and tested whether P-selectin surface expression and monocyte adherence were reduced after HLA I Ab stimulation. Transfection with siRNA targeting integrin β_4 drastically diminished integrin β_4 protein levels without affecting Akt or ERK levels (Fig. 1A), or cell surface HLA I expression (Fig. 1B). In line with previous results, ECs treated with either anti–HLA-A2 Ab or anti–HLA-B12 Ab significantly upregulated cell surface P-selectin (Fig. 1C). The salient feature of the data shown in Fig. 1 is that ECs with significantly reduced integrin β_4 expression retained the capacity to exocytose P-selectin (Fig. 1C) as compared with cells transfected with nontargeting siRNA. Concordantly, knockdown of integrin β_4 had no effect on HLA I Ab-induced monocyte adherence (Fig. 1D), which was not significantly different compared with control siRNA conditions (Fig. 1E). These experiments indicate that HLA I induces P-selectin externalization through an integrin β_4–independent pathway and raised the possibility that HLA molecules interact with other, as yet unidentified coreceptors to rapidly upregulate cell surface P-selectin expression and promote monocyte adherence.

HLA I physically associates with TLR4

Several previous studies suggest that HLA II is functionally linked to TLRs in innate immune cells (27–31), but it is not known whether HLA I interacts physically and functionally with TLRs in ECs. As a first step to explore this possibility, we determined the protein expression of different TLRs in ECs and used human monocytes or Ramos cells, which are known to express multiple TLRs, as positive controls. ECs expressed TLR3, TLR4, TLR5, and TLR10, as shown by Western blot analysis. In contrast, TLR1, TLR2, TLR6, TLR7, TLR8, or TLR9 was not detected (Supplemental Fig. 1A). Importantly, only TLR4 was detected on the surface of ECs by flow cytometry (Supplemental Fig. 1B). In addition, ECs express the Toll/IL-1R domain–containing adaptors TIRAP, MyD88, and TRIF, but not TRAM, the MyD88-independent component of TLR4 signaling (Supplemental Fig. 1C, 1D).

The preceding results prompted us to determine whether any of the endothelial-expressed TLRs physically associates with HLA I, as judged by coimmunoprecipitation. ECs were left untreated or stimulated with HLA I Ab. TLR4, which is the only TLR expressed on the surface of ECs, was also the only TLR detected when HLA I was pulled down (Fig. 2A). In addition, MD2, MyD88, and TIRAP were also found in the complex with HLA I, and their association was increased in cells treated with HLA I Ab (Fig. 2A). TIRAP is an adaptor protein that connects MyD88 with TLR4 (32). In contrast, TRIF was not detected in HLA I immunoprecipitates (Fig. 2A). Similar results were obtained when cells were challenged with an Ab that binds HLA-A2 (Fig. 2B). These results suggest that HLA I physically associates with TLR4 in ECs at the cell surface. Reciprocal experiments using TLR4 pulldown confirmed that HLA I associated with TLR4 (Fig. 2C, 2D). Because we demonstrated previously that HLA I interacts physically with integrin β_4, we asked whether this integrin was present in the HLA I/TLR4 complex. Integrin β_4 was not detected in TLR4 immunoprecipitates (Fig. 2C). Similarly, pulldown of integrin β_4 yielded an increased association with HLA I in response to HLA I stimulation, but TLR4 was not detected (Fig. 2E). Furthermore, knockdown of integrin β_4 did not alter the association of TLR4 with HLA I (Fig. 2F) despite extensive loss of integrin β_4 protein (Fig. 2G). These experiments used coimmunoprecipitation of endogenous rather than expressed tagged proteins because molecular complexes between expressed proteins of the TLR system might represent artifacts of protein overexpression (33). Our results indicate that HLA I molecules form two separate signaling complexes at the cell surface, that is, with either integrin β_4 or TLR4.

Knockdown of TLR4 impairs HLA I–induced P-selection expression at the surface of ECs

Because HLA I promotes P-selectin expression at the cell surface in an integrin β_4–independent manner, we tested whether the HLA I/TLR4 complex, identified in the current study, mediates P-selectin externalization. To determine whether TLR4 was required for EC exocytosis of P-selectin in response to HLA I Abs, we tested

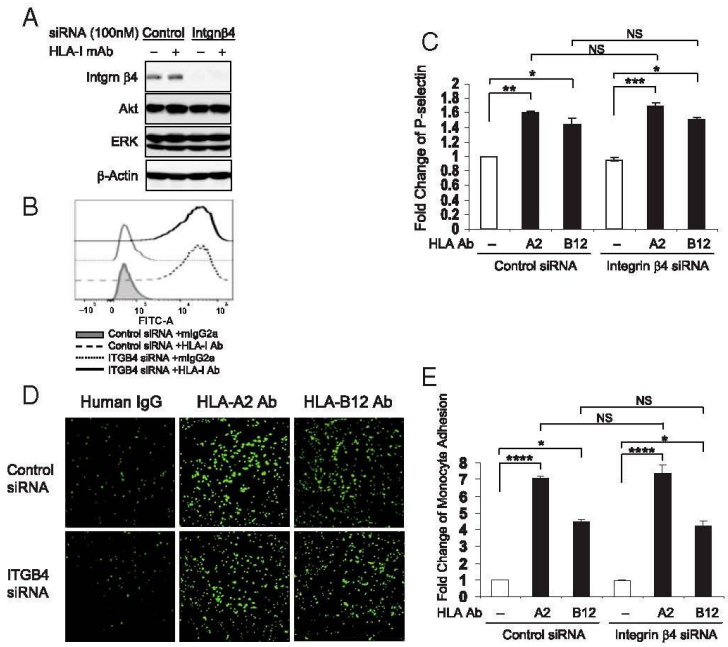

FIGURE 1. HLA I Ab induces P-selectin expression and monocyte adhesion through an integrin β_4–independent pathway on human ECs. (**A**) ECs were transfected with 100 nM single duplex siRNA against the integrin β_4 subunit (sequence, 5′-GAGAGCAGCUUCCAAAUCA-3′) or with nontargeting control siRNA and were incubated for 48 h. Cells were lysed and subjected to Western blotting analysis with Abs against integrin β_4 (205 kDa), Akt, and ERK and with β-actin as a loading control. (**B**) Expression of HLA I on the surface of ECs transfected with siRNAs was analyzed by flow cytometry with the HLA I–specific Ab W6/32 or isotype control mouse IgG2a. Negative control cells transfected with nontargeting control siRNA + mouse IgG2a are shown as a filled peak in half-offset histography, whereas the dashed line represents cells transfected with control siRNA + HLA I Ab, the dotted line represents cells transfected with integrin β_4 siRNA + mouse IgG2a, and the thick solid line represents cells transfected with integrin β_4 siRNA + HLA I Ab. (**C**) ECs were transfected with integrin β_4–specific siRNA or control siRNA (100 nM each). After 48 h, cells were stimulated with anti–HLA-A2 or anti–HLA-B12 human mAb (1 μg/ml) for 30 min. Cell surface P-selectin was stained on unpermeabilized cells with sheep anti-human P-selectin Ab followed by donkey anti-sheep HRP-conjugated secondary Ab, detected by adding tetramethylbenzidine substrate and measuring the OD at 650 nm. The bar graph shows the fold change of the mean ± SEM of the OD value from triplicate wells for each condition. $*p < 0.05$, $**p < 0.01$, $***p < 0.001$ analyzed by one-way ANOVA with Tukey's multiple comparison test. Results represent at least three independent experiments. (**D** and **E**) ECs were transfected with integrin β_4–specific siRNA or control siRNA (100 nM each). ECs were stimulated with HLA-A2 or HLA-B12 human mAb (1 μg/ml) for 30 min. CFSE-labeled Mono Mac 6 (MM6) with an FcγR blockade was added to HLA I Ab-stimulated EC monolayers. Adherence of MM6 cells was measured by a Nikon Eclipse Ti live cell inverted microscope with a ×4 objective lens and (E) analyzed with CellProfiler. Bar graph represents fold change of adherent MM6 mean ± SEM from at least three independent experiments. $*p < 0.05$, $****p < 0.0001$ analyzed by one-way ANOVA with a Tukey's multiple comparison test.

P-selectin expression under TLR4 or MyD88 knockdown with siRNA. TLR4 siRNA specifically reduced TLR4 expression, but not HLA I or signaling adaptor molecules (Fig. 3A, 3C). Similarly, MyD88 siRNA reduced MyD88 protein but not TLR4 or HLA I (Fig. 3B, 3D). When either TLR4 or MyD88 was knocked down, HLA I Ab treatment failed to elicit P-selectin exocytosis (Fig. 3E). As a control, we verified that LPS-induced P-selectin was also abrogated under TLR4 or MyD88 deficiency (Fig. 3F). These results were substantiated using immunofluorescence imaging of cell surface P-selectin and externalized vWF, another component stored in the WPB. Neither VWF nor P-selectin was externalized by HLA I Ab in ECs that had been treated with TLR4 or MyD88 siRNAs (Fig. 3G). A pharmacological inhibitor of TLR4, TAK242 (34), also blocked HLA I Ab-induced P-selectin presentation (Fig. 3G). In contrast, siRNA targeting TLR3 or TRIF had no detectable effect (Fig. 3G).

TLR4 associates with HLA I to increase monocyte adherence to ECs

We and others previously showed that HLA Ab-induced P-selectin supported increased adherence of monocytes and platelets to endothelium (18, 25, 35). In this study, we demonstrate that HLA I induces P-selectin externalization through a novel interaction with TLR4. Consequently, we tested whether loss of TLR4 impairs P-selectin externalization and dampened monocyte adhesion to the endothelium. First, we corroborated that treatment of ECs with HLA I Ab markedly increased monocyte adhesion (2.7-fold). Similar results were obtained in ECs stimulated with either the TLR4 agonist LPS or thrombin, as positive controls, but not elicited by treatment with mouse IgG2a or non-HLA Ab CD105 (Fig. 4A, 4B). As observed with P-selectin surface expression, siRNA knockdown of TLR4 or MyD88, or pretreatment with the TLR4 inhibitor TAK242, markedly reduced monocyte adhesion to endothelium stimulated with HLA I Abs (Fig. 4C, 4D). In contrast, siRNA against TLR3 or TRIF had no effect (Fig. 4C, 4D). As controls, we found that TLR4 or MyD88 siRNA blocked monocyte adherence to LPS-stimulated endothelium, whereas siRNA-mediated knockdown of TLR3 or TRIF did not produce any appreciable inhibitory effect (Fig. 4C, 4E).

Given the results shown in Fig. 4, it was important to rule out that the effects of HLA I Ab were due to LPS contamination. To this end, we tested whether polymyxin B, a potent LPS neutralizer, has any effect on monocyte binding to ECs in response to Ab-mediated

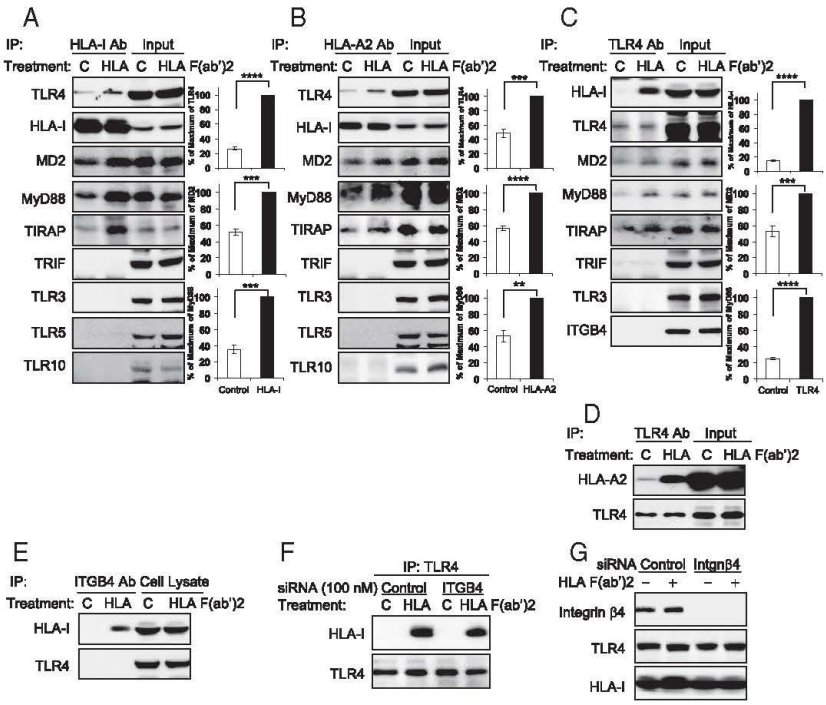

FIGURE 2. Ligation of HLA I on ECs with Ab triggers formation of a signal complex containing TLR4 and HLA I. (**A**–**C**) ECs were stimulated with the $F(ab')_2$ fragments of W6/32 (a pan Ab against HLA I) or with a control mouse IgG2a $F(ab')_2$ fragment for 20 min. Cell lysates were subjected to immunoprecipitation (IP) with (A) W6/32, (B) anti–HLA-A2 human mAb, (C) TLR4 Ab (HTA125) and analyzed by Western blotting with Abs against the H chain of HLA I (EMR8-5), TLR4 (120 kDa), MyD88 (33 kDa), MD2 (20–25 kDa), TIRAP (30 kDa), TRIF (66 kDa), TLR3 (115 kDa), TLR5 (110–120 kDa), TLR10 (90 kDa), or (C) integrin β_4 (205 kDa) as indicated to the left of the blots. For each sample, 5% of the total cell lysate that was used in the immunoprecipitation was loaded as an input control. Data are representative of three independent experiments. Protein bands (A and B) TLR4, MD2, and MyD88 and (C) HLA I, MD2, and MyD88 were quantified by densitometry scan and the results are expressed as the mean ± SEM percentage of the maximal extent of protein. The data presented in (A)–(C) are representative of at least three independent experiments. $^{**}p < 0.01$, $^{***}p < 0.001$, $^{****}p < 0.0001$ analyzed by Student *t* test. (**D**) ECs were stimulated as described in (A), cell lysates were immunoprecipitated with an Ab against TLR4 (HTA125), and samples were analyzed by Western blotting with the HLA-A2 Ab (BB7.2) or TLR4 Ab. For each sample, 5% of the total cell lysate that was used in the immunoprecipitation reaction was loaded as an input control. Data are representative of three independent experiments. (**E**) ECs were stimulated as described in (A), cell lysates were immunoprecipitated with an integrin β_4 Ab, and samples were analyzed by Western blotting with the HLA I H chain (EMR8-5) or TLR4 Ab. For each sample, 5% of the total cell lysate that was used in the immunoprecipitation reaction was loaded as an input control. Data are representative of three independent experiments. (**F** and **G**) ECs were transfected with 100 nM integrin β_4 siRNA or control siRNA. After 48 h, ECs were stimulated with the $F(ab')_2$ fragments of W6/32 or with control IgG2a $F(ab')_2$ for 20 min. (F) Cell lysates were immunoprecipitated with an Ab against TLR4 (HTA125), and samples were analyzed by Western blotting with Ab against HLA I H chain EMR8-5 or TLR4 Ab. Data are representative of two independent experiments. (G) ECs were subjected to Western blotting analysis with Abs against integrin β_4, TLR4, and HLA I (EMR8-5). Data are representative of three independent experiments.

crosslinking of HLA I. Initially, we verified that pretreatment with polymyxin B completely blocked LPS-stimulated monocyte adhesion (Fig. 5A, 5B). Next, we excluded the presence of TLR4 ligand in our HLA Ab preparations by testing monocyte adherence induced by HLA Ab in the absence or presence of polymyxin B (Fig. 5C), at the concentration that neutralized LPS. Although purified LPS itself increased monocyte adherence to endothelium, polymyxin B did not significantly affect HLA I Ab-induced monocyte binding (Fig. 5C, 5D). In addition, ligation of HLA I with the mAb W6/32 stimulated an increase in monocyte adhesion on ECs transfected with nontargeting siRNA (Fig. 5C). Knockdown of TLR4 or MyD88 with siRNA or pretreated with TAK242 inhibited HLA Ab-induced monocyte adhesion to ECs (Fig. 5C). Similar to W6/32 treatment alone, W6/32 treated with polymyxin B also stimulated increased monocyte adhesion on ECs transfected with control siRNA, which eliminated the possibility of contamination by LPS. Knockdown of TLR4 or MyD88 with siRNA or pretreated with TAK242 inhibited PB + HLA I Ab-stimulated monocyte adhesion on ECs. Both W6/32 and W6/32 + polymyxin B–mediated monocyte adhesion was not affected by TLR3 siRNA and TRIF siRNA (Fig. 5C, 5D).

HLA I is required for TLR4-mediated P-selectin externalization and monocyte binding

Thus far, our results demonstrated that TLR4 is a coreceptor for HLA I mediating rapid Ab-induced P-selectin externalization and monocyte adhesion. We next interrogated whether HLA I was reciprocally required for TLR4-triggered endothelial responses elicited by LPS. Stimulation of ECs with LPS resulted in complex formation between HLA I, MyD88, and TLR4, but not TRIF, as shown by coimmunoprecipitation of HLA I (Fig. 6A) and reciprocal pulldown of TLR4 (Fig. 6B). Knockdown of HLA I in ECs prevented LPS-induced externalization of P-selectin and vWF release (Fig. 6C), as

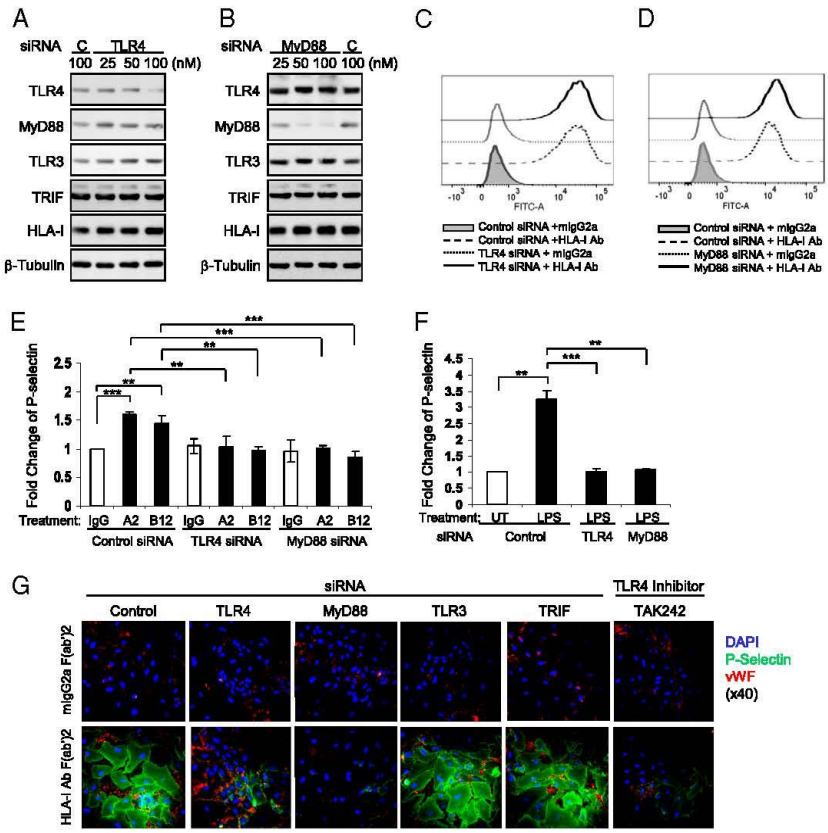

FIGURE 3. Knockdown of TLR4 or MyD88 inhibits HLA I–stimulated P-selectin expression and vWF release on ECs. (**A**) ECs were transfected with 100 nM control siRNA or with 25, 50, or 100 nM TLR4 siRNA, or (**B**) with 25, 50, or 100 nM MyD88 siRNA or 100 nM control siRNA for 48 h. Cells were lysed and analyzed by Western blotting with Abs against TLR4, MyD88, TLR3, TRIF, and HLA I, and with β-tubulin as a loading control. (**C** and **D**) Expression of HLA I on the surface of ECs transfected with siRNAs was analyzed by flow cytometry with the HLA I Ab W6/32 or isotype control mouse IgG2a. Negative control cells transfected with nontargeting control siRNA + mouse IgG2a are shown as a filled peak in a half-offset histogram, whereas the dashed line represents cells transfected with control siRNA + HLA I mAb, the dotted line represents cells transfected with (C) TLR4 siRNA,\ or (D) MyD88 siRNA + mouse IgG2a, and the thick solid line represents cells transfected with (C) TLR4 siRNA or (D) MyD88 siRNA + HLA I mAb, respectively. Data are representative of three independent experiments. (**E**) ECs were transfected with TLR4 siRNA, MyD88 siRNA, or control siRNA (100 nM each). After 48 h, cells were stimulated with anti–HLA-A2 or anti–HLA-B12 human mAb (1 μg/ml) for 30 min. The cells were fixed with freshly prepared 4% PFA, and cell surface P-selectin was stained on unpermeabilized cells with sheep anti-human P-selectin Ab followed by donkey anti-sheep HRP secondary Ab, detected by adding tetramethylbenzidine substrate and measuring the OD at 650 nm. Bar graph shows fold change of the mean ± SEM of OD from triplicate wells for each condition. $^{**}p < 0.01$, $^{***}p < 0.001$ analyzed by one-way ANOVA with a Tukey's multiple comparison test. Data are representative of at least three independent experiments. (**F**) ECs were transfected with TLR4 siRNA, MyD88 siRNA, or control siRNA (100 nM each). After 48 h, cells were stimulated with LPS (0.1 μg/ml) for 30 min. Cell surface P-selectin was stained on unpermeabilized cells with sheep anti-human P-selectin Ab followed by anti-sheep HRP secondary Ab, detected by adding tetramethylbenzidine substrate and measuring OD at 650 nm. Bar graph shows fold change of the mean ± SEM of OD from triplicate wells for each condition. $^{**}p < 0.01$, $^{***}p < 0.001$ analyzed by one-way ANOVA with a Tukey's multiple comparison test. Data are representative of at least three independent experiments. (**G**) ECs were transfected with TLR3, TRIF, TLR4, MyD88, or control siRNA (100 nM each) for 48 h, or pretreated with TLR4 inhibitor TAK242 (1.0 μM) for 30 min, and cells were stimulated with anti–HLA I Ab $F(ab')_2$ fragment or mouse IgG2a $F(ab')_2$ fragment (1 μg/ml) for 30 min. Cells were fixed with freshly prepared 4% PFA, and surface P-selectin was stained on unpermeabilized cells with mouse anti-human P-selectin mAb (mouse IgG1) and rabbit anti-human vWF Ab followed by Alexa Fluor 488 rabbit anti-mouse IgG1, Alexa Fluor 594 goat anti-rabbit IgG (H+L), and DAPI. Six middle fields per dish were imaged with a Zeiss LSM 880 fluorescence microscope using a ×40 objective lens. Data are representative of at least three independent experiments.

well as monocyte adherence to endothelium (Fig. 6D, 6E). In contrast, we found that knockdown of HLA I did not prevent expression of ICAM-1 or E-selectin in response to treatment with LPS for 18 h (data not shown). Collectively, our results demonstrate that HLA I functions as a coreceptor for TLR4-mediated rapid P-selectin externalization and monocyte adhesion.

Discussion

Donor-specific HLA Abs can contribute to AMR by binding to the HLA molecules on the surface of ECs and triggering intracellular signaling, leading to EC activation and leukocyte recruitment. Despite the importance of understanding these processes to identify novel targets to prevent or treat AMR, the molecular mechanisms

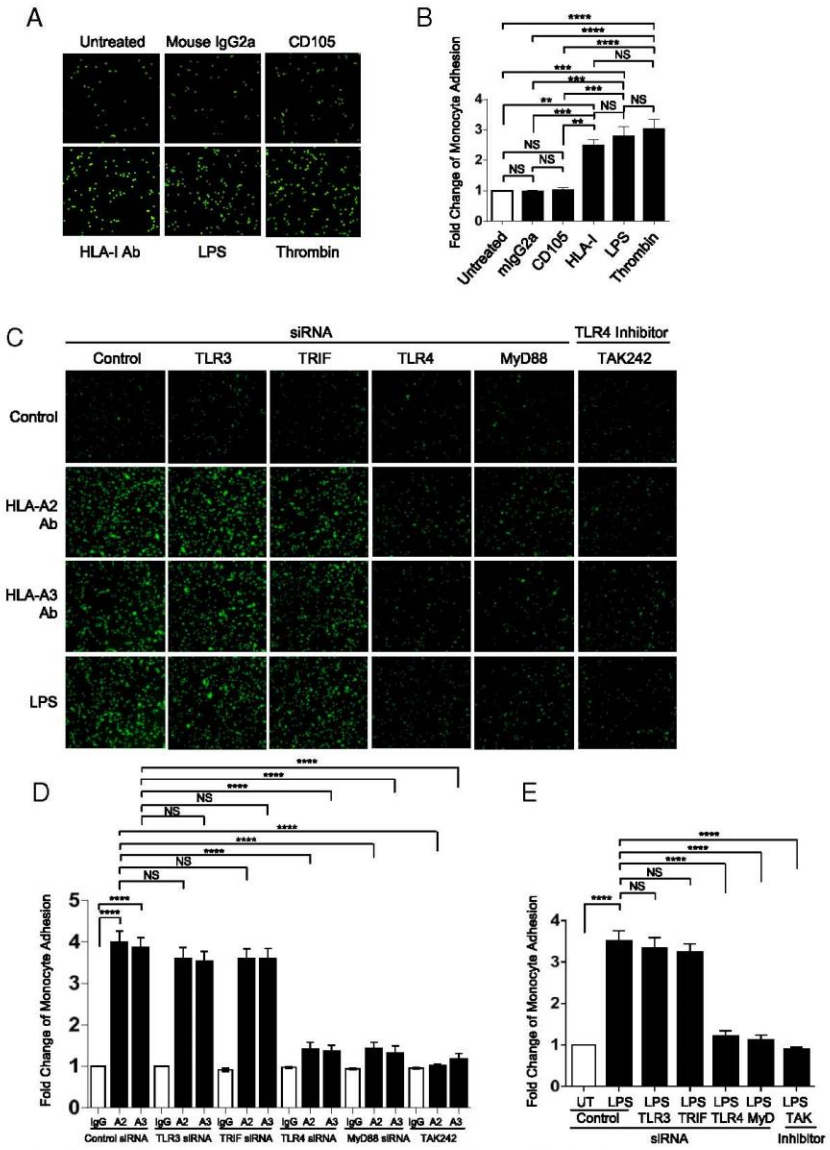

FIGURE 4. Knockdown TLR4 or MyD88 inhibits HLA I–mediated monocyte adhesion on ECs. (**A**) ECs were untreated or treated with HLA I Ab, LPS, thrombin, anti-CD105 Ab, or mouse IgG2a for 30 min. CFSE-labeled fresh isolated monocytes from healthy donors with an FcγR blockade were added to stimulated endothelial monolayers. (**C**) ECs were transfe-cted with TLR3, TRIF, TLR4, MyD88, or control siRNA (100 nM each) for 48 h or treated with TLR4 inhibitor TAK242 (1.0 μM) for 30 min. Cells were untreated or stimulated with anti–HLA-A2 or anti–HLA-A3 human mAb (1 μg/ml) or LPS (0.1 μg/ml) for 30 min. CFSE-labeled fresh isolated monocytes from healthy donors with an FcγR blockade were added to stimulated endothelial monolayers. Adherence of monocytes was measured by a fluorescence microscope with a ×4 objective lens and analyzed with ImageJ. (**B**, **D**, and **E**) Bar graphs represent fold change of adherent monocyte mean ± SEM from (A) and (C). $^{**}p < 0.01$, $^{***}p < 0.001$, $^{****}p < 0.0001$ analyzed by one-way ANOVA with a Tukey's multiple comparison test. Data represent at least four independent experiments using three different ECs from three different donors and fresh isolated monocytes from three different healthy donors.

involved remain incompletely understood. Our previous work demonstrated that HLA I forms a molecular complex with integrin β_4 in response to Ab binding (12). Integrin β_4, acting as a coreceptor, mediates HLA I–induced signaling pathways, including Src/FAK, ERK, and PI3K/AKT/mTORC1, leading to EC proliferation and migration. In addition to these signaling pathways and cellular responses, HLA I crosslinking also elicits rapid trafficking of P-selectin to the surface of ECs, which plays a pivotal role in the capture of monocytes that are critical in the pathogenesis of vascular inflammation in AMR (15). Surprisingly, we show in the present study

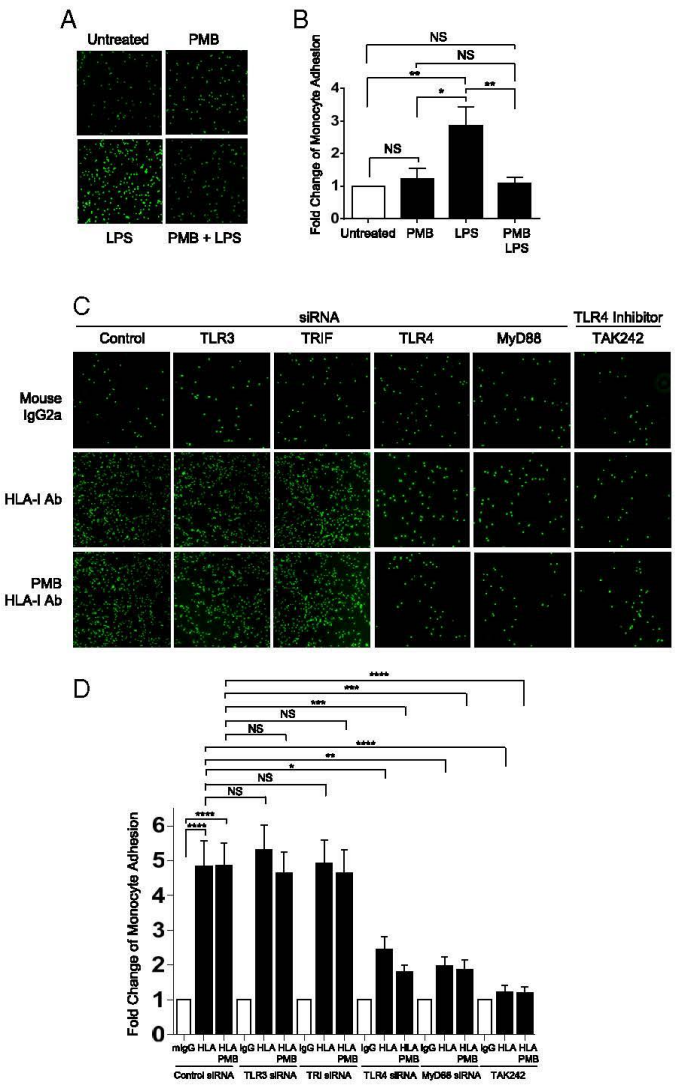

FIGURE 5. Knockdown TLR4 or MyD88 inhibits HLA I Ab-mediated human peripheral blood monocyte adhesion on ECs. (**A**) ECs were untreated or treated with polymyxin B (PMB), or LPS, or PMB+LPS. (**C**) ECs were transfected with 100 nM TLR3, TRIF, TLR4, MyD88, or control siRNA for 48 h, or pretreated with TAK242 for 30 min. Cells were stimulated anti anti–HLA I mAb (1 mg/ml) or PMB preincubated HLA I Ab for 30 min. (A and C) CFSE-labeled primary human monocytes with an FcγR blockade were added to Ab-activated endothelial monolayer. Adherence of monocytes was measured by fluorescence microscopy using a ×4 objective lens and analyzed with ImageJ. (**B** and **D**) Bar graph represents fold change of monocyte adherent mean ± SEM from three independent experiments. $*p < 0.05$, $**p < 0.01$, $***p < 0.001$, $****p < 0.0001$ analyzed by one-way ANOVA with a Tukey's multiple comparison test. Data are representative of a minimum of three independent experiments.

that integrin β_4 is not required for surface expression of P-selectin and monocyte capture to ECs in response to HLA I crosslinking. These new findings prompted us to hypothesize that in addition to integrin β_4, HLA I coopts other surface molecules that have the capacity to transduce intracellular signals that elicit P-selectin externalization and monocyte recruitment.

A recent study demonstrated that TLR4 mediates P-selectin externalization in ECs in response to intravascular hemolysis (21) and previous studies indicated that HLA II interacts functionally with TLRs (27, 28), but it was not known whether HLA I interacts physically and functionally with these receptors in ECs. We therefore focused on TLRs as possible mediators of HLA I–induced P-selectin expression and monocyte adhesion to ECs. As a first step to investigate this possibility, we found that ECs express TLR3, TLR4, TLR5, and TLR10. Of significance, TLR4 was the only TLR detected on the EC surface. Consequently, we performed coimmunoprecipitation experiments to examine whether HLA I and TLR4 form a physical complex in these cells. Stimulation of ECs with anti-HLA Ab increased the amount of complex formation between HLA I and TLR4, as shown by Western blot analysis of either HLA I or TLR4 immunoprecipitates. These findings prompted us to determine whether HLA I couples with TLR4 to induce P-selectin externalization, vWF release, and monocyte adhesion to ECs.

We found that siRNA-mediated knockdown of TLR4 inhibited HLA I Ab-stimulated P-selectin expression, vWF release, and monocyte recruitment on ECs, strongly implicating TLR4 in HLA I signal transduction. TLR4 is the only TLR that signals both through MyD88 to induce proinflammatory cytokines and via TRIF to

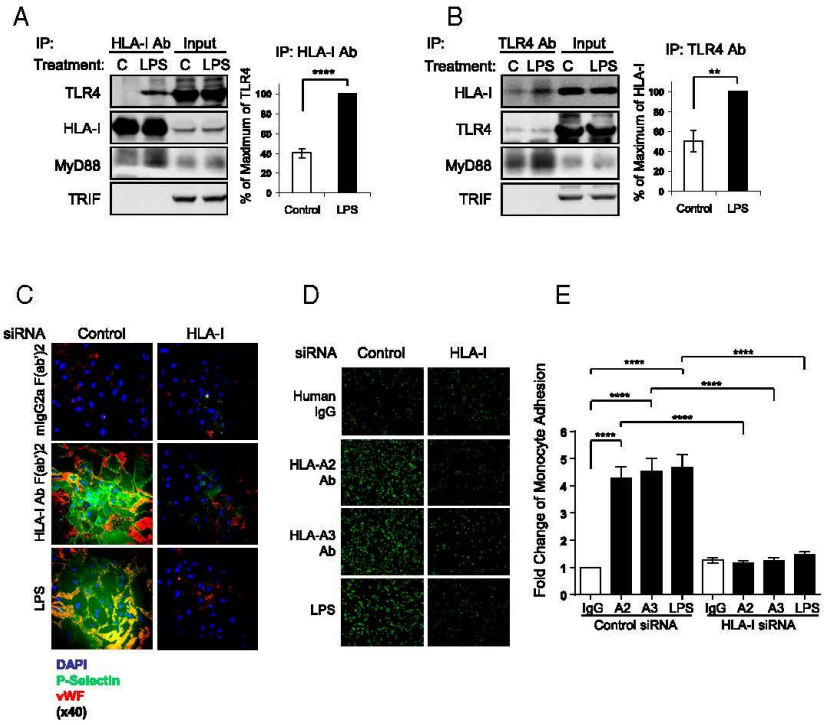

FIGURE 6. An HLA I/TLR4 signaling complex is required to induce LPS-mediated P-selectin. (**A** and **B**) ECs were stimulated with LPS (0.1 μg/ml) for 15 min, and cell lysates were subjected to immunoprecipitation (A) with HLA I pan Ab W6/32 or (B) with TLR4 Ab and analyzed by Western blotting with Abs against the H chain of HLA I (EMR8-5), TLR4, MyD88, or TRIF, as indicated to the left of the blots. For each sample, 5% of the total cell lysate that was used in the immunoprecipitation was loaded as an input control. Protein bands (A) TLR4 and (B) HLA I were quantified by a densitometry scan, and the results are expressed as the mean ± SEM percentage of the maximal extent of protein. $^{**}p < 0.01$, $^{****}p < 0.0001$ analyzed by a Student *t* test. Data are representative of three independent experiments. (**C** and **D**) ECs were transfected with 100 nM HLA I or control siRNA for 48 h. (C) Cells were stimulated with anti–HLA I Ab $F(ab')_2$ fragment, mouse IgG2a $F(ab')_2$ fragment (1 μg/ml), or LPS (0.1 μg/ml) for 30 min. Cells were fixed with freshly prepared 4% PFA, and surface P-selectin was stained on unpermeabilized cells with mouse anti-human P-selectin mAb (mouse IgG1) and rabbit anti-human vWF Ab followed by Alexa Fluor 488 rabbit anti-mouse IgG1, Alexa Fluor 594 goat anti-rabbit IgG (H+L), and DAPI. Six middle fields per dish were image with a Zeiss LSM 880 fluorescence microscope using a ×40 objective lens. Data are representative of three independent experiments. (D) ECs were stimulated anti–HLA-A2, anti–HLA-A3 human mAb (1 μg/ml), or human IgG1 or LPS (0.1 μg/ml) for 30 min. CFSE-labeled primary human monocytes with an FcγR blockade were added to stimulated endothelial monolayers. Adherence of monocytes was measured by a fluorescence microscope using a ×4 objective lens and analyzed with ImageJ software. (**E**) Bar graph represents fold change of monocyte adherent mean ± SEM from at least three independent experiments. $^{**}p < 0.01$, $^{****}p < 0.0001$ analyzed by (A and B) Student *t* test or (E) one-way ANOVA with a Tukey's multiple comparison test. Data are representative of three independent experiments.

induce type I IFN (36). Of significance, TLR4/MyD88 signals from the cell surface, whereas signaling from TLR4/TRIF occurs from endosomes (37). Accordingly, the new signaling complex identified in this study between HLA I and TLR4 signals from the EC surface and contains MyD88. Furthermore, siRNA-mediated knockdown of MyD88 prevented P-selectin surface expression induced by Ab binding to HLA I as effectively as knockdown of TLR4 or treatment with the TLR4 inhibitor TAK242. Our results imply that TLR4 is a novel coreceptor for HLA I to stimulate P-selectin externalization and monocyte capture on activated ECs, although the interaction between anti–class I Ab, HLA-I, and TLR4 may activate additional mechanisms that increase monocyte adhesion that remain to be identified. Taken together with our previous results (12), we propose that in response to Ab binding, HLA I molecules form two separate signaling complexes at the surface of ECs, that is, one with integrin β_4 and another with TLR4/MyD88 to regulate different EC functions of great significance in the pathogenesis of AMR. A corollary of this conclusion is that the TLR4/MyD88 emerges as a new target for therapeutic interventions in the context of AMR.

Our data also reveal that TLR4 and HLA I form a molecular signaling complex in response to bacterial LPS promoting endothelial P-selectin exocytosis and leukocyte recruitment. These results implicate HLA I molecules in the generation of innate immune responses. Consistent with this possibility, associations between MHC molecules and TLRs have been reported to enhance TLR-mediated cellular activation and antimicrobial effector mechanisms. Ab ligation of HLA II on human monocytes induced MyD88 expression followed by NF-κB activation and proinflammatory cytokine production (29). Deficiency in MHC class II expression by macrophages and dendritic cells attenuated the production of proinflammatory cytokines and type I IFN triggered by TLR3, TLR4, or TLR9 signaling (30). Furthermore, coexpression of HLA II molecules and TLR4 enhanced macrophage production of the antimicrobial peptide human β-defensin 2 after treatment with LPS (27). Moreover, bacterial superantigen exotoxins, signaling through HLA II, upregulate

the transcription and membrane expression of TLR4 in human monocytes (31). Further elucidation of molecular interactions between HLA I and TLR4 may well provide new insights into the regulation of inflammatory responses to infectious pathogens in the vasculature.

One of the most intriguing questions raised by the identification of two separate signaling complexes induced by Ab-induced HLA I activation is their functional interaction in the context of AMR. Substantial evidence indicates that surface-expressed P-selectin and ICAM-1 cooperate in promoting monocyte adhesion to the endothelium during their recruitment. Previously, we demonstrated that treatment of ECs with HLA I Ab not only induces P-selectin surface expression but also firm adhesion of monocytes via ICAM-1 (17). These studies revealed that mTOR plays a critical role in promoting ICAM-1–mediated firm monocyte adhesion whereas Ca^{2+} flux stimulates P-selectin externalization. Given the results presented in the current study, we speculate that the two signaling complexes formed by HLA I play a key role in orchestrating the cooperative interaction between P-selectin surface expression and ICAM-1 in monocyte recruitment. Specifically, the HLA I/integrin β_4 complex mediates mTOR-dependent firm monocyte adhesion via ICAM-1 while the HLA I/TLR4 complex identified in this study mediates the P-selection externalization, the first step in monocyte interaction with ECs. Thus, we postulate that the concomitant functions of both HLA I signaling complexes cooperate in inducing monocyte recruitment, a critical event in the inflammatory cascade implicated in AMR.

In conclusion, donor-specific HLA Abs are increasingly recognized to contribute to AMR by binding to HLA molecules on the surface of ECs and triggering intracellular signaling pathways leading to EC activation and leukocyte recruitment, but the molecular mechanisms involved remain incompletely understood. The mechanistic experiments presented in the present study identify, to our knowledge for the first time, TLR4 as novel coreceptor for HLA I to upregulate rapid P-selectin surface expression and stimulate monocyte recruitment on activated ECs. Taken together with our previous studies, we propose that HLA I molecules form two separate physical complexes at the EC surface, that is, with either integrin β_4 or TLR4, thereby mediating an array of signaling pathways leading to EC activation. We postulate that the concomitant functions of both signaling complexes formed by HLA I in ECs cooperate in inducing monocyte recruitment, a critical event in the inflammatory cascade implicated in AMR. A corollary of this conclusion is that the novel HLA I/TLR4/MyD88 signaling axis in ECs emerges as a new target for therapeutic intervention to prevent monocyte recruitment to the graft and prevent AMR.

Acknowledgments

We thank Timothy J. Thauland from Dr. Manish Butte's laboratory (Department of Pediatrics), James Sinnett-Smith from Dr. Enrique Rozengurt's laboratory (Department of Medicine), Jing Zhang from Dr. Yuan Zhai's laboratory, and Hirofumi Hirao from Dr. Jerzy W. Kupiec-Weglinski's laboratory (Department of Surgery), David Geffen School of Medicine, University of California, Los Angeles, for assistance in fluorescence microscopy.

Disclosures

The authors have no financial conflicts of interest.

References

1. Hart, A., D. Singh, S. J. Brown, J. H. Wang, and B. L. Kasiske. 2021. Incidence, risk factors, treatment, and consequences of antibody-mediated kidney transplant rejection: a systematic review. *Clin. Transplant.* 35: e14320.
2. Reed, E. F., A. J. Demetris, E. Hammond, S. Itescu, J. A. Kobashigawa, N. L. Reinsmoen, E. R. Rodriguez, M. Rose, S. Stewart, N. Suciu-Foca, et al.; International Society for Heart and Lung Transplantation. 2006. Acute antibody-mediated rejection of cardiac transplants. *J. Heart Lung Transplant.* 25: 153–159.
3. Singh, N., J. Pirsch, and M. Samaniego. 2009. Antibody-mediated rejection: treatment alternatives and outcomes. *Transplant. Rev. (Orlando)* 23: 34–46.
4. Merola, J., D. D. Jane-Wit, and J. S. Pober. 2017. Recent advances in allograft vasculopathy. *Curr. Opin. Organ Transplant.* 22: 1–7.
5. Terasaki, P. I., and M. Ozawa. 2004. Predicting kidney graft failure by HLA antibodies: a prospective trial. *Am. J. Transplant.* 4: 438–443.
6. Wang, M., N. J. Patel, X. Zhang, E. P. Kransdorf, B. Azarbal, M. M. Kittleson, L. S. C. Czer, J. A. Kobashigawa, and J. K. Patel. 2021. The effects of donor-specific antibody characteristics on cardiac allograft vasculopathy. *Clin. Transplant.* 35: e14483.
7. Jin, Y. P., M. C. Fishbein, J. W. Said, P. T. Jindra, R. Rajalingam, E. Rozengurt, and E. F. Reed. 2004. Anti-HLA class I antibody-mediated activation of the PI3K/Akt signaling pathway and induction of Bcl-2 and Bcl-xL expression in endothelial cells. *Hum. Immunol.* 65: 291–302.
8. Jin, Y. P., Y. Korin, X. Zhang, P. T. Jindra, E. Rozengurt, and E. F. Reed. 2007. RNA interference elucidates the role of focal adhesion kinase in HLA class I-mediated focal adhesion complex formation and proliferation in human endothelial cells. *J. Immunol.* 178: 7911–7922.
9. Jin, Y. P., R. P. Singh, Z. Y. Du, A. K. Rajasekaran, E. Rozengurt, and E. F. Reed. 2002. Ligation of HLA class I molecules on endothelial cells induces phosphorylation of Src, paxillin, and focal adhesion kinase in an actin-dependent manner. *J. Immunol.* 168: 5415–5423.
10. Jin, Y. P., N. M. Valenzuela, M. E. Ziegler, E. Rozengurt, and E. F. Reed. 2014. Everolimus inhibits anti-HLA I antibody-mediated endothelial cell signaling, migration and proliferation more potently than sirolimus. *Am. J. Transplant.* 14: 806–819.
11. Jindra, P. T., Y. P. Jin, E. Rozengurt, and E. F. Reed. 2008. HLA class I antibody-mediated endothelial cell proliferation via the mTOR pathway. *J. Immunol.* 180: 2357–2366.
12. Zhang, X., E. Rozengurt, and E. F. Reed. 2010. HLA class I molecules partner with integrin β_4 to stimulate endothelial cell proliferation and migration. *Sci. Signal.* 3: ra85.
13. Cleator, J. H., W. Q. Zhu, D. E. Vaughan, and H. E. Hamm. 2006. Differential regulation of endothelial exocytosis of P-selectin and von Willebrand factor by protease-activated receptors and cAMP. *Blood* 107: 2736–2744.
14. Naß, J., J. Terglane, and V. Gerke. 2021. Weibel Palade bodies: unique secretory organelles of endothelial cells that control blood vessel homeostasis. *Front. Cell Dev. Biol.* 9: 813995.
15. Valenzuela, N. M., and E. F. Reed. 2017. Antibody-mediated rejection across solid organ transplants: manifestations, mechanisms, and therapies. *J. Clin. Invest.* 127: 2492–2504.
16. Denis, C. V., P. André, S. Saffaripour, and D. D. Wagner. 2001. Defect in regulated secretion of P-selectin affects leukocyte recruitment in von Willebrand factor-deficient mice. *Proc. Natl. Acad. Sci. USA* 98: 4072–4077.
17. Salehi, S., R. A. Sosa, Y. P. Jin, S. Kageyama, M. C. Fishbein, E. Rozengurt, J. W. Kupiec-Weglinski, and E. F. Reed. 2018. Outside-in HLA class I signaling regulates ICAM-1 clustering and endothelial cell-monocyte interactions via mTOR in transplant antibody-mediated rejection. *Am. J. Transplant.* 18: 1096–1109.
18. Valenzuela, N. M., A. Mulder, and E. F. Reed. 2013. HLA class I antibodies trigger increased adherence of monocytes to endothelial cells by eliciting an increase in endothelial P-selectin and, depending on subclass, by engaging FcγRs. *J. Immunol.* 190: 6635–6650.
19. Valenzuela, N. M., and E. F. Reed. 2013. Antibodies in transplantation: the effects of HLA and non-HLA antibody binding and mechanisms of injury. *Methods Mol. Biol.* 1034: 41–70.
20. Belcher, J. D., C. Chen, J. Nguyen, L. Milbauer, F. Abdulla, A. I. Alayash, A. Smith, K. A. Nath, R. P. Hebbel, and G. M. Vercellotti. 2014. Heme triggers TLR4 signaling leading to endothelial cell activation and vaso-occlusion in murine sickle cell disease. *Blood* 123: 377–390.
21. Merle, N. S., R. Paule, J. Leon, M. Daugan, T. Robe-Rybkine, V. Poillerat, C. Torset, V. Frémeaux-Bacchi, J. D. Dimitrov, and L. T. Roumenina. 2019. P-selectin drives complement attack on endothelium during intravascular hemolysis in TLR-4/heme-dependent manner. *Proc. Natl. Acad. Sci. USA* 116: 6280–6285.
22. Parham, P., C. J. Barnstable, and W. F. Bodmer. 1979. Use of a monoclonal antibody (W6/32) in structural studies of HLA-A,B,C, antigens. *J. Immunol.* 123: 342–349.
23. Erl, W., C. Weber, C. Wardemann, and P. C. Weber. 1995. Adhesion properties of Mono Mac 6, a monocytic cell line with characteristics of mature human monocytes. *Atherosclerosis* 113: 99–107.
24. Erl, W., P. C. Weber, and C. Weber. 1998. Monocytic cell adhesion to endothelial cells stimulated by oxidized low density lipoprotein is mediated by distinct endothelial ligands. *Atherosclerosis* 136: 297–303.
25. Valenzuela, N. M., L. Hong, X. D. Shen, F. Gao, S. H. Young, E. Rozengurt, J. W. Kupiec-Weglinski, M. C. Fishbein, and E. F. Reed. 2013. Blockade of P-selectin is sufficient to reduce MHC I antibody-elicited monocyte recruitment in vitro and in vivo. *Am. J. Transplant.* 13: 299–311.
26. Valenzuela, N. M., K. R. Trinh, A. Mulder, S. L. Morrison, and E. F. Reed. 2015. Monocyte recruitment by HLA IgG-activated endothelium: the relationship between IgG subclass and FcγRIIa polymorphisms. *Am. J. Transplant.* 15: 1502–1518.
27. Frei, R., J. Steinle, T. Birchler, S. Loeliger, C. Roduit, D. Steinhoff, R. Seibl, K. Büchner, R. Seger, W. Reith, and R. P. Lauener. 2010. MHC class II molecules enhance Toll-like receptor mediated innate immune responses. *PLoS One* 5: e8808.
28. Shio, M. T., G. S. Hassan, W. A. Shah, A. Nadiri, Y. El Fakhry, H. Li, and W. Mourad. 2014. Coexpression of TLR2 or TLR4 with HLA-DR potentiates the

superantigenic activities of *Mycoplasma* arthritidis-derived mitogen. *J. Immunol.* 192: 2543–2550.
29. Kissner, T. L., G. Ruthel, S. Alam, R. G. Ulrich, S. Fernandez, and K. U. Saikh. 2011. Activation of MyD88 signaling upon staphylococcal enterotoxin binding to MHC class II molecules. *PLoS One* 6: e15985.
30. Liu, X., Z. Zhan, D. Li, L. Xu, F. Ma, P. Zhang, H. Yao, and X. Cao. 2011. Intracellular MHC class II molecules promote TLR-triggered innate immune responses by maintaining activation of the kinase Btk. *Nat. Immunol.* 12: 416–424.
31. Sinha-Datta, U., I. Horikawa, E. Michishita, A. Datta, J. C. Sigler-Nicot, M. Brown, M. Kazanji, J. C. Barrett, and C. Nicot. 2004. Transcriptional activation of hTERT through the NF-kappaB pathway in HTLV-I-transformed cells. *Blood* 104: 2523–2531.
32. Bovijn, C., A. S. Desmet, I. Uyttendaele, T. Van Acker, J. Tavernier, and F. Peelman. 2013. Identification of binding sites for myeloid differentiation primary response gene 88 (MyD88) and Toll-like receptor 4 in MyD88 adapter-like (Mal). *J. Biol. Chem.* 288: 12054–12066.
33. Sampaio, N. G., M. Kocan, L. Schofield, K. D. G. Pfleger, and E. M. Eriksson. 2018. Investigation of interactions between TLR2, MyD88 and TIRAP by bioluminescence resonance energy transfer is hampered by artefacts of protein overexpression. *PLoS One* 13: e0202408.
34. Matsunaga, N., N. Tsuchimori, T. Matsumoto, and M. Ii. 2011. TAK-242 (resatorvid), a small-molecule inhibitor of Toll-like receptor (TLR) 4 signaling, binds selectively to TLR4 and interferes with interactions between TLR4 and its adaptor molecules. *Mol. Pharmacol.* 79: 34–41.
35. Yamakuchi, M., N. C. Kirkiles-Smith, M. Ferlito, S. J. Cameron, C. Bao, K. Fox-Talbot, B. A. Wasowska, W. M. Baldwin III, J. S. Pober, and C. J. Lowenstein. 2007. Antibody to human leukocyte antigen triggers endothelial exocytosis. *Proc. Natl. Acad. Sci. USA* 104: 1301–1306.
36. Yamamoto, M., S. Sato, H. Hemmi, K. Hoshino, T. Kaisho, H. Sanjo, O. Takeuchi, M. Sugiyama, M. Okabe, K. Takeda, and S. Akira. 2003. Role of adaptor TRIF in the MyD88-independent Toll-like receptor signaling pathway. *Science* 301: 640–643.
37. Kagan, J. C., T. Su, T. Horng, A. Chow, S. Akira, and R. Medzhitov. 2008. TRAM couples endocytosis of Toll-like receptor 4 to the induction of interferon-β. *Nat. Immunol.* 9: 361–368.

Chapter 3 – Antibody-induced Vascular Inflammation Skews Infiltrating Macrophages to a Novel Remodeling Phenotype in a Model of Transplant Rejection

Received: 4 December 2019 | Revised: 15 March 2020 | Accepted: 7 April 2020

DOI: 10.1111/ajt.15934

ORIGINAL ARTICLE

AJT

Antibody-induced vascular inflammation skews infiltrating macrophages to a novel remodeling phenotype in a model of transplant rejection

Xuedong Wei[1,2] | Nicole M. Valenzuela[1] | Maura Rossetti[1] | Rebecca A. Sosa[1] | Jessica Nevarez-Mejia[1] | Gregory A. Fishbein[1] | Arend Mulder[3] | Jayeeta Dhar[4] | Karen S. Keslar[4] | William M. Baldwin III[4] | Robert L. Fairchild[4] | Jianquan Hou[2] | Elaine F. Reed[1]

[1]Department of Pathology and Laboratory Medicine, David Geffen School of Medicine, University of California, Los Angeles, California

[2]Department of Urology, The First Affiliated Hospital of Soochow University, Suzhou, Jiangsu, China

[3]Department of Immunohaematology and Bloodtransfusion, Leiden University Medical Center, Leiden, Netherlands

[4]Lerner Research Institute and Transplant Center, Department of Pathology, Case Western Reserve University School of Medicine, Cleveland Clinic, Cleveland, Ohio

Correspondence
Elaine F. Reed
Email: ereed@mednet.ucla.edu

Funding information
National Institute of Allergy and Infectious Diseases, Grant/Award Number: U19AI128913, PO1AI120944, RO1AI042819, RO1AI135201 and U01AI124319; Jiangsu Provincial Medical Youth Talent, Grant/Award Number: QNRC2016739; Science and Technology Development Program of Suzhou, Grant/Award Number: SYS201601, CXTDB2017009 and GSWS2019033; Jiangsu Provincial Key Medical Discipline, Grant/Award Number: ZDXKA2016012; CTOT NanoString Core, Grant/Award Number: UO1 AI063594

HLA donor-specific antibodies (DSAs) binding to vascular endothelial cells of the allograft trigger inflammation, vessel injury, and antibody-mediated rejection (AMR). Accumulation of intragraft-recipient macrophages is a histological characteristic of AMR, which portends worse outcome. HLA class I (HLA I) DSAs enhance monocyte recruitment by activating endothelial cells and engaging FcγRs, but the DSA-activated donor endothelial influence on macrophage differentiation is unknown. In this study, we explored the consequence of DSA-activated endothelium on infiltrating monocyte differentiation. Here we show that cardiac allografts from murine recipients treated with MHC I DSA upregulated genes related to monocyte transmigration and Fc receptor stimulation. Human monocytes co-cultured with HLA I IgG-stimulated primary human endothelium promoted monocyte differentiation into $CD68^{+}CD206^{+}CD163^{+}$macrophages (M(HLA I IgG)), whereas HLA I $F(ab')_2$ stimulated endothelium solely induced higher CD206 (M(HLA I $F(ab')_2$)). Both macrophage subtypes exhibited significant changes in discrete cytokines/chemokines and unique gene expression profiles. Cross-comparison of gene transcripts between murine DSA-treated cardiac allografts and human co-cultured macrophages identified overlapping genes. These findings uncover the role of HLA I DSA-activated endothelium in monocyte differentiation, and point to a novel, remodeling phenotype of infiltrating macrophages that may contribute to vascular injury.

KEYWORDS

alloantibody, animal models: murine, basic (laboratory) research/science, immunobiology, macrophage/monocyte biology: differentiation/maturation, rejection: antibody-mediated (AMR), translational research/science, vascular biology

Abbreviations: Ab, antibody; AMR, antibody-mediated rejection; DSA, donor-specific antibody; EC, endothelial cell; M(HLA I $F(ab')_2$), macrophages differentiated by endothelium activated with HLA IgG $F(ab')_2$ fragment; M(HLA IgG), macrophages differentiated by endothelium activated with intact HLA IgG; TV, transplant vasculopathy.

1 | INTRODUCTION

In antibody-mediated autoimmune and inflammatory vascular diseases, antibodies binding to lumenal endothelial cells (ECs) trigger inflammatory signaling, thereby contributing to autoimmune vasculitis,[1-3] atherosclerosis,[4,5] and rejection of solid organ transplants. The production of MHC/HLA donor-specific antibodies (DSAs) after transplantation of kidney, heart, liver, and lung allografts occurs in up to 50% of patients by 10 years.[6,7] DSAs mediate acute and chronic antibody-mediated rejection (AMR) and are associated with lower long-term graft survival.[8] AMR manifests as endothelial injury and vascular inflammation, consisting predominantly of macrophages[9] and evidence of complement deposition in the vessels of the graft.[10] Chronic exposure of the allograft to DSAs and repeated injury can culminate in transplant vasculopathy (TV), which is a leading cause of allograft loss and patient death.[11-14]

Anti-EC antibodies contribute to vascular inflammation by activating endothelium directly, and through FcγR engagement on effector immune cells.[3] The binding of HLA I antibodies to donor endothelium also causes injury by multiple concurrent mechanisms, including Fc-independent agonistic HLA signaling[15,16] and IgG Fc-dependent activation of the classical complement cascade and recruitment of leukocyte effector cells.[17-20] Antibody ligation of HLA I triggers Weibel Palade Body (WPB) exocytosis and induces P-selectin expression, which in turn promotes recipient platelet, monocyte, NK cell, and neutrophil capture and infiltration into the graft.[18,21] P-selectin–induced monocyte tethering is further enhanced through secondary interactions between the Fc portion of IgG and Fcγ receptors (FcγRs) on myeloid and lymphoid cells,[17-19] promoting Mac-1–mediated ,firm adhesion to intercellular adhesion molecule 1 (ICAM-1) on ECs. These in vitro findings are supported by clinical and experimental evidence that allografts undergoing AMR exhibit characteristic macrophage infiltrates that promote graft injury and graft dysfunction.[16,18,22] Collectively, these data support the critical role for macrophages in the pathogenicity of AMR.

Macrophages mature into heterogeneous subtypes with distinct effector functions, and they play important roles in tissue homeostasis, host defense to pathogens, and disease pathogenesis.[23,24] The effector functions of macrophages develop after transendothelial cell migration into the tissue and interaction with activating stimuli such as cytokines, chemokines, growth factors, immunoglobulin Fcγ receptors, and Toll-like receptor (TLR) agonists.[24,25] Macrophages are associated with both rejection and allograft fibrosis. M1-like macrophages were described to promote acute cellular rejection,[26,27] whereas the M2-like subtype may dampen alloimmune responses and contribute to tissue repair, remodeling, and chronic rejection.[28-31] Although macrophages are the principal component of AMR lesions, no studies have attempted to define their functional and phenotypic characteristics, especially in the context of HLA DSAs.

In the current study, we sought to understand if antibody-stimulated endothelium could induce monocyte differentiation toward a specialized macrophage phenotype. Using a mouse model of acute AMR and an in vitro transwell co-culture model with human primary cells, we identified two novel macrophage subtypes: one polarized through direct contact with HLA I antibody-activated endothelium: M(HLA I $F(ab')_2$)—with increased $CD68^+CD206^+$ expression; and M(HLA I IgG) receiving a second activating signal via FcγR engagement that prompted an increase in $CD163^+$ expression. This work dissects the Fc-independent and Fc-dependent effects of endothelium and HLA DSAs on macrophage differentiation, processes that are relevant to both acute and chronic AMR.

2 | MATERIALS AND METHODS

2.1 | Murine cardiac allografts

B10.A (H-2^a) hearts (K^k, D^d, L^d, IE^k, IA^k) were transplanted heterotopically to immunodeficient C57BL/6 (B6 $Rag1^{-/-}$; H-2^b) mice as described previously.[32] One week postoperatively, a mixture of IgG1 (AF3–12.1.3), IgG2a (16.1.2N), and IgG2b (15.1.5P) antibodies to H-2^a (BioXCell, West Lebanon, NH) was transferred intraperitoneally at a dose of 100 mg for each antibody. Control animals received the same dose of isotype control antibodies (MOPC-21, C1.18, and MPC-11; BioXCell). Antibody injections were administered 4 times on alternate days, and the mice were euthanized 1 hour after the fourth injection.

2.2 | Immunohistochemistry and nanostring for cardiac allografts

Samples containing full cross-sections through the cardiac grafts were immediately fixed in acid methanol and processed for immunohistochemistry as detailed in Data S1. RNA was isolated from homogenates of 3 experimental and 3 control allografts for gene expression measurements by NanoString. RNA was hybridized to the Mouse PanCancer Immune Profiling Panel supplemented with 10 genes.

2.3 | HLA antibodies

mAbs against HLA-A2 and A3 were derived from human hybridomas.[33] $F(ab')_2$ fragments of mAbs were generated using Ides/FABricator.[19] Anti-CD105 was from Millipore. Isotype control was from Sigma-Aldrich.

2.4 | Cells and culture

Primary human ECs were isolated from aortic rings as described previously.[15,19] Human primary monocytes were isolated from healthy donors as reported previously[17] and detailed in Data S1. Methods for monocyte–endothelial cell co-culture are provided in the Data S1.

2.5 | Flow cytometric analysis of macrophage subtypes

Macrophage phenotypes were assessed by flow cytometry using the fluorochrome-labeled antibodies described in the Supplement, acquired on an LSRFortessa (BD Biosciences), and the data were analyzed using FlowJo version 10 (Figure S6).

2.6 | Cytokine/chemokine detection by multiplex assay

Cytokine/chemokine measurements were performed using human 38-plex kits (Millipore, HCYTMAG-60K-PX38) and analyzed on a Luminex 200 instrument as detailed in the Data S1.[34]

2.7 | Gene expression analysis of human macrophages

RNA expression of 594 genes was measured using the nCounter Human Immunology v2 panel (Data S1).

2.8 | In vitro *macrophage and dendritic cell differentiation*

In vitro induction of polarized macrophages and dendritic cells from human monocytes was performed as described previously (Data S1).[35-39]

2.9 | Statistical analysis

Data are shown by box and whisker graphs with a range of min to max and all plots, or presented as mean ± SEM or mean ± SD. Statistical differences between groups were determined using paired *t* tests or repeated-measures 1-way ANOVA followed by multiple correction (Dunnett, Sidak, or Fisher least significant differences (LSD) as recommended by the GraphPad Prism software). $P < .05$ was considered statistically significant. For hierarchical clustering, individual genes or cytokines were normalized by Z-score, and then euclidean distance with average linkage was used. Analyses were performed in R or nSolver Analysis Software 3.0 (nanoString Technologies).

3 | RESULTS

3.1 | DSA induces acute endothelial and macrophage responses in cardiac allografts

To test the effects of DSAs on cardiac allografts in the absence of T cells, we transplanted B10.A ($H\text{-}2^a$) hearts to immunodeficient C57BL/6 (B6 $Rag1^{-/-}$; $H\text{-}2^b$) mice. A week after transplantation when perioperative inflammation had subsided, a mixture of IgG1, -2a, and -2b monoclonal antibodies to $H\text{-}2^a$ was injected intraperitoneally. Control mice received isotype matched control IgG. The antibody injections were administered 4 times on alternate days, and the mice were euthanized 1 hour after the fourth injection. Immunohistology confirmed that DSAs induced features characteristic of acute antibody-mediated rejection, including diffuse C4d deposition on capillary endothelium and increased numbers of intravascular and perivascular macrophages (Figure 1). Antibody-induced injury was manifested by capillary dilatation and endothelial cell swelling (Figure 1, insets). Macrophage activation was indicated by more stellate morphology in grafts from DSA-treated recipients compared to the quiescent fusiform macrophages in control grafts.

3.2 | DSAs upregulate gene expression, indicative of monocyte stimulation by Fc receptors and transmigration through activated endothelium

DSA-induced changes in gene expression in cardiac allograft tissue identified 27 differentially expressed genes (DEGs) between DSA-treated and isotype-treated recipient allografts at a $P < .1$ significance level ($n = 3$). All DEGs had increased expression in DSA-treated recipient allografts compared to isotype control allografts. Nine of the top 10 upregulated genes were related to monocyte and macrophage function (Table 1; Table S1). Six of these genes code for chemotactic proteins (*CXCL1*, *CCL2*, *CCL7*, and *CCL12*) or receptors (*CX3CR1* and *GPR183*). Two of the monocyte chemotactic proteins (CCL2/MCP-1 and CCL7/MCP-3) have been implicated in transmigration of human monocytes through activated ECs in vitro.[40] In addition, production of MCP-1 and CXCL1 (KC) were found to be increased when macrophages bind to DSAs on ECs in vitro.[41] These findings prompted us to investigate in detail the DSA-induced transmigration of human monocytes, by employing an in vitro model with human primary monocytes and ECs.

3.3 | HLA I antibody–activated ECs promote the differentiation of human peripheral blood monocytes into $CD68^+CD206^+CD163^+$ macrophages through Fc-dependent and Fc-independent mechanisms

Because the in vivo findings indicated that DSA induces genes implicated in Fcγ receptor activation of monocytes and transmigration of monocytes, we tested whether HLA I antibody binding to ECs altered the function of interacting human peripheral blood monocytes. To mimic the process of monocyte transendothelial cell extravasation into the allograft during AMR, we developed an in vitro EC-monocyte co-culture system in which monocytes adhere to HLA I antibody-activated ECs, transmigrate, and are then allowed to differentiate into macrophages over a period of 5 days (Figure 2A). To determine

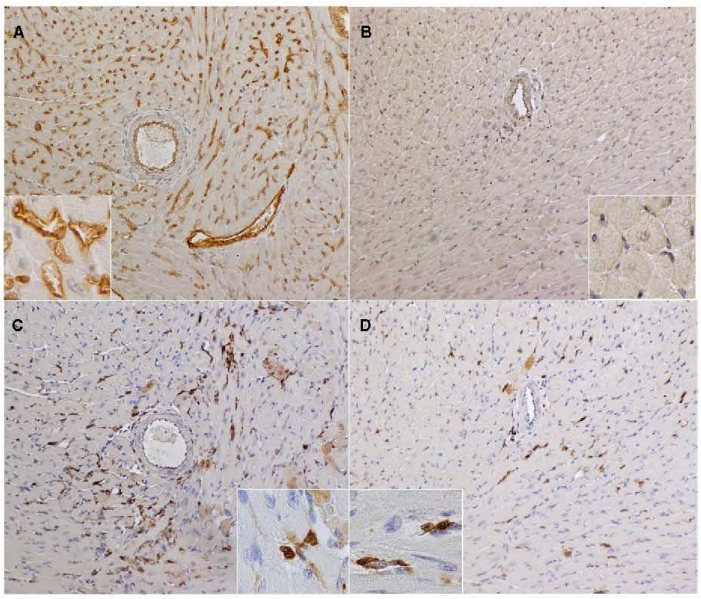

FIGURE 1 Immunohistology for C4d and Mac 2. C4d deposits are diffuse in capillaries, arteries, and veins of graft from DSA-treated mouse (A), but no C4d was detected in graft from isotype control–treated mouse (B). Higher magnification demonstrates that capillaries with C4d deposits are dilated and ECs are swollen (inset A). Mac2+ macrophages are more numerous in the graft from DSA-treated mouse (C) than in graft from isotype control–treated mouse (D). Higher magnification demonstrates qualitative differences in Mac2 staining of intra- and pericapillary macrophages (insets of C and D)

the effect of HLA I antibody–activated endothelium on macrophage polarization, ECs were pretreated with HLA I IgG before the addition of purified monocytes. Both intact and the $F(ab')_2$ fragment of HLA I IgG stimulation significantly increased the numbers of transmigrated cells compared to untreated and hIgG-treated ECs (Figure 2B; Figure S1). Expression of CD68, CD206, and CD163 on the transmigrated macrophages was significantly increased after co-culture with HLA I IgG–activated ECs, but not on those co-cultured with irrelevant human IgG-pretreated ECs (Figure 3A; Figure S2). There was no significant difference in expression of CD64, CD86, or CD1a. Given that CD68 is a pan-macrophage marker, these data suggest that the HLA I IgG–activated ECs increased monocyte transmigration and induced their differentiation. Activation of endothelium with tumor necrosis factor α (TNF-α), a pro-inflammatory stimulus, increased the expression of CD206, but not CD163 and CD68 (Figure 3A). To address the role of the Fc region in monocyte differentiation, we stimulated ECs with an HLA I $F(ab')_2$. There was no difference in CD206 expression between macrophages induced by intact HLA I IgG vs $F(ab')_2$ (Figure 3A; Figure S2). However, CD163 was significantly lower on M(HLA I $F(ab')_2$) (Figure 3A; Figure S2), implying that CD163 expression relies on the monocyte FcγR engagement by HLA I IgG Fc region, whereas CD206 does not.

We found previously that antibody crosslinking of HLA I was sufficient to increase adhesion of monocytes in a P-selectin–dependent manner. To determine if monocyte differentiation was specifically induced by HLA I antibody–mediated EC activation, or required FcγRs, we co-cultured monocytes with anti-CD105 mIgG2a–stimulated ECs. Anti-CD105 mIgG2a binds to endoglin on EC surface and to FcγRs on human monocytes,[42] but does not trigger EC exocytosis.[17] Control CD105 mIgG2a–treated ECs did not increase the expression of either CD206 or CD163 on monocytes compared to untreated ECs (Figure 3B), indicating that M(HLA I IgG) differentiation is dependent on the HLA I antibody–induced EC activation, even in the presence of Fc-FcγR ligation.

3.4 | HLA I antibody–activated ECs increased cytokine/chemokine production by M(HLA I IgG)

To investigate the functional capacity of M(HLA I IgG), we collected co-culture supernatants on day 4 and examined the production of 38 cytokines and chemokines. Eight analytes were detected above the lower limit of quantitation (LLOQ). Cytokines/chemokines clustered into 3 main groups: control, HLA I antibody, and TNF-α stimulated (Figure 4A). ECs alone, monocytes alone or untreated/IgG-treated co-cultures produced few detectable cytokines and chemokines. In contrast, HLA I antibody (intact IgG and $F(ab')_2$ and TNF-α treatment induced high expression of cytokines and chemokines in EC monocyte co-cultures. IL-6, IL-8/CXCL8, IL-10, MIP-1β/CCL4, and GROα/CXCL1 were significantly increased in HLA I IgG–stimulated co-cultures compared to untreated and isotype control–treated co-cultures (Figure 4B), whereas the differences in MDC/CCL22 and MIP-1β/CCL4 were not significant. There was no difference between M(HLA I IgG) and M(HLA I $F(ab')_2$) co-cultures, except for a trend toward increased IL-10 in M(HLA I IgG) compared to M(HLA I $F(ab')_2$) co-cultures ($P = .1801$) (Figure 4B).

We did not observe changes in cytokine production from HLA antibody–stimulated endothelium alone (Figure 4A,B), whereas

TABLE 1 The 27 differentially expressed genes (DEGs) in DSA- vs isotype-treated cardiac allografts

Gene symbol	*P*	FC
Complement related		
CD55	.007	1.5
C7	.071	2.6
C1S1	.097	1.4
Costimulatory molecules		
CD79B	.063	1.4
Immune/cellular response		
IL1RN	.002	2.2
GPR183	.034	2.0
PTGS2	.073	2.6
CD200	.073	1.4
CD9	.093	1.6
TMEM173	.097	1.5
ITGA2B	.099	17.3
LRP1	.075	1.2
Phagocytosis		
CLEC5A	.091	1.5
Adhesion molecules		
EMR1	.063	1.6
SELE	.073	3.6
Signaling and transcription factors		
TBP	.05	1.2
FOS	.056	1.6
POU2F2	.08	1.4
EGR2	.067	2.4
Chemokines/cytokines		
CCL7	.0118	3.2
CXCL1	.041	1.6
CCL12	.052	1.7
CX3CR1	.056	1.7
CCL2	.06	3.7
PPBP	.076	17.0
CSF1	.09	1.3
CXCL14	.09	1.4

Note: Data analyzed by Student *t* test of gene expression counts ($P < .1$) between HLA I DSA–treated mice allograft recipients and isotype-treated controls (n = 3). GPR183 (EBI2) expressed on macrophages leads to calcium mobilization and to directed cell migration. FOS (cFos) suppresses the expression of inducible nitric oxide synthase (iNOS) and pro-inflammatory cytokines.
Abbreviation: FC, fold change.

positive control TNF-α induced the secretion of numerous cytokines and chemokines as expected (Figure S3). These results indicate that interaction of activated macrophages with HLA I antibody–activated endothelium is necessary to induce cytokine/chemokine production.

3.5 | Co-culture with HLA I antibody–stimulated ECs dramatically changes the macrophage transcriptional profile

To further explore macrophage functional changes induced by ECs stimulated with intact and $F(ab')_2$ HLA antibody, we analyzed gene expression in transmigrated monocytes after 5 days using Nanostring Human Immunology Panel. The volcano plots (Figure 5A) compare gene expression among M(EC), M(HLA I IgG), and M(HLA I $F(ab')_2$. Compared to M(EC), 43 genes were differentially expressed (38 increased and 5 decreased) in M(HLA I IgG) and 13 DEGs (11 increased, 2 decreased) in M(HLA I $F(ab')_2$). Eleven genes increased in both M(HLA I IgG) and M(HLA I $F(ab')_2$) compared with M(EC) (Table 2). In addition, 14 genes were differentially expressed comparing M(HLA I IgG) to M(HLA I $F(ab')_2$), suggesting that the Fc component of HLA antibody promotes additional gene expression. As a result, a total of 53 DEGs from the 3 comparisons were identified (Table 2; Table S2).

Unsupervised hierarchical clustering of the expression patterns of the 53 DEGs (Figure 5B; Figure S4) revealed 3 groups. Compared to M(EC), 5 genes in group 1 DEGs were downregulated in both M(HLA I IgG) and M(HLA I $F(ab')_2$), whereas 36 group 3 DEGs were upregulated in both conditions. Twelve group 2 DEGs were upregulated in M(HLA I IgG), but downregulated in M(HLA I $F(ab')_2$).

These DEGs encode complement-related, costimulatory, immune/cellular response, phagocytosis, adhesion, signaling and transcription factors, chemokines/cytokines, and growth and differentiation related molecules (Table 2). Compared to M(EC), most of these DEGs were significantly increased in M(HLA I IgG) (Table 2; Figure S4), such as: *C1QA*, *C1QB*, *CD59*, *SERPING1*, *CTSC*, *CR1*, *JAK3*, *MAF*, *S1PR1*, and *TNFAIP3*. Compared to M(HLA I IgG), complement-related *(C1QA*, *C1QB*, *C2)*, costimulatory *(CD83)*, adhesion *(ICAM4)*, signaling and transcription factors *(EGR1*, *EGR2*, *MAF*, *SOCS3*, *TNFAIP3)*, and chemokines/cytokines genes (eotaxin-2/*CCL24*, *MIP-1α/CCL3*, *MIP-1β/CCL4*, *CCRL2*, *GROα/CXCL1*) were lower than in M(HLA $F(ab')_2$). Chemokines/cytokines genes *MIP-1α/CCL3*, *MIP-1β/CCL4*, *GROα/CXCL1*, and *IL1B* were decreased in M(HLA I $F(ab')_2$) compared to the untreated M(EC) (Table 1; Figure S4). These data suggest that, compared to HLA I $F(ab')_2$, HLA I IgG induces a broader spectrum of immunological functions in macrophages.[38,43]

3.6 | M(HLA I IgG) is a novel macrophage subset with distinct features compared to classically polarized macrophages

To understand whether HLA I antibody–activated ECs poise transmigrated monocytes to unique, not-yet-described macrophage phenotypes, we generated cytokine-polarized control macrophage subsets to compare with M(HLA I IgG) and M(HLA I $F(ab')_2$). Consistent with previous studies,[44-46] M(IFN-γ) were $CD64^{hi}CD14^{lo}CD206^{lo}CD163^{lo}$; M(IL-4) were

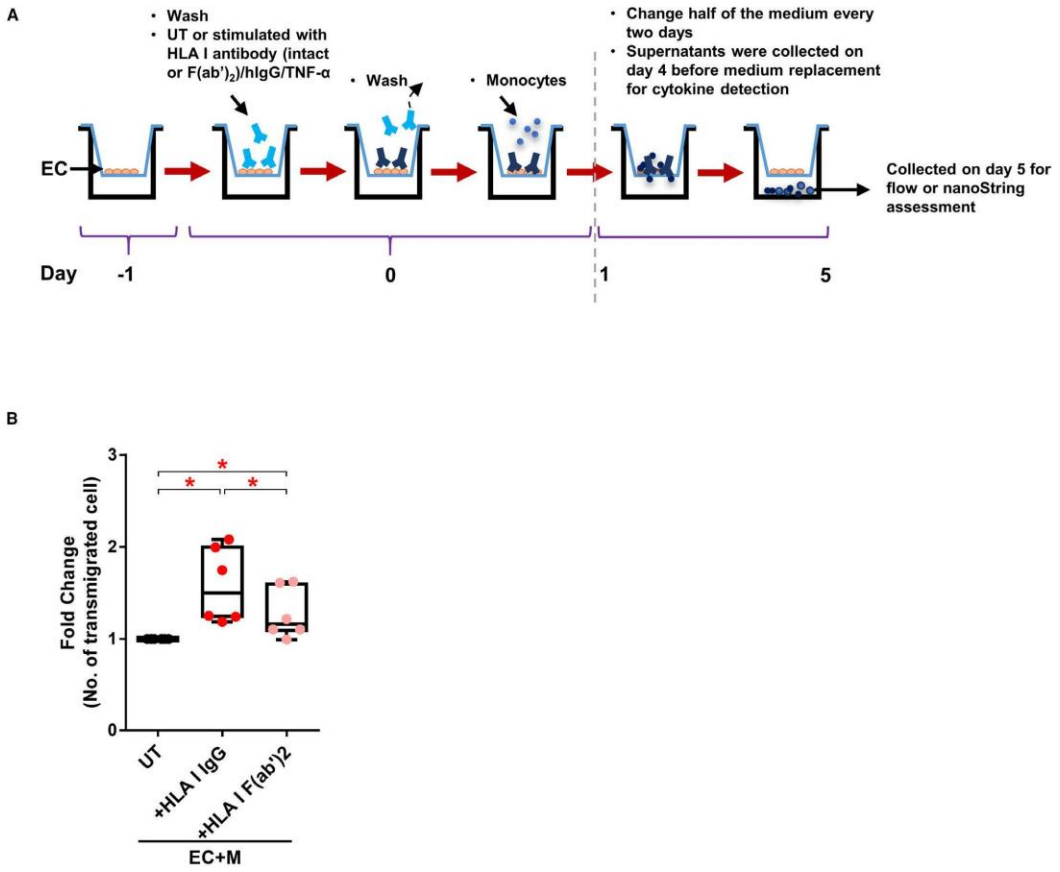

FIGURE 2 HLA I IgG stimulation increased the transmigration of human monocytes. A, ECs were seeded in the upper chamber on day −1 and grown to a confluent monolayer. On day 0, the ECs were washed and starved for 4 h, and then left unstimulated (UT) or stimulated with 1 μg/mL HLA I antibody (intact or $F(ab')_2$) or hIgG for an additional hour. For TNF-α stimulation, 10 ng/mL TNF-α was added at the beginning of the EC starvation. The unbound antibodies and TNF-α were extensively washed away before adding the monocytes. The cells were co-cultured for 5 d before phenotype or gene expression assessments. During the co-culture, half of the medium was replaced every 2 d, before which the supernatants were collected for cytokine detection. B, Transmigrated mononuclear cells were imaged on day 2 before medium replacement and counted. Fold changes in mean numbers of transmigrated mononuclear cells co-cultured with unstimulated (UT), HLA IgG, or HLA I $F(ab')_2$ stimulated ECs are shown by box and whiskers graph. Data were from 2 independent experiments using 2 monocyte donors cultured with ECs from 3 donors. *$P < .05$ was analyzed by repeated-measures one-way ANOVA with Sidak tests

$CD206^{hi}CD68^{hi}CD14^{lo}CD64^{lo}CD163^{lo}$; and M(IL-10) were $CD163^{hi}CD14^{hi}CD68^{hi}CD86^{lo}$. For M(hIgG + lipopolysaccharide [LPS]), several markers, including CD64, CD68, CD163, and CD1a, were significantly decreased, whereas no cell surface protein that we assessed was increased, as reported[46] (Figure 6A; Figure S4). mDCs were $CD1a^{hi}CD86^{hi}CD206^{hi}$.[47] These phenotypes were distinct from that observed in M(HLA I IgG), which exhibited coexpression of CD163 and CD206.

When comparing M(HLA I IgG) to these controls, we found that the expression of GRO/CXCL1, MCP-1/CCL2, MDC/CCL22, and TNF-α was consistent with those of M(IL-10). However, M(HLA I IgG) also shared some properties with M(hIgG + LPS) as well as M(IFN-γ), such as IL-6, IL-8/CXCL8 and MCP-1/CCL2 (Figure 6B), indicating a distinct subtype of M(HLA I IgG).

Finally, we compared the expression of the 53 DEGs identified in M(HLA I IgG) and M(HLA I $F(ab')_2$) with that of macrophages polarized by cytokines (Figure 7A). Hierarchical clustering based on the overall expression pattern of these DEGs indicate that antibody-stimulated conditions were indeed different, and were more similar to M(IL-10), and secondly to M(IL-4),

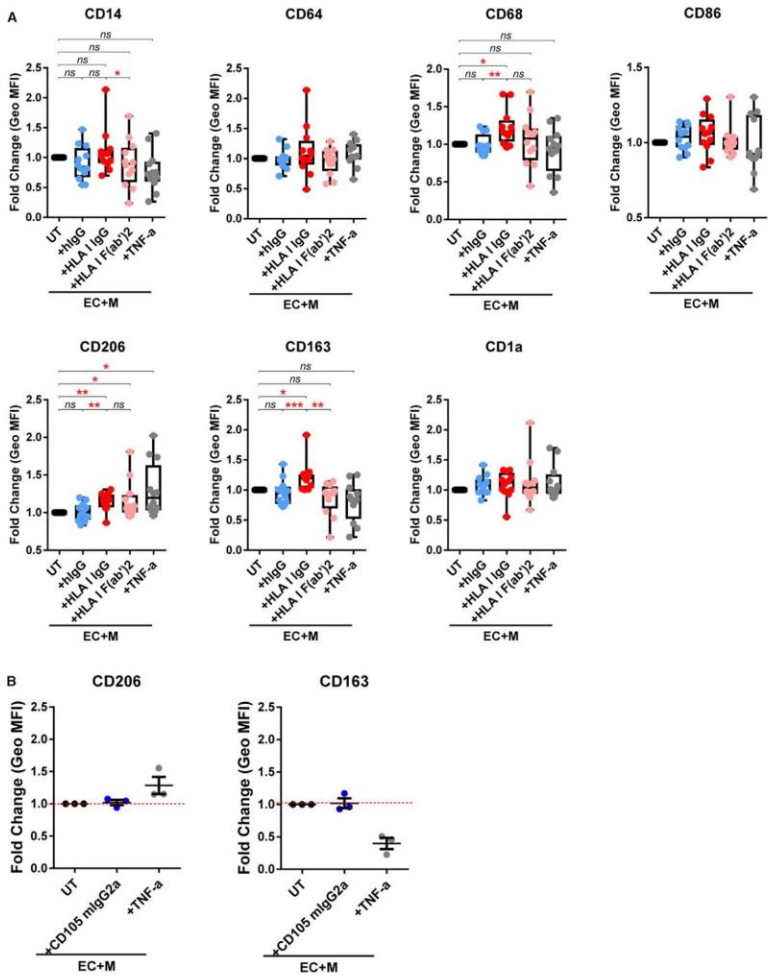

FIGURE 3 HLA I IgG–activated EC-induced differentiation of monocytes into $CD68^{+}CD206^{+}CD163^{+}$ macrophages. A, Monocytes were co-cultured with unstimulated (UT), or HLA I IgG, HLA I F(ab′), hIgG, or TNF-α stimulated ECs as in Figure 1. On day 5, the macrophages in the lower chamber were collected and the assessments of surface marker expression were performed using flow cytometry. Results are expressed as fold change of Geo MFI value against EC+M+UT by box and whiskers graph. *$P < .05$, **$P < .01$ and ***$P < .001$ were analyzed by repeated measures one-way ANOVA with Sidak tests. B, Before the addition of monocytes, ECs were left untreated (UT) or treated with CD105 mIgG2a at 1 μg/mL (+CD105 mIgG2a) or TNF-α (10 ng/mL) (+TNF-α) and then co-cultured for 5 d. The cells in the lower chamber were collected and assessed for the expression of CD206 and CD163 using flow cytometry. Data are expressed as mean ± SEM fold change of Geo MFI value against EC+M+UT. The data in (A) represent 4 independent experiments with 4 monocyte donors against ECs from 3 donors. Data in (B) were from one experiment using one monocyte donor against ECs from 3 donors

than to LPS-treated macrophages (M(hIgG + LPS) and M(IFN-γ)) (Figure 7B). For M(HLA I IgG), 13 of the 53 DEGs were shared with M(IL-4), 20 with M(IL-10), and 11 with both (Figure 6C). Notably, 4 of the unshared 9 DEGs in M(HLA I IgG) were also dramatically increased in M(hIgG + LPS), and 3 of them were pro-inflammatory genes, suggesting that some similarity exists between the M(HLA I IgG) and the M(hIgG + LPS). M(HLA I $F(ab')_2$) shared 18 genes with M(IL-4), 16 with M(IL-10), and 14 with both (Figure 7C). These data suggest that M(HLA I IgG) exhibits a distinct pattern of gene expression that is a unique phenotype not consistent with any of the canonical cytokine-stimulated conditions described to date.

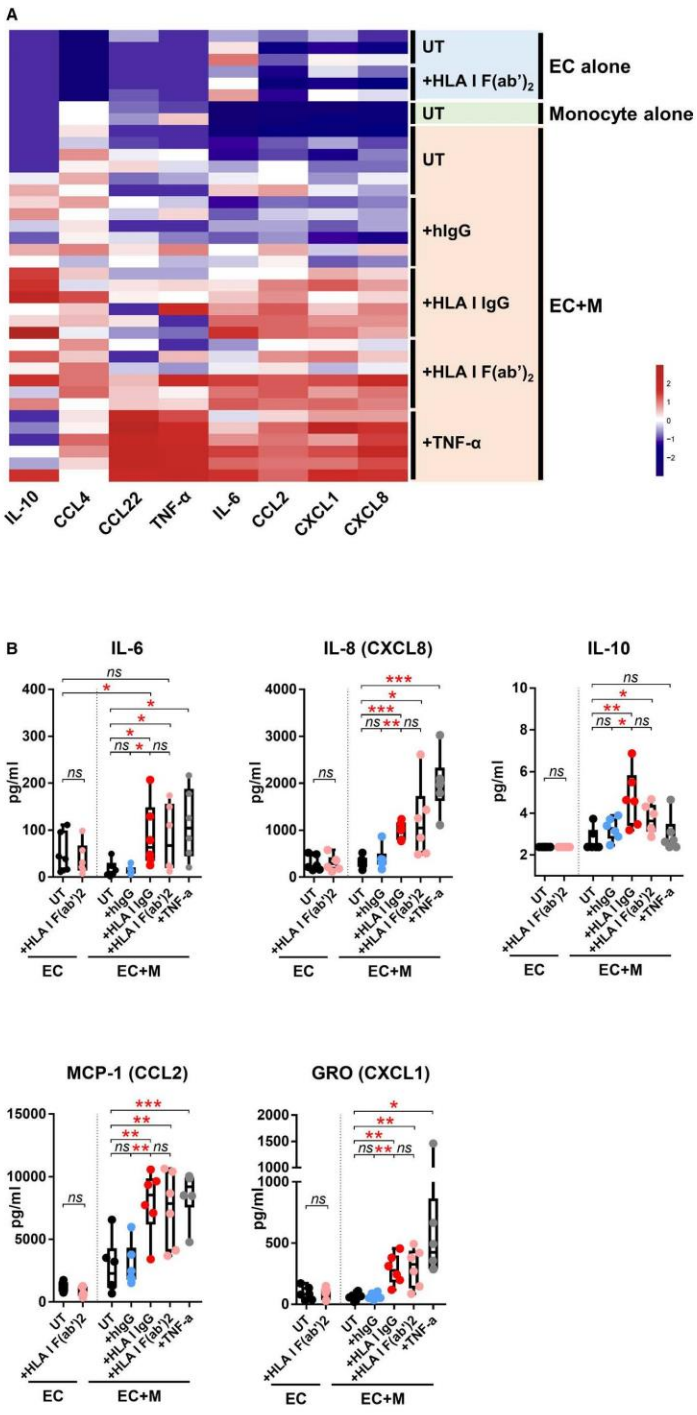

FIGURE 4 HLA I antibody–activated ECs increased cytokine/chemokine production by M(HLA I IgG). A, Co-culture supernatants were collected on day 4 before medium replacement for cytokine detection. The data were Z-scaled and normalized by cytokine, and hierarchical clustering was performed. B, Statistical analysis of the data shown in (A). The data in (B) are represented by box and whisker plots and analyzed by repeated-measures 1-way ANOVA with Fisher LSD tests. *$P < .05$, **$P < .01$ and ***$P < .001$. The data represent 2 independent experiments using 2 monocyte donors against ECs from 3 donors

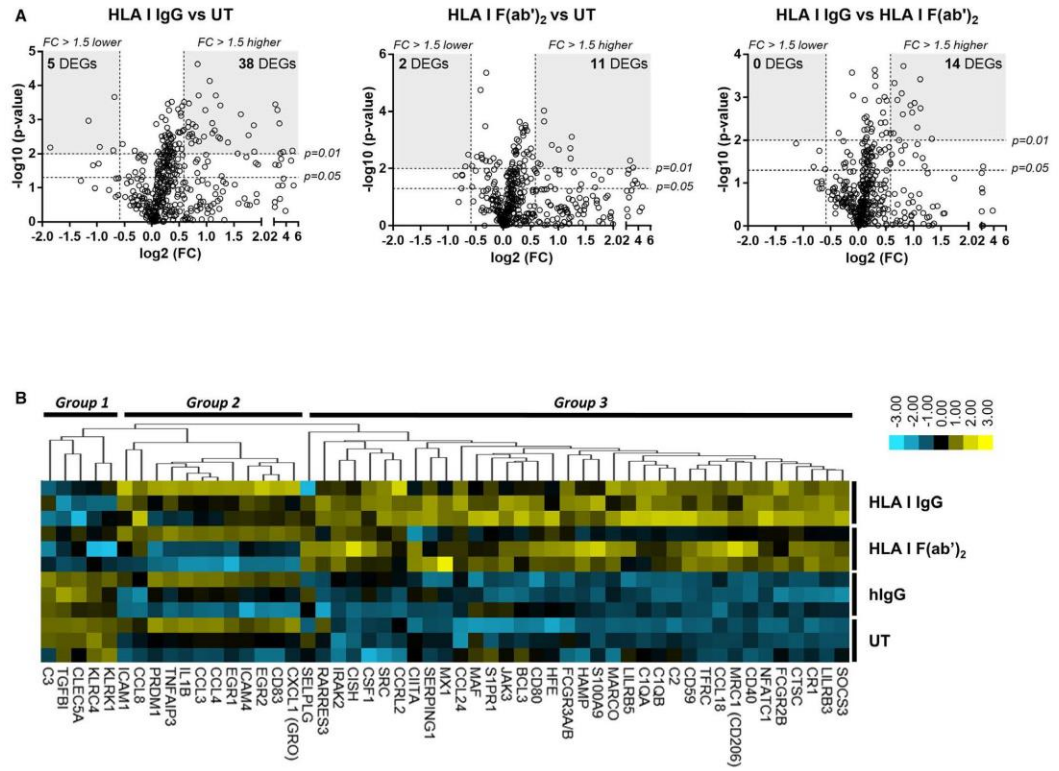

FIGURE 5 Volcano plots of the NanoString data and heatmap of the 53 differentially expressed genes (DEGs) in HLA I antibody–induced macrophages. After 5 d co-culture with unstimulated (UT), or HLA I IgG, HLA I F(ab′)$_2$, hIgG stimulated ECs, macrophages in the lower chambers were collected and lysed in RLT buffer for NanoString analysis. A, Volcano plots of log2 (fold change, FC) on x-axis vs −log10 (*P*-value) on y-axis from the comparisons of the gene expression in each 2 of the HLA I IgG, HLA I F(ab′)$_2$ and UT groups. Each circle represents one gene. For each comparison, genes with a $P < .01$ and absolute FC > 1.5 were considered DEGs and highlighted in gray. B, Hierarchical clustering and heatmap of 53 DEGs, *Z*-scaled and normalized by gene. Groups 1, 2, and 3 indicate the 3 gene clusters with differential expression patterns across the 3 conditions. Data were obtained coculturing 2 monocyte donors against the ECs from 3 donors

3.7 | Human in vitro M(HLA I IgG) and M(HLA I F(ab′)$_2$) polarized macrophages share similar DEGs with murine DSA-treated cardiac grafts

To identify if human in vitro co-culture macrophages contain DEGs analogous to murine cardiac allografts treated with a MHC I DSA mixture, we performed a comparative analysis between DEGs from both parties. Overall, 11 DEGs overlapped between the human in vitro and the murine in vivo data (Table 3). The DEGs encoded immune/cellular responses, chemokines/cytokines, transcription factors, phagocytosis, and complement-related proteins. Both M(HLA I IgG) and M(HLA I F(ab′)$_2$) independently shared 7 analogous DEGs compared with the DEGs from DSA-treated grafts. Shared DEGs between M(HLA I IgG) and DSA-treated grafts included genes related to immune responses *(IL1RN)*, chemokines *(CXCL1, CCL2,* and *CSF1)*, signaling transcription factors *(EGR2* and *POU2F2)*, and phagocytosis *(CLEC5A)*. Shared DEGs between M(HLA I F(ab′)$_2$) and DSA-treated grafts also included genes related to immune/cellular response *(GRP183* and *PTGS2)*, cytokines/chemokines *(CXCL1, CCL2,* and *CSF1)*, phagocytosis *(CLEC5A)*, and complement *(C1S1)*. Five DEGs *(CXCL1, EGR2, PTGS2, CLEC5A,* and *TMEM173)* were identified as significantly different between M(HLA I IgG) and M(HLA F(ab′)$_2$. Finally, four DEGs were shared across all 3 groups: M(HLA I IgG), M(HLA I F(ab′)$_2$), and MHC I DSA-treated allografts. These four genes included chemokines/cytokines *(CXCL1, CCL2,* and *CSF1)*, and phagocytosis *(CLEC5A)*.

4 | DISCUSSION

Herein we describe for the first time that ECs activated by HLA I IgG skew monocytes toward a novel macrophage polarization

TABLE 2 The 53 differentially expressed genes (DEGs) in co-cultured macrophages

	IgG vs UT		$F(ab')_2$ vs UT		IgG vs $F(ab')_2$	
Gene symbol	*P*	FC	*P*	FC	*P*	FC
Complement-related						
C1QA	**	2.32	ns	-	**	2.19
C1QB	**	3.40	**	1.55	**	2.10
C2	****	1.79	**	1.32	**	1.37
C3	**	0.61	*	0.68	ns	–
CD59	**	1.62	*	1.33	ns	–
SERPING1	***	2.38	ns	–	ns	–
Costimulatory molecules						
CD40	***	3.09	*	2.44	ns	–
CD80	**	7.36	*	4.89	ns	–
CD83	**	1.68	ns	-	**	1.64
Immune/cellular response						
CIITA	**	2.97	*	2.67	ns	–
CTSC	***	1.51	**	1.29	**	1.18
KLRC4	**	0.45	*	0.55	ns	–
KLRK1	**	0.52	*	0.59	ns	–
LILRB3	**	1.59	**	1.35	*	1.18
LILRB5	**	1.74	ns	–	ns	–
MX1	**	1.65	*	2.04	ns	–
S100A9	**	1.58	*	1.50	ns	–
Phagocytosis						
CLEC5A	**	0.28	*	0.60	*	0.46
CR1	****	2.08	***	1.67	*	1.25
MARCO	**	2.62	**	2.01	ns	–
MRC1	**	1.68	*	1.51	ns	–
Fcγ receptors						
FCGR2B	**	2.15	**	1.38	**	1.56
FCGR3A/B	**	2.16	****	1.67	ns	–
Adhesion molecules						
ICAM1	**	1.74	*	1.19	*	1.47
ICAM4	**	2.22	ns	-	***	2.18
SELPLG	ns	–	***	2.37	ns	–
TGFBI	***	0.62	****	0.75	*	0.83
Signaling and transcription factors						
BCL3	**	1.50	ns	–	*	1.30
CISH	**	11.13	*	13.74	ns	–
EGR1	**	1.25	ns	–	***	1.57
EGR2	**	1.74	ns	–	***	1.73
IRAK2	**	2.37	**	2.33	ns	–
JAK3	**	8.24	**	6.25	ns	–
MAF	**	1.67	*	1.27	**	1.30
NFATC1	**	1.94	***	1.35	*	1.40
PRDM1	ns	–	**	0.65	*	1.49
S1PR1	***	5.87	*	3.44	*	1.72

(Continues)

TABLE 2 (Continued)

Gene symbol	IgG vs UT		$F(ab')_2$ vs UT		IgG vs $F(ab')_2$	
	P	FC	*P*	FC	*P*	FC
SOCS3	***	4.56	**	2.34	**	1.97
SRC	***	1.60	*	1.30	***	1.24
TNFAIP3	*	1.42	ns	—	**	1.67
Chemokines/cytokines						
CCL18	**	3.64	*	3.13	ns	—
CCL24	**	32.47	*	10.91	**	2.52
CCL3	*	1.30	**	0.76	***	1.76
CCL4	*	1.39	**	0.72	**	2.03
CCL8	**	1.59	ns	-	*	1.52
CCRL2	***	1.81	***	1.30	***	1.39
CXCL1	*	1.30	**	0.76	**	1.75
IL1B	ns	—	**	0.62	ns	—
Growth/differentiation factors/others						
CSF1	*	8.90	**	8.89	ns	—
HAMP	***	1.97	*	2.02	ns	—
HFE	**	1.82	**	1.60	ns	—
TFRC	***	2.25	**	1.84	ns	—
RARRES3	*	4.61	ns	-	**	1.93

Note: The data were from two independent experiments using two monocyte donors against the ECs from 3 donors. UT, IgG, and F(ab')2 represent monocytes co-cultured with unstimulated or HLA I IgG antibody (intact or F(ab')2) stimulated endothelial cells.

Abbreviations: FC, fold change; —, not applicable.

ns $P > .05$,

*$P < .05$,

**$P < .01$,

***$P < .001$, and

****$P < .0001$ were analyzed by repeated measures 1-way ANOVA with Fisher LSD tests of gene expression counts.

state through the synergistic actions of EC activation and FcγR ligation. Using an in vivo mouse model of acute AMR, we identified DSA upregulated genes related to monocyte stimulation by Fcγ receptors and transmigration through DSA-activated endothelium. Cardiac allografts from recipients treated with MHC I DSA had an increased expression of transcripts associated with macrophage recruitment, adhesion, and immune/cellular response. To directly examine the mechanisms of MHC I DSA on macrophage polarization, we utilized an in vitro model of human peripheral blood monocytes transmigrating through HLA I IgG–activated endothelial monolayers. These macrophages had concurrent expression of CD163 and CD206, enhanced production of IL-10, IL-6, IL-8/CXCL8, MCP-1/CCL2, and GROα/CXCL1, and increased expression of transcripts involved in antigen presentation and regulation of complement cascades. In vitro co-cultured polarized macrophages and in vivo DSA-exposed allografts shared analogous DEGs involved in macrophage recruitment and immune cellular/response.

HLA I outside-in signaling promotes monocyte adhesion and recruitment by triggering mobilization of WPBs, induction of P-selectin, ICAM-1 clustering, and subsequent leukocyte capture and firm adhesion to the activated endothelium, a process partially mediated by the Fc-FcγR interaction between the HLA I IgG and the monocytes.[17,19,20] The question addressed in this work is whether the HLA I antibody modifies monocyte differentiation during recruitment and transendothelial migration.

Once monocytes transmigrate into the subendothelial connective tissue, they differentiate into distinct phagocytes including macrophages and DCs. Historically, macrophages were classified into two major functional subgroups termed M1 and M2, with distinct functions.[38,48] M1 or "classically activated" macrophages differentiate in response to interferon-gamma (IFN-γ) or TLR ligands, whereas M2 or "alternatively activated" macrophages develop in the presence of IL-10, IL-4, or IL-13 and mediate tissue repair and promote fibrosis.[24,25,48] However, the current viewpoint is that the M1/M2 nomenclature underrepresents the actual functional heterogeneity of macrophage subtypes, which are now classified based on their interaction with different immunological stimuli (ie, growth factors, cytokines, bacterial products), rather than attributing them to distinct subsets.[23,38] Indeed, monocyte co-culture, even with unstimulated endothelium, triggered phenotypic changes[49] and changes in gene expression.[50]

A

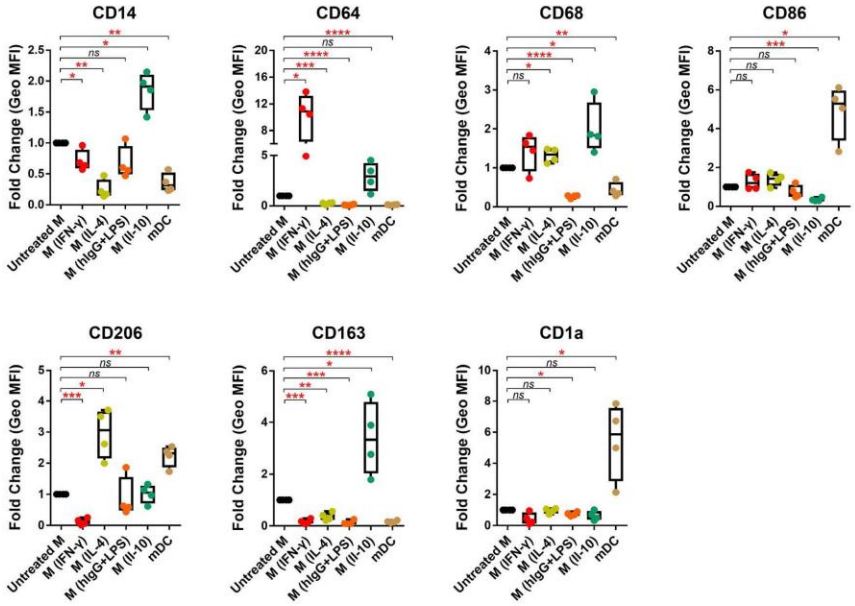

B

Cytokines (ng/ml)	Polarized macrophages						M (HLA I Ab)	
	Untreated M	M (IFN-γ)	M (IL-4)	M (hIgG+LPS)	M (IL-10)	mDC	IgG	$F(ab')_2$
TNF-α	2.27±0.03	21.55±9.90	2.28±0.54	5774.00±3869.00	1.06±0.17	8025.00±6032.00	-	-
IL-6	1.35±0.72	11.05±12.13	0.84±0.00	10589.00±1474.00	0.84±0.00	4825.00±5683.00	↑	↑
CXCL8	244.80±132.90	207.20±117.30	31.16±8.25	18821.00±1046.00	163.10±25.75	9252.00±5828.00	↑	↑
CCL4	14.05±2.93	11.42±8.47	26.00±3.10	5280±1667.00	19.50±0.55	10604.00±7642.00	-	↑
IL-10	4.00±1.97	2.38±0.00	3.75±0.42	788.80±542.00	N/A	102.00±121.40	↑	↑
CXCL1	39.21±5.33	18.27±7.34	12.53±3.05	15705.00±0.00	54.44±9.01	1223.00±1437.00	↑	↑
CCL22	13.21±7.43	2.88±0.00	504.70±344.00	5819.00±5670.00	3.15±0.38	14857.00±0.00	-	-
CCL2	637.00±186.60	6533.00±3907.00	222.80±174.20	10177.00±613.80	7179.00±1520.00	9481.00±83.44	↑	↑

FIGURE 6 Characterization of in vitro polarized macrophages and dendritic cells (DCs). A, Freshly isolated human peripheral monocytes from 4 different donors were left unstimulated (untreated M), or stimulated with IFN-γ (50 ng/mL), IL-4 (40 ng/mL), hIgG (10 μg/mL, precoated) + LPS (100 ng/mL), IL-10 (50 ng/mL) or IL-4 (20 ng/mL) + GM-CSF (50 ng/mL) + LPS (100 ng/mL, on day 4) for 5 d to induce M(IFN-γ), M(IL-4), M(hIgG + LPS), M(IL-10), and mature DCs (mDCs), respectively. Stimuli and half of the culture medium were refreshed every 2 d. Expression of 7 surface markers were measured by flow cytometry. Results are expressed as fold change of Geo MFI value against untreated M, and shown by box and whisker plots. Statistical significance *P < .05, **P < .01, ***P < .001, and ****P < .0001 was analyzed by repeated-measures 1-way ANOVA with Dunnett tests compared to untreated M. B, Cell culture supernatants from polarized macrophages were collected on day 4 before medium replacement, and assessed for cytokines using 38-plex Luminex. Cytokine concentrations are shown as mean ± SD. Measurement of IL-10, used as stimuli to generate M(IL-10), was not included in the analysis and indicated by "N/A." Table 5B represents the cytokine levels from Figure 3. ↑indicates increased vs –unchanged cytokine expression in M(HLA I IgG) and M(HLA I $F(ab')_2$). Data were from 4 independent experiments using 3 ECs with 4 monocyte donors

Less is known about monocyte emigration and differentiation during antibody-mediated vascular inflammation. In the setting of AMR, HLA crosslinking by antibodies on the EC induces EC activation and intracellular signaling. Our data suggest that this process is specific for HLA I and requires EC activation.[17] Because the IgG subclass and FcγR polymorphisms regulate HLA I IgG–promoted monocyte

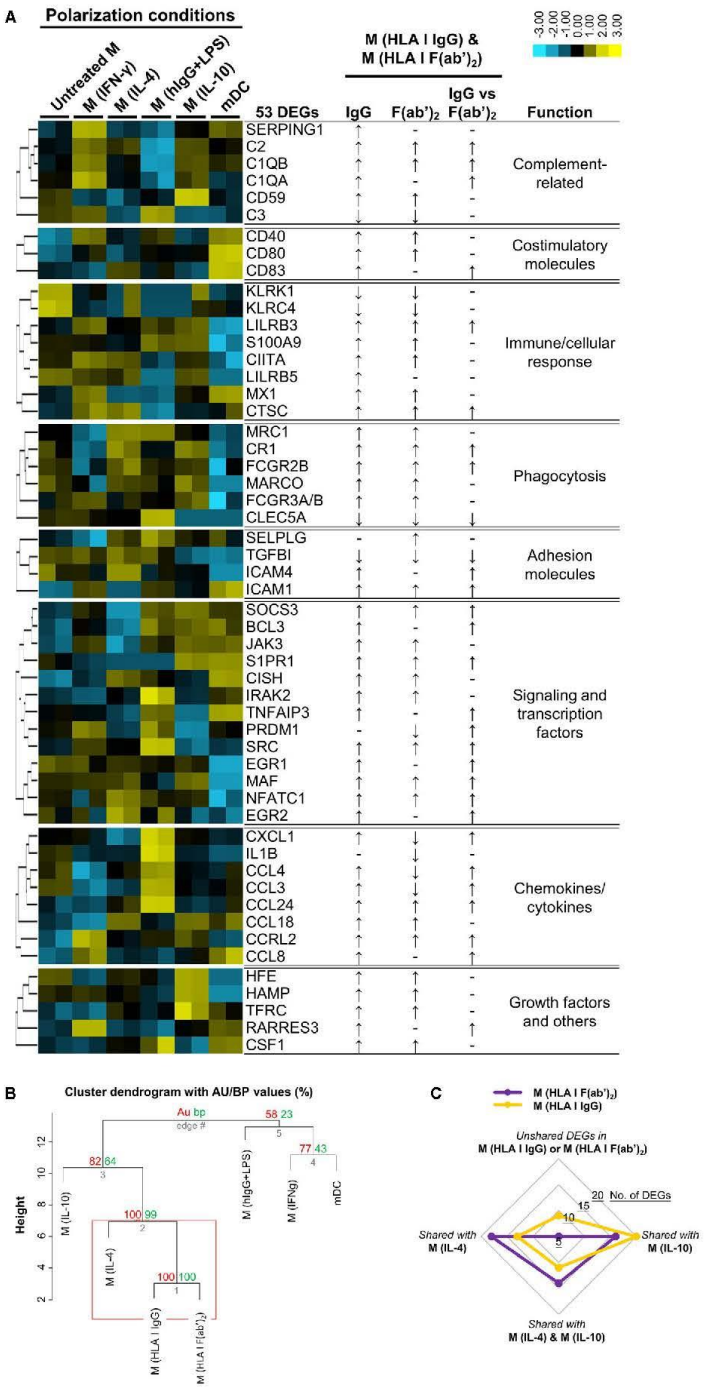

FIGURE 7 HLA I antibody–polarized macrophages exhibit a unique transcriptional profile. A, Heat map shows expression of the 53 DEGs in macrophages from 2 independent experiments using 2 monocyte donors polarized using canonical stimuli compared to expression of DEGs in M(HLA I IgG) and M(HLA I F(ab')$_2$) obtained by testing 2 monocyte donors against 3 ECs. ↑, ↓, and – indicate upregulated, downregulated, and unchanged, respectively, referring to the data in Table 1. B, Hierarchical clustering was used to compare the pattern of gene expression between the control cultures, M(HLA I IgG) and M(HLA I F(ab')$_2$). C, For macrophages polarized using canonical stimuli, DEGs were defined as an absolute fold change >1.5. The radar chart shows the difference in the numbers of DEGs shared with between M(HLA I IgG) and M(HLA I F(ab')$_2$ and M(IL-4) and M(IL-10)

TABLE 3 The 11 differentially expressed genes (DEGs) similar across in vitro human co-cultured macrophages and DSA-treated cardiac grafts

Mice allografts		IgG vs UT		$F(ab')_2$ vs UT		IgG vs $F(ab')_2$		
Gene symbol	*P*	*P*	FC	*P*	FC	*P*	FC	Function
IL1RN	.002	*	2.42	ns	1.92	ns	1.23	Immune/cellular response
GPR183	.034	ns	1.00	*	0.84	ns	1.2	Immune/cellular response
CXCL1	.041	*	1.47	**	0.87	**	1.75	Chemokines/cytokines
CCL2	.060	*	1.78	**	1.94	ns	0.97	Chemokines/cytokines
EGR2	.067	**	1.74	ns	1.02	***	1.73	Signaling/ transcription
PTGS2	.073	ns	1.46	**	0.68	*	2.3	Immune/cellular response
POU2F2	.080	*	1.23	ns	1.09	ns	1.18	Signaling/ transcription
CSF1	.090	*	8.90	**	8.89	ns	1.09	Chemokines/cytokines
CLEC5A	.091	**	0.28	*	0.60	*	0.46	Phagocytosis
TMEM173	.097	ns	1.23	ns	1.03	*	1.2	Immune/cellular response
C1S1	.097	ns	37.3	*	26.5	ns	1.2	Complement-related

Note: Left: In vivo mouse cardiac allograft differentially expressed genes with $P < .1$ between HLA I DSA–treated allograft recipients and isotype-treated controls (n = 3). Right: UT, Ab, and $F(ab')_2$ represent monocytes co-cultured with unstimulated, HLA I antibody (intact or $F(ab')_2$) stimulated endothelial cells, respectively.

Abbreviation: FC, fold change.

ns $P > .05$,

*$P < .05$,

**$P < .01$,

***$P < .001$, and

****$P < .0001$ were analyzed by repeated measures 1-way ANOVA with Fisher's LSD tests of gene expression counts.

adhesion,[17,19] we used HLA I $F(ab')_2$ in parallel to see whether the HLA I IgG Fc region took part in driving differential polarization. Our results indicate the critical role of antibody Fc region in further M(HLA I IgG) differentiation, as M(HLA I IgG) express CD206 and CD163 concurrently. Similarly, hemoglobin/haptoglobin stimulation promotes concomitant expression of CD206 and CD163 in macrophages, termed M(Hb).[51]

Several studies have reported that antibody ligation of HLA I molecules on ECs directly triggered production of cytokines, chemokines,[52,53] and growth factors, of which some have been shown to augment M2-like polarization of macrophages.[54-57] In our model, stimulation with HLA I antibody did not induce cytokine production directly from ECs. Instead, cell-cell contact of monocytes with antibody-activated ECs was required for cytokine production. This inconsistency may be due to differences in EC vascular origin, passage number, and/or HLA antibody concentrations. However, recruited human monocytes trigger a regulatory pathway of cytokine-mediated signaling at the EC interface, substantiating cross talk between the monocyte and EC in vascular inflammation.[58] The mechanism(s) underlying how HLA antibody–activated ECs instruct monocyte differentiation needs to be investigated.

Although endothelial-polarized macrophages shared some patterns of gene and cytokine expression with cytokine-activated macrophages, there was no complete overlap with macrophages derived in the presence of prototypic stimuli. EC activated by HLA I crosslinking (HLA I $F(ab')_2$) induced expression of genes in macrophages typical of alternatively activated macrophages. When macrophages also received FcγR signaling, numerous genes characteristic of M(IFNγ) were enhanced. Many of these additional genes overlapped with M(hIgG + LPS), indicating the involvement of the HLA I IgG Fc region in monocyte differentiation. Thus, the present data suggest that the HLA I IgG–enhanced monocyte differentiation occurs not only by activating ECs, but also through the action of the antibody Fc region. These features suggest that the M(HLA I IgG) is a previously undescribed subtype of alternatively activated macrophage.

Our study also provides phenotypic markers for M(hIgG + LPS), which had remained elusive so far.[45,46] Indeed, we found several surface markers (CD64, CD68, CD163, CD1a) that were significantly decreased in M(hIgG + LPS), which was to some extent consistent with the findings of others.[59]

MHC I DSA–treated allografts shared overlapping genes with in vitro co-cultured human macrophages. Although difficult to classify allograft DEGs to specific cell-types from bulk transcriptomes, many genes have been previously described to be associated with macrophage recruitment (eg, *CCL2* and *CXCL1*),[40,41] polarization (eg, *CSF1*),[60] immune responses (*GPR183*),[61] and phagocytosis (*CLEC5A*)[62] CXCL1 and CCL2 were also increased in vitro in co-culture supernatants from M(HLA I IgG) and M(HLA I $F(ab')_2$). Banff 2017 identified several transcripts (*CX3CR1*, *FCGR3A*, *CD163*, and *CD206*) in renal AMR that overlap with our M(HLA I) signature.[63]

Moreover, CD68 is a component of the ISHLT working formulation to identify intravascular macrophages in heart allografts with AMR.[64] None of the 27 DEGs are included in CD16a-inducible transcripts following in vitro crosslinking on purified NK cells that are also expressed during AMR of kidney grafts.[65] Nonetheless, NK cell transcripts related to Fc-receptor stimulation warrants further investigation. Overall, our in vitro data using human primary cells and in vivo murine studies further implicate DSA in the development of distinct macrophages specific to AMR. The clinical relevance and mechanisms by which these $CD206^+$ and $CD163^+$ macrophages may contribute to the processes of acute and chronic transplant rejection need to be elucidated. Notably, $CD163^+$ macrophages were identified within fibrotic areas of patient renal allografts[28] and $CD206^+$ macrophages were increased within murine renal allografts with chronic rejection.[30] Studies are underway to validate these findings in biopsies from patients with AMR. This macrophage subset could be an attractive therapeutic target for patients with DSAs at risk of TV.

The ECs used in the current study were isolated from human aortic rings, which may not reflect the positional identity and heterogeneity of ECs from different vascular beds. This study mainly probed the effect of HLA I antibody–activated ECs on monocyte differentiation. Whether and how HLA II antibodies activate the ECs and drive monocyte differentiation is a subject of ongoing study. Although our mouse model of AMR indicated macrophage polarization via Fc receptors and transmigration across DSA-activated endothelium, further transcriptome profiling of isolated graft-infiltrating macrophages will be critical. We show that the HLA-I antibody–activated ECs can drive monocyte differentiation, but further study is required to determine what biological impact the macrophages, in turn, have on the intimal cells that contributes to vascular disease.

In conclusion, our findings demonstrate the ability of antibody-induced vascular inflammation to promote monocyte polarization to a unique $CD68^+CD206^+CD163^+$ macrophage phenotype. The increase in genes indicative of monocyte stimulation by Fc receptors and transmigration through activated endothelium in murine cardiac allografts suggests a pathogenic role of these macrophages in tissue injury that remains to be elucidated.

ACKNOWLEDGMENTS

The authors express their thanks to OneLegacy and all the organ and tissue donors and their families for giving the gift of life by their generous donation. The authors would like to acknowledge Dr Nina Dvorina for her expert immunohistochemical stains, and the efforts of the Clinical Trials in Organ Transplantation Core at Cleveland Clinic Nanostring Core. This work was supported in part by NIH U19AI128913, PO1AI120944, U01AI124319, RO1AI042819 (to E.F.R.), RO1AI135201 (to E.F.R. and R.L.F.); by the Jiangsu Provincial Medical Youth Talent QNRC2016739 and Science and Technology Development Program of Suzhou SYS201601, CXTDB2017009, GSWS2019033 (to X.W.); by the Jiangsu Provincial Key Medical Discipline ZDXKA2016012 (to J.H.); and by the Clinical Trials in Organ Transplantation Core at Cleveland Clinic NanoString Core UO1 AI063594 (to R.L.F.).

DISCLOSURE

The authors of this manuscript have no conflicts of interest to disclose as described by the *American Journal of Transplantation*.

DATA AVAILABILITY STATEMENT

The data that support the findings of this study are available from the corresponding author upon reasonable request.

ORCID

Xuedong Wei https://orcid.org/0000-0003-2000-2620
Nicole M. Valenzuela https://orcid.org/0000-0003-2024-5382
Maura Rossetti https://orcid.org/0000-0003-3347-6200
Rebecca A. Sosa https://orcid.org/0000-0002-9860-6830
Jessica Nevarez-Mejia https://orcid.org/0000-0003-3390-4818
Gregory A. Fishbein https://orcid.org/0000-0002-3632-5654
Arend Mulder https://orcid.org/0000-0001-7805-7064
Robert L. Fairchild https://orcid.org/0000-0002-7107-5259
Jianquan Hou https://orcid.org/0000-0001-9416-3713
Elaine F. Reed https://orcid.org/0000-0002-3524-545X

REFERENCES

1. Guilpain P, Mouthon L. Antiendothelial cells autoantibodies in vasculitis-associated systemic diseases. *Clin Rev Allergy Immunol*. 2008;35(1-2):59-65.
2. Legendre P, Régent A, Thiebault M, Mouthon L. Anti-endothelial cell antibodies in vasculitis: a systematic review. *Autoimmun Rev*. 2017;16(2):146-153.
3. Florey OJ, Johns M, Esho OO, Mason JC, Haskard DO. Antiendothelial cell antibodies mediate enhanced leukocyte adhesion to cytokine-activated endothelial cells through a novel mechanism requiring cooperation between Fc{gamma}RIIa and CXCR1/2. *Blood*. 2007;109(9):3881-3889.
4. Iseme RA, McEvoy M, Kelly B, et al. A role for autoantibodies in atherogenesis. *Cardiovasc Res*. 2017;113(10):1102-1112.
5. Matsuura E, Atzeni F, Sarzi-Puttini P, Turiel M, Lopez LR, Nurmohamed MT. Is atherosclerosis an autoimmune disease. *BMC Med*. 2014;12:47.
6. Wiebe C, Gibson IW, Blydt-Hansen TD, et al. Evolution and clinical pathologic correlations of de novo donor-specific HLA antibody post kidney transplant. *Am J Transplant*. 2012;12(5):1157-1167.
7. Zhang Q, Hickey M, Drogalis-Kim D, et al. Understanding the correlation between DSA, complement activation and antibody mediated rejection in heart transplant recipients. *Transplantation*. 2018;102(10):e431-e438.
8. Clerkin KJ, Farr MA, Restaino SW, et al. Donor-specific anti-HLA antibodies with antibody-mediated rejection and long-term outcomes following heart transplantation. *J Heart Lung Transplant*. 2017;36(5):540-545.
9. Valenzuela NM, Reed EF. Antibody-mediated rejection across solid organ transplants: manifestations, mechanisms, and therapies. *J Clin Invest*. 2017;127(7):2492-2504.
10. Loupy A, Toquet C, Rouvier P, et al. Late failing heart allografts: pathology of cardiac allograft vasculopathy and association with antibody-mediated rejection. *Am J Transplant*. 2016;16(1):111-120.
11. Roux A, Bendib Le Lan I, Holifanjaniaina S, et al. Antibody-mediated rejection in lung transplantation: clinical outcomes

and donor-specific antibody characteristics. *Am J Transplant*. 2016;16(4):1216-1228.
12. Wong KL, Taner T, Smith BH, et al. Importance of routine antihuman/leukocyte antibody monitoring: de novo donor specific antibodies are associated with rejection and allograft vasculopathy after heart transplantation. *Circulation*. 2017;136(14):1350-1352.
13. Tran A, Fixler D, Huang R, Meza T, Lacelle C, Das BB. Donor-specific HLA alloantibodies: impact on cardiac allograft vasculopathy, rejection, and survival after pediatric heart transplantation. *J Heart Lung Transplant*. 2016;35(1):87-91.
14. Loupy A, Vernerey D, Viglietti D, et al. Determinants and outcomes of accelerated arteriosclerosis: major impact of circulating antibodies. *Circ Res*. 2015;117(5):470-482.
15. Jin YP, Korin Y, Zhang X, Jindra PT, Rozengurt E, Reed EF. RNA interference elucidates the role of focal adhesion kinase in HLA class I-mediated focal adhesion complex formation and proliferation in human endothelial cells. *J Immunol*. 2007;178(12):7911-7922.
16. Jindra PT, Hsueh A, Hong L, et al. Anti-MHC class I antibody activation of proliferation and survival signaling in murine cardiac allografts. *J Immunol*. 2008;180(4):2214-2224.
17. Valenzuela NM, Mulder A, Reed EF. HLA class I antibodies trigger increased adherence of monocytes to endothelial cells by eliciting an increase in endothelial P-selectin and depending on subclass, by engaging FcγRs. *J Immunol*. 2013;190(12):6635-6650.
18. Valenzuela NM, Hong L, Shen XD, et al. Blockade of p-selectin is sufficient to reduce MHC I antibody-elicited monocyte recruitment in vitro and in vivo. *Am J Transplant*. 2013;13(2):299-311.
19. Valenzuela NM, Trinh KR, Mulder A, Morrison SL, Reed EF. Monocyte recruitment by HLA IgG-activated endothelium: the relationship between IgG subclass and FcγRIIa polymorphisms. *Am J Transplant*. 2015;15(6):1502-1518.
20. Salehi S, Sosa RA, Jin Y-P, et al. Outside-in HLA class I signaling regulates ICAM-1 clustering and endothelial cell-monocyte interactions via mTOR in transplant antibody-mediated rejection. *Am J Transplant*. 2018;18(5):1096-1109.
21. Yamakuchi M, Kirkiles-Smith NC, Ferlito M, et al. Antibody to human leukocyte antigen triggers endothelial exocytosis. *Proc Natl Acad Sci USA*. 2007;104(4):1301-1306.
22. Pilmore HL, Painter DM, Bishop GA, McCaughan GW, Eris JM. Early up-regulation of macrophages and myofibroblasts: a new marker for development of chronic renal allograft rejection. *Transplantation*. 2000;69(12):2658-2662.
23. Liberale L, Dallegri F, Montecucco F, Carbone F. Pathophysiological relevance of macrophage subsets in atherogenesis. *Thromb Haemost*. 2017;117(1):7-18.
24. Das A, Sinha M, Datta S, et al. Monocyte and macrophage plasticity in tissue repair and regeneration. *Am J Pathol*. 2015;185(10):2596-2606.
25. Mantovani A, Biswas SK, Galdiero MR, Sica A, Locati M. Macrophage plasticity and polarization in tissue repair and remodelling. *J Pathol*. 2013;229(2):176-185.
26. Mannon RB. Macrophages: contributors to allograft dysfunction, repair, or innocent bystanders. *Curr Opin Organ Transplant*. 2012;17(1):20-25.
27. Azad TD, Donato M, Heylen L, et al. Inflammatory macrophage-associated 3-gene signature predicts subclinical allograft injury and graft survival. *JCI Insight*. 2018;3(2). https://doi.org/10.1172/jci.insight.95659
28. Ikezumi Y, Suzuki T, Yamada T, et al. Alternatively activated macrophages in the pathogenesis of chronic kidney allograft injury. *Pediatr Nephrol*. 2015;30(6):1007-1017.
29. Toki D, Zhang W, Hor KLM, et al. The role of macrophages in the development of human renal allograft fibrosis in the first year after transplantation. *Am J Transplant*. 2014;14(9):2126-2136.
30. Wu C, Zhao Y, Xiao X, et al. Graft-infiltrating macrophages adopt an M2 phenotype and are inhibited by purinergic receptor P2X7 antagonist in chronic rejection. *Am J Transplant*. 2016;16(9):2563-2573.
31. Zhao Y, Chen S, Lan P, et al. Macrophage subpopulations and their impact on chronic allograft rejection versus graft acceptance in a mouse heart transplant model. *Am J Transplant*. 2018;18(3):604-616.
32. Rahimi S, Qian Z, Layton J, Fox-Talbot K, Baldwin WM 3rd, Wasowska BA. Non-complement- and complement-activating antibodies synergize to cause rejection of cardiac allografts. *Am J Transplant*. 2004;4(3):326-334.
33. Mulder A, Kardol MJ, Arn JS, et al. Human monoclonal HLA antibodies reveal interspecies crossreactive swine MHC class I epitopes relevant for xenotransplantation. *Mol Immunol*. 2010;47(4):809-815.
34. Sosa RA, Zarrinpar A, Rossetti M, et al. Early cytokine signatures of ischemia/reperfusion injury in human orthotopic liver transplantation. *JCI Insight*. 2016;1(20):e89679.
35. Mosser DM, Edwards JP. Exploring the full spectrum of macrophage activation. *Nat Rev Immunol*. 2008;8(12):958-969.
36. Martinez FO, Sica A, Mantovani A, Locati M. Macrophage activation and polarization. *Front Biosci*. 2008;13:453-461.
37. Gordon S, Martinez FO. Alternative activation of macrophages: mechanism and functions. *Immunity*. 2010;32(5):593-604.
38. Murray P, Allen J, Biswas S, et al. Macrophage activation and polarization: nomenclature and experimental guidelines. *Immunity*. 2014;41(1):14-20.
39. Rehman A, Hemmert KC, Ochi A, et al. Role of fatty-acid synthesis in dendritic cell generation and function. *J Immunol*. 2013;190(9):4640-4649.
40. Williams MR, Sakurai Y, Zughaier SM, Eskin SG, McIntire LV. Transmigration across activated endothelium induces transcriptional changes, inhibits apoptosis, and decreases antimicrobial protein expression in human monocytes. *J Leukoc Biol*. 2009;86(6):1331-1343.
41. Lee C-Y, Lotfi-Emran S, Erdinc M, et al. The involvement of FcR mechanisms in antibody-mediated rejection. *Transplantation*. 2007;84(10):1324-1334.
42. Bruhns P. Properties of mouse and human IgG receptors and their contribution to disease models. *Blood*. 2012;119(24):5640-5649.
43. Fuentes-Duculan J, Suárez-Fariñas M, Zaba LC, et al. A subpopulation of CD163-positive macrophages is classically activated in psoriasis. *J Invest Dermatol*. 2010;130(10):2412-2422.
44. Mantovani A, Sica A, Sozzani S, Allavena P, Vecchi A, Locati M. The chemokine system in diverse forms of macrophage activation and polarization. *Trends Immunol*. 2004;25(12):677-686.
45. Ambarus CA, Krausz S, van Eijk M, et al. Systematic validation of specific phenotypic markers for in vitro polarized human macrophages. *J Immunol Methods*. 2012;375(1–2):196-206.
46. Ambarus CA, Santegoets KCM, van Bon L, et al. Soluble immune complexes shift the TLR-induced cytokine production of distinct polarized human macrophage subsets towards IL-10. *PLoS ONE*. 2012;7(4):e35994.
47. Xia CQ, Kao KJ. Heparin induces differentiation of CD1a+ dendritic cells from monocytes: phenotypic and functional characterization. *J Immunol*. 2002;168(3):1131-1138.
48. Italiani P, Boraschi D. From monocytes to M1/M2 macrophages: phenotypical vs. functional differentiation. *Front Immunol*. 2014;5:514.
49. Tso C, Rye KA, Barter P. Phenotypic and functional changes in blood monocytes following adherence to endothelium. *PLoS ONE*. 2012;7(5):e37091.
50. Thomas-Ecker S, Lindecke A, Hatzmann W, Kaltschmidt C, Zänker KS, Dittmar T. Alteration in the gene expression pattern of primary monocytes after adhesion to endothelial cells. *Proc Natl Acad Sci USA*. 2007;104(13):5539-5544.

51. Finn AV, Nakano M, Polavarapu R, et al. Hemoglobin directs macrophage differentiation and prevents foam cell formation in human atherosclerotic plaques. *J Am Coll Cardiol*. 2012;59(2):166-177.
52. Reyes-Vargas E, Pavlov IY, Martins TB, Schwartz JJ, Hill HR, Delgado JC. Binding of anti-HLA class I antibody to endothelial cells produce an inflammatory cytokine secretory pattern. *J Clin Lab Anal*. 2009;23(3):157-160.
53. Naemi FM, Carter V, Kirby JA, Ali S. Anti-donor HLA class I antibodies: pathways to endothelial cell activation and cell-mediated allograft rejection. *Transplantation*. 2013;96(3):258-266.
54. Roca H, Varsos ZS, Sud S, Craig MJ, Ying C, Pienta KJ. CCL2 and interleukin-6 promote survival of human CD11b+ peripheral blood mononuclear cells and induce M2-type macrophage polarization. *J Biol Chem*. 2009;284(49):34342-34354.
55. Mauer J, Chaurasia B, Goldau J, et al. Signaling by IL-6 promotes alternative activation of macrophages to limit endotoxemia and obesity-associated resistance to insulin. *Nat Immunol*. 2014;15(5):423-430.
56. Sierra-Filardi E, Nieto C, Domínguez-Soto Á, et al. CCL2 shapes macrophage polarization by GM-CSF and M-CSF: identification of CCL2/CCR2-dependent gene expression profile. *J Immunol*. 2014;192(8):3858-3867.
57. Li N, Qin J, Lan L, et al. PTEN inhibits macrophage polarization from M1 to M2 through CCL2 and VEGF-A reduction and NHERF-1 synergism. *Cancer Biol Ther*. 2015;16(2):297-306.
58. Chimen M, Yates CM, McGettrick HM, et al. Monocyte subsets coregulate inflammatory responses by integrated signaling through TNF and IL-6 at the endothelial cell interface. *J Immunol*. 2017;198(7):2834-2843.
59. Ricardo SD, van Goor H, Eddy AA. Macrophage diversity in renal injury and repair. *J Clin Invest*. 2008;118(11):3522-3530.
60. Jones CV, Ricardo SD. Macrophages and CSF-1: implications for development and beyond. *Organogenesis*. 2013;9(4):249-260.
61. Preuss I, Ludwig M-G, Baumgarten B, et al. Transcriptional regulation and functional characterization of the oxysterol/EBI2 system in primary human macrophages. *Biochem Biophys Res Commun*. 2014;446(3):663-668.
62. Xiong W, Wang H, Lu L, et al. The macrophage C-type lectin receptor CLEC5A (MDL-1) expression is associated with early plaque progression and promotes macrophage survival. *J Transl Med*. 2017;15(1):234.
63. Haas M, Loupy A, Lefaucheur C, et al. The Banff 2017 Kidney Meeting Report: revised diagnostic criteria for chronic active T cell-mediated rejection, antibody-mediated rejection, and prospects for integrative endpoints for next-generation clinical trials. *Am J Transplant*. 2018;18(2):293-307.
64. Berry GJ, Burke MM, Andersen C, et al. The 2013 International Society for Heart and Lung Transplantation Working Formulation for the standardization of nomenclature in the pathologic diagnosis of antibody-mediated rejection in heart transplantation. *J Heart Lung Transplant*. 2013;32(12):1147-1162.
65. Parkes MD, Halloran PF, Hidalgo LG. Evidence for CD16a-mediated NK cell stimulation in antibody-mediated kidney transplant rejection. *Transplantation*. 2017;101(4):e102-e111.

SUPPORTING INFORMATION

Additional supporting information may be found online in the Supporting Information section.

How to cite this article: Wei X, Valenzuela NM, Rossetti M, et al. Antibody-induced vascular inflammation skews infiltrating macrophages to a novel remodeling phenotype in a model of transplant rejection. *Am J Transplant*. 2020;20:2686–2702. https://doi.org/10.1111/ajt.15934

Chapter 4 – HLA Class I Antibody-activated Endothelium Mediates Monocyte Polarization into CD206+ M2-Macrophages with MMP9 Secretion via TLR4 Signaling and P-selectin

Abstract

HLA donor-specific antibodies (DSA) elicit a cascade of alloimmune responses against the graft vasculature, leading to endothelial cell (EC) activation and monocyte infiltration during antibody-mediated rejection (AMR). Recurrent AMR episodes promote chronic inflammation and remodeling, leading to thickening of the arterial intima or cardiac allograft vasculopathy (CAV). Intragraft-recipient macrophages serve as a diagnostic marker in AMR however, their mechanisms of polarization and function remain unclear. In this study, we utilized an *in vitro* transwell co-culture system to explore the mechanisms of monocyte-to-macrophage polarization induced by HLA I DSA activated ECs. Anti-HLA I (IgG or $F(ab')_2$) antibody-activated ECs induced the polarization of M2-macrophages with increased CD206 expression and MMP9 secretion. However, inhibition of TLR4 signaling or PSLG-1-P-selectin interactions significantly decreased both CD206 and MMP9. Monocyte adherence to Fc-P-selectin coated plates induced M2-macrophages with increased CD206 and MMP9. Moreover, FcyR-IgG interactions synergistically enhanced both pro- and active-MMP9 in conjunction with P-selectin. Transcriptomic analysis of arterial regions from DSA+CAV+ rejected cardiac allografts and multiplex-immunofluorescent staining illustrated the expression of CD68+CD206+CD163+MMP9+ M2-macrophages within the neointima of CAV affected lesions. These findings reveal a novel mechanism linking HLA I antibody-activated endothelium to the generation of M2-macrophages which secrete vascular remodeling proteins contributing to AMR and CAV pathogenesis.

Introduction

Antibody-mediated rejection (AMR) remains a significant clinical challenge impacting both long-term allograft and patient survival post-transplantation. AMR is defined by multifaceted immunological responses which are primarily driven by donor-specific antibodies (DSA) targeting polymorphic human leukocyte antigens (HLA I and HLA II) on the graft vasculature. Specifically, DSA promotes the recruitment and activation of circulating leukocytes (e.g., T-cells, monocytes, and NK-cells), and triggers complement activation resulting in endothelial cell (EC) injury[4,5]. In cardiac allografts, AMR is diagnosed using endomyocardial biopsies (EMBs) and is characterized by distinct features including EC swelling, microvascular inflammation (subendothelial mononuclear infiltration), presence of intravascular CD68+ macrophages, and potential complement C4d deposition[10]. Repeated episodes of AMR contribute to a persistent state of chronic inflammation, triggering vascular remodeling characterized by the migration and proliferation of ECs and smooth muscle cells[20]. This pathological process leads to the progressive thickening of the intimal layer and eventual occlusion of the vasculature, a condition referred to as cardiac allograft vasculopathy (CAV)[20,24].

HLA DSA can further enhance AMR and contribute to the development of CAV by activating EC intracellular signaling cascades and facilitating the recruitment of infiltrating monocytes. For example, HLA I DSA can trigger EC signaling pathways such as FAK/Src, PI3K/AKT, and mTOR leading to EC proliferation, migration, and upregulation of survival proteins (BCL-2 and BCL-XL)[12,13,65,66]. Moreover, HLA I out-side-in signaling can stimulate EC cytoskeletal rearrangements (via mTOR, RhoA/ROCK) resulting in increased clustering of ICAM-1 at the cell surface, thereby facilitating firm adhesion of monocytes to ECs[14]. In addition, our recent findings have illustrated that anti-HLA I antibodies stimulate the formation of a molecular complex between HLA I and Toll-like receptor 4 (TLR4) on the surface of ECs[16]. TLR4 signaling via adaptor proteins (MyD88 and TIRAP) results in Weibel-Palade bodies (WPBs) exocytosis of P-selectin thereby mediating

monocyte tethering at the surface of ECs[16]. Monocyte and EC adhesive interactions mediated by PSGL-1 and P-selectin are further strengthened through interactions between the Fc portion of HLA I IgG and Fcy-receptors (FcyRs) expressed on monocytes[17,19].

In both preclinical and clinical studies, graft-infiltrating monocytes and macrophages have been consistently linked to poorer outcomes in kidney and heart transplantation[28-32]. Macrophages accumulate within the vascular lumens in EMBs and have been observed to increase in density during episodes of AMR and HLA DSA[10,67]. Macrophages can also be found within the neointima and adventitia of CAV affected lesions in both rejected human cardiac allografts and mouse models of chronic AMR[22,68]. Despite the high prevalence of macrophages in rejecting allografts, their mechanisms of polarization, phenotype, and function remain elusive. In general, M1 macrophages have been linked to acute rejection as they secrete pro-inflammatory cytokines, generate harmful reactive oxygen species (ROS), and exhibit expression of co-stimulatory molecules (e.g., CD80/CD86) which can amplify T-cell mediated activation[9,47]. Conversely, M2 macrophages (subdivided into M2a, M2b, and M2c) are linked with chronic rejection as they promote tissue remodeling through the secretion anti-inflammatory cytokines, pro-angiogenic growth factors (e.g., TGF-α, VEGF, and PDGF), and matrix metalloproteinases (MMPs)[9,44,47]. Nonetheless, recent studies have emphasized the oversimplification of the M1/M2 paradigm in transplantation, as macrophages can be activated by various environmental stimuli and exhibit remarkable plasticity[69,70]. Moreover, only a limited number of studies have specifically investigated macrophage polarization and function in the context of HLA DSA activated endothelium[71-73].

Studies in our lab have revealed that anti-HLA I antibody-activated ECs induce monocyte polarization into M2-like macrophages through both Fc-dependent and Fc-independent mechanisms[71]. In an *in vitro* co-culture model using transwell inserts, monocytes which transmigrated across anti-HLA I $F(ab')_2$ antibody-activated ECs differentiated into CD206+ (mannose receptor C type 1 (MRC1)) M2-like macrophages after 5 days of co-culture. Meanwhile,

monocytes that transmigrated across anti-HLA I IgG antibody-activated ECs differentiated into M2-like CD206+ macrophages with an added increase in CD163 (hemoglobin scavenger receptor). Given that monocytes undergo multiple adhesive interactions during trans endothelial cell transmigration, we investigated whether EC adhesion molecules, such as P-selectin, which are upregulated in response to HLA I DSA impact M2-macrophage polarization. Moreover, building on our previous findings demonstrating that HLA I DSA triggers EC signaling via TLR4, resulting in increased surface expression of P-selectin, we furthered explored whether blocking TLR4 signaling or inhibiting PSGL-1-P-selectin interactions would impede M2-macrophage polarization and M2-related functions.

In this study, we found that blocking TLR4 signaling or inhibiting PSGL-1-P-selectin interactions decreased CD206 expression and MMP9 secretion in anti-HLA I (IgG or $F(ab')_2$) antibody-activated EC polarized macrophages. These results reinforce our previous findings indicating that CD206 expression is not dependent on Fc-interactions. Moreover, our findings suggest that P-selectin plays a pivotal role in regulating M2-macrophage phenotype and function in a model of vascular inflammation induced by anti-HLA I DSA. We also validated the expression of CD68+CD206+CD163+MMP9+ M2-macrophages within vessels of CAV+DSA+ rejected cardiac allografts. In conclusion, we propose a novel mechanism by which HLA I antibody-activated endothelium promotes the generation of M2-macrophage with the capacity to secrete proteins involved in vascular remodeling, thereby contributing to the development of CAV.

Materials and Methods

Study Approval

This study was approved by the University of California, Los Angeles Institutional Review Board IRB#18-001275. Formalin-fixed paraffin embedded (FFPE) tissue from rejected cardiac allografts were provided by the UCLA Translational Pathology Core Lab (TPCL).

HLA I antibodies and primary EC lines

Human monoclonal allele-specific antibodies against HLA-A2/A28 (IgG1, clone SN607D8) and A3/A11/A24 (IgG1, clone MUL2C6) were derived from human hybridomas and purified via protein A chromatography were kindly provided by Dr. Sebastiaan Heidt[74]. HLA I $F(ab')_2$ fragments were generated using FabRICATOR/IdeS (Genovis) in accordance with the manufacturer's protocol. The binding capacities HLA I IgG and HLA I $F(ab')_2$ antibodies have been previously validated via flow cytometry[71]. Primary human aortic ECs were isolated from the aortic rings of deceased donor hearts (B114) or were obtained from ATCC (3F1153), and cultured as previously described[19,71,75]

Transwell co-culture

The transwell co-culture model used in this study has been previously reported by Xuedong et al., *AJT* 2020[71]. Briefly, ECs ($0.2x10^5$) were plated in complete M199 medium in the upper chamber of 0.1% Gelatin coated transwell inserts (3-µm size pore, Corning) in 24-well plates on day -1. On day 0, ECs were incubated with M199 + 0.2% FBS for four hours followed by stimulation with HLA I IgG or HLA I $F(ab')_2$ (1µg/mL), hIgG isotype control (1µg/mL) (Sigma-Aldrich), or left untreated for 1 hour. To simulate the activation of ECs by allele-specific HLA I DSA, EC3F1153 were stimulated by HLA-A2 and B114 were stimulated with HLA-A3 antibodies in accordance with EC HLA typing[71]. After stimulation, ECs were washed to removed unbound antibodies and placed in complete RPMI 1640 + 10% FBS. Then, freshly isolated human primary monocytes (0.5×10^5) were plated above ECs in transwell insert (2.5 monocytes per 1 EC ratio) and incubated for 5 days. Half of the media was replenished on days 2 and 4. On day 5, cells in the bottom chamber were detached and stained for phenotype analysis. TLR4 pharmacological inhibitor TAK242 (1µM) or anti-P-selectin blocking antibody (5ug/mL) (R&D Systems) were added for 30 minutes prior to stimulating ECs with HLA I antibodies. For validation experiments, monocytes were pre-incubated with r-PSGL-1-Ig antibody (20 ug/mL) prior to seeding in transwell

insert as previously described[17]. Knockdown of EC TLR4 via SiRNA prior to plating in transwell insert was performed as previously described[16].

Macrophage polarization using solid-phase assay.

On day -1, 96-well plates were coated with of Fc-P-selectin or Fc-ICAM-1 chimeric proteins (10 µg/mL) (R&D Systems), hIgG isotype control (10 µg/mL), 5% BSA, or ELISA reaction buffer (50mM carbonate-bicarbonate) used to coat plates (Bioworld) and placed at 4℃ overnight. On day 0, all wells were blocked with 5% BSA for >30 minutes at room temperature and washed twice with 1x PBS. Freshly isolated primary monocytes (0.5×10^5) were plated in complete RPMI 1640 + 10% FBS medium for 5 days. For Fc-blocked conditions, monocytes were pre-treated with Fc-receptor blocking solution (BioLegend) as recommended by manufacturer (5µL of Fc-block per 1×10^6 cells). Half of the media was replenished on days 2 and 4. Cells were detached using Accutase (Innovative Cell) and collected for phenotype analysis. Cytokine polarized (M1, M2a, M2b, M2c, and mDC) macrophages were generated as previously described[71].

Flow cytometry phenotype analysis

Collected cells were first stained with Live/Dead fixable blue cell stain kit (Invitrogen) following manufacturer's protocol to determine viability. Cells were then washed twice with 1x PBS and incubated for 30 minutes with CD206-APC/Cy7 (clone 15-2) (BioLegend) at 4C. Stain cells were acquired on an LSRFortessa™ (BD Biosciences, San Jose, CA) flow cytometer and data was analyzed using FlowJo version 10.8.

MMP9 Western blot and Elisa Assays

The preparation of cell lysates for Western blot was carried as previously described[76]. Briefly, cells were lysed using 2x Laemmli SDS Sample buffer (Bio-Rad) + Dithiothreitol (DTT). After resolving the cell lysates through SDS-PAGE overnight, the proteins were transferred onto polyvinylidene difluoride membranes (Millipore) for 2 hours. The membranes were blocked using

5% nonfat dry milk in TBS (pH 7.4) containing 0.05% Tween 20 (TBST) for 1 hour at room temperature and incubated overnight with MMP9 antibody (9D4.2) Pro and Active (Millipore Sigma) at 2ug/mL (1:500) dilution or with GAPDH antibody (0411) (Santa Cruz Biotech) at 1:2000 dilution. The blots were then incubated with HRP-conjugated secondary antibodies and developed with ELC (Bio-Rad). The protein bands were scanned using Epson Perfection V700 photo scanner (Epson) and were quantified using ImageJ program. MMP9 secretion from transwell cell culture supernatants (at day 4) was examined using human MMP9 ELISA Kit (Abcam (ab246539)) following manufacturer's protocol.

RNA Digital Spatial Profiling (DSP), data normalization, and deconvolution.

Whole transcriptomic digital spatial profiling (DSP) of arterial regions from CAV+DSA+ rejected cardiac allografts (N=3; 2 females, 1 male) was performed by NanoString Technologies (Seattle, WA) as part of the Technology Access Program (TAP) as per Merritt et al., *Nat Biotechnol* 2020[77]. Briefly, FFPE slides underwent mild proteinase K digestion followed by incubation with a whole transcriptome cocktail (18,504 transcripts) of UV-(PC)-oligonucleotide-labeled mRNA probes. After hybridization steps, slides were loaded into the DSP instrument and geometric AOIs were selected based on the presence CD68+ CD163+ macrophages localized within CD34+ arterial vessels as previously determined via immunofluorescent staining. To analyze AOIs, a programmable digital micromirror device (DMD) was employed. This enabled the precise illumination of the AOI with UV light, facilitating region-specific release of PC-oligos. The released indexing oligonucleotides were gathered through microcapillary aspiration, placed into a microplate, and then digitally counted utilizing the Next-Generation Sequencing (NGS). The GeoMx analysis suite was used for quality control (QC) and normalization of RNA data. Outlier probes were removed using Grubbs test within a target and AOI (biological probe QC). The data for each AOI was then scaled to the 3rd quartile of all selected targets (Q3) and normalized to the average (+2SD) of negative controls (NegProbe). RNA data is reported as a signal to noise ratio

(SNR) to negative controls (NegProbe). RNA deconvolution for obtaining cell fraction estimates across all arterial AOIs was derived using CIBERSORT as previously described[78].

Multiplex-immunofluorescent staining of cardiac allografts

Multiplex-immunofluorescent staining of cardiac explants was performed by UCLA TPCL. The TSA-based Opal method was used for immunofluorescence (IF) staining (Opal Polaris 7-Color Automation IHC Kit; Akoya Biosciences, Marlborough, MA, USA; Catalogue No. NEL871001KT). Since TSA and DAB oxidation are both peroxidase-mediated reactions, the primary antibody conditions and order of staining determined using DAB detection were directly applied to the fluorescent assays, unlike conventional IHC wherein a chromogenic peroxidase substrate is used for antigen detection, each antibody is paired with an individual Opal fluorophore for visualization. The Opal fluorophores were used at a 1 in 100 dilution, as recommended by Akoya when using the Leica BOND RX. As such, a fluorescent singleplex was performed for each biomarker and compared to the appropriate chromogenic singleplex to assess staining performance. Once each target was optimized in uniplex slides, the Opal 5 multiplexed assay was used to generate multiple staining slides. TMA slides Staining was performed consecutively Leica BOND RX by using the same steps as those used in uniplex IF, and the detection for each marker was completed before application of the next antibody. The sequence of antibodies for multiplex staining was determined for panel combination is: CD31 (opal 480), CD68 (opal 520), CD206 (opal570), CD163 (opal 620), MMP9 (opal 690). All fluorescently labelled slides were scanned on the Vectra Polaris (Akoya Biosciences) at 40× magnification using appropriate exposure times. The data from the multispectral camera were analyzed by the imaging InForm software (Akoya Biosciences).

Statistical analysis

Data presented in **Figure 1**, **Figure 2**, and **Figure 3** was analyzed using paired repeated measures one-way ANOVA (Fisher least significant differences (LSD)) with bar graphs showing ±SEM. Data in **Figure 4** was examined using unpaired repeated measures one-way ANOVA (Fishers LSD) or unpaired student T-test (**Figure 4E**). Statistical significance was determined as $p < 0.05$ (*), $p < 0.01$(**), $p < 0.001$(***) $p < 0.0001$(****)) using GraphPad Prism software v9.0.

Results

Macrophage CD206 expression is induced via TLR4 upregulation of P-selectin in HLA I antibody-activated ECs.

Prior findings in our lab have shown that monocytes co-cultured with HLA I (IgG or F(ab')$_2$) antibody-activated ECs promoted monocyte differentiation into CD206+ M2 macrophages[71]. Moreover, given that HLA I (IgG or F(ab')$_2$) antibodies mediate EC P-selectin surface expression via TLR4 signaling, we questioned whether inhibiting TLR4 signaling or blocking PSGL-1-P-selectin interactions altered macrophage CD206 expression[16]. To simulate the process of monocyte transmigration across HLA I antibody-activated ECs, we utilized our previously published *in vitro* transwell co-culture model[71]. Using this model, monocytes adhere to HLA I (IgG or F(ab')$_2$) antibody-activated ECs (in the top chamber (insert)), and transmigrate (to the bottom chamber) where they differentiate into macrophages over a 5-day period. In this study, ECs were pre-treated with a TLR4 pharmacological inhibitor (TAK242) or an anti-P-selectin blocking antibody prior to (and during) stimulation with HLA I (IgG or F(ab')$_2$). Results show that both HLA I (IgG or F(ab')$_2$) conditions significantly increased macrophage CD206 expression compared to hIgG isotype treated ECs. However, the addition of TAK242 or anti-P-selectin blocking antibody (α-P-selectin Ab) significantly reduced CD206 expression in both HLA I (IgG or F(ab')$_2$) conditions (**Figure 4-1A**). Alternatively, macrophage CD206 expression also decreased when monocytes

were pre-treated with rPSGL-1-Ig (prior to plating in transwell) in both HLA I (IgG or F(ab')$_2$) conditions (**Figure 4-1B**).

To further validate whether HLA I (IgG or F(ab')$_2$) antibody-activated EC signaling via TLR4 drives macrophage CD206 expression, we knocked down EC TLR4 expression using small interfering RNAs (siRNA). Results illustrated that knockdown of TLR4 significantly reduced CD206 expression compared to HLA I (IgG or F(ab')$_2$) control SiRNA conditions (**Figure 4-1C**).

Finally, to confirm the specificity of P-selectin in eliciting macrophage CD206 expression, we employed a solid-phase assay in which culture plates were coated with Fc-P-selectin or Fc-ICAM-1, chimeric proteins. Monocytes were pre-treated with Fc-receptor block to eliminate Fc-receptor interactions and plates coated with hIgG antibody isotype (containing an Fc-portion) were used as controls. Following a five-day culture, monocytes cultured in Fc-P-selectin coated plates exhibited a significant increase in CD206 macrophage expression compared to macrophages polarized in plates coated with coating buffer only, hIgG isotype control, and 5% BSA (**Figure 4-1D**). Moreover, macrophages polarized in Fc-ICAM-1 protein coated plates did not significantly increase CD206 expression, further suggesting that upregulation of CD206 by macrophages is P-selectin specific.

MMP9 is upregulated in HLA I (IgG or F(ab')$_2$) co-cultures and is regulated by TLR4 and P-selectin.

High levels of MMP9 in rejecting allografts have been associated with driving inflammatory and fibrotic responses in both AMR and CAV pathogenesis[79,80]. Given that M2-macrophages are known to secrete MMP9, we investigated whether macrophages polarized by HLA I (IgG or F(ab')$_2$) antibody-activated ECs also showed elevated levels of MMP9 secretion. Cell culture supernatants from our transwell *in vitro* co-culture model were collected on day 4 assessed for MMP9 secretion using ELISA. Results indicated that both HLA I (IgG or F(ab')$_2$) antibody-

activated EC conditions displayed a significant increase in MMP9 secretion compared to UT and hIgG isotype controls (**Figure 4-2A**). Cytokine polarized M2a (IL-4) macrophages (which we have shown to exhibit high expression of CD206) also displayed moderate MMP9 secretion[71]. Nevertheless, M2b (hIgG + LPS) polarized macrophages exhibited the highest levels of MMP9 secretion compared to all conditions.

To determine if TLR4 signaling and/or P-selectin surface expression in HLA I (IgG or $F(ab')_2$) antibody-activated EC conditions contributed to the observed increased in MMP9, we assayed supernatants from transwell experiments that employed TAK242 and α-P-selectin Ab via ELISA. Results revealed that the addition of either TAK242 or α-P-selectin Ab significantly reduced MMP9 secretion in both HLA I (IgG or $F(ab')_2$) conditions (**Figure 4-2B**). Supernatants from untreated ECs only or EC + HLA I $F(ab')_2$ did not secrete MMP9.

Monocyte interactions with Fc-P-selectin and hIgG induce macrophage pro- and active-MMP9 expression.

To validate the specificity of P-selectin in eliciting macrophage MMP9 expression, we used our solid phase assay as seen in **Figure 4-1D**. Given that ELISA results measured overall MMP9 secretion and MMP9 can exist in both pro and active forms, we utilized Western blot analysis to determine which form of MMP9 was produced by macrophages (**Figure 4-3A**). Monocytes were left untreated or pre-treated with Fc-block before plating in Fc-P-selectin or hIgG isotype coated plates. Results illustrated that both pro (92kDa) and active (82kDa) forms of MMP9 were significantly increased when macrophages were cultured on Fc-P-selectin coated plates compared to plates coated with coating buffer and 5% BSA, under both untreated and Fc-blocked conditions (**Figure 4-3B**). Moreover, plates coated with hIgG also exhibited higher levels of both pro and active MMP9, although levels were reduced in Fc-blocked compared to untreated conditions. Notably, all conditions showed decreased levels of pro and active MMP9 in Fc-blocked compared to untreated conditions (**Figure 4-3C**). These findings suggested that while P-selectin

alone induces MMP9 expression, additional stimuli via FcyRs may act synergistically to further increase in MMP9 expression.

Arterial regions from rejected cardiac allografts exhibit M2-macrophage transcripts and MMP9 as a top M2-macrophage associated gene.

In order to examine the expression of M2-macrophage associated transcripts within CAV affected lesion, a total of 14 arterial regions of interest (AOIs) from CAV+DSA+ rejected cardiac allografts (N=3; 1 male, 2 female) were subjected to whole transcriptomic analysis via DSP. Arterial regions were selected on the presence of CD68+CD163+ macrophages localized within CD34+ vessels (**Figure 4-4A**). The expression of *CD68*, *CD206* (*MRC1*), and *CD163* were significantly elevated compared to internal negative RNA probes (NegProbe) (**Figure 4-4B**). Additionally, activating FcyRs known to be expressed in circulating monocytes (and NK cells) such as *FCGR1A* (CD64) and *FCGR3A* (CD16) were also significantly increased compared to NegProbe. The expression of activating FcyRs was significantly higher compared the inhibitory FcyR, *FCGR2B*. *FCGR2B* was not significantly elevated compared NegProbe. CIBERSORT RNA data deconvolution furthered revealed that M2-macrophages exhibited the broadest distribution across all arterial regions and were significantly elevated compared to M0 macrophages (**Figure 4-4C**). Top M2 associated-transcripts included remodeling proteins/cytokines *MMP9*, *MS4A6S*, *CCL18, and AIF1* while M1 included inflammatory proteins/cytokines *IRF8, CCL4, ADAMDEC1, and HCK* (**Figure 4-4D and Table 4-1**). Notably, MMP9 expression levels across arterial regions was significantly elevated compared NegProbe (**Figure 4-4E**).

CD206+CD163+MMP9+ M2-macrophages are found within vascular neointimal lesions of CAV+DSA+ rejected cardiac allografts

Multiplex-immunofluorescent staining was used to validate the M2-macrophage phenotype observed in our *in vitro* and DSP RNA studies. CAV+DSA+ rejected cardiac allografts used in our

DSP analysis (PID1-3) were stained for M2-macrophage markers. A total of 7/14 vessels examined via DSP contained moderate-to-high levels of neointima formation. We confirmed the presence of CD68+CD206+CD163+ macrophages in arterial regions that exhibited neointimal lesions. Moreover, we validated co-expression of MMP9 in CD206+, CD163+, and double positive cells (**Figure 5**).

Discussion

Recent findings in our lab have demonstrated that anti-HLA I (IgG or F(ab')$_2$) antibody crosslinking to HLA I molecules on ECs stimulates the formation of a molecular complex between HLA I and TLR4. TLR4 signaling triggers the exocytosis of WPBs and surface expression of P-selectin, therefore facilitating monocyte tethering to ECs[16]. In this study, we further illustrated that monocyte stimulation via PSGL-1-P-selectin promotes their polarization into M2-like macrophages with enhanced functionality. Specifically, anti-HLA I (IgG or F(ab')$_2$) antibody-activated EC polarized macrophages significantly increased both CD206 expression and MMP9 secretion. However, when TLR4 signaling or PSGL-1-P-selectin interactions were inhibited, macrophages significantly reduced CD206 and MMP9. While macrophage expression of CD206 and MMP9 was determined to be Fc-independent, our results suggest that activating FcyR-IgG interactions may act synergistically with P-selectin to further increase MMP9 secretion. Concurrently, FcyR-IgG interactions have been shown to promote macrophage expression of CD163 when co-culture with anti-HLA I IgG antibody-activated ECs[71]. Considering these findings, we found evidence of CD68+ macrophages co-expressing CD206, CD163, and MMP9 within arterial lesions of CAV+DSA+ human rejected cardiac allografts.

While studies investigating the influence of vascular interactions on monocyte-to-macrophage polarization remain limited, existing studies substantiate the concept that activated ECs can induce transcriptional changes in monocytes as well as guide their differentiation into M2-like macrophages. Specifically, interactions during trans endothelial cell migration can activate

extensive intracellular signaling cascades in both EC and monocytes in order to promote the directional and efficient migration/extravasation of monocytes across the vessel wall[37,38,81]. Moreover, mouse-derived primary ECs have been shown to provide a selective niche for the polarization of hematopoietic progenitor cells into pro-angiogenic M2-like macrophages with increased *CD206/MRC1* and *VEGFA* expression[82]. Furthermore, a recent study identified that anti-HLA II $F(ab')_2$ antibody-activated ECs co-cultured with peripheral blood mononuclear cells (PBMCs) for 5-days promoted monocyte differentiation into CD68+CD163+ M2-macrophages[72].

Our findings pinpoint P-selectin as a principal regulator of monocyte activation during monocyte transmigration across anti-HLA I (IgG or $F(ab')_2$) antibody-activated ECs. Prior studies have highlighted the capacity of P-selectin as a potent regulator of cell function in various immune cell types[83,84]. Specifically, macrophage adherence activates PSGL-1/Akt/mTOR-dependent signaling, promoting macrophage chemotaxis and phagocytosis[85]. Similarly, monocyte adherence to P-selectin induces PSGL-1/mTOR/eIF4E signaling regulating the surface protease receptor, UPAR which recognizes and binds to the matrix protein, Vitronectin[40]. Monocyte adherence to P-selectin coated plates, as well as interactions with P-selectin expressed on activated platelets, has been shown to induce monocyte secretion of cytokines/chemokines (e.g., TNF-α, IL-6, IL-8, IL-12, and CCL2 (MCP-1)), and tissue factors, which facilitate platelet adherence to ECs[86-89].

Our data proposes a novel mechanistic framework suggesting that anti-HLA I antibody-activated ECs promote the differentiation of M2-like macrophages capable of secreting key vascular remodeling proteins such as MMP9 (**Figure 4-6**). These findings highlight the potential role of these macrophages in exacerbating AMR and CAV pathogenesis. Specifically, MMP9 can directly degrade extracellular matrix (ECM) proteins (e.g., collagen, fibronectin, laminin, etc.) increasing vascular permeability and facilitating SMC migration[90,91]. MMP9 can also activate inflammatory cytokines (e.g., TNF-α and IL-1β) and pro-angiogenic factors (e.g., TGF-β and VEGF) which

contribute to the formation of fibrotic lesions[91]. Although the production of MMP9 by monocytes has been linked to the process of transmigration, our studies specifically identified that PSGL-1-P-selectin interactions act as a main elicitor of MMP9 production upon monocyte tethering to the endothelium[92]. Moreover, increased MMP9 levels are sustained once monocytes polarized into macrophages. In conjunction with these findings, activated platelets (expressing P-selectin) have been shown act as a secondary stimulus enhancing monocyte synthesis of MMP9 when cultured with immobilized ECM proteins such as collagen[93].

Monocyte engagement with Fc-P-selectin induced polarized macrophage secretion of both pro and active forms of MMP9. Although MMP9 is normally synthesized and secreted in a pro-form, there is evidence that MMP9 may also be activated intracellularly[94]. It may also be possible that MMP9 is activated extracellularly and taken back up. Monocytes treated with Fc-receptor block decreased MMP9 secretion compared to untreated, suggesting that activating FcyRs enhance MMP9 secretion. Increased expression of FcyRs on macrophages has been shown to results in higher production of MMPs in rheumatoid arthritis[95]. Concurrently, M2b macrophages which are polarized by immune complexes (hIgG + LPS) exhibited the highest secretion of MMP9.

Various *in vitro* and *in vivo* studies have emphasized the benefits of inhibiting PSGL-1-P-selectin axis in rejecting allografts[18,96-99]. Particularly, our group has demonstrated that administration of rPSGL-1-Ig markedly decreases antibody-induced monocyte infiltration in a mouse cardiac allograft model of AMR[18]. Nonetheless, findings in this study suggest that inhibiting P-selectin may have broader implications, as it may also regulate the function of intra-graft macrophages. Moreover, our studies underscore TLR4 as a novel therapeutic approach that could be used to regulate HLA I antibody-activated EC signaling, monocyte infiltration, and macrophage polarization. Targeting TLR4 in combination with concurrent therapies may allow for new avenues for inhibiting the multiple mechanisms of HLA antibody-mediated injury and fibrotic lesion development.

Both transcriptomic analysis via DSP and multiplex-immunofluorescent staining validated the expression of CD68+CD206+CD163+MMP9+ M2-like macrophages within neointimal lesions of CAV+DSA+ rejected cardiac allografts. Moreover, we identified positive expression of activating FcyRs (CD64 and CD16), further suggesting the potential involvement of FcyR-IgG interactions in the activation of monocytes. Prior studies have indicated the presence of M2-macrophages in rejecting allografts[100-103]. For example, kidney allograft biopsies from patients with chronic-active AMR showed a predominance of CD163+ macrophages (68%)[101]. This macrophage phenotype was also observed within fibrotic areas of biopsies from patients with chronic kidney allograft injury[102]. Moreover, a study by Chatterjee et al., illustrated the expression of CD68+CD163+CD206+ macrophages within CAV lesions along with the expression of IL-10[103]. A recent transwell *in vitro* study has shown that anti-HLA II $F(ab')_2$ antibody-activated ECs increase secretion of IL-10, which promotes macrophage expression of CD163[72]. Finally, the expression of *MRC1* (CD206) and *MMP9* were found to be significantly higher within the neointimal luminal layer in CAV rejecting grafts compare to non-transplanted (control) hearts[104]. Although it is possible that macrophage production of MMP9 may be induced by other stimuli, such as Th1 cells which can induce macrophage secretion of MMP9 *in vitro*, our studies highlight an alternative mechanism by which HLA I DSA may also induce pro-fibrotic functions in macrophages[105].

Further studies are needed to fully understand the mechanisms of macrophage polarization by anti-HLA I antibody-activated ECs during AMR and CAV development. For example, although we have previously shown that HLA I (IgG and $F(ab')_2$) transwell co-cultures exhibit distinct cytokine/chemokine profiles, the cytokines/chemokines regulated by TLR4 signaling or by P-selectin adhesion remain to be determined. Also, it remains essential to validate the catalytic potential of MMP9 secreted by co-cultured macrophages. Additionally, this study utilized ECs isolated from human aortic rings as oppose microvascular or coronary ECs which are normally

found in EMBs or CAV lesions, respectively. Finally, this study only focused on examining how HLA I DSA-activated ECs guide macrophage polarization, whereas the mechanisms of macrophage polarization by HLA II DSA remains to be determined.

In conclusion, our findings elucidate the mechanisms by which HLA I antibody-activated ECs induce macrophage expression of CD206 and MMP9 secretion via TLR4 mediated P-selectin surface expression. FcyR-IgG interactions may also act synergistically with P-selectin to further increase MMP9. The presence of CD68+ M2-macrophages co-expressing CD206, CD163, and MMP9 within neointimal lesions is likely to have a substantial impact on exacerbating the severity of AMR episodes and promoting vascular remodeling in CAV.

Acknowledgements

The authors would like to extend their gratitude to the organ donors and their families for their generous gifts of life and knowledge. We express our thanks to the NanoString Technology Access Program (TAP) and UCLA TPCL for their resources. The authors would like to acknowledge Dr. Yunfeng Li for her expertise on multiplex-immunofluorescence staining.

Sources of Funding

This study was funded by the NIH Grant R01AI135201 (EFR, NMV, and RLF), NIH Grant R21AI156592 (EFR and RLF), the NIH Ruth L. Kirschstein National Research Service Award (NRSA) T32HL069766 (JNM), and the UCLA Eugene V. Cota Robles Fellowship (JNM).

Author contributions

JNM, EFR, and NMV designed the research study. JNM and YPJ performed experiments and data analysis. JNM, HCP, and RP analyzed transcriptomic data. RAS and GAF identified patient allografts. SH provided HLA I antibodies. ER, WMB and RLF provided feedback and contributed to the design of the study. All authors read and approved the manuscript.

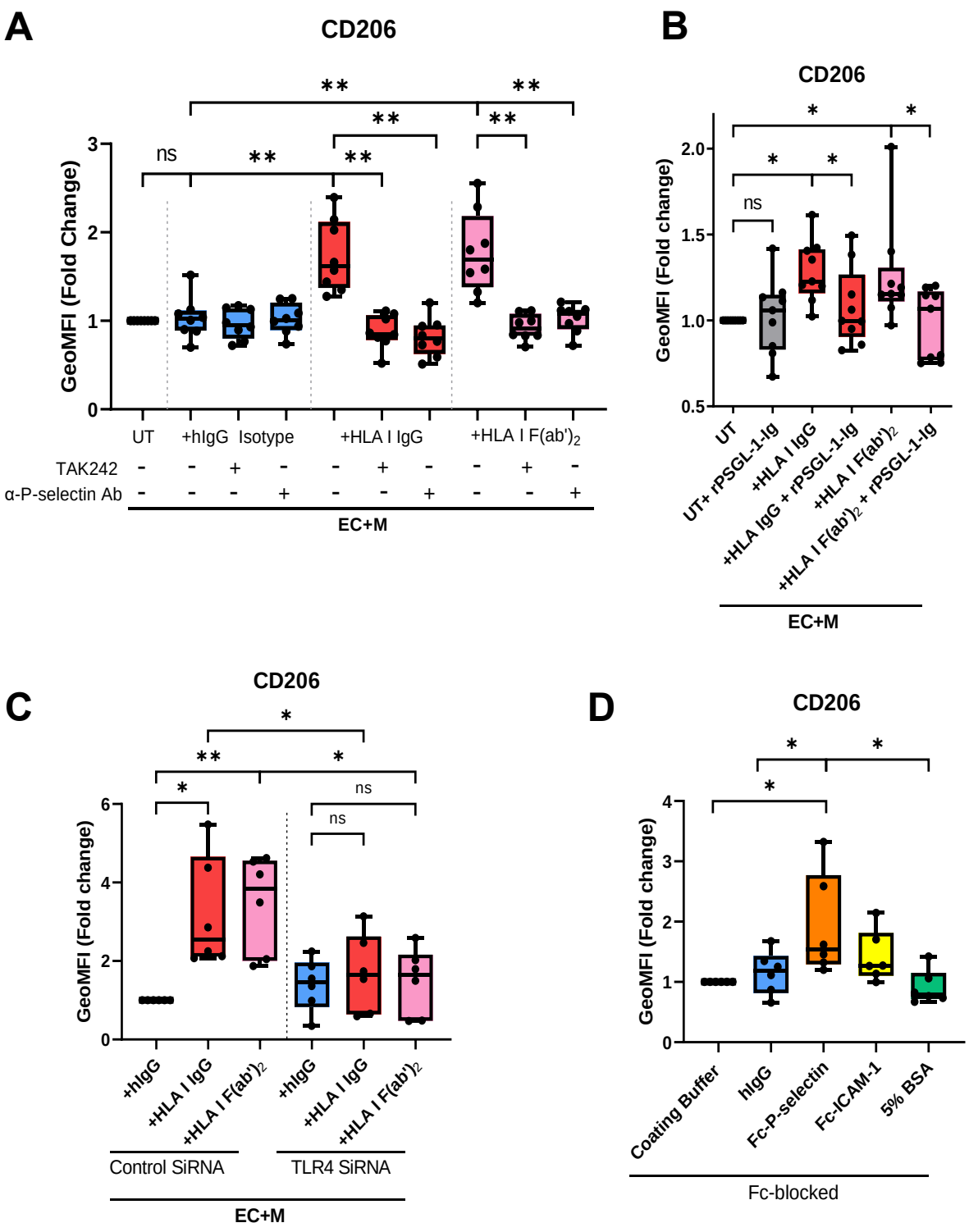
A
CD206
GeoMFI (Fold Change)
ns
UT
+hIgG Isotype
+HLA I IgG
+HLA I F(ab')2
TAK242
α-P-selectin Ab
EC+M
B
CD206
GeoMFI (Fold change)
UT
UT+ rPSGL-1-Ig
+HLA I IgG
+HLA IgG + rPSGL-1-Ig
+HLA I F(ab')2
+HLA I F(ab')2 + rPSGL-1-Ig
EC+M
C
CD206
GeoMFI (Fold change)
+hIgG
+HLA I IgG
+HLA I F(ab')2
Control SiRNA
TLR4 SiRNA
EC+M
D
CD206
GeoMFI (Fold change)
Coating Buffer
hIgG
Fc-P-selectin
Fc-ICAM-1
5% BSA
Fc-blocked

Figure 4-1: Upregulation of P-selectin via TLR4 signaling in anti-HLA I (IgG and F(ab')$_2$) antibody-active ECs induces M2-macrophage marker CD206.

A) Transwell (EC+M) co-culture model in which ECs are seeded in the upper chamber (insert) and grown to confluency at day -1. On day 0, ECs are washed and placed in starvation media for 4 hours, followed by stimulation with hIgG isotype, HLA I IgG, or HLA I F(ab')$_2$ (1ug/mL) or left untre ated (UT) for 1 hour. In order to inhibit EC signaling via TLR4 or adhesive interactions via P-selectin, TAK242 (1uM) or α-P-selectin blocking antibody (Ab) (5ug/mL) were added 30 minutes before and during incubation with HLA I antibodies. Next, ECs are washed to removed unbound antibodies and cultured with primary monocytes. Transmigrated cells in the bottom chamber are collected for phenotype analysis on day 5. Half of the media is replenished on days 2 and 4. **A)** EC stimulation with anti-HLA I IgG or F(ab')$_2$ increases M2-macrophage marker CD206. Addition of TAK242 or α-P-selectin Ab significantly reduces CD206 expression. **B)** Monocytes pre-treated with rPSGL-1-Ig antibody (20 ug/mL) prior to plating in transwell insert significantly decrease macrophage expression of CD206 compared to anti-HLA I IgG or HLA I F(ab')$_2$ EC treated conditions. **C)** knockdown of EC TLR4 via SiRNA prior to plating on transwell insert significantly decreased macrophage CD206 expression compared to Control SiRNA ECs. **D)** Monocytes pre-treated with Fc-receptor block and cultured with Fc-P-selectin chimeric protein coated plates (5 days) polarize into macrophages with significantly higher expression of CD206 compared to cells cultured with hIgG isotype coated plates or coating buffer only. Fc-ICAM-1 and 5% BSA coated plates were included as controls. Statistical significance was analyzed by paired repeated measures one-way ANOVA ($p < 0.05$ (*) and $p < 0.01$(**) from N=3 monocyte donors across two EC lines (B114 and 3F1153).

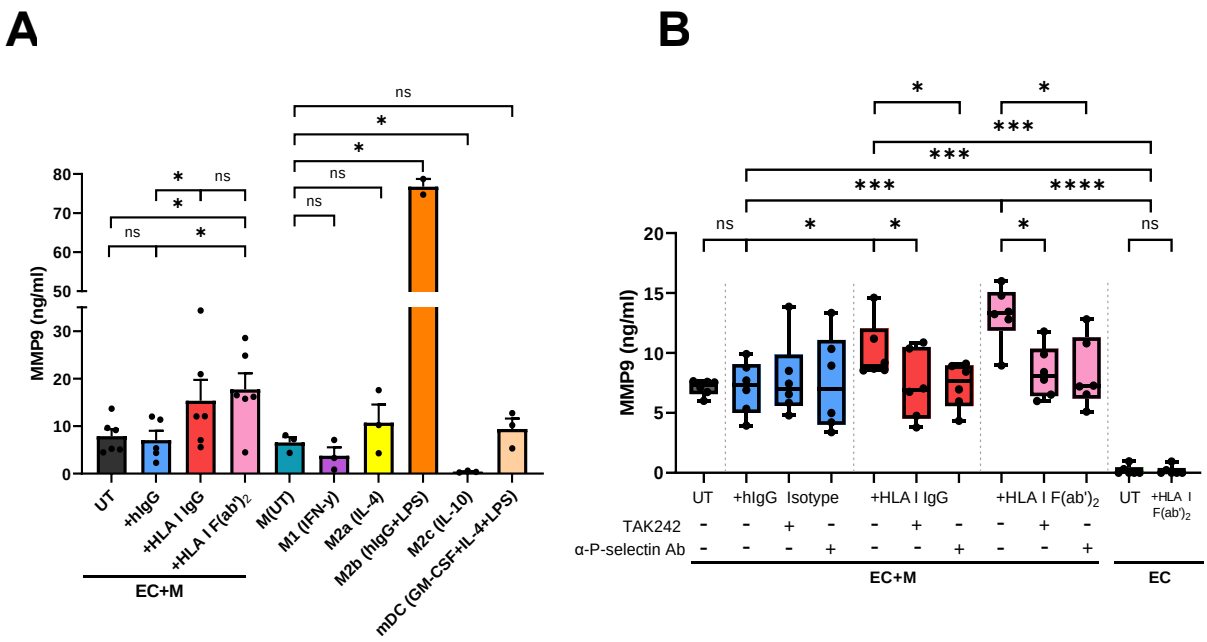

Figure 4-2: Macrophage secretion of MMP9 increases in HLA I (IgG and F(ab')$_2$) antibody-activated EC conditions and is regulated via TLR4 signaling and P-selectin.

A) Transwell (EC+M) co-culture supernatants from day 4 were examined via ELISA assay for MMP9. Anti-HLA I IgG and HLA I F(ab')$_2$ (1ug/mL) EC stimulated conditions significantly increased MMP9 compared to hIgG isotype controls. MMP9 secretion at day 4 from cytokine polarized macrophages (M1 (IFN-γ), M2a (IL-4), M2b (hIgG+LPS), M2c (IL-10), and mDC (GM-CSF+IL-4+LPS)) was also measured as comparative controls. M2b macrophages exhibited the highest secretion of MMP9. **B)** MMP9 secretion in transwell co-cultures (EC+M) significantly decreases in HLA I IgG and HLA I F(ab')$_2$ conditions when inhibiting TLR4 signaling via TAK242 and P-selectin interactions using α-P-selectin Ab. Untreated ECs or ECs + HLA I F(ab')$_2$ supernatants did not secrete MMP9. Data in bar graphs shown as ±SEM. Statistical significance was analyzed by paired repeated measures one-way ANOVA ($p < 0.05$ (*), $p < 0.01$(**), $p < 0.001$(***) $p < 0.0001$(****) from N=3 monocyte donors across two EC lines (B114 and 3F1153)).

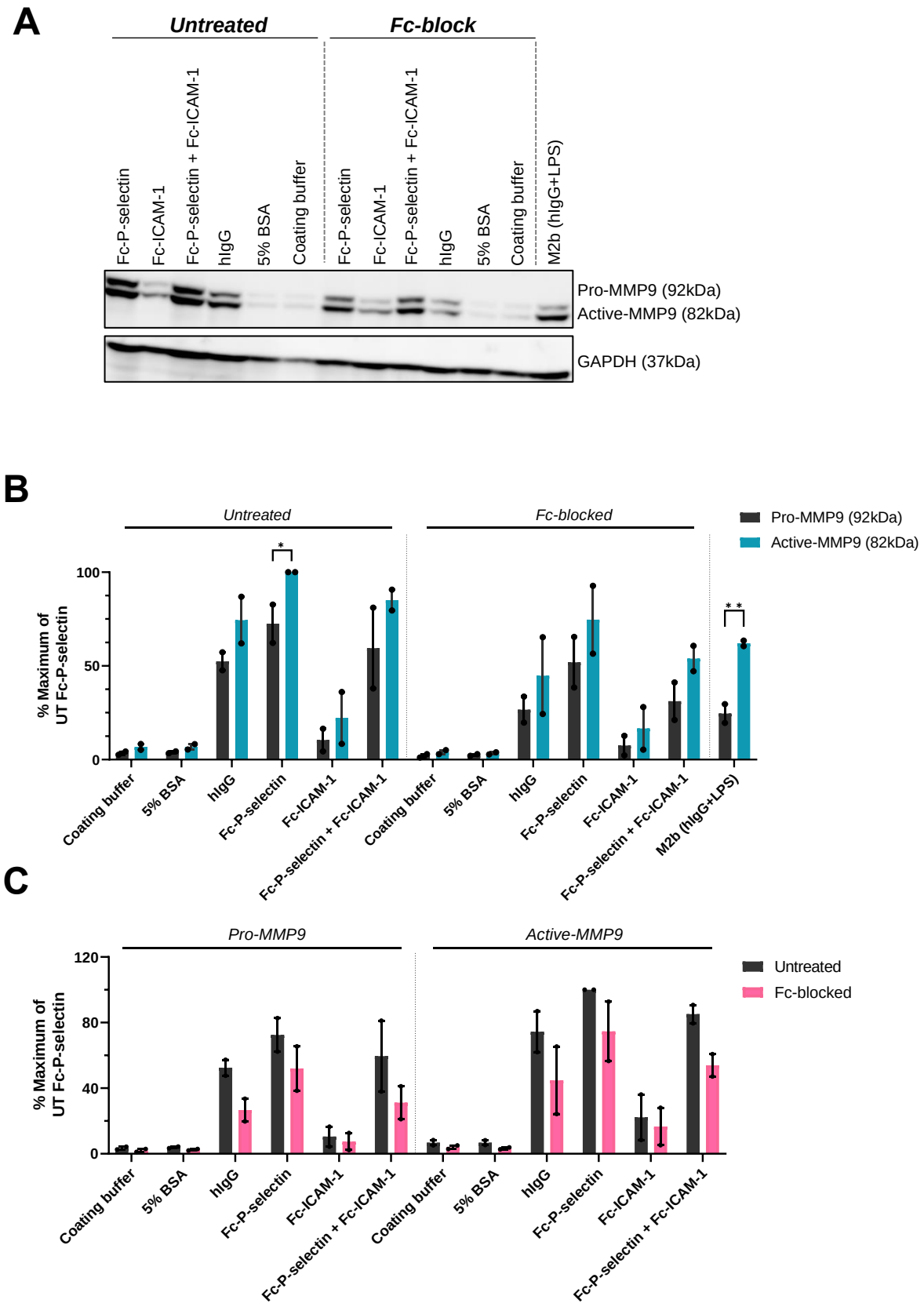
A
Untreated
Fc-block
Fc-P-selectin
Fc-ICAM-1
Fc-P-selectin + Fc-ICAM-1
hIgG
5% BSA
Coating buffer
Fc-P-selectin
Fc-ICAM-1
Fc-P-selectin + Fc-ICAM-1
hIgG
5% BSA
Coating buffer
M2b (hIgG+LPS)
Pro-MMP9 (92kDa)
Active-MMP9 (82kDa)
GAPDH (37kDa)
B
Untreated
Fc-blocked
Pro-MMP9 (92kDa)
Active-MMP9 (82kDa)
% Maximum of UT Fc-P-selectin
100
50
0
*
* *
Coating buffer
5% BSA
hIgG
Fc-P-selectin
Fc-ICAM-1
Fc-P-selectin + Fc-ICAM-1
Coating buffer
5% BSA
hIgG
Fc-P-selectin
Fc-ICAM-1
Fc-P-selectin + Fc-ICAM-1
M2b (hIgG+LPS)
C
Pro-MMP9
Active-MMP9
Untreated
Fc-blocked
% Maximum of UT Fc-P-selectin
120
80
40
0
Coating buffer
5% BSA
hIgG
Fc-P-selectin
Fc-ICAM-1
Fc-P-selectin + Fc-ICAM-1
Coating buffer
5% BSA
hIgG
Fc-P-selectin
Fc-ICAM-1
Fc-P-selectin + Fc-ICAM-1

Figure 4-3: P-selectin and FcyR-IgG adhesive interactions induce the polarization of macrophages with increased MMP9 secretion.

A) Monocytes cultured (5-days) on plates coated with Fc-P-selectin, Fc-ICAM-1, Fc-P-selectin+Fc-ICAM-1, hIgG, 5% BSA, or coating buffer were subjected to Western blot analysis to detect pro-MMP9 (92kDa) and activated-MMP9 (82kDa). **B)** Untreated (left) or Fc-blocked (right) pre-treated monocytes cultured in Fc-P-selectin and hIgG coated plates increased both pro and active MMP9 compared to those cultured in Fc-ICAM-1, 5% BSA, or with coating. There was higher expression of active-MMP9 in hIgG and Fc-P-selectin conditions. M2b (hIgG + LPS) polarized macrophages which showed high secretion of MMP9 by ELISA assay were used as comparative controls. **C)** Untreated monocytes in hIgG and Fc-P-selectin conditions showed higher MMP9 secretion compared to those pre-treated with Fc-block. This suggests that FcyR-IgG interactions may act synergistically with P-selectin in inducing MMP9. Quantified data was normalized to GAPDH control. Data in bar graphs shown as ±SEM. Statistical significance was analyzed by repeated measures one-way ANOVA ($p < 0.05$ (*), $p < 0.01$(**), $p < 0.001$(***) $p < 0.0001$(****).

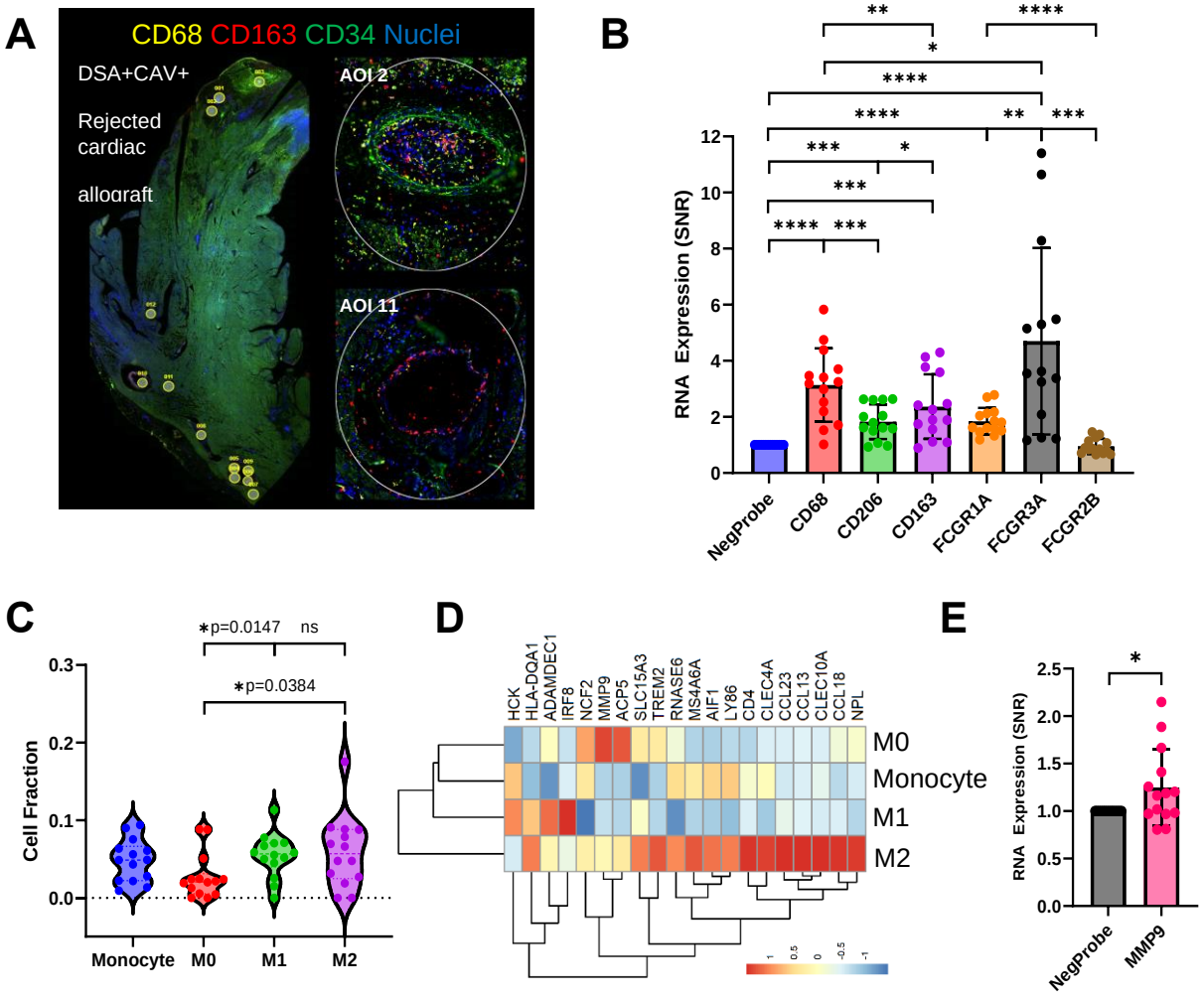
A
CD68 CD163 CD34 Nuclei
DSA+CAV+
Rejected cardiac allograft
AOI 2
AOI 11
B
RNA Expression (SNR)
NegProbe
CD68
CD206
CD163
FCGR1A
FCGR3A
FCGR2B
C
Cell Fraction
*p=0.0147
ns
*p=0.0384
Monocyte
M0
M1
M2
D
HCK
HLA-DQA1
ADAMDEC1
IRF8
NCF2
MMP9
ACP5
SLC15A3
TREM2
RNASE6
MS4A6A
AIF1
LY86
CD4
CLEC4A
CCL23
CCL13
CLEC10A
CCL18
NPL
M0
Monocyte
M1
M2
E
RNA Expression (SNR)
NegProbe
MMP9

Figure 4-4: M2-macrophage transcripts are elevated within vascular lesions of CAV+DSA+ rejected cardiac allografts.

A) A total of 14 arterial areas of interest (AOIs) from CAV+DSA+ rejected cardiac explants (N=3; 1 male, 2 female) were selected on the presence of CD68+CD163+ macrophages localized within CD34+ arteries and subjected to GeoMx digital spatial profiling (DSP). Representative image shows explant tissue from PID1 along with two selected AOIs containing CD68+CD163+ macrophages. **B)** The expression of M2-macrophage transcripts (*CD68*, *CD163*, and *CD206*) and activating Fc-receptors (*FCGR1A* and *FCGR3A*) were significantly elevated compared to the internal negative RNA probe (Negprobe) across all 14 AOIs. **C)** M2-macrophage cell fractions (derived by CIBERSORT cellular deconvolution) are more broadly distributed compared to M0 macrophages across all 14 AOIs. **D)** Top-20 macrophage-associated genes per macrophage subtype based on CIBERSORT deconvolution. **E)** MMP9 RNA expression is significantly elevated compared to Negprobe across the 14 AOIs. RNA data is normalized to internal negative controls (NegProbe) and shown as signal to noise ratio (SNR). Statistical significance was analyzed by unpaired repeated measures one-way ANOVA or unpaired student T-test ($p < 0.05$ (*), $p < 0.01$(**), $p < 0.001$(***) $p < 0.0001$(****)).

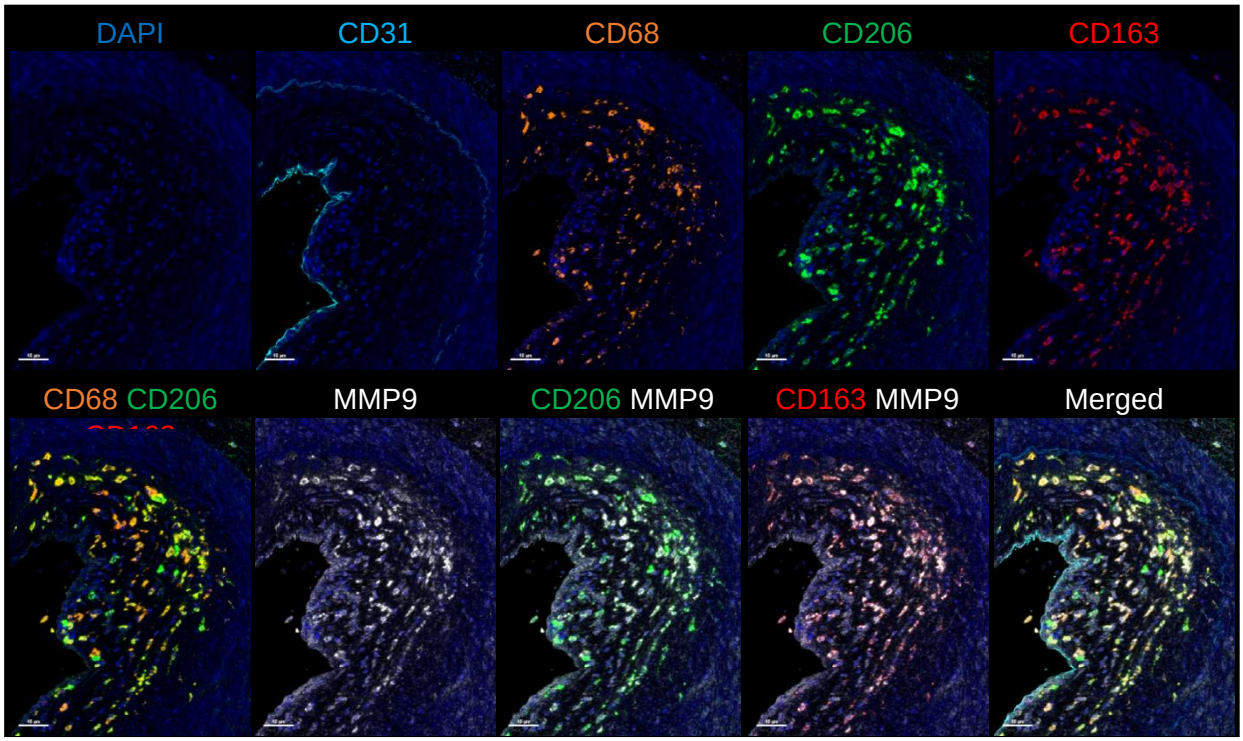

Figure 4-5: CD68+CD206+CD163+MMP9+ M2-macrophages accumulate within vascular neointimal lesions of CAV+ DSA+ rejected cardiac allografts.

Multiplex-immunofluorescent staining of DSA+CAV+ rejected cardiac allografts (PID1-3) for M2-macrophage markers (CD68, CD206, and CD163) found within the neointima luminal layer as observed by CD31+ endothelial cells lining the vessel (bar=40um). MMP9 co-localized with CD206+, CD163+, and CD206+CD163+ double-positive cells confirming *in vitro* transwell co-culture studies and spatial profiling RNA data deconvolution results.

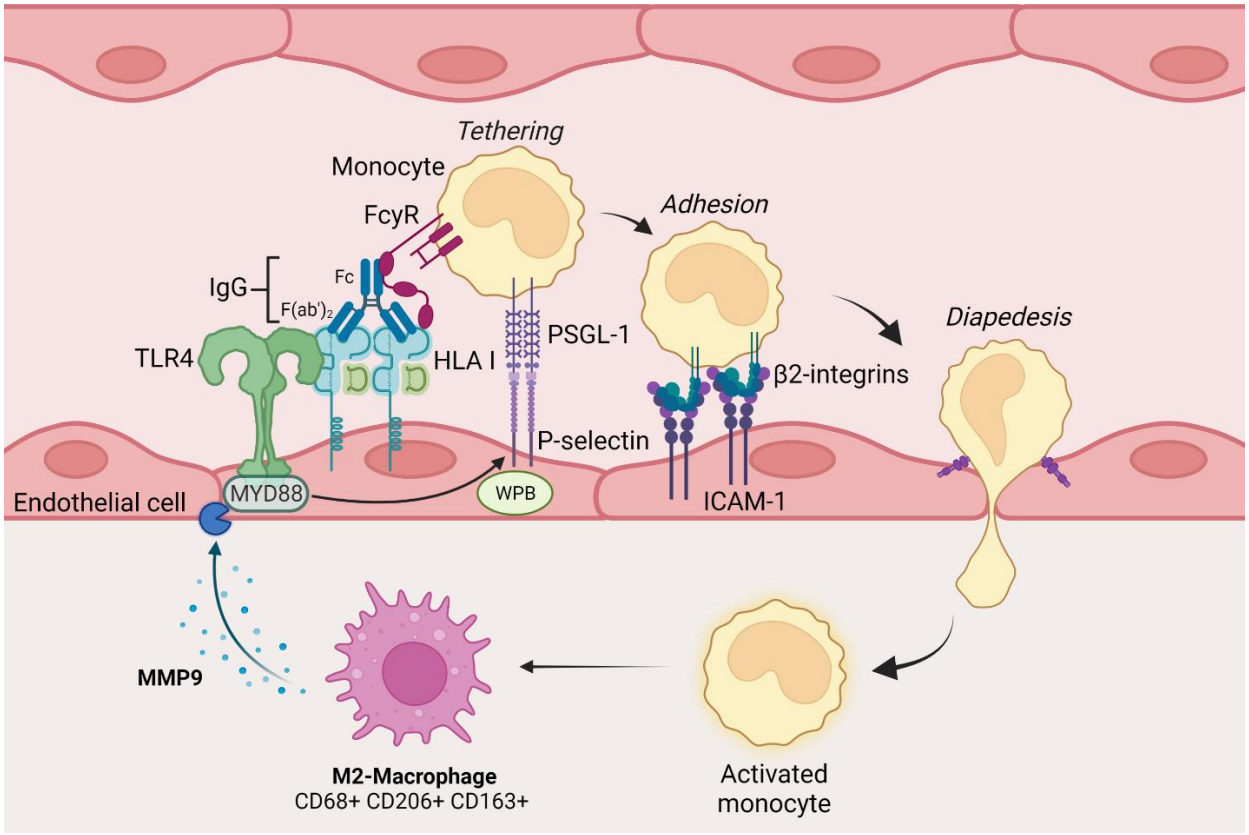

Figure 4-6: HLA I DSA-activated endothelium induces monocyte differentiation into CD68+CD163+CD206+MMP9+ M2-macrophages.

HLA I (IgG or F(ab')$_2$) antibody crosslinking to HLA I molecules on endothelial cells (ECs) stimulates the formation of a molecular complex between HLA I and Toll-like receptor 4 (TLR4). TLR4 signaling via MyD88 triggers the exocytosis of Weibel-Palade bodies (WPBs) and surface expression of P-selectin. Monocytes tether to the surface of ECs via PSGL-1-P-selectin and undergo a secondary stimulus via FcyR-IgG interactions. In this study, we identified that HLA I (IgG or F(ab')$_2$) antibody-activated ECs induce M2-macrophages with increased CD206 expression and MMP9 secretion. The increase in CD206 and MMP9 was directly linked to PSGL-1-P-selectin interactions. We have shown previously that FcyR-IgG interactions can also induce an added increase of M2c marker, CD163. Macrophage secretion of MMP9 can directly degrade ECM component (e.g., Collagen) and activates pro-angiogenic cytokines (e.g., TGF-β and VEGF)

promoting vascular remodeling and fibrosis leading to formation of neointima as observed in CAV lesions. Figure created with BioRender.com.

Table 4-1: Top 20 Monocyte/Macrophage-associated genes based on CIBERSORT RNA data deconvolution matrix.

	Monocyte	M0	M1	M2
1	NCF2	MMP9	IRF8	MMP9
2	MNDA	NCF2	CCL4	MS4A6A
3	MS4A6A	ACP5	ADAMDEC1	CCL18
4	AIF1	CHI3L1	HCK	AIF1
5	HCK	IGSF6	SIGLEC1	NCF2
6	CLEC7A	C5AR1	SAMSN1	CD4
7	LST1	SLC15A3	TLR2	ACP5
8	LY86	ADAMDEC1	CCL8	CLEC4A
9	TLR2	EGR2	C3AR1	CCL13
10	CD37	CLEC7A	HLA-DQA1	LY86
11	C5AR1	HCK	MNDA	SLC15A3
12	RNASE6	FPR3	SLC15A3	CLEC10A
13	CFP	CCL18	CHI3L1	CCL23
14	CD4	MNDA	MMP9	HLA-DQA1
15	CCL4	RNASE6	LST1	RNASE6
16	CLEC4A	LST1	GPR183	ADAMDEC1
17	P2RY13	TREM2	AIF1	HCK
18	IGSF6	CCL4	CD4	NPL
19	IRF8	IRF8	CD86	TREM2
20	CD300A	AIF1	CLIC2	IRF8

Chapter 5 – Spatial Multi-omics of Arterial Regions from Cardiac Allograft Vasculopathy Rejected Grafts Reveal Mechanistic Insights into the Pathogenesis of Chronic Antibody-Mediated Rejection

Abstract

Cardiac allograft vasculopathy (CAV) causes late-graft failure and mortality after heart transplantation. Donor-specific antibodies (DSA) lead to chronic endothelial cell (EC) injury, inflammation, and arterial intima thickening. We characterized immune cells in rejected cardiac allografts and identified protein and transcriptomic signatures distinguishing early and late CAV lesions. GeoMx digital spatial profiling (DSP) was used to analyze arterial areas of interest (AOIs) from CAV+DSA+ rejected cardiac allografts (N=3; 22 AOIs total). AOIs were categorized based on CAV neointimal thickening and underwent whole transcriptome and protein profiling. AOIs with low neointima showed increased markers for activated inflammatory infiltrates, EC activation transcripts, and gene modules involved in metalloproteinase activation and TP53 regulation of caspases. Inflammatory and apoptotic proteins correlated with inflammatory modules in low neointima AOIs. High neointima AOIs exhibited elevated TGFβ-regulated transcripts and modules enriched for platelet activation/aggregation. Proteins associated with growth factors/survival correlated with modules enriched for proliferation/repair in high neointima AOIs. Key transcripts involved in proliferation, migration, and EndoMT were significantly associated with increasing neointima scores. Our findings suggest protein and transcriptomic profiles linked to CAV progression, indicating a transition from early inflammatory lesions to later proliferative/pro-fibrotic lesions.

Introduction

Cardiac allograft vasculopathy (CAV) remains a major clinical challenge limiting long-term graft and patient survival following heart transplantation. Approximately 29% of heart transplant recipients develop CAV by 5 years and 47% by 10 years post-transplant[106]. CAV lesions are characterized by concentric intimal thickening of the vascular wall consisting of proliferating myofibroblast and inflammatory immune infiltrates[20]. Although both immunological and non-immunological processes contribute to CAV pathogenesis, the exact mechanisms mediating disease progression remain unclear. Episodes of antibody-mediated rejection (AMR) in which donor specific antibodies (DSA) target human leukocyte antigens (HLA) present on vascular endothelial cells (ECs) have been increasingly recognized as a major risk factor contributing to CAV[107]. Specifically, DSA can activate EC intracellular signaling cascades inducing EC proliferation, migration, and increased surface expression of adhesion molecules promoting monocyte and NK cell recruitment[5,12,14-16]. Moreover, DSA can directly mediate EC-injury by triggering activation of the classical complement cascade[5]. Recurring episodes of AMR contribute to chronic inflammation eliciting EC injury and apoptosis. CD4+ and CD8+ T-cells activated by HLA alloantigen recognition are also commonly found in the adventitia and neointima of CAV rejected hearts. Specifically, memory T helper (Th) 1 secreting pro-inflammatory cytokines such as IFN-y and TNF-α can attract and activate CD8+ cytotoxic T cells and NK cells[20]. T cells also secrete transforming-growth factor-β (TGF-β) which significantly contributes to fibrosis and remodeling by upregulating collagen synthesis in SMCs and stimulating macrophage secretion of matrix metalloproteinases[108]. The process of endothelial-to-mesenchymal transition (EndoMT) remains another distinguishing characteristic contributing to CAV. EndoMT is a phenomenon in which ECs gradually lose EC markers and increase mesenchymal cell. A combination of inflammatory stimuli, low or disturbed shear flow, vascular stiffness (activating WNT/β-catenin), and metabolic dysregulation (e.g., high glucose) can all cause EndoMT via different signaling pathways[109].

Overall, numerous immunological mechanisms involving both innate and adaptive immune responses have been shown to contribute to the initiation and progression of neointimal development in CAV. Recent studies using endomyocardial biopsies (EMBs) have elucidated DSA and/or AMR-specific bulk-RNA signatures which contribute to CAV[110-112]. However, as CAV mainly affects large and small epicardial and intramyocardial arteries, EMBs may not exactly reflect the immune and/or vascular signatures contributing to neointima formation. Therefore, the proteomic and transcriptomic signatures revealing specific activated markers and regulatory pathways from DSA+CAV+ affected vessels as observed in rejected cardiac explants remains to be elucidated. In this study, we used GeoMx digital spatial profiling (DSP) to examine both the whole transcriptome and targeted protein profiles of arterial regions scored with varying levels of neointima progression. Using a multi-omics approach, we explored differences between arterial regions containing low and high neointimal scores thereby identifying potential immune proteins, enriched transcripts, and pathways involved in neointima progression.

Methods

Study approval

The use of human cardiac rejected explants for this study was approved by the University of California, Los Angeles Institutional Review Board (IRB#18-001275). Formalin-fixed paraffin embedded (FFPE) tissue from rejected cardiac explants were obtained from the UCLA Translational Pathology Core Lab (TPCL).

Arterial vessel selection and pathological characteristics.

A total of 22 geometric areas of interest (AOIs) capturing the entire artery (14 AOIs) or portions of arteries (as part of larger vessels) (8 AOIs) were selected across three cardiac allograft explants from CAV+DSA+ patients (N=3; 2 females PID1, PID2 and 1 male PID3). All 22 arterial areas of interest (AOIs) included the neointima, media, and adventitia, encompassing all components of

the vessel **(Figure 5-1A**). Given the similarity in protein and transcript expression between the 14 AOIs (capturing entire arteries) and the 22 AOIs dataset (**Supplementary Figure 5-1**), we conducted downstream analysis using all 22 AOIs. Patient demographics and clinical information are summarized in **Supplementary Table 5-1**. The 22 AOIs included 10 vessels from PID1, five vessels from PID2, and seven vessels from PID3. Hematoxylin and eosin (H&E) staining was used to score arteries based on the level of CAV progression/neointimal thickening by the pathologist. In total, 11 arteries were scored with 'low' neointima (+/- minimal and 1+ mild) and 11 with 'high' neointima (2+ moderate, 3+ significant, and 4+ very significant) (**Supplementary Table 5-2**). H&E images were captured using Zeiss microscope and examined using ZEISS ZEN lite Software v3.3.

Targeted protein and whole transcriptome GeoMx digital spatial profiling (DSP)

Multiplex digital spatial profiling of protein and RNA in fixed tissues was performed by NanoString Technologies (Seattle, WA) as part of the Technology Access Program (TAP) as per Merritt et al., *Nat Biotechnol* 2020[77]. For protein DSP, FFPE slides underwent antigen retrieval and were incubated with a cocktail of 73 UV-photocleavable (PC)-oligonucleotide-labeled primary antibodies. The antibody cocktail included a total of seven pre-defined protein panels (**Supplementary Table 5-3**). For RNA DSP, consecutive FFPE slide cross-sections from the same patient explants underwent mild proteinase K digestion followed by incubation with a whole transcriptome cocktail (18,504 transcripts) of UV-PC-oligo labeled mRNA probes. After antibody incubation or hybridization steps, slides were loaded into the DSP instrument and geometric AOIs were selected based on previously defined arterial regions scored for CAV by the pathologist (**Supplementary Table 5-2**). AOIs were profiled using a programmable digital micromirror device (DMD) that directs UV light to exactly illuminate the AOI and release PC-oligos in a region-specific manner. The released indexing oligonucleotides are collected via microcapillary aspiration,

dispensed into a microplate, and digitally counted using the single-molecule counting nCounter System for protein or Next Generation Sequencing (NGS) readout for RNA.

Data normalization using NanoString's GeoMx analysis suite

The GeoMx analysis suite was used for quality control (QC) and normalization of both protein and RNA datasets. Digital nCounter counts corresponding to protein probes were normalized by internal spike-in controls followed by normalization to the average of negative IgG probes. Whole genome transcriptomic RNA probes underwent QC and Grubbs test to remove outlier probes within a target and AOI (biological probe QC). Each AOI's data was scaled to the 3rd quartile of all selected targets (Q3) and normalized to the average (+2SD) of negative controls (NegProbe-WTX). Normalized counts for both protein and RNA datasets are reported as a signal to noise ratio (SNR) to internal negative controls.

WGCNA analysis, gene regulatory networks (GNRs), and data deconvolution

Whole gene co-expression network analysis (WGCNA) was used to define modules of co-expressed transcripts containing a minimum of 10 transcripts. Modules with correlation >0.75 were merged[113]. In total, 313 modules containing eigengene values were generated using the whole genome dataset. The expression of each module is reported by the module eigengene, defined as the first principal component of the expression matrix or average weighted expression profile of the module. Enriched pathways for each module were identified using Reactome. To identify underlying transcription factor regulation of identified gene expression profiles, gene regulatory network (GRN) analysis was performed using R package *SCENIC*[113]. RNA deconvolution for obtaining cell type abundance estimates across all arterial AOIs was derived using SpatialDecon algorithm with immune matrix platform as previously described[114].

Multiplex-immunofluorescent staining

Multiplex-immunofluorescent staining of cardiac explants was performed by UCLA TPLC. The TSA-based Opal method was used for immunofluorescence (IF) staining (Opal Polaris 7-Color Automation IHC Kit; Akoya Biosciences, Marlborough, MA, USA; Catalogue No. NEL871001KT). Since TSA and DAB oxidation are both peroxidase-mediated reactions, the primary antibody conditions and order of staining determined using DAB detection were directly applied to the fluorescent assays, unlike conventional IHC wherein a chromogenic peroxidase substrate is used for antigen detection, each antibody is paired with an individual Opal fluorophore for visualization. The Opal fluorophores were used at a 1 in 100 dilution, as recommended by Akoya when using the Leica BOND RX. As such, a fluorescent singleplex was performed for each biomarker and compared to the appropriate chromogenic singleplex to assess staining performance. Once each target was optimized in uniplex slides, the Opal 6 multiplexed assay was used to generate multiple staining slides. TMA slides Staining was performed consecutively Leica BOND RX by using the same steps as those used in uniplex IF, and the detection for each marker was completed before application of the next antibody. The sequence of antibodies for multiplex staining was determined for panel combination is: CD31 (opal 480), SMA (opal 520), Vinmentin (opal570), UBAP2L (opal 620), CD45 (opal 690). All fluorescently labelled slides were scanned on the Vectra Polaris (Akoya Biosciences) at 40× magnification using appropriate exposure times. The data from the multispectral camera were analyzed by the imaging InForm software (Akoya Biosciences).

Statistical Analysis

Identification of differentially expressed proteins (DEPs), differentially expressed genes (DEGs), and differentially expressed WGCNA modules between AOIs with low and high neointima were determined using linear mixed-effects model, including patient ID as a random effect variable. Results were considered significant at $Log_2FC > 1$ and *p-value* < 0.05 for **Figures 5-4B, C** (**Table. 5-1**) and *p-value* < 0.05 for **Figure 5-4D**. Statistical significance in **Figure 5-2C** was determined

using Pearson correlation coefficient test, significant at *p-value* < 0.05. Results in **Table 5-3** (and **supplementary Figure 5-4**) were determined using Spearman correlation $p < 0.05$ (*), $p < 0.01$(**), $p < 0.001$(***) in GraphPad Prism software v9.3.1.

Results

Arterial AOIs express protein markers related to immune-cell activation and cell death.

Arterial AOIs from three CAV+DSA+ rejected cardiac explants (PID1-3; 2 females and 1 male; (**Figure 5-1A**) were spatially profiled using a 73-protein panel (**Supplementary Table 5-3**). A total of 41 protein markers were similarly expressed across all 22 arterial AOIs (SNR>1 in blue) (**Figure 5-1B**). To assess variability in the structural make-up of the 22 captured AOIs, we additionally examined expressed proteins (SNR>1) in the 14 AOIs that encompassed entire arteries. Notably, all 41 proteins exhibited similar levels of expression (SNR>1) in both 22 AOI and 14 AOI datasets (**Supplementary Figure 5-1A**). Therefore, downstream analysis was conducted using all 22 AOIs. Specifically, all 22 AOIs expressed markers involved in immune cell activation and cytotoxicity (CD44, GZMB and HLA-DR), apoptosis (cleaved caspase 9, BAD, and p53) and cell survival (BCLXL) showed moderate expression. This was accompanied by the expression of CD45+ immune infiltrates including macrophages (CD68), T cells (CD4 and CD8), NK cells (CD56), monocytes (CD14), and dendritic cells (CD11c) in order of expression. Phosphorylated proteins in the MAPK and PI3K/AKT signaling pathway (p44/42 MAPK ERK1/2, pan-AKT, and phospho-AKT1) were detected at moderate-to-low levels. Stimulator of interferons genes (STING) and TNFSF4/OX40L, a memory T cell survival inducing ligand also showed moderate-to-low levels of expression (**Supplementary Table 5-4**). Protein correlation matrix analysis across all AOIs revealed significant associations between apoptotic and anti-apoptotic proteins (e.g., BAD and BCLXL), T cell markers (CD3 and CD8), and signaling cascades (Phospho-AKT1 (S473) and Pan-Ras) (**Supplementary Figure 5-2 and Supplementary Table 5-5**).

Top transcripts in arteries encode for DSA-mediated immune responses and vascular remodeling.

Transcriptomic analysis identified a total of 10,746 genes with an average SNR>1 and coefficient of variation (COV)>0.19 across all 22 arterial AOIs. A total of 74 transcripts had an average SNR>10 (excluding ribosomal and ATP genes) (**Figure 5-2A**). Similar findings were observed when examining 14 AOIs capturing entire arteries (10,122 transcripts with SNR>1 and COV>0.19). Specifically, among the top 70 transcripts (average SNR>10) identified in the 14 AOIs, there was almost complete overlap (65/70) with the top 74 transcripts observed in the 22 AOIs (**Supplementary Figure 5-1B**). Subsequently, we proceeded our analysis utilizing all 22 AOIs. The top two transcripts included *PTBP1,* a regulator of inflammation, and *ADAM15* which mediates endothelial hyperpermeability during inflammation[115,116]. Immunoglobulin transcripts (e.g., *IGKC* and *IGHG1/2/3/4*) were also highly elevated. This was accompanied by the expression of HLA class I (*HLA-B*), IFN-y inducible HLA class II molecules (e.g., *HLA-DRB1* and *HLA-DRA*), and HLA class II chaperone transcripts (*CD74*)[117]. AOIs also exhibited a relatively high expression of transcripts described in vascular remodeling, angiogenesis, platelet activation, cell proliferation, migration, and immune infiltration (*IGFBP7*, *TMSB4X*, *FLNA*, *TIMP1*, *MAZ*, *CRYAB*, *TMEM106C*)[118-123]. Metascape gene enrichment analysis of the top 231 transcripts (average SNR>5) revealed that AOIs were enriched in pathways relating to EC angiogenesis (‘*VEGFA-VEGFR2 signaling pathway’*), DSA activation (‘*immunoglobulin mediated immune responses’*), thrombosis (‘*platelet degranulation’*), and pro-inflammatory cytokines (‘*IL-18 signaling pathway’*) (**Figure 5-2B**). Highly expressed transcripts most likely were attributed to fibroblast, ECs, macrophages, and memory CD8 T-cells as these were most prominent cell types by cellular abundance counts (**Figure 5-3A**). Specifically, CD8 protein expression significantly correlated with CD8 memory abundance counts (and not CD8 naïve T-cells) further suggesting the presence of memory T-cells (**Figure 5-3B**). Additionally, we identified CD45, CD8, CD56, CD20, CD127, and CD11c protein markers significantly correlated with RNA counterpart expression validating the level of expression of these cell types in each AOI (**Figure 5-2C**).

Arterial AOIs with low neointima exhibit higher inflammation and cell death while AOIs with high neointima exhibit remodeling and fibrotic profiles.

Although all arteries were found to exhibit similar protein markers of both innate and adaptive immune infiltrates, we questioned whether the degree of inflammation varied between AOIs scored with a low (+/- minimal and 1+ mild) or high (2+ moderate, 3+ significant, and 4+ very significant) neointima (N=11 AOIs for each condition). Unsupervised clustering of the 41 proteins (SNR>1) illustrated that AOIs with low neointima clustered closer together and displayed higher protein expression (**Figure 5-4A**). This was also observed when clustering AOIs for each individual patient (**Supplementary Figure 5-3**). A total of 8 differentially expressed proteins (DEPs) were increased in arteries with low neointima (**Figure 5-4B**). These included markers involved in T-cell clonal expansion/survival (TNFSF4/OX40L), memory T-cells (CD45RO and CD127), checkpoint inhibitors (TIM-3), monocytes (CD14), regulators of PI3K/AKT signaling (INPP4B), MAPK signaling (pan-Ras), and pro-apoptotic proteins (p53) (**Table 5-1**). AOIs with low neointima also upregulated *VWF* (indicative of EC activation)[124]. Meanwhile, AOIs with high neointima significantly increased TGFβ-regulated genes (*CSRP1* and *TAGLN)* and adipocyte differentiation factor (*ADIRF/APM2*) (**Figure 5-4C and Table 5-1**)[125-127].

To further explore transcriptional differences between low and high neointima AOIs, we utilized whole gene co-expression network analysis (WGCNA) to define modules of co-expressed transcripts[113]. AOIs with low neointima upregulated three modules (ME21, ME22, and ME118), two of which were enriched for '*Activation of matrix metalloproteinases*' and '*TP53 regulation of caspase activators and caspases'*. High neointima AOIs upregulated one module (ME50) enriched for pathways involved in '*Platelet activation, signaling and aggregation*' (**Figure 5-4D and Table 5-2**). Gene regulatory network (GRN) analysis enabled the identification of key transcription factors correlating co-expression modules. Specifically, ME21 and ME118 highly correlated with inflammatory driven transcription factors *SREBF2* and *NFATC1*,

respectively[128,129]. Meanwhile, ME50 highly correlated with *NR2F2*, which promotes cell proliferation and TGF-β-dependent epithelial-to-mesenchymal transition (EMT) (**Figure 5-4D and Table 5-2**)[130].

Additionally, we identified that numerous protein markers encoding inflammatory infiltrates (e.g., CD45, CD44, CD8, OX40L, GZMB) and apoptosis (p53 and BAD) highly correlated with co-expressing modules enriched for '*interferon gamma signaling*', '*Toll-like receptor cascades*', '*NF-kB phosphorylation*' and '*TP53 regulation of caspase activators and caspases*' (ME65, 77, 91, 118, 242, and 304) only in AOIs with low neointima. Alternatively, proteins associated with growth factor receptors (EGFR), regulators of cell growth/division (NF1), smooth muscle cell markers (SMA), and cell survival proteins (BCL-XL) significantly correlated with modules enriched for '*MAPK1/MAPK3 signaling*', '*signaling by FGFR*', '*FGFR2 ligand binding and activation*', and '*VEGFA-VEGFR2 pathway*' (ME161, 205, 206) only in AOIs with high neointima (**Table 5-3 and supplementary Figure 5-4**). Cellular deconvolution reinforced neointimal differences since AOIs with high neointima exhibited a significantly higher number of fibroblasts, while AOIs with low neointima contained a higher number of classical monocytes (**Figure 5-3C**).

CAV lesion progression is associated with distinct gene expression signatures and gene regulatory networks.

To identify genes associated with different stages of neointima, we performed a linear regression of neointima score on normalized expression of each gene. From principal component analysis of genes significantly associated with neointima score (n=245), we identified the first principal component (PC1) as increasing in a stepwise manner with increasing neointima score (**Figure 5-5A**). Finally, to identify key genes and GRNs which may be driving vessel occlusion, we tested for genes/GRNs associated with PC1 score. A total of 36 genes were significantly associated with PC1 by linear regression analysis (adjusted *p-value* < 0.05) (**Figure 5-5B and Supplementary Table 5-6**). Specifically, arteries with mild neointima (+/-) contained heat shock proteins

(*CRYAB/HSBP5* and *HSPB7*) which increase in response to inflammatory stress[123,131]. Vessels with minimal neointima (1+) increased the antigen T-cell receptor (*TARP*) which promotes tumor cell proliferation and migration[132]. Vessels with moderate neointima (2+) increased a set of genes described in remodeling and EMT (*TAGLN*, *CSRP1, and FLNA*)[120,125,126]. Vessels with significant neointima (3+) only increased ubiquitin and RNA-binding protein (*UBAP2L*), a principal mediator of EMT/fibrosis and emerging biomarker and therapeutic target of EndoMT in cancer[133,134]. Finally, arteries with very significant neointima (4+) increased early growth response-1 (*EGR1*) and *FOS* transcription factors, implicated in cancer progression and fibrosis[135,136]. Notably, transcripts involved in inhibiting tumor cell proliferation, EMT/fibrosis (*OGN*) and anti-inflammatory regulators (*ZFP36*) were also identified in vessels with moderate (2+) and very significant neointima (4+), respectively[137,138]. Major GRNs associated with increasing neointima also included transcription factors involved promoting cell proliferation, migration, EMT/EndoMT, fibrosis (*NF2F2, JUN, HEY, ATF3, ATF4, and FOXP1)* and angiogenesis (*RUNX1*)[130,139-144] (**Figure 5-5C**).

Neointima driven genes resided within scores of +/-, 2+, and 4+, suggesting sequential stages in which genes may be turned on-and-off. Notably, UBAP2L was only increased in AOIs with a score of 3+. Since UBAP2L has been reported as a key mediator of EMT in cancer, we questioned whether it was also expressed in arterial AOIs as a possible mediator of EndoMT. Multiplex immunofluorescent staining of cardiac explants revealed that UBAP2L co-localized with CD31+ ECs and Vimentin+ mesenchymal cells. CD31+ ECs also co-expressed Vimentin suggesting activation toward mesenchymal phenotype. UBAP2L did not co-localize with SMA+ or CD45+ cells (**Figure 5D**). A total of 16/22 (72%) of arterial AOIs expressed UBAP2L co-localized within CD31+Vimentin+ ECs and CD31-Vimentin+ mesenchymal cells. Specifically, 9/11 (81%) high neointima AOIs while only 7/11 (63%) of low neointima AOIs expressed UBAP2L.

Discussion

Herein, we utilized GeoMx DSP technology to examine both the protein and transcriptomic expression of arterial AOIs from HLA DSA+CAV+ rejected cardiac explants. Among the 22 arterial regions examined, we identified similarly expressed protein markers relating to innate and adaptive immune cells, cell activation, and cell death. Whole transcriptome analysis highlighted transcripts involved in DSA-mediated responses and vascular remodeling. Moreover, we demonstrated that AOIs with low neointima exhibit higher inflammatory and cell death profiles while AOIs with high neointima exhibit lesions undergoing proliferation, migration, and EndoMT/fibrosis. Finally, we identified key genes (e.g., *UBAP2L*) and transcription factors associated with increasing neointima scores, many implicated in promoting proliferation, migration, and EMT/fibrosis. By examining the similarities and heterogeneities between arterial regions, we present a unique approach to further delineate the potential stages of CAV progression.

Macrophages and T cells have been found to accumulate within the neointima of human CAV affected vessels[10,22]. This is concordant with our study as CD68+ and CD4/CD8+ markers were the top immune infiltrates in both protein and RNA cell abundance datasets. Monocyte recruitment may occur in the early phases of CAV as we observed significantly higher protein expression of CD14 and classical monocytes counts in arteries with low neointima. HLA DSA can rapidly increase intracellular calcium and endothelial presentation of P-selectin, which supports monocyte binding[16,18]. Notably, CD68 protein expression significantly correlated with module ME206 in high neointima AOIs. ME206 was enriched for pathways related to '*Fc gamma receptor dependent phagocytosis*' indicative of polarized macrophage specific functions[71].

Endothelial cell injury is a major hallmark of AMR and in the early phases of CAV. Specifically, high protein expression of CD8+ T cells, CD44 activation marker, cleaved caspase 9, and GZMB together suggest cell-targeted injury via the perforin/granzyme apoptosis pathway by cytotoxic T-

cells. Human coronary arteries with advanced atherosclerosis and CAV lesions have been shown to exhibit high levels of GZMB localized within infiltrating leukocytes underlying the endothelium, in the deep intima, and in perivascular infiltrates in the adventitia[145]. GZMB-induced cell apoptosis can be enhanced by the pro-apoptotic protein BAD (BCL-2 associated agonist of cell death) or hindered by the anti-apoptotic BCL-2 family protein, BCL-XL. These regulatory proteins shared similar protein expression levels to GZMB and exhibited the highest significant correlation with each other. This is likely because activated BAD binds to and inhibits the anti-apoptotic function of BCL-XL[146]. Expression of EC anti-apoptotic proteins can be potentiated by antibody ligation of HLA class I and II molecules which activate the PI3K/AKT pathway and upregulation of BCL-2 and BCL-XL[13]. Hence, ECs may acquire anti-apoptotic defense mechanisms that promote EndoMT via HLA outside in signaling.

Arterial AOIs also showed high expression of transcripts associated with DSA-mediated responses including multiple immunoglobulins (IgGs), suggesting the presence of antibody secreting cells such as B cells and/or plasma cells. Since CD20 protein expression across AOIs was relatively low (SNR=1.21), it is likely that these IgG transcripts are encoded by mature plasma cells (which decrease CD20 expression). This was confirmed in a study by Chattejee et al., in which majority of the CD138+ differentiated plasma cells around CAV affected coronary arteries from rejected explants secreted IgG[103]. Moreover, microarray studies by Wehner et al., have shown a strong immunoglobulin transcriptome in CAV rejected explants in contrast to atherosclerosis[147].

All arteries shared high expression for transcripts associated with EC and SMC activation, remodeling, angiogenesis, and platelet activation[118-122]. We compared transcripts with an average SNR > 5 to those identified in pathological AMR+DSA+ EMBs reported by Loupy et al. using microarray technology[110]. Similarly, we detected the expression of IFN-γ inducible genes (HLA class II transcripts), and NK-cell activation (*FCGR3A*). However, our results may not fully

encompass the transcriptomic profile described by studies using EMBs due to anatomical differences within the heart. These differences have been emphasized in a mouse model of chronic AMR[68].

Multi-omics analysis between AOIs with low and high neointima proposes a sequential time-frame of the vascular changes leading to CAV. Specifically, ‘early’ lesions exhibit higher inflammatory profiles consisting of lymphocyte and monocyte infiltrates, while 'late’ lesions contain higher proliferative and fibromuscular/mesenchymal tissue with lower inflammation. These observations are in accordance with the results of Huibers et al. who identified three histopathological patterns of CAV characterized by inflammatory lesions, increased SMCs, followed by fibrotic lesions[148]. AOIs with low neointima mainly exhibit features of burnt-out vasculitis (thickening of the vessel wall) or endothelialitis (cells beneath the endothelium). Based on the significantly higher memory T-cell and cell death markers in low neointima AOIs, we speculate that T-cells infiltrate subendothelial regions where they proliferate and mediate EC-injury. The accumulation of T-cells expressing perforin-containing granules in the subendothelial region of early CAV lesions has been previously reported[149]. OX40L (*TNFRSF4*) was the highest DEP between low and high neointima AOIs. OX40L (expressed on APCs, NK cell, activated CD4 T-cells, ECs and mast cells) binds to OX40+ antigen activated T-cells stimulating T-cell proliferation, clonal expansion/survival, and effector cytokine release[150]. Studies using mouse heart transplant models have highlighted the benefits of OX40L blockade in promoting graft survival by inducing Tregs[151]. AOIs with low neointima showing early vascular inflammation and cell death were supported by increased VWF and ME118 (enriched for TP53 activation of caspases), which significantly correlated with NFATC1, a regulator of cytotoxic CD8+ T-cells. AOIs with low neointima showed early vascular inflammation and cell death characteristics, supported by increased *VWF* and ME118 (enriched for TP53 activation of caspases). ME118 correlated significantly with *NFATC1*, a key regulator of cytotoxic CD8+ T-cells[129].

Alternatively, AOIs with high neointima mainly demonstrated features of ongoing neointima expansion as seen by an increase in transcripts involved in myofibroblast differentiation (*CSRP1*), and remodeling (*TAGLN*)[125,126]. AOIs with high neointima upregulated pathways related to '*Platelet activation, signaling and aggregation*' (ME50). DSA crosslinking to MHC I antigens induces Weibel-Palade bodies (WPb) exocytosis of P-selectin and vWF which can increase platelet and leukocyte infiltration which aggravate vessel pathology[16-18,152].

High neointima AOIs also increased GRNs involved in cell proliferation (*JUN*), EndoMT (*NR2F2*, *HEY2*, and *FOXP1*), angiogenesis (*RUNX1*) and fibrosis (*ATF3* and *ATF4*)[125,130,139-144]. Notably, DEGs (*CSRP1* and *TAGLN*) and GRNs (*NR2F2*, *ATF3*, *FOXP1*) encompassed genes which promote EndoMT by regulating or being induced by TGF-β[125,126,130,141]. Similar findings were observed by linear regression analysis as key genes involved tumor cell proliferation, migration, EMT/fibrosis, and anti-inflammatory modulators (*ZFP36*) associated with increasing neointima scores. Intriguingly, inhibitors of EMT/fibrosis were also identified in high neointima AOIs in both GRN (*GLIS2*) and linear regression (*OGN*) results[137,153]. This raises potential targetable mechanisms which may help delay CAV progression.

Furthermore, we identified UBAP2L as a new potential regulator of EndoMT in CAV. UBAP2L is a major regulator of EMT via numerous mechanisms. This includes positively regulating the transcription factor SNAIL1 which suppresses E-cadherin expression and by sustaining cell proliferation via regulating cyclins and PI3K/Akt signaling[133,134]. Cancer cells overexpressing UBAP2L are characterized by upregulating mesenchymal factors (N-cadherin and Vimentin). Our findings suggest that CD31+Vimentin+UBAP2L+ ECs may be in an intermediate stage of EndoMT. AOIs with high neointima also contained CD31-Vimentin+UBAP2L+ mesenchymal cells which may be at a more terminal stage of EndoMT but still undergoing proliferation and growth possibly induced by UBAP2L.

Finally, neointimal differences became more apparent as the majority of markers encoding effector immune cell infiltrates significantly correlated with inflammatory co-modules enriched for IFN-y signaling, TLR cascades, and NF-kB phosphorylation. Meanwhile, the majority of protein markers associated with cell growth factors and proliferation (e.g., EGFR and NF1) correlated with profibrotic modules enriched for FGFR, FDFR2, and VEGFA-VEGFR2 signaling (**Table 3**). Antibody ligation of HLA I and HLA II molecules stimulates EC cell proliferation and migration via activation of PI3K/AKT, ERK, and mTOR signaling[12,15,65]. Moreover, anti-HLA I antibodies can mediate an increase in FGFR cell surface expression[76].Together, these findings reinforce the notion that ECs and SMCs undergo active proliferative, migrative, and pro-fibrotic signals contributing to vessel occlusion.

In summary, our data suggest a temporal progression whereby initial inflammation by mononuclear cell infiltrates in the intima later promote proliferative and fibrotic responses. Although it is difficult to predict whether AOIs with low neointima will indeed progress into arteries with high neointima, our findings emphasize on the degree of arterial heterogeneity in CAV rejected explants. Lu et al. have reported similar findings regarding the heterogeneity of CAV lesions in a pathological study[22].

While our study reveals novel profiles in arteries from DSA+CAV+ rejected cardiac explants, there remains a few limitations to be addressed. First, DSP analysis represents data from a selected region rather than at the single-cell level. On-going studies are focused on identifying cell-type specific profiles. Furthermore, the geometric regions analyzed in this study encompassed various arterial components, including the neointima, media, and adventitia. Hence, our findings do not distinguish specific signatures associated with distinct compartments of the vessel. Further investigations employing more targeted region selection are needed to delineate these compartments. Second, despite encountering variability in patient characteristics, no significant correlations were found between patient age at transplant and neointima score nor with time post-transplant and neointima score. Thirdly, further studies are needed to characterize patient

explants from DSA-negative and native ischemic heart disease controls to validate the results of this study. Finally, our results feature novel differences between low and high neointima AOIs however, further longitudinal studies are needed to confirm the fate of low neointimal arteries.

To our knowledge, this is the first spatial multi-omics study examining arterial vessels with varying degree of neointima formation in DSA+CAV+ rejected cardiac allografts. Our findings further accentuate on the degree of vessel heterogeneity and profiles not usually identified by pathology alone. We anticipate this newly generated dataset can serve as resource for future high throughput or basic studies investigating the mechanisms of DSA mediated injury and CAV development.

Acknowledgements

We would like to thank the NanoString Technology Access Program (TAP) for this opportunity and UCLA TPCL for their resources. Finally, the authors thank the organ donors and their families for their generous gifts of life and knowledge.

Sources of Funding

This study was funded by the National Institute of Allergy and Infectious Diseases (NIH) Grant R01AI135201 (EFR, RLF, NMV), NIH Grant R21AI156592 (EFR, RLF), the NIH Ruth L. Kirschstein National Research Service Award (NRSA) T32HL069766 (JNM), and the UCLA Eugene V. Cota Robles Fellowship (JNM).

Author Contributions

JNM and EFR designed research study. JNM and HCP performed data analysis. RAS, GAF, and WMB identified patient tissue, region selection, and grading. NMV, WMB, and RLF contributed to the design of the study. JNM and EFR wrote the manuscript. All authors read and approved the manuscript.

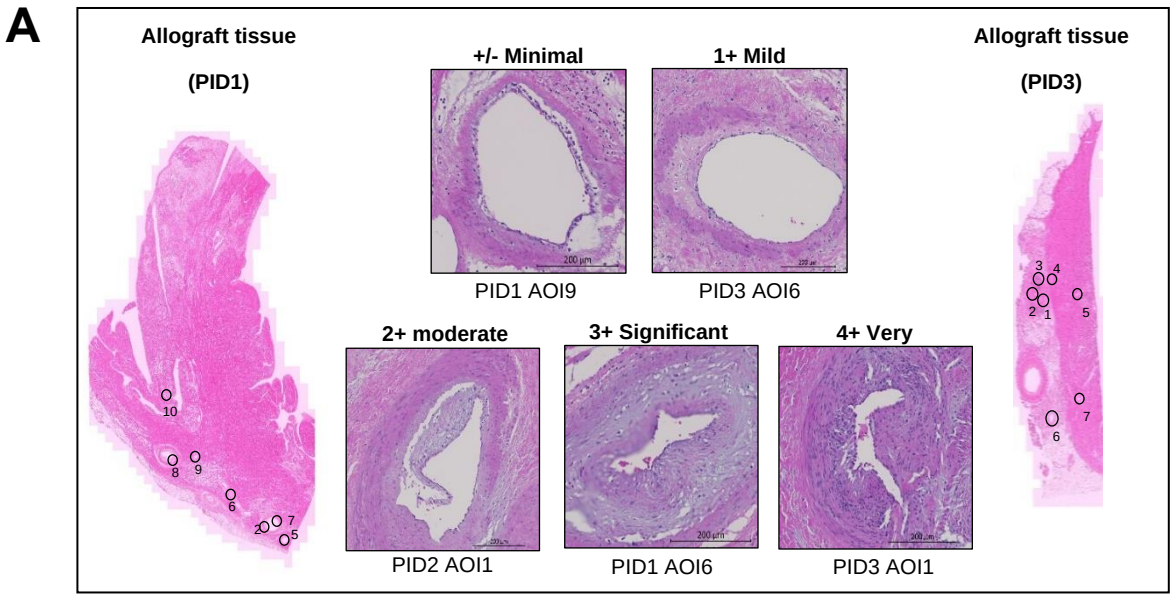
A
Allograft tissue
(PID1)
+/- Minimal
1+ Mild
Allograft tissue
(PID3)
PID1 AOI9
PID3 AOI6
2+ moderate
3+ Significant
4+ Very
PID2 AOI1
PID1 AOI6
PID3 AOI1

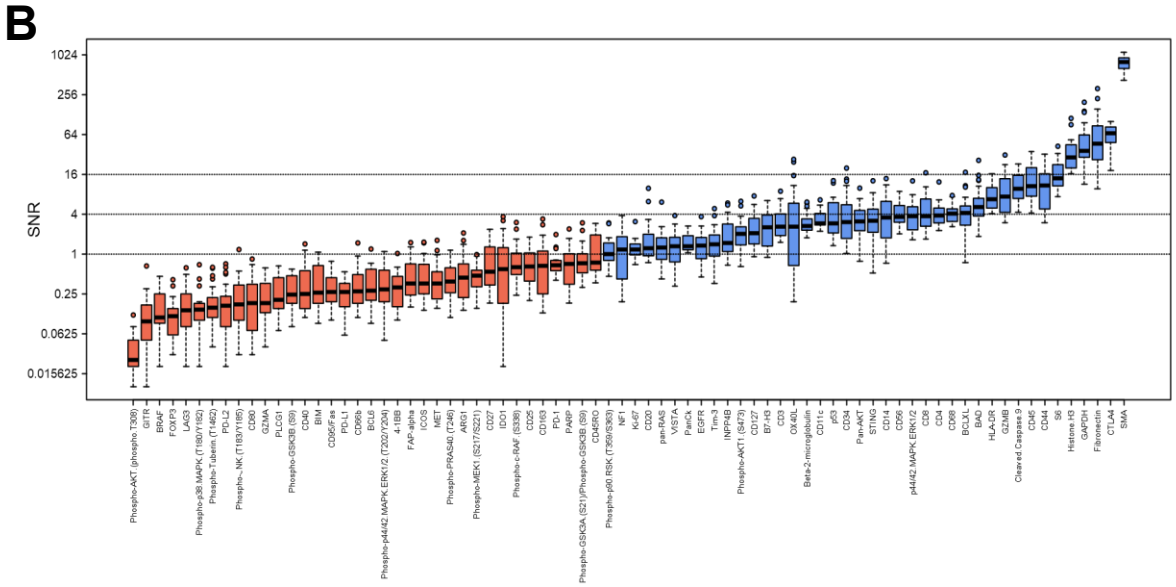
B
SNR
1024
256
64
16
4
1
0.25
0.0625
0.015625

Figure 5-1: Arterial regions from cardiac allograft vasculopathy (CAV) rejected grafts exhibit varying degrees of neointimal thickening and express 41 protein markers.

A) A total of 22 arterial areas of interest (AOIs) from CAV+DSA+ patients (PID1-3; 2 females and 1 male) were subjected to protein and RNA digital spatial profiling (DSP). In total, 11 AOIs were scored with 'low' neointima (+/- minimal and 1+ mild) and 11 with 'high' neointima (2+ moderate, 3+ significant, and 4+ very significant) by H&E staining (bar=200µm). **B)** Protein profiling identified a total of 41 protein markers which were similarly expressed across all 22 AOIs (average SNR>1 in blue). Protein data was normalized to the average of negative IgG controls and reported as a signal to noise ratio (SNR). Proteins with an average SNR<1 (in red) were considered not expressed.

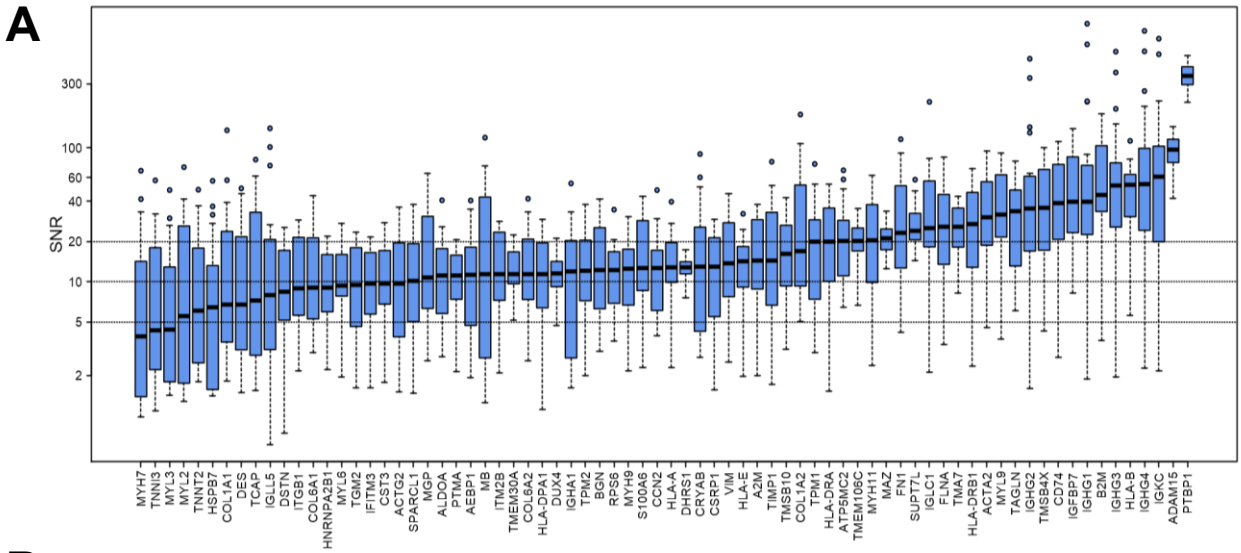
A
SNR
300
100
60
40
20
10
5
2
MYH7 TNNI3 MYL3 MYL2 TNNT2 HSPB7 COL1A1 DES TCAP IGLL5 DSTN ITGB1 COL6A1 HNRNPA2B1 MYL6 TGM2 IFITM3 CST3 ACTG2 SPARCL1 MGP ALDOA PTMA AEBP1 MB ITM2B TMEM30A COL6A2 HLA-DPA1 DUX4 IGHA1 TPM2 BGN RPS6 MYH9 S100A6 CCN2 HLA-A DHRS1 CRYAB CSRP1 VIM HLA-E A2M TIMP1 TMSB10 COL1A2 TPM1 HLA-DRA ATP5MC2 TMEM106C MYH11 MAZ FN1 SUPT7L IGLC1 FLNA TMA7 HLA-DRB1 ACTA2 MYL9 TAGLN IGHG2 TMSB4X CD74 IGFBP7 IGHG1 B2M IGHG3 HLA-B IGHG4 IGKC ADAM15 PTBP1

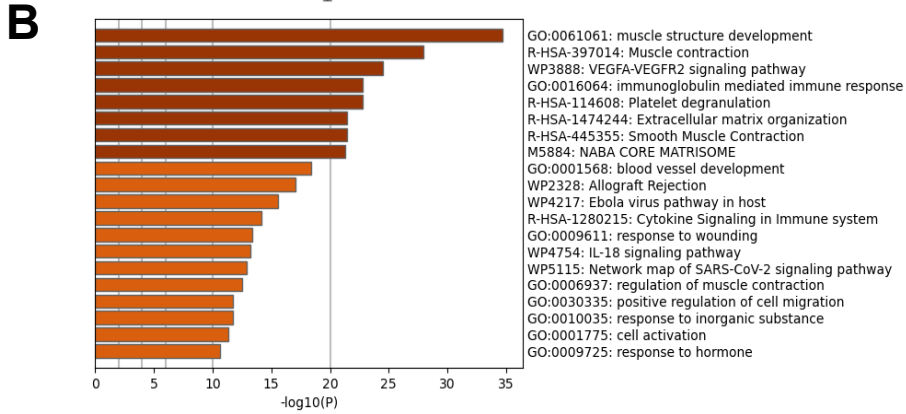
B
GO:0061061: muscle structure development
R-HSA-397014: Muscle contraction
WP3888: VEGFA-VEGFR2 signaling pathway
GO:0016064: immunoglobulin mediated immune response
R-HSA-114608: Platelet degranulation
R-HSA-1474244: Extracellular matrix organization
R-HSA-445355: Smooth Muscle Contraction
M5884: NABA CORE MATRISOME
GO:0001568: blood vessel development
WP2328: Allograft Rejection
WP4217: Ebola virus pathway in host
R-HSA-1280215: Cytokine Signaling in Immune system
GO:0009611: response to wounding
WP4754: IL-18 signaling pathway
WP5115: Network map of SARS-CoV-2 signaling pathway
GO:0006937: regulation of muscle contraction
GO:0030335: positive regulation of cell migration
GO:0010035: response to inorganic substance
GO:0001775: cell activation
GO:0009725: response to hormone
0 5 10 15 20 25 30 35
-log10(P)

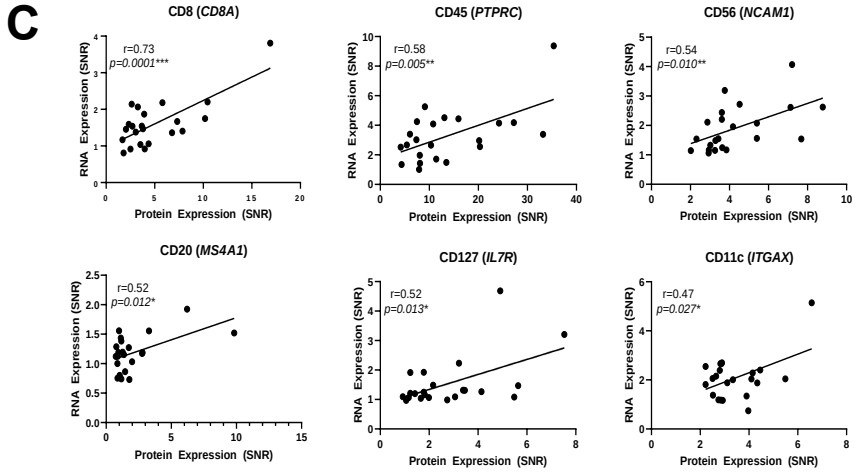
C
CD8 (CD8A)
r=0.73
p=0.0001***
CD45 (PTPRC)
r=0.58
p=0.005**
CD56 (NCAM1)
r=0.54
p=0.010**
CD20 (MS4A1)
r=0.52
p=0.012*
CD127 (IL7R)
r=0.52
p=0.013*
CD11c (ITGAX)
r=0.47
p=0.027*
RNA Expression (SNR)
Protein Expression (SNR)

Figure 5-2: Top transcripts in arterial AOIs encode for DSA-mediated immune responses and vascular remodeling.

A) Expression levels of the top 74 transcripts (average SNR>10) ranked by median values (excluding ribosomal and ATP transcripts). Whole genome RNA data was normalized to the average (+2SD) of internal negative controls (NegProbe-WTX) and is reported as a signal to noise ratio (SNR). **B)** Pathway enrichment analysis of the top 231 transcripts (with average SNR>5) using Metascape. **C)** The protein expression of CD8, CD45, CD56, CD20, CD127, and CD11c exhibited a significantly positive correlation with RNA counterpart expression. Statistical significance was determined using Pearson correlation test ($p<0.05$ (*), $p<0.01$(**), $p<0.001$(***).

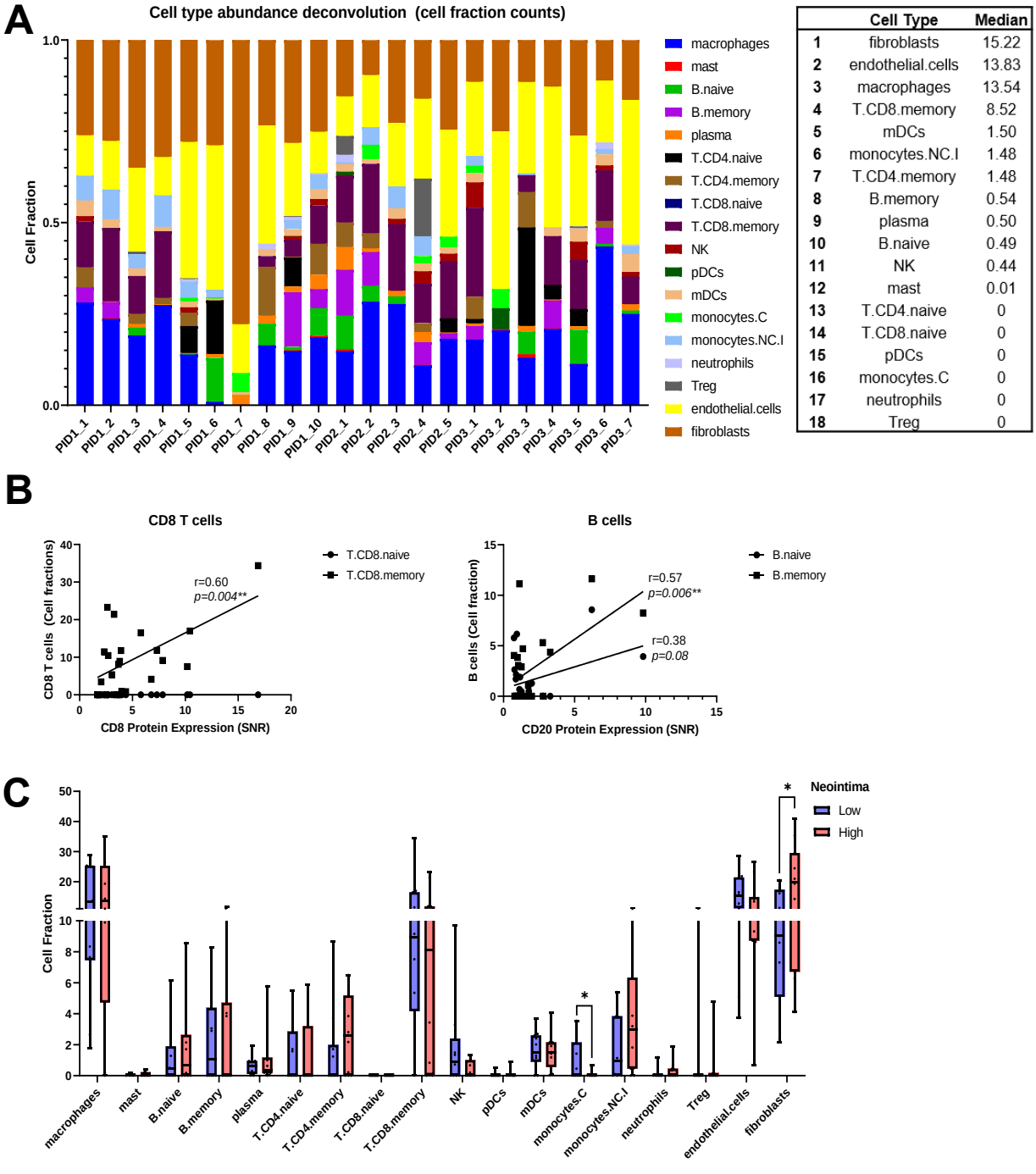

	Cell Type	Median
1	fibroblasts	15.22
2	endothelial.cells	13.83
3	macrophages	13.54
4	T.CD8.memory	8.52
5	mDCs	1.50
6	monocytes.NC.I	1.48
7	T.CD4.memory	1.48
8	B.memory	0.54
9	plasma	0.50
10	B.naive	0.49
11	NK	0.44
12	mast	0.01
13	T.CD4.naive	0
14	T.CD8.naive	0
15	pDCs	0
16	monocytes.C	0
17	neutrophils	0
18	Treg	0

Figure 5-3: Fibroblast, endothelial cells, macrophages, and memory CD8 T-cells showed highest expression across all arterial AOIs.

A) RNA data deconvolution of cell type abundance estimates across all arterial AOIs was derived using SpatialDecon algorithm. Fibroblast, ECs, macrophages, and memory CD8 T-cells were the most prominent cell types across AOIs. **B)** Deconvolution cell fraction counts for CD8+ memory T-cells and CD20 memory B-cells significantly correlated with protein expression counterparts (SNR counts) (determined by Pearson correlation coefficient test ($p < 0.01$ (**)). **C)** Cell fraction counts for each cell type between low and high neointima AOIs. Classical monocytes were significantly elevated in AOIs with low neointima while fibroblast cell fractions were higher in AOIs with high neointima Significance was determined by non-paired *student T-test* ($p < 0.05$ (*)).

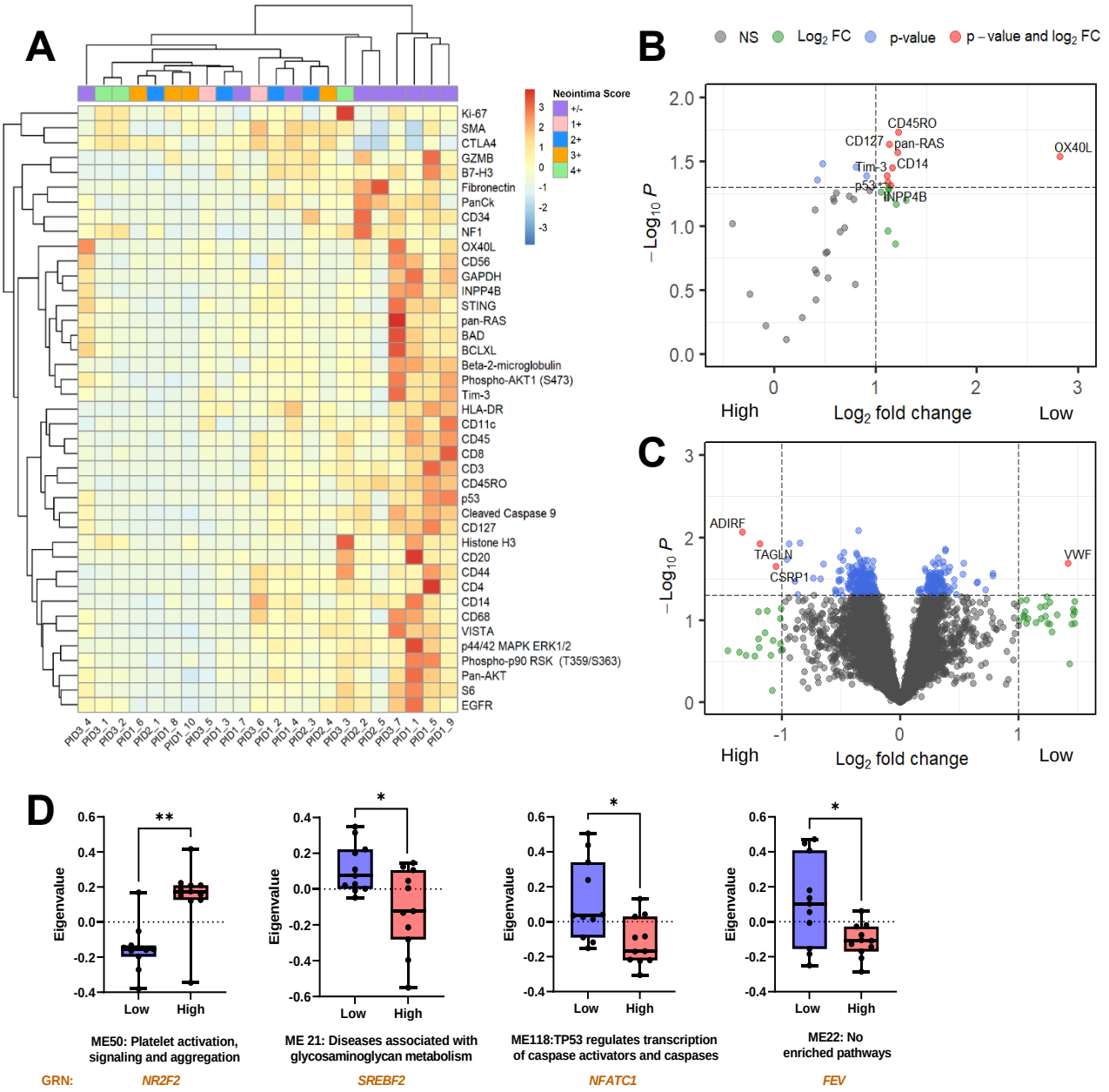
A
Neointima Score
+/-
1+
2+
3+
4+
Ki-67
SMA
CTLA4
GZMB
B7-H3
Fibronectin
PanCk
CD34
NF1
OX40L
CD56
GAPDH
INPP4B
STING
pan-RAS
BAD
BCLXL
Beta-2-microglobulin
Phospho-AKT1 (S473)
Tim-3
HLA-DR
CD11c
CD45
CD8
CD3
CD45RO
p53
Cleaved Caspase 9
CD127
Histone H3
CD20
CD44
CD4
CD14
CD68
VISTA
p44/42 MAPK ERK1/2
Phospho-p90 RSK (T359/S363)
Pan-AKT
S6
EGFR
PID3_4 PID3_1 PID3_2 PID1_6 PID2_1 PID1_8 PID1_10 PID3_5 PID1_3 PID1_7 PID3_6 PID1_2 PID1_4 PID2_3 PID2_4 PID3_3 PID2_2 PID2_5 PID3_7 PID1_1 PID1_5 PID1_9
B
NS
Log2 FC
p-value
p – value and log2 FC
CD45RO
CD127
pan-RAS
OX40L
Tim-3
CD14
p53
INPP4B
−Log10 P
High
Log2 fold change
Low
C
ADIRF
TAGLN
CSRP1
VWF
−Log10 P
High
Log2 fold change
Low
D
Eigenvalue
Low
High
ME50: Platelet activation, signaling and aggregation
ME 21: Diseases associated with glycosaminoglycan metabolism
ME118:TP53 regulates transcription of caspase activators and caspases
ME22: No enriched pathways
GRN:
NR2F2
SREBF2
NFATC1
FEV

Figure 5-4: Arterial AOIs containing high and low neointima exhibit differences in protein and RNA expression.

A) Unsupervised clustering of the 41 expressed proteins (average SNR>1) across all 22 arterial AOIs. **B)** Differentially expressed proteins (DEPs) (in red dots) between AOIs with low and high neointima. **C)** Differentially expressed genes (DEGs) between AOIs with low and high neointima (in red dots). **D)** Weighted gene co-expression network analysis (WGCNA) was used to generate gene modules (ME) of co-expressed genes. Expression of each module is represented by eigengene values (Eigenvalue). Module names were defined by Reactome pathway enrichment analysis. Arterial AOIs with low neointima increased ME21, ME22, and ME118 while AOIs with high neointima increased ME50. The highest positively correlated gene regulatory network (GNR) for each module is included below (orange text). Statistical significance for volcano plots ($Log_2FC>1$ and $p\text{-value}<0.05$) and for comparing modules (Eigenvalues) was determined using linear mixed-effects model (including PID as random effects) using in R software ($p<0.05$ (*) and $p<0.01$ (**)).

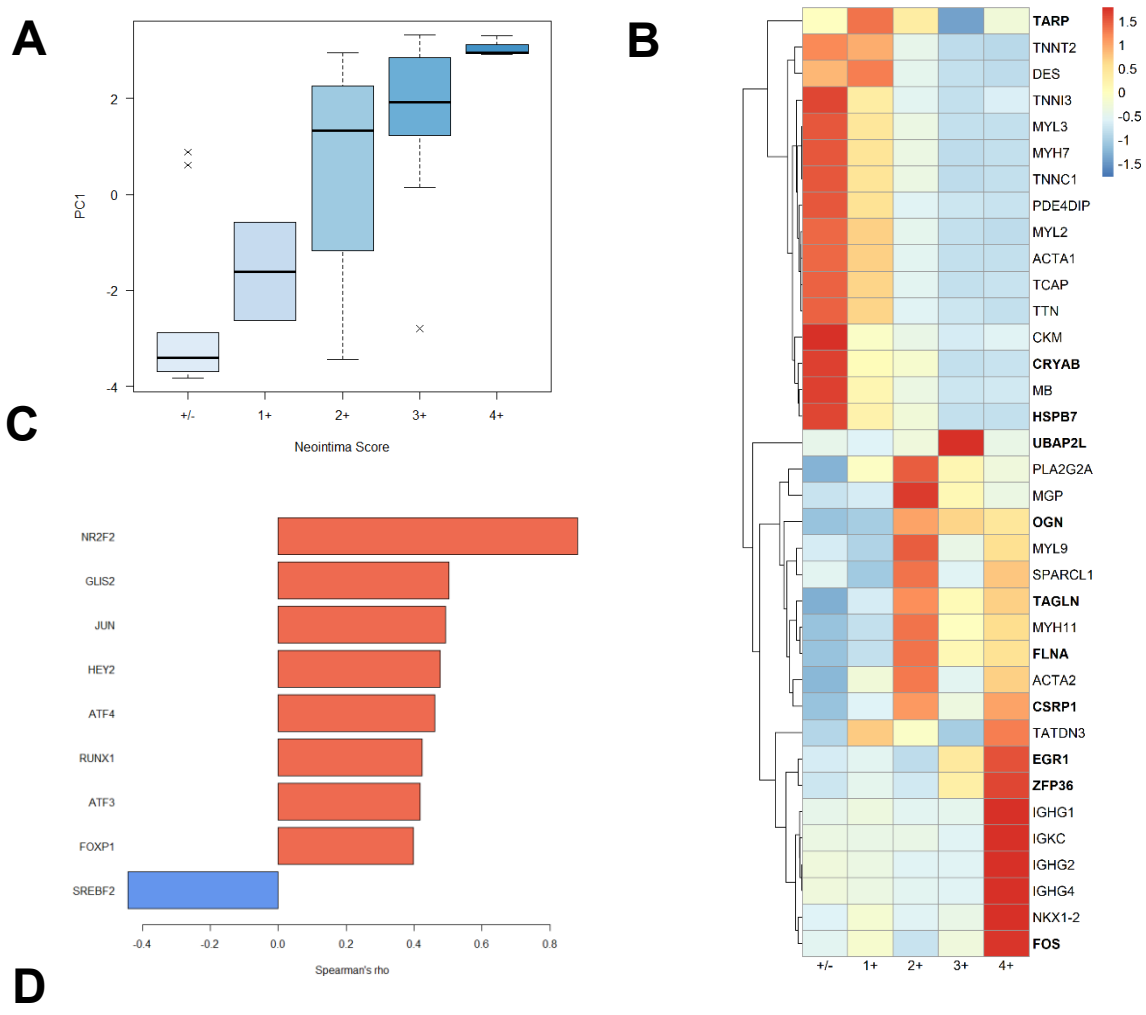
A
PC1
2
0
-2
-4
+/-
1+
2+
3+
4+
Neointima Score
B
TARP
TNNT2
DES
TNNI3
MYL3
MYH7
TNNC1
PDE4DIP
MYL2
ACTA1
TCAP
TTN
CKM
CRYAB
MB
HSPB7
UBAP2L
PLA2G2A
MGP
OGN
MYL9
SPARCL1
TAGLN
MYH11
FLNA
ACTA2
CSRP1
TATDN3
EGR1
ZFP36
IGHG1
IGKC
IGHG2
IGHG4
NKX1-2
FOS
1.5
1
0.5
0
-0.5
-1
-1.5
+/-
1+
2+
3+
4+
C
NR2F2
GLIS2
JUN
HEY2
ATF4
RUNX1
ATF3
FOXP1
SREBF2
-0.4
-0.2
0.0
0.2
0.4
0.6
0.8
Spearman's rho
D
SMA
Viment
CD31
CD45
UBAP2
SMA
UBAP2
Vimentin
UBAP2L
CD31
UBAP2
CD45
UBAP2
Merged

Figure 5-5: A total of 36 genes and 9 gene regulatory networks (GNRs) were significantly associated with neointima score.

A) From principal component analysis of genes significantly associated with neointima score (n=245), we identified the first principal component (PC1) as increasing in a stepwise manner with increasing neointima score. **B)** A total of 36 genes were significantly associated (Adjusted *p-value* < *0.05*) with PC1 showed distinct patterns with increasing neointima score. Genes in bold have been characterized to promote cell proliferation, migration, epithelial-to-mesenchymal transition (EMT) and fibrosis (p-values found in **Supplementary Table 6**). **C)** A total of 9 gene regulatory networks (GNRs) correlated with PC1 and therefore increasing neointima score (*p-value* < *0.05*). **D)** UBAP2L co-localized with CD31+ ECs and Vimentin+ mesenchymal cells within the neointima. Representative image shows PID1 AOI 8 which exhibits significant neointima (3+) (scale bar=50μm).

Tables

Table 5-1: Differentially expressed proteins (DEPs) and differentially expressed genes (DEGs) between low and high neointima AOIs.

	Protein	Log_2FC	*p-value*
1	OX40L	2.82	*0.029*
2	CD45RO	1.23	*0.019*
3	pan-RAS	1.22	*0.027*
4	CD14	1.17	*0.035*
5	INPP4B	1.15	*0.049*
6	CD127	1.14	*0.023*
7	p53	1.12	*0.046*
8	Tim-3	1.11	*0.041*
	Gene	**Log2FC**	***p-value***
1	*VWF*	1.42	*0.021*
2	*CSRP1*	-1.05	*0.022*
3	*TAGLN*	-1.18	*0.012*
4	*ADIRF*	-1.33	*0.009*

Table 5-2: Differentially expressed modules between low and high neointima AOIs and highest positively correlated gene regulatory network (GNR) (*p-value* < 0.5).

Module name	Total genes	Representative genes[a]	Enriched pathway[b] (genes in enriched pathways)	GNR	Neointima
ME21	8	ASCL5, CLDN7, CLEC4F, CTRB1, GPC5, NECTIN4, NKAIN4, TMEM97	Cell-cell junction organization (NECTIN4,CLDN7), Activation of Matrix Metalloproteinases (CTRB1), Diseases associated with glycosaminoglycan metabolism (GPC5)	SREBF2	↑Low
ME22	7	ABCC8, HOXD12, RXFP2, SHOC1, WRAP73, ZNF283, ZNF649	NA	FEV	↑Low
ME50	10	GRAMD1C, ITIH3, ITIH4, LURAP1L, MRPS14, PAWR, RAD51B, REXO5, RHOB, SMTN, ZDHHC11	Platelet activation, signaling and aggregation (RHOB/ITIH4/ITIH3), Diseases of DNA repair (RAD51B)	NR2F2	↑High
ME118	15	ACSM3, ARHGAP28, CITED1, CNPY1, EFCAB8, F9, ITGAX, KCNJ13, KCP, MMP26, MTNR1A, OR1Q1, PRICKLE4, SEPTIN3, SLC25A15, SMG9, TMEM14A, TMEM269, TP63, TRAIP	TP53 Regulates Transcription of Caspase Activators and Caspases (TP63), Activation of the TFAP2 (AP-2) family of transcription factors (CITED1), Gamma-carboxylation of protein precursors (F9), Urea cycle (SLC25A15)	NFATC1	↑Low

a: Genes with expression pattern best representative of combined module of co-expressed genes
b: Enrichment pathway defined by Reactome and (genes in enriched pathways)

Table 5-3: Highly correlated proteins with WGCNA modules between low and high neointima AOIs.

		Low Neointima AOIs			High Neointima AOIs				
Module	**Protein**	**r**	***p-value***		**r**	***p-value***		**Representative genes[a]**	**Enriched pathway[b] (genes in enriched pathway)**
ME65	B7-H3	0.78	**	*0.006*	-0.08	*ns*	*0.818*	CD80, GGACT, OR52M1, PALD1, PTK7, SMIM41	Costimulation by the CD28 family (CD80)
	GZMB	0.76	**	*0.009*	-0.34	*ns*	*0.313*		
	Fibronectin	0.75	*	*0.011*	-0.51	*ns*	*0.114*		
ME77	Ki-67	0.71	*	*0.018*	0.73	*	*0.014*	ABCA6, APOC3, ATE1, CC2D1A, CD163, CDKL3, CHI3L1, DSTYK, H4C9, HK3, HLA-DQA1, HLA-DQB1, IFT27, ITGAX, KLHDC4, MAP3K8, PCYOX1L, PFKFB3, PLA1A, PLTP, TFRC, TNC, TRAPPC2L, TREML2, TRIM14, ZC3H12A, ZNF394, ZNF461	Costimulation by the CD28 family (HLA-DQB1, MAP3K8, HLA-DQA1), Interferon gamma signaling (HLA-DQB1/HLA-DQA1, TRIM14), HDL remodeling (PLTP, APOC3)
	CD8	0.68	*	*0.025*	0.35	*ns*	*0.286*		
	CD68	0.67	*	*0.028*	0.12	*ns*	*0.735*		
	CD44	0.65	*	*0.037*	0.14	*ns*	*0.694*		
	CD45	0.64	*	*0.04*	0.28	*ns*	*0.402*		
ME91	GZMB	0.74	*	*0.013*	-0.07	*ns*	*0.839*	B3GNT8, IRAK2, ITM2A, KNOP1, NUDCD2, PMEL, SCN3A, SP140, ZBTB18, ZDHHC17	Toll-like Receptor Cascades (IRAK2), O-linked glycosylation of mucins (B3GNT8), TAK1 activates NFkB by phosphorylation and activation of IKKs complex (IRAK2), L1CAM interactions (SCN3A)
	p53	0.65	*	*0.037*	0.61	*ns*	*0.052*		
ME118	GZMB	0.67	*	*0.028*	-0.75	**	*0.01*	ACSM3, ARHGAP28, CITED1, CNPY1, EFCAB8, F9, ITGAX, KCNJ13, KCP, MMP26, MTNR1A, OR1Q1, PRICKLE4, SEPTIN3, SLC25A15, SMG9, TMEM14A, TMEM269, TP63, TRAIP	TP53 Regulates Transcription of Caspase Activators and Caspases (TP63), Activation of the TFAP2 (AP-2) family of transcription factors (CITED1), Gamma-carboxylation of protein precursors (F9), Urea cycle (SLC25A15)
	Fibronectin	0.62	*	*0.048*	-0.04	*ns*	*0.924*		
ME242	CD56	0.8	**	*0.005*	-0.03	*ns*	*0.946*	CNMD, DTYMK, GORAB, METTL21A, NOL7, STUB1, TRAF6, ZBTB4, ZNF772	TGF-beta receptor signaling activates SMADs (STUB1), TAK1 activates NFkB by phosphorylation and activation of IKKs complex (TRAF6), Protein methylation (METTL21A)
	OX40L	0.8	**	*0.005*	-0.2	*ns*	*0.557*		
	BAD	0.62	*	*0.048*	-0.35	*ns*	*0.299*		
ME304	Ki-67	0.79	**	*0.006*	0.12	*ns*	*0.735*	BRI3BP, C9, CRYBB2, DZIP1, GALNT13, GBP3, ITGAX, LUZP2, NQO2, OAS1, SLC25A32, USHBP1	Interferon gamma signaling (OAS1, GBP3)
	HLA-DR	0.73	*	*0.01*	0.59	*ns*	*0.056*		
	Tim-3	0.68	*	*0.025*	0.38	*ns*	*0.244*		
ME161	NF1	-0.2	*ns*	*0.562*	0.86	**	*0.001*	CASP3, CORT, DCAF8L2, FRS3, ISM1, NSRP1, PITHD1, SFRP5, SHC3, WDR5B	MAPK1/MAPK3 signaling (FRS3/SHC3), Signaling by FGFR (FRS3), Apoptotic factor-mediated response (CASP3)
	Fibronectin	-0.54	*ns*	*0.094*	0.65	*	*0.034*		
	SMA	0.09	*ns*	*0.796*	0.63	*	*0.044*		
ME205	EGFR	0.09	*ns*	*0.796*	0.8	**	*0.005*	ASCL3, FGFBP2, KIF1A, OR2G3, OTUD1	FGFR2b ligand binding and activation (FGFBP2), COPI-dependent Golgi-to-ER retrograde traffic (KIF1A)
	STING	0.17	*ns*	*0.615*	0.78	**	*0.006*		
	Histone H3	-0.25	*ns*	*0.468*	0.69	*	*0.023*		
ME206	CD11c	0.25	*ns*	*0.451*	0.79	**	*0.006*	BARHL1, C19orf71, ELMO2, FSCB, SHCBP1, ULK4	PTK6 Regulates RHO GTPases, RAS GTPase and MAP kinases (ELMO2), Fcgamma receptor (FCGR) dependent phagocytosis (ELMO2), VEGFA-VEGFR2 Pathway (ELMO2), PTK6 Regulates RHO GTPases, RAS GTPase and MAP kinases (ELMO2)
	CD34	-0.17	*ns*	*0.615*	0.77	**	*0.007*		
	NF1	-0.29	*ns*	*0.381*	0.71	*	*0.018*		
	Phospho-AKT1 (S473)	-0.12	*ns*	*0.735*	0.7	*	*0.02*		
	CD68	-0.04	*ns*	*0.924*	0.69	*	*0.023*		
	BCLXL	-0.01	*ns*	*0.99*	0.68	*	*0.025*		
	S6	0.07	*ns*	*0.839*	0.66	*	*0.031*		
	SMA	-0.21	*ns*	*0.539*	0.66	*	*0.031*		
	Fibronectin	-0.04	*ns*	*0.924*	0.64	*	*0.04*		
	EGFR	0.03	*ns*	*0.946*	0.63	*	*0.044*		
	VISTA	-0.29	*ns*	*0.386*	0.62	*	*0.048*		

a: Genes with expression pattern best representative of combined module of co-expressed genes

b: Enrichment pathway defined by Reactome and (genes in enriched pathway)

Statistical significance was determined using Spearman correlation test ($p<0.05$ (*) and $p<0.01$(**) in GraphPad Prism software v9.3.1.

Graphed results are shown in supplementary figure 3.

Supplementary Materials

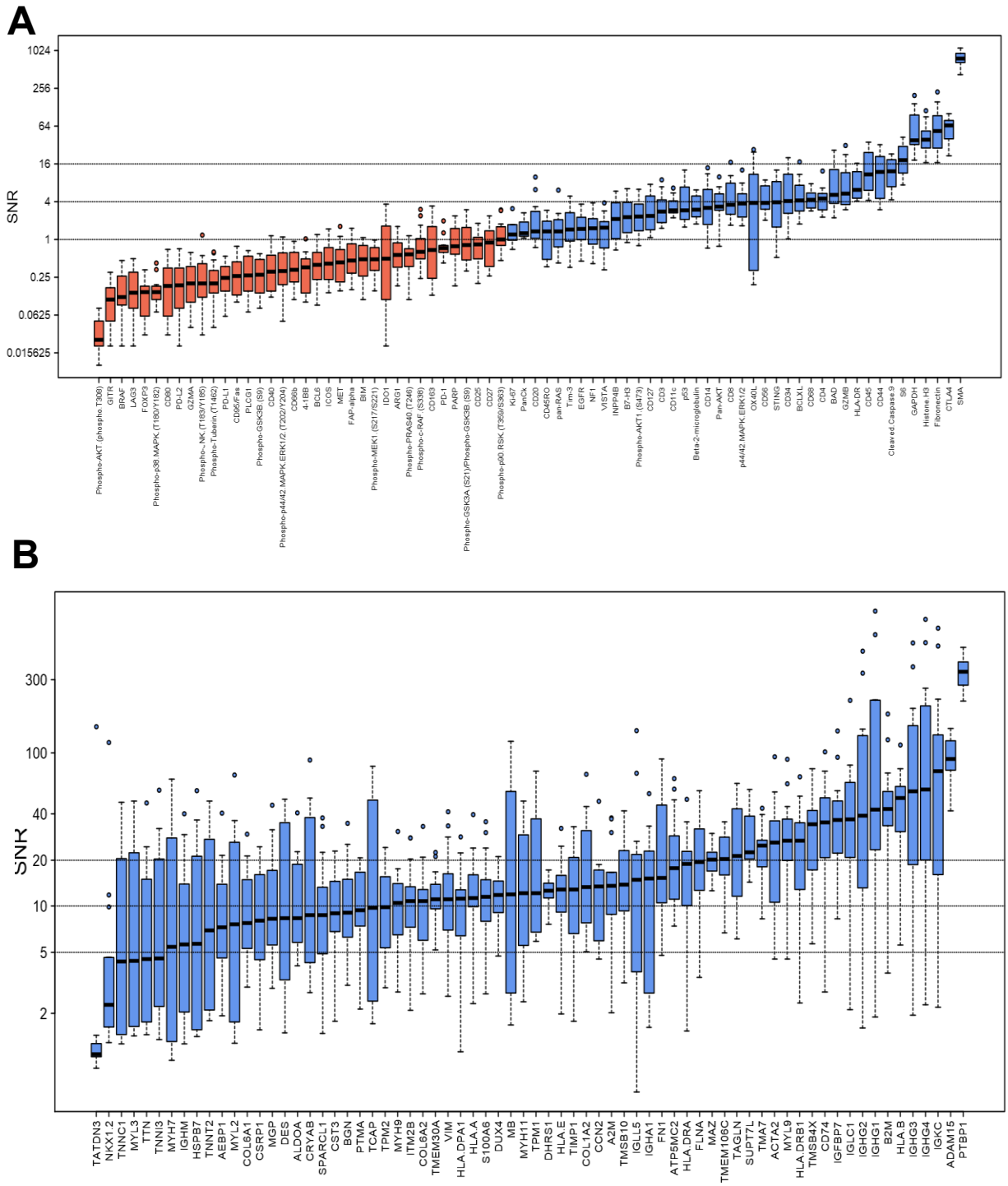

Supplementary Figure 5-1: Highly expressed proteins and transcripts across 14 areas of interest (AOIs) encompassing entire arteries. A) Protein profiling identified a total of 43 protein markers which were similarly expressed across 14 AOIs capturing whole arteries (average SNR>1 in blue). The expressed protein markers observed in the 14 AOIs (capturing entire arteries) were consistent with those expressed in the 22 AOIs dataset. Protein data was normalized to the average of negative IgG controls and reported as a signal to noise ratio (SNR). Proteins with an average SNR<1 (in red) were considered not expressed. **B)** Expression levels of the top 70 transcripts (average SNR>10) across 14 AOIs. Nearly all of the top 70 transcripts exhibited significant overlap (65/70) with the top 74 transcripts identified in the 22 AOI dataset. Data is ranked by median values (excluding ribosomal and ATP transcripts). Whole genome RNA data was normalized to the average (+2SD) of internal negative controls (NegProbe-WTX) and is reported as a signal to noise ratio (SNR).

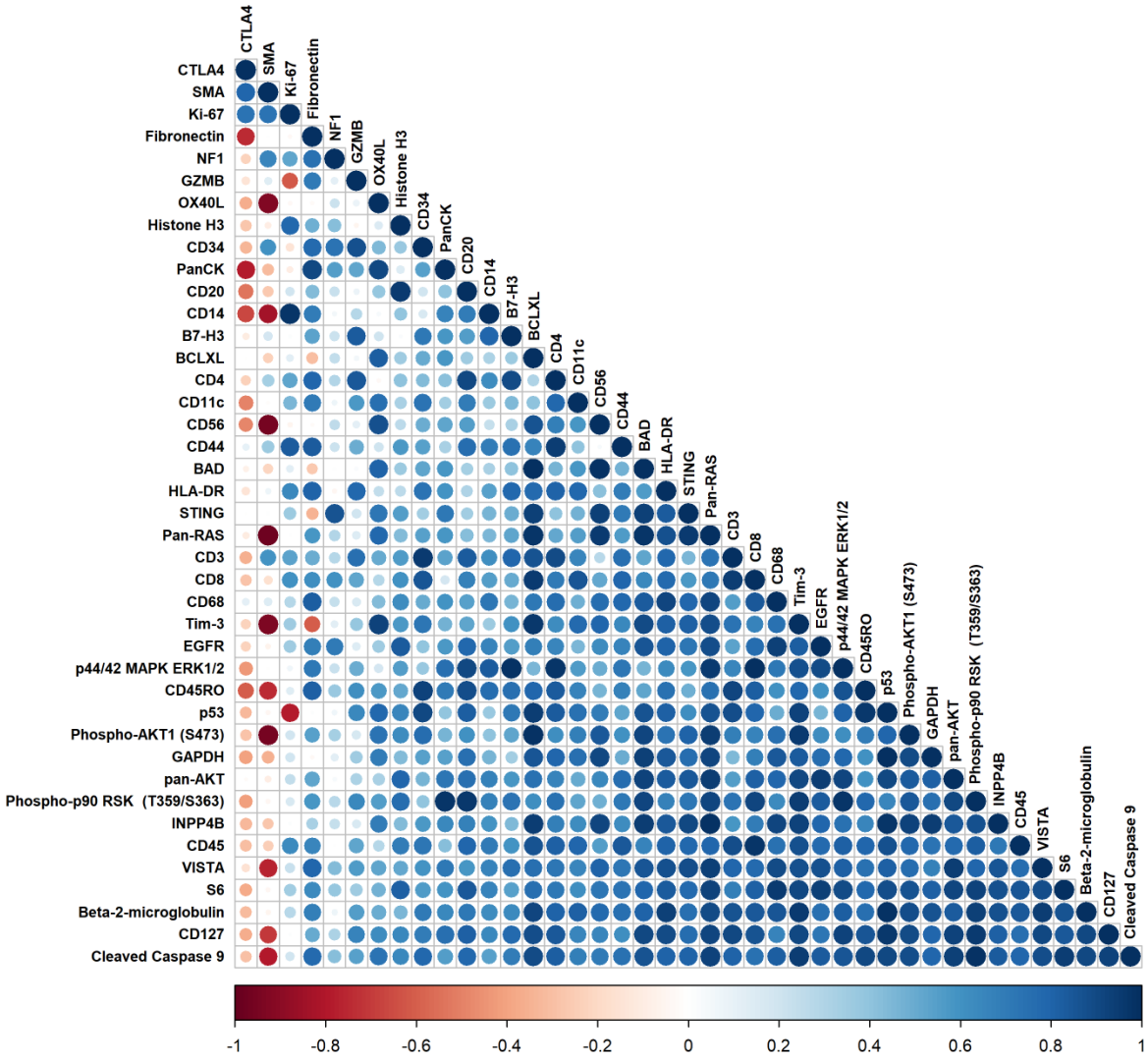

Supplementary Figure 5-2: Proteins highly correlate with one another across all 22 arterial AOIs. Correlation matrix illustrating positively correlated proteins (in blue) and negatively correlated proteins (red). Dot size corresponds to correlation values. Correlation p-values can be found in **Supplementary Table 5**. Correlation matrix was generated using 'GeneralCorr' package in R Software.

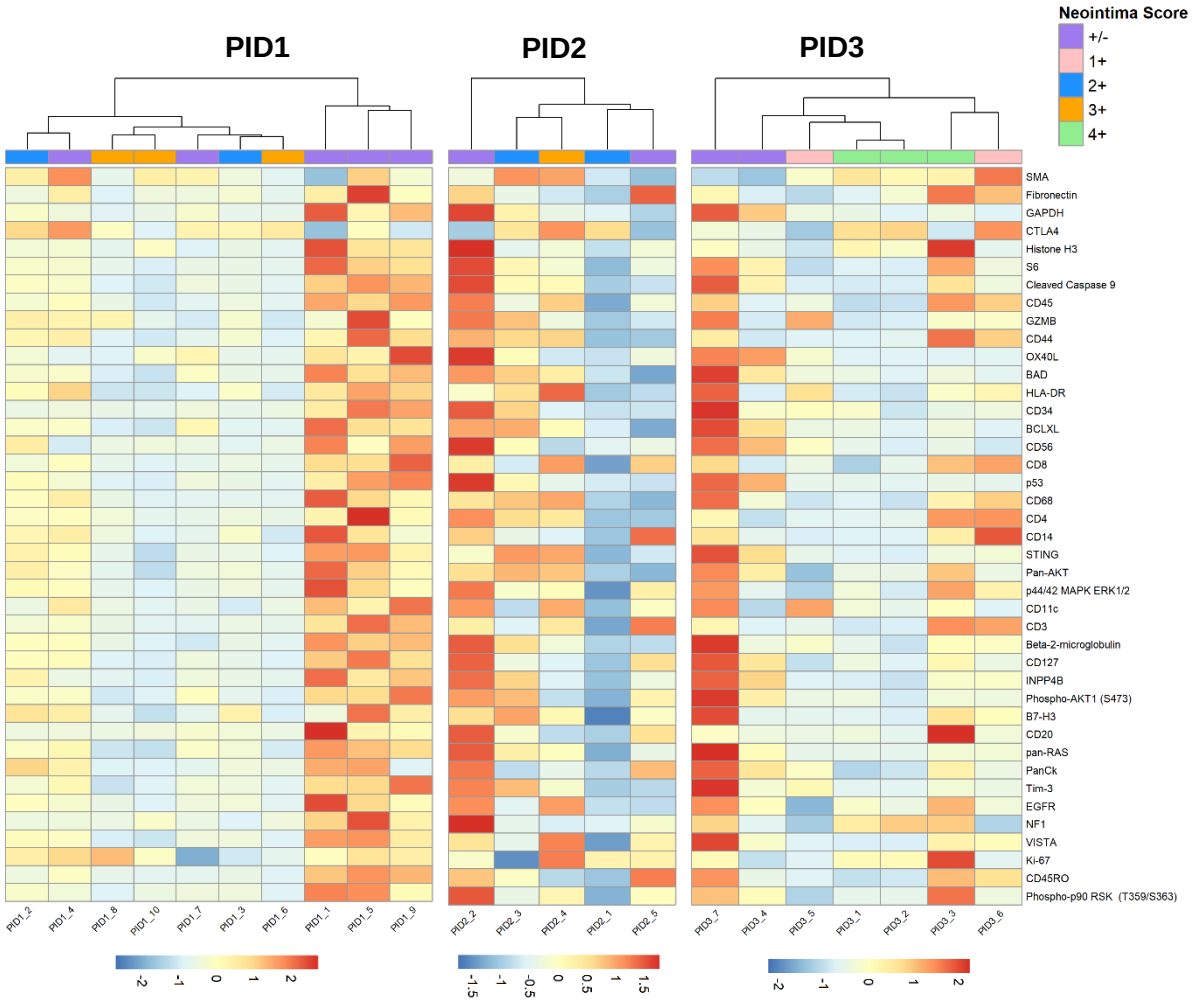

Supplementary Figure 5-3: Arterial AOIs with low neointima show higher protein expression compared to AOIs with high neointima for each patient (PID) explant. Unsupervised clustering of all 22 arterial regions for each PID illustrates that AOIs containing low neointima scores (+/- minimal and 1+ mild) showed relatively higher expression of protein markers compared to AOIs scored with high neointima (2+ moderate, 3+ significant, and 4+ very significant). Heatmaps were generated using ‘pheatmap’ package in R software v4.1.1.

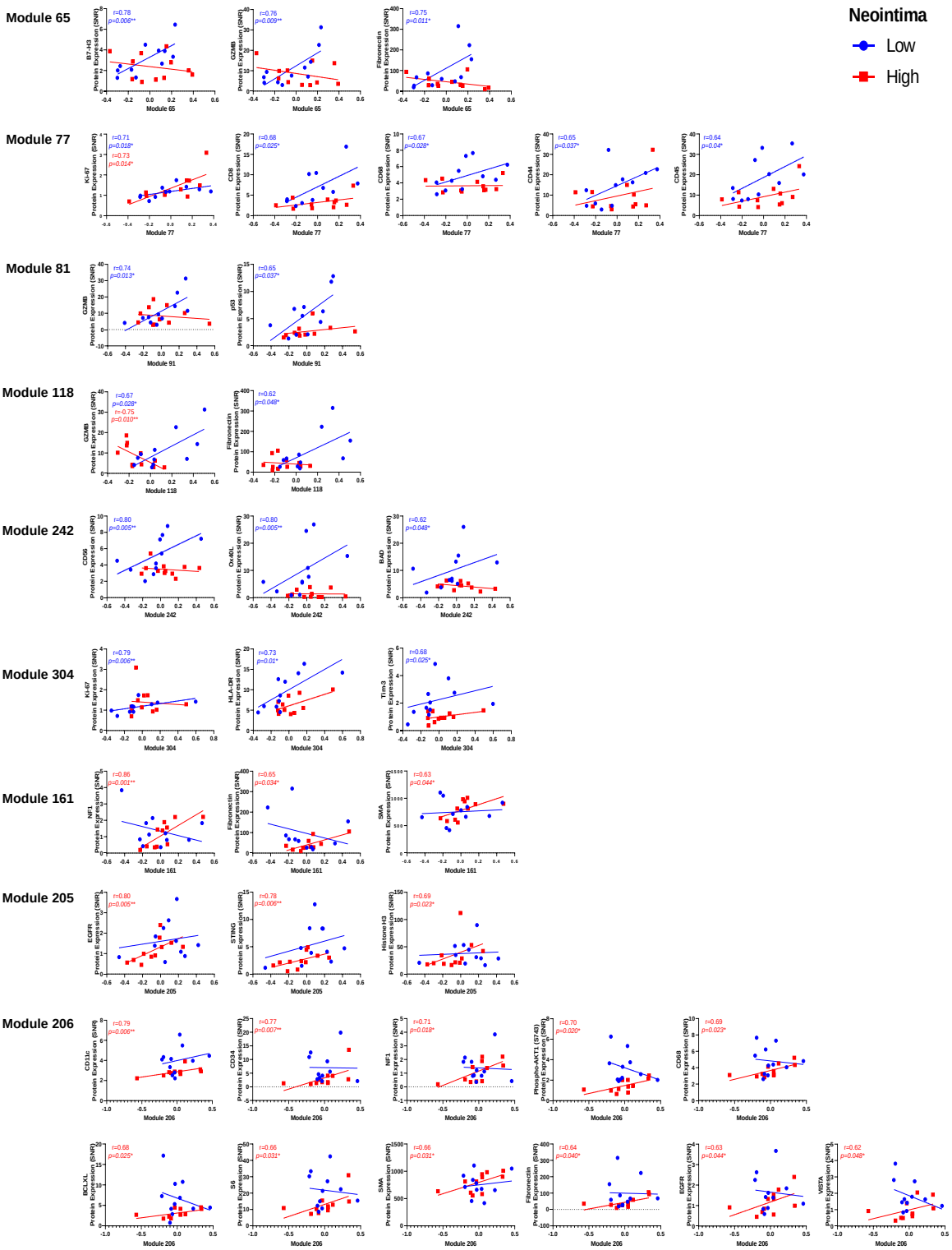
Module 65
Module 77
Module 81
Module 118
Module 242
Module 304
Module 161
Module 205
Module 206
Neointima
Low
High

Supplementary Figure 5-4: Arterial AOIs with low and high neointima differentially correlated with WGCNA modules. Proteins involved in immune infiltration and activation (e.g., CD45 and GZMB) and apoptosis (p53 and BAD) more highly correlated with WGCNA modules enriched for inflammatory pathways (ME65, 77, 91, 118, 242, and 304) in low neointima AOIs. Proteins involved in repair and fibrotic tissue progression (E.g., NF1 and EGFR) more highly correlated with modules enriched for cell proliferation, migration, and fibrosis (ME161, 205, 206) in AOIs with high neointima. Statistical significance was determined using Spearman correlation test ($p<0.05$ (*) and $p<0.01$(**) in GraphPad Prism software v9.3.1. Summarized results are shown in **Table 3**.

Supplementary Tables

Supplementary Table 5-1: Cardiac explant tissue patient (PID) information.

PID	Sex	Age at Tx	Race	Etiology	Donor Age	Donor Sex	Donor Race	HLA MM	DSA	AMR	AMR specific treatments	Maintance Treatments	Explant Collection (yrs-post Tx)	Block tissue section
1	F	3	White	Congenital	unknown	unknown	unknown	7/8	A2, A69, A66:02, A34:02	Suspicious	unknown	Tacrolimus, sirolimus, prednisone	9	unknown
2	F	12	Hispanic/ Latino	Dilated myopathy: Idiopathic	23	M	White	4/8	A24, DR51 and AT1R	Suspicious	ATG, Rituximab, steroids, plasmapheresis	Tacrolimus, sirolimus, prednisone	6	Proximal posterior decending artery+posterior left ventricle+posterior papillary muscle
3	M	59	Arab or Middle Eastern	Dilated myopathy: Ischemic	53	M	Hispanic/ Latino	8/8	A2, DR7, and DQ2	No	ATG, steroids	Tacrolimus, prednisone, mycophenolate	2	Right coronary artery to posterior decending artery

Supplementary Table 5-2: AOI characteristics for each patient.

	PID_AOI	Vessel Size	Neointima Score	Neointima Level	AOI surface area
1	PID1_1	Small	+/-	Low	329263.8
2	PID1_2	Medium	2+	High	321196.4
3	PID1_3	Medium	2+	High	334999
4	PID1_4	Medium	+/-	Low	267510.9
5	PID1_5	Small	+/-	Low	320404
6	PID1_6	Small	3+	High	303792.3
7	PID1_7	Medium	+/-	Low	325248.6
8	PID1_8	Medium	3+	High	303022.8
9	PID1_9	Small	+/-	Low	324421.5
10	PID1_10	Small	3+	High	258791.9
11	PID2_1	Medium	2+	High	325248.6
12	PID2_2	Small	+/-	Low	180822.8
13	PID2_3	Small	2+	High	165501.7
14	PID2_4	Medium	3+	High	336621.1
15	PID2_5	Medium	+/-	Low	322007.3
16	PID3_1	Medium	4+	High	282375.5
17	PID3_2	Medium	4+	High	315628.9
18	PID3_3	Small	4+	High	130200.7
19	PID3_4	Small	+/-	Low	278590.4
20	PID3_5	Small	1+	Low	326839.5
21	PID3_6	Small	1+	Low	323631.3
22	PID3_7	Small	+/-	Low	335831.6

Supplementary Table 5-3: Target proteins within NanoString Digital Spatial Profiling (DSP) Panels.

Controls	Immune Cell Profiling	IO Drug Target	Immune Activation	Immune Cell Typing	PI3K/AKT Signaling	MAPK Signaling	Cell Death
Rb IgG	PD-1	4-1BB	CD127	CD45RO	Phospho-AKT1 (S473)	BRAF	BAD
Ms IgG1	CD68	LAG3	CD25	FOXP3	Phospho-GSK3B (S9)	EGFR	BCL6
Ms IgG2a	HLA-DR	OX40L	CD80	CD34	Phospho-GSK3A (S21)/Phospho-GSK3B (S9)	Phospho-c-RAF (S338)	BCLXL
Histone H3	Ki-67	Tim-3	ICOS	CD66b	INPP4B	Phospho-JNK (T183/Y185)	CD95/Fas
S6	B2M	VISTA	PD-L2	FAP-alpha	PLCG1	Phospho-MEK1 (S217/S221)	GZMA
GAPDH	CD11c	ARG1	CD40	CD14	Phospho-PRAS40 (T246)	Phospho-p38 MAPK (T180/Y182)	NF1
	CD20	B7-H3	CD44	CD163	Phospho-Tuberin (T1462)	Phospho-p44/42 MAPK ERK1/2 (T202/Y204)	Cleaved Caspase 9
	CD3	IDO1	CD27		Pan-AKT	pan-RAS	p53
	CD4	STING			MET	p44/42 MAPK ERK1/2	PARP
	CD45	GITR				Phospho-p90 RSK (T359/S363)	BIM
	CD56						
	CD8						
	CTLA4						
	GZMB						
	PD-L1						
	PanCk						
	SMA						
	Fibronectin						

*IO=Immune oncology

Supplementary Table 5-4: Median protein expression across all arterial AOIs.

	Protein marker (*Gene name*)	Median
1	SMA (*SMN1*)	797.03
2	CTLA4	66.95
3	Fibronectin (*FN1*)	46.43
4	GAPDH (*GAPDHS*)	36.31
5	Histone H3 (*H3C1*)	28.79
6	S6 (*RPS6*)	13.92
7	CD44	10.85
8	CD45 (*PTPRC*)	10.56
9	Cleaved Caspase 9 (CASP9)	9.74
10	GZMB	7.38
11	HLA-DR (*HLA-DRA*)	6.72
12	BAD	5.16
13	BCLXL (*BCL2L1*)	4.15
14	CD68	4.09
15	CD4	3.77
16	CD8 (*CD8A*)	3.74
17	p44/42 MAPK ERK1/2 (*MAPK1*)	3.69
18	CD56 (*NCAM1*)	3.62
19	CD14	3.54
20	STING (*STING1*)	3.18
21	pan-AKT (*AKT1*)	3.14
22	CD34	3.06
23	p53 (*TP53*)	2.92
24	CD11c (ITGAX)	2.91
25	Beta-2-microglobulin (*B2M*)	2.67
26	TNFSF4 (*OX40L*)	2.61
27	CD3 (*CD3D*)	2.59
28	B7-H3 (*CD276*)	2.56
29	CD127 (*IL7R*)	2.08
30	Phospho-AKT1 (S473) (*AKT1*)	2.03
31	INPP4B	1.47
32	Tim-3 (*HAVCR2*)	1.40
33	EGFR	1.33
34	PanCK (*KRT18*)	1.32
35	VISTA (VSIR)	1.31
36	Pan-RAS (KRAS)	1.25
37	CD20 (*MS4A1*)	1.21
38	Ki-67 (*MKI67*)	1.18
39	Neurofibromin 1 (*NF1*)	1.17
40	Phospho-p90 RSK (T359/S363)(*RPS6KA1*)	1.00
41	CD45RO (*PTPRC*)	0.74

Supplementary Table 5-5: Top 30 positive correlations and four negative correlations across all arterial AOIs.

	Protein vs. Protein		Correlation	*p-value*
1	BAD	BCLXL	1.00	*2.25E-13*
2	Cleaved Caspase 9	Pan-RAS	0.93	*6.00E-11*
3	INPP4B	Pan-RAS	0.98	*8.72E-11*
4	S6	Pan-RAS	0.93	*9.71E-10*
5	CD127	Pan-RAS	0.92	*1.58E-09*
6	CD8	CD3	0.95	*3.42E-09*
7	S6	CD127	0.9	*1.13E-08*
8	Phospho-AKT1 (S473)	Pan-RAS	0.94	*1.40E-08*
9	BAD	Tim-3	0.94	*1.59E-08*
10	CD44	CD4	0.95	*3.89E-08*
11	CD127	p44/42 MAPK ERK1/2	0.92	*4.51E-08*
12	CD127	Phospho-p90 RSK (T359/S363)	0.96	*4.82E-08*
13	BCLXL	Pan-RAS	0.95	*7.27E-08*
14	p44/42 MAPK ERK1/2	Phospho-p90 RSK (T359/S363)	0.92	*1.00E-07*
15	pan-AKT	Pan-RAS	0.94	*1.24E-07*
16	CD3	VISTA	0.99	*1.49E-07*
17	BCLXL	Tim-3	0.93	*1.59E-07*
18	Pan-RAS	VISTA	0.97	*1.86E-07*
19	INPP4B	Phospho-AKT1 (S473)	0.93	*1.93E-07*
20	CD3	CD45RO	0.97	*2.09E-07*
21	CD45RO	CD3	0.92	*2.09E-07*
22	Phospho-p90 RSK (T359/S363)	Pan-RAS	0.92	*2.26E-07*
23	p44/42 MAPK ERK1/2	VISTA	0.93	*2.60E-07*
24	Phospho-AKT1 (S473)	CD127	0.91	*2.76E-07*
25	INPP4B	CD127	0.93	*3.92E-07*
26	CD127	Cleaved Caspase 9	0.91	*3.92E-07*
27	Tim-3	GAPDH	0.97	*4.45E-07*
28	p53	Tim-3	0.93	*6.11E-07*
29	CD45	VISTA	0.99	*6.55E-07*
30	BCLXL	STING	0.95	*7.93E-07*
1	CTLA4	CD20	-0.70	*0.006*
2	CTLA4	OX40L	-0.67	*0.009*
3	CTLA4	CD45RO	-0.78	*0.028*
4	SMA	CD56	-0.97	*0.038*

Supplementary Table 6-6: PC1 vs. increasing neointima significant genes.

	Gene	*adj. p-value*
1	MB	*3.63654E-09*
2	TATDN3	*9.97889E-08*
3	MYH7	*3.59311E-07*
4	TCAP	*4.95505E-07*
5	MYL2	*4.26353E-06*
6	TNNT2	*8.91826E-06*
7	DES	*4.33708E-05*
8	ACTA1	*4.33708E-05*
9	MYL3	*4.33708E-05*
10	TNNC1	*6.19108E-05*
11	PLA2G2A	*8.82703E-05*
12	MYH11	*0.000209127*
13	TNNI3	*0.0002321*
14	HSPB7	*0.000387171*
15	NKX1-2	*0.000457262*
16	TAGLN	*0.000510579*
17	TTN	*0.00051905*
18	FOS	*0.000930395*
19	IGKC	*0.001197936*
20	IGHG1	*0.001423819*
21	FLNA	*0.002969703*
22	CRYAB	*0.003049202*
23	EGR1	*0.004200763*
24	ACTA2	*0.004200763*
25	MYL9	*0.01269158*
26	CSRP1	*0.01269158*
27	CKM	*0.01366143*
28	TARP	*0.014182583*
29	ZFP36	*0.018360154*
30	OGN	*0.018360154*
31	UBAP2L	*0.018376166*
32	IGHG2	*0.018376166*
33	IGHG4	*0.030398856*
34	PDE4DIP	*0.042808341*
35	MGP	*0.044618653*
36	SPARCL1	*0.044766688*

Chapter 6 – Conclusion

Ineffectiveness of current HLA DSA therapies in preventing AMR and chronic rejection

The generation of donor-specific antibodies (DSAs) targeting human leukocyte antigen (HLA) Class I and Class II molecules expressed on the graft endothelium are strongly linked to reduced long-term graft survival and remain a significant risk factor following solid organ transplantation. Specifically, transplant recipients with preformed DSAs face an elevated risk of acute rejection, chronic rejection, and eventual allograft loss across all solid organs[154-158]. Despite the utilization of various therapies, such as I.V. immunoglobulin and plasmapheresis, to mitigate DSA production pre- and post-transplantation, their efficacy is limited in terms of long-term effects[159]. Moreover, while anti-CD20 immunotherapies, such as Rituximab, effectively target B-cells, they have limited impact on plasma cells, which are responsible for the production of majority of serum antibodies[160]. Instead, proteosome inhibitors (e.g., bortezomib and carfilzomib) in combination with plasmapheresis and rituximab have been used for desensitization[161]. Costimulatory blockade such as cytotoxic T lymphocytes-associated protein-4-Ig (CTLA4-Ig) prevent DSA production only when given in the first 2 weeks after sensitization or in low-risk pre-transplant patients[162-164]. Moreover, therapies aimed at inhibiting the activation complement, such as Eculizumab, have shown limited efficacy in preventing both acute AMR and chronic rejection[165,166]. In addition, although mTOR inhibitors (sirolimus and everolimus) inhibit vascular smooth muscle cell and fibroblast proliferation, thereby slowing down the progression of cardiac allograft vasculopathy (CAV), they do not necessarily prevent chronic rejection[24,167-171]. In conclusion, there is a pressing need for a deeper understanding of the immunological mechanisms underlying AMR and CAV for the development of effective therapeutics capable of preventing vascular immunogenicity and chronic rejection.

Key findings and future directions

In this dissertation, we investigated the mechanisms of HLA Class I DSA-activated endothelium induced signaling and the effect on monocyte-to-macrophage polarization and functions. First, using an *in vitro* approach, we identified that primary human aortic endothelial cells (HAECs) exhibit surface expression of Toll-like receptor 4 (TLR4). Next, utilizing both co-immunoprecipitation and multiplex-immunofluorescent approaches, we identified that anti-HLA I (IgG and $F(ab')_2$) antibody crosslinking to HLA I molecules induces the formation of a molecular complex between HLA I and TLR4[16]. The formation of this complex was independent of HLA I complex formation with integrin-β4 (ITGB4). Signaling via TLR4 and adaptor protein, MyD88 induces the extravasation of Weibel-Palade bodies (WPbs) containing P-selectin[16]. Surface expression of P-selectin mediates monocyte capture to ECs via monocyte P-selectin glycoprotein ligand-1 (PSGL-1)[16]. Monocyte capture to ECs is followed by strong adhesive interactions mediated by EC expression of intracellular adhesion molecule 1 (ICAM-1)[12]. Complex formation between HLA I and ITGB4 have been shown to activate mTOR/RhoA/ROCK signaling which mediate ICAM-1 clustering at the surface of ECs[9]. Together, these findings suggest that HLA I DSA trigger distinct EC functions via two separate signaling pathways both of which facilitate monocyte recruitment and infiltration into the allograft. Future directions entail validating our results in microvascular and coronary artery ECs, given that these specific vessel types are the ones affected, as observed in endomyocardial biopsies (EMBs) and in cases of CAV, respectively. Moreover, ongoing studies in our lab are focused on utilizing a TLR4 and HLA Class II deficient mouse model of chronic AMR to further delineate the role of TLR4. Currently, there are no therapies directly aimed at preventing the recruitment of allograft infiltrating leukocytes. Therefore, these findings highlight TLR4 receptor as a novel target for potential therapeutic intervention.

Second, we elucidated that HLA I (IgG and $F(ab')_2$) antibody-activated ECs skew infiltrating monocytes to novel M2-like remodeling phenotypes[71]. Specifically, using an *in vitro* transwell

model, we identified that monocytes co-cultured with HLA I IgG-stimulated ECs differentiated into CD68+CD206+CD163+ macrophages. On the other hand, monocytes co-cultured with HLA I $F(ab')_2$-stimulated ECs only upregulated CD206. These findings suggested that monocyte Fc-gamma receptor (FcγR) interactions with the Fc-portion of IgG also impact macrophage phenotype. Moreover, both macrophage subtypes (HLA I IgG and HLA I $F(ab')_2$ polarized), exhibited a distinct transcriptomic profile compared to UT or hIgG isotype polarized macrophages. Moreover, co-culture secretions exhibited upregulation of discrete cytokines/chemokines. Cross-comparison of macrophage phenotype and transcriptome revealed that HLA I IgG and $F(ab')_2$ antibody-EC polarized macrophages exhibited the highest similarity to M2a (IL-4) and M2c (IL-10) cytokine polarized macrophage controls. On going studies remain focused on understanding the kinetics and origins of cytokine/chemokine secretions within co-culture conditions. Also, it remains unknown how specific cytokine/chemokines influence macrophage polarization. In addition, further research is need to explore the potential of these macrophages as antigen-presenting cells (APCs) and their ability to activate T-cells. Notably, we have also identified that all transwell polarized macrophages (including UT, hIgG isotype, TNF-α, HLA I IgG and $F(ab')_2$), exhibit significantly higher phagocytosis and efferocytosis potential compare to cytokine polarized macrophages (data not shown). These findings highlight the role of the endothelium and the process of monocyte transmigration in enhancing macrophage functions.

Third, building upon prior findings, we next aimed to determine the mechanisms of macrophage polarization and function induced by HLA I DSA antibody-activated ECs. Given that HLA I DSA signals via TLR4 to induced P-selectin surface expression on ECs, we investigated how blocking TLR4 signaling (via TAK242) or inhibiting P-selectin-PSGL-1 interactions impacted macrophage phenotype. *In vitro* transwell co-culture experiments showed that anti-HLA I (IgG or $F(ab')_2$) antibody-activated ECs polarized macrophages increased CD206 expression and matrix metalloproteinase-9 (MMP9) secretion. However, both CD206 and MMP9 levels were reduced

when inhibiting TLR4 signaling or P-selectin-PSGL-1 interactions. Solid phase adhesion studies confirmed the significant role of P-selectin as a major inducer of macrophage CD206 and MMP9 expression. In addition, through western blot analysis, we observed a synergistic effect between FcγR-IgG interactions and P-selectin in enhancing macrophage MMP9 expression. Lastly, we confirmed the presence of CD68+CD206+CD163+MMP9+ M2-macrophages within the CAV affected lesions of DSA+ rejected cardiac allografts. These findings highlight the role of HLA I antibody-activated endothelium in the polarization of M2-macrophages with capacity to secrete vascular remodeling proteins which can contribute to both AMR inflammation and CAV development. Future studies for this research entail further delineating how other adhesion molecules (e.g., ICAM-1 and CD31/PECAM-1) may influence macrophage polarization[37]. Moreover, it remains crucial to validate this novel macrophage phenotype in longitudinally stored EMBs with varying levels of AMR diagnosis (e.g., pAMR0 versus pAMR2+). Subsequently, studies examining macrophage transcriptomic expression at the single-cell level from either EMBs or CAV rejected specimens remain vital for further characterizing macrophage functions within rejecting grafts. Our results highlight the role of FcγR-IgG interactions in influencing monocyte recruitment, polarization, and function. Circulating IgGs can also activate complement (via C1q complex binding to Fc-portion of IgG), and FcγRIIIa/CD16+ NK-cells can also adhere to ECs via FcγR interactions[4,19]. Past studies utilizing IgG-degrading enzyme of *Streptococcus pyogenes* (IdeS) have gathered attention due to their ability to abolish complement activation in an animal model of AMR and for patient desensitization[172-176]. Nonetheless, these studies poise concerns due to the possibility of allergic reactions to bacterial enzymes and the reoccurrence of IgGs. Therefore, findings in this study emphasize TLR4 and P-selectin as novel therapeutic targets for mitigating vessel immunogenicity during AMR.

Finally, spatial multi-omics of arterial regions from CAV+ DSA+ rejected cardiac allografts allowed further understanding into the molecular processes regulating neointimal formation and CAV

development. Arterial regions with different neointima levels were analyzed using transcriptomic and proteomic profiling. Low neointimal regions displayed elevated inflammatory profiles, while high neointima regions showed characteristics of fibrotic and remodeling processes. Specifically, we identified key gene modules, gene regulatory networks, and key transcripts associated with specific neointima scores. Moreover, we identified ubiquitin associated protein 2 like (UBAP2L) as a potential new regulator of endothelial-to-mesenchymal transition (EndoMT) in CAV. Given that treatment options for CAV remain limited, these results form the foundation for the identification of novel biomarkers. Future studies should prioritize the validation of increased transcripts and proteins identified in our digital spatial profiling (DSP) analysis, particularly focusing on their secretion and detectability in plasma as potential diagnostic markers. This remains crucial, as current non-invasive screening methods like AlloMap only assess the risk of acute rejection and lack reliable marker molecules for standardized clinical parameters[177,178]. Moreover, studies using the molecular microscope diagnostic system (MMDx) on cardiac allograft EMBs have been shown to show discrepancies when compared to histological characteristics and AMR grading[179,180].

Conclusion

All in all, the findings of our study shed light on a novel mechanism underlying vessel immunogenicity mediated by HLA I DSA. We have demonstrated the ability of HLA I DSA to initiate intracellular signaling cascades in ECs, leading to subsequent effects on macrophage polarization and function. These discoveries form the foundation for the development of innovative therapeutics aimed at preventing the infiltration and activation of leukocytes in graft rejection. By understanding and targeting these specific pathways, we can potentially enhance the long-term survival of transplanted organs and improve the outcomes of transplantation procedures.

Bibliography

1. Heim C, Gocht A, Weyand M, Ensminger S. New Targets for the Prevention of Chronic Rejection after Thoracic Organ Transplantation. *Thorac Cardiovasc Surg*. Jan 2018;66(1):20-30. doi:10.1055/s-0037-1615290

2. Sun Q, Yang Y. Late and chronic antibody-mediated rejection: main barrier to long term graft survival. *Clin Dev Immunol*. 2013;2013:859761. doi:10.1155/2013/859761

3. United Network for Organ Sharing (UNOS). https://unos.org/data/transplant-trends/?gclid=Cj0KCQjw7aqkBhDPARIsAKGa0oIt6eg_7ZfYR2p1zrNHS-uyF-wxbJk6Ey_nqmsN5CdNHQ8MEFGZJ3UaAqXqEALw_wcB

4. Valenzuela NM, Reed EF. Antibody-mediated rejection across solid organ transplants: manifestations, mechanisms, and therapies. *J Clin Invest*. Jun 30 2017;127(7):2492-2504. doi:10.1172/jci90597

5. Thomas KA, Valenzuela NM, Reed EF. The perfect storm: HLA antibodies, complement, FcγRs, and endothelium in transplant rejection. *Trends Mol Med*. May 2015;21(5):319-29. doi:10.1016/j.molmed.2015.02.004

6. Valenzuela NM, Reed EF. Antibodies in transplantation: the effects of HLA and non-HLA antibody binding and mechanisms of injury. *Methods Mol Biol*. 2013;1034:41-70. doi:10.1007/978-1-62703-493-7_2

7. Siu JHY, Surendrakumar V, Richards JA, Pettigrew GJ. T cell Allorecognition Pathways in Solid Organ Transplantation. *Front Immunol*. 2018;9:2548. doi:10.3389/fimmu.2018.02548

8. Pontrelli P, Rascio F, Castellano G, Grandaliano G, Gesualdo L, Stallone G. The Role of Natural Killer Cells in the Immune Response in Kidney Transplantation. *Front Immunol*. 2020;11:1454. doi:10.3389/fimmu.2020.01454

9. Salehi S, Reed EF. The divergent roles of macrophages in solid organ transplantation. *Curr Opin Organ Transplant*. Aug 2015;20(4):446-53. doi:10.1097/mot.0000000000000209

10. Berry GJ, Burke MM, Andersen C, et al. The 2013 International Society for Heart and Lung Transplantation Working Formulation for the standardization of nomenclature in the pathologic diagnosis of antibody-mediated rejection in heart transplantation. *J Heart Lung Transplant*. Dec 2013;32(12):1147-62. doi:10.1016/j.healun.2013.08.011

11. Loupy A, Cazes A, Guillemain R, et al. Very late heart transplant rejection is associated with microvascular injury, complement deposition and progression to cardiac allograft vasculopathy. *Am J Transplant*. Jul 2011;11(7):1478-87. doi:10.1111/j.1600-6143.2011.03563.x

12. Zhang X, Rozengurt E, Reed EF. HLA class I molecules partner with integrin β4 to stimulate endothelial cell proliferation and migration. *Sci Signal*. Nov 23 2010;3(149):ra85. doi:10.1126/scisignal.2001158

13. Jin YP, Fishbein MC, Said JW, et al. Anti-HLA class I antibody-mediated activation of the PI3K/Akt signaling pathway and induction of Bcl-2 and Bcl-xL expression in endothelial cells. *Hum Immunol*. Apr 2004;65(4):291-302. doi:10.1016/j.humimm.2004.01.002

14. Salehi S, Sosa RA, Jin YP, et al. Outside-in HLA class I signaling regulates ICAM-1 clustering and endothelial cell-monocyte interactions via mTOR in transplant antibody-mediated rejection. *Am J Transplant*. May 2018;18(5):1096-1109. doi:10.1111/ajt.14544

15. Jin YP, Valenzuela NM, Zhang X, Rozengurt E, Reed EF. HLA Class II-Triggered Signaling Cascades Cause Endothelial Cell Proliferation and Migration: Relevance to Antibody-Mediated Transplant Rejection. *J Immunol*. Apr 1 2018;200(7):2372-2390. doi:10.4049/jimmunol.1701259

16. Jin YP, Nevarez-Mejia J, Terry AQ, et al. Cross-Talk between HLA Class I and TLR4 Mediates P-Selectin Surface Expression and Monocyte Capture to Human Endothelial Cells. *J Immunol*. Oct 1 2022;209(7):1359-1369. doi:10.4049/jimmunol.2200284

17. Valenzuela NM, Mulder A, Reed EF. HLA class I antibodies trigger increased adherence of monocytes to endothelial cells by eliciting an increase in endothelial P-selectin and, depending on subclass, by engaging FcγRs. *J Immunol*. Jun 15 2013;190(12):6635-50. doi:10.4049/jimmunol.1201434

18. Valenzuela NM, Hong L, Shen XD, et al. Blockade of p-selectin is sufficient to reduce MHC I antibody-elicited monocyte recruitment in vitro and in vivo. *Am J Transplant*. Feb 2013;13(2):299-311. doi:10.1111/ajt.12016

19. Valenzuela NM, Trinh KR, Mulder A, Morrison SL, Reed EF. Monocyte recruitment by HLA IgG-activated endothelium: the relationship between IgG subclass and FcγRIIa polymorphisms. *Am J Transplant*. Jun 2015;15(6):1502-18. doi:10.1111/ajt.13174

20. Jansen MA, Otten HG, de Weger RA, Huibers MM. Immunological and Fibrotic Mechanisms in Cardiac Allograft Vasculopathy. *Transplantation*. Dec 2015;99(12):2467-75. doi:10.1097/tp.0000000000000848

21. Lund LH, Edwards LB, Kucheryavaya AY, et al. The Registry of the International Society for Heart and Lung Transplantation: Thirty-second Official Adult Heart Transplantation Report--2015; Focus Theme: Early Graft Failure. *J Heart Lung Transplant*. Oct 2015;34(10):1244-54. doi:10.1016/j.healun.2015.08.003

22. Lu WH, Palatnik K, Fishbein GA, et al. Diverse morphologic manifestations of cardiac allograft vasculopathy: a pathologic study of 64 allograft hearts. *J Heart Lung Transplant*. Sep 2011;30(9):1044-50. doi:10.1016/j.healun.2011.04.008

23. Tambur AR, Pamboukian SV, Costanzo MR, et al. The presence of HLA-directed antibodies after heart transplantation is associated with poor allograft outcome. *Transplantation*. Oct 27 2005;80(8):1019-25. doi:10.1097/01.tp.0000180564.14050.49

24. Chih S, Chong AY, Mielniczuk LM, Bhatt DL, Beanlands RS. Allograft Vasculopathy: The Achilles' Heel of Heart Transplantation. *J Am Coll Cardiol*. Jul 5 2016;68(1):80-91. doi:10.1016/j.jacc.2016.04.033

25. Delgado JF, Reyne AG, de Dios S, et al. Influence of cytomegalovirus infection in the development of cardiac allograft vasculopathy after heart transplantation. *J Heart Lung Transplant*. Aug 2015;34(8):1112-9. doi:10.1016/j.healun.2015.03.015

26. Cho JG, Lee A, Chang W, Lee MS, Kim J. Endothelial to Mesenchymal Transition Represents a Key Link in the Interaction between Inflammation and Endothelial Dysfunction. *Front Immunol*. 2018;9:294. doi:10.3389/fimmu.2018.00294

27. Javaheri A, Saha N, Lilly SM. How to Approach the Assessment of Cardiac Allograft Vasculopathy in the Modern Era: Review of Invasive Imaging Modalities. *Curr Heart Fail Rep*. Apr 2016;13(2):86-91. doi:10.1007/s11897-016-0283-y

28. Bergler T, Jung B, Bourier F, et al. Infiltration of Macrophages Correlates with Severity of Allograft Rejection and Outcome in Human Kidney Transplantation. *PLoS One*. 2016;11(6):e0156900. doi:10.1371/journal.pone.0156900

29. Bräsen JH, Khalifa A, Schmitz J, et al. Macrophage density in early surveillance biopsies predicts future renal transplant function. *Kidney Int*. Aug 2017;92(2):479-489. doi:10.1016/j.kint.2017.01.029

30. Tinckam KJ, Djurdjev O, Magil AB. Glomerular monocytes predict worse outcomes after acute renal allograft rejection independent of C4d status. *Kidney Int*. Oct 2005;68(4):1866-74. doi:10.1111/j.1523-1755.2005.00606.x

31. Abe T, Su CA, Iida S, et al. Graft-derived CCL2 increases graft injury during antibody-mediated rejection of cardiac allografts. *Am J Transplant*. Aug 2014;14(8):1753-64. doi:10.1111/ajt.12780

32. Liu X, Lu Y, Lian Y, et al. Macrophage Depletion Improves Chronic Rejection in Rats With Allograft Heart Transplantation. *Transplant Proc*. Apr 2020;52(3):992-1000. doi:10.1016/j.transproceed.2019.12.037

33. Eltzschig HK, Eckle T. Ischemia and reperfusion--from mechanism to translation. *Nat Med*. Nov 7 2011;17(11):1391-401. doi:10.1038/nm.2507

34. Guibert EE, Petrenko AY, Balaban CL, Somov AY, Rodriguez JV, Fuller BJ. Organ Preservation: Current Concepts and New Strategies for the Next Decade. *Transfus Med Hemother*. 2011;38(2):125-142. doi:10.1159/000327033

35. Ponticelli C. The mechanisms of acute transplant rejection revisited. *J Nephrol*. Mar-Apr 2012;25(2):150-8. doi:10.5301/jn.5000048

36. Jiang X, Tian W, Sung YK, Qian J, Nicolls MR. Macrophages in solid organ transplantation. *Vasc Cell*. Mar 11 2014;6(1):5. doi:10.1186/2045-824x-6-5

37. Gerhardt T, Ley K. Monocyte trafficking across the vessel wall. *Cardiovasc Res*. Aug 1 2015;107(3):321-30. doi:10.1093/cvr/cvv147

38. van Buul JD, Hordijk PL. Signaling in leukocyte transendothelial migration. *Arterioscler Thromb Vasc Biol*. May 2004;24(5):824-33. doi:10.1161/01.ATV.0000122854.76267.5c

39. Shi C, Simon DI. Integrin signals, transcription factors, and monocyte differentiation. *Trends Cardiovasc Med*. Jul 2006;16(5):146-52. doi:10.1016/j.tcm.2006.03.002

40. Mahoney TS, Weyrich AS, Dixon DA, McIntyre T, Prescott SM, Zimmerman GA. Cell adhesion regulates gene expression at translational checkpoints in human myeloid leukocytes. *Proc Natl Acad Sci U S A*. Aug 28 2001;98(18):10284-9. doi:10.1073/pnas.181201398

41. Shapouri-Moghaddam A, Mohammadian S, Vazini H, et al. Macrophage plasticity, polarization, and function in health and disease. *J Cell Physiol*. Sep 2018;233(9):6425-6440. doi:10.1002/jcp.26429

42. Bashir S, Sharma Y, Elahi A, Khan F. Macrophage polarization: the link between inflammation and related diseases. *Inflamm Res*. Jan 2016;65(1):1-11. doi:10.1007/s00011-015-0874-1

43. Fairweather D, Cihakova D. Alternatively activated macrophages in infection and autoimmunity. *J Autoimmun*. Nov-Dec 2009;33(3-4):222-30. doi:10.1016/j.jaut.2009.09.012

44. Barron L, Wynn TA. Fibrosis is regulated by Th2 and Th17 responses and by dynamic interactions between fibroblasts and macrophages. *Am J Physiol Gastrointest Liver Physiol*. May 2011;300(5):G723-8. doi:10.1152/ajpgi.00414.2010

45. Schulz D, Severin Y, Zanotelli VRT, Bodenmiller B. In-Depth Characterization of Monocyte-Derived Macrophages using a Mass Cytometry-Based Phagocytosis Assay. *Sci Rep*. Feb 13 2019;9(1):1925. doi:10.1038/s41598-018-38127-9

46. Gordon S, Plüddemann A. Macrophage Clearance of Apoptotic Cells: A Critical Assessment. *Front Immunol*. 2018;9:127. doi:10.3389/fimmu.2018.00127

47. Li J, Li C, Zhuang Q, et al. The Evolving Roles of Macrophages in Organ Transplantation. *J Immunol Res*. 2019;2019:5763430. doi:10.1155/2019/5763430

48. Liu Y, Kloc M, Li XC. Macrophages as Effectors of Acute and Chronic Allograft Injury. *Curr Transplant Rep*. Dec 2016;3(4):303-312. doi:10.1007/s40472-016-0130-9

49. Famulski KS, Kayser D, Einecke G, et al. Alternative macrophage activation-associated transcripts in T-cell-mediated rejection of mouse kidney allografts. *Am J Transplant*. Mar 2010;10(3):490-7. doi:10.1111/j.1600-6143.2009.02983.x

50. Mitchell RN. Graft vascular disease: immune response meets the vessel wall. *Annu Rev Pathol*. 2009;4:19-47. doi:10.1146/annurev.pathol.3.121806.151449

51. Castro-Dopico T, Clatworthy MR. Fcγ Receptors in Solid Organ Transplantation. *Curr Transplant Rep*. 2016;3(4):284-293. doi:10.1007/s40472-016-0116-7

52. Clynes R, Maizes JS, Guinamard R, Ono M, Takai T, Ravetch JV. Modulation of immune complex-induced inflammation in vivo by the coordinate expression of activation and inhibitory Fc receptors. *J Exp Med*. Jan 4 1999;189(1):179-85. doi:10.1084/jem.189.1.179

53. Bournazos S, Wang TT, Ravetch JV. The Role and Function of Fcγ Receptors on Myeloid Cells. *Microbiol Spectr*. Dec 2016;4(6)doi:10.1128/microbiolspec.MCHD-0045-2016

54. Bournazos S, Ravetch JV. Fcγ receptor pathways during active and passive immunization. *Immunol Rev*. Nov 2015;268(1):88-103. doi:10.1111/imr.12343

55. Guilliams M, Bruhns P, Saeys Y, Hammad H, Lambrecht BN. The function of Fcγ receptors in dendritic cells and macrophages. *Nat Rev Immunol*. Feb 2014;14(2):94-108. doi:10.1038/nri3582

56. Ben Mkaddem S, Benhamou M, Monteiro RC. Understanding Fc Receptor Involvement in Inflammatory Diseases: From Mechanisms to New Therapeutic Tools. *Front Immunol*. 2019;10:811. doi:10.3389/fimmu.2019.00811

57. Fadel FI, Elshamaa MF, Salah A, et al. FcγRIIa defunctioning polymorphism in paediatric patients with renal allograft. *Cent Eur J Immunol*. 2017;42(4):363-369. doi:10.5114/ceji.2017.72817

58. Paul P, Picard C, Sampol E, et al. Genetic and Functional Profiling of CD16-Dependent Natural Killer Activation Identifies Patients at Higher Risk of Cardiac Allograft Vasculopathy. *Circulation*. Mar 6 2018;137(10):1049-1059. doi:10.1161/circulationaha.117.030435

59. Paul P, Pedini P, Lyonnet L, et al. FCGR3A and FCGR2A Genotypes Differentially Impact Allograft Rejection and Patients' Survival After Lung Transplant. *Front Immunol*. 2019;10:1208. doi:10.3389/fimmu.2019.01208

60. Akesson P, Moritz L, Truedsson M, Christensson B, von Pawel-Rammingen U. IdeS, a highly specific immunoglobulin G (IgG)-cleaving enzyme from Streptococcus pyogenes, is

inhibited by specific IgG antibodies generated during infection. *Infect Immun*. Jan 2006;74(1):497-503. doi:10.1128/iai.74.1.497-503.2006

61. Collin M, Olsén A. EndoS, a novel secreted protein from Streptococcus pyogenes with endoglycosidase activity on human IgG. *Embo j*. Jun 15 2001;20(12):3046-55. doi:10.1093/emboj/20.12.3046

62. Lin HY, Chang KT, Hung CC, et al. Effects of the mTOR inhibitor rapamycin on monocyte-secreted chemokines. *BMC Immunol*. Sep 26 2014;15:37. doi:10.1186/s12865-014-0037-0

63. Weichhart T, Haidinger M, Katholnig K, et al. Inhibition of mTOR blocks the anti-inflammatory effects of glucocorticoids in myeloid immune cells. *Blood*. Apr 21 2011;117(16):4273-83. doi:10.1182/blood-2010-09-310888

64. van den Bosch TP, Kannegieter NM, Hesselink DA, Baan CC, Rowshani AT. Targeting the Monocyte-Macrophage Lineage in Solid Organ Transplantation. *Front Immunol*. 2017;8:153. doi:10.3389/fimmu.2017.00153

65. Jin YP, Valenzuela NM, Ziegler ME, Rozengurt E, Reed EF. Everolimus inhibits anti-HLA I antibody-mediated endothelial cell signaling, migration and proliferation more potently than sirolimus. *Am J Transplant*. Apr 2014;14(4):806-19. doi:10.1111/ajt.12669

66. Jindra PT, Jin YP, Rozengurt E, Reed EF. HLA class I antibody-mediated endothelial cell proliferation via the mTOR pathway. *J Immunol*. Feb 15 2008;180(4):2357-66. doi:10.4049/jimmunol.180.4.2357

67. Xu L, Collins J, Drachenberg C, Kukuruga D, Burke A. Increased macrophage density of cardiac allograft biopsies is associated with antibody-mediated rejection and alloantibodies to HLA antigens. *Clin Transplant*. May 2014;28(5):554-60. doi:10.1111/ctr.12348

68. Tsuda H, Dvorina N, Keslar KS, et al. Molecular Signature of Antibody-Mediated Chronic Vasculopathy in Heart Allografts in a Novel Mouse Model. *Am J Pathol*. Jul 2022;192(7):1053-1065. doi:10.1016/j.ajpath.2022.04.003

69. Liberale L, Dallegri F, Montecucco F, Carbone F. Pathophysiological relevance of macrophage subsets in atherogenesis. *Thromb Haemost*. Jan 5 2017;117(1):7-18. doi:10.1160/th16-08-0593

70. Murray PJ, Allen JE, Biswas SK, et al. Macrophage activation and polarization: nomenclature and experimental guidelines. *Immunity*. Jul 17 2014;41(1):14-20. doi:10.1016/j.immuni.2014.06.008

71. Wei X, Valenzuela NM, Rossetti M, et al. Antibody-induced vascular inflammation skews infiltrating macrophages to a novel remodeling phenotype in a model of transplant rejection. *Am J Transplant*. Oct 2020;20(10):2686-2702. doi:10.1111/ajt.15934

72. Guo Y, Zheng B, Tian P, et al. HLA class II antibody activation of endothelial cells induces M2 macrophage differentiation in peripheral blood. *Clin Exp Nephrol*. Apr 2023;27(4):309-320. doi:10.1007/s10157-022-02307-9

73. Pabois A, Pagie S, Gérard N, et al. Notch signaling mediates crosstalk between endothelial cells and macrophages via Dll4 and IL6 in cardiac microvascular inflammation. *Biochem Pharmacol*. Mar 15 2016;104:95-107. doi:10.1016/j.bcp.2016.01.016

74. Mulder A, Kardol MJ, Arn JS, et al. Human monoclonal HLA antibodies reveal interspecies crossreactive swine MHC class I epitopes relevant for xenotransplantation. *Mol Immunol*. Jan 2010;47(4):809-15. doi:10.1016/j.molimm.2009.10.004

75. Jin YP, Korin Y, Zhang X, Jindra PT, Rozengurt E, Reed EF. RNA interference elucidates the role of focal adhesion kinase in HLA class I-mediated focal adhesion complex formation and proliferation in human endothelial cells. *J Immunol*. Jun 15 2007;178(12):7911-22. doi:10.4049/jimmunol.178.12.7911

76. Jin YP, Singh RP, Du ZY, Rajasekaran AK, Rozengurt E, Reed EF. Ligation of HLA class I molecules on endothelial cells induces phosphorylation of Src, paxillin, and focal adhesion kinase in an actin-dependent manner. *J Immunol*. Jun 1 2002;168(11):5415-23. doi:10.4049/jimmunol.168.11.5415

77. Merritt CR, Ong GT, Church SE, et al. Multiplex digital spatial profiling of proteins and RNA in fixed tissue. *Nat Biotechnol*. May 2020;38(5):586-599. doi:10.1038/s41587-020-0472-9

78. Newman AM, Liu CL, Green MR, et al. Robust enumeration of cell subsets from tissue expression profiles. *Nat Methods*. May 2015;12(5):453-7. doi:10.1038/nmeth.3337

79. Campbell LG, Ramachandran S, Liu W, et al. Different roles for matrix metalloproteinase-2 and matrix metalloproteinase-9 in the pathogenesis of cardiac allograft rejection. *Am J Transplant*. Mar 2005;5(3):517-28. doi:10.1111/j.1600-6143.2005.00744.x

80. Vanhoutte D, van Almen GC, Van Aelst LN, et al. Matricellular proteins and matrix metalloproteinases mark the inflammatory and fibrotic response in human cardiac allograft rejection. *Eur Heart J*. Jul 2013;34(25):1930-41. doi:10.1093/eurheartj/ehs375

81. Imhof BA, Aurrand-Lions M. Adhesion mechanisms regulating the migration of monocytes. *Nat Rev Immunol*. Jun 2004;4(6):432-44. doi:10.1038/nri1375

82. He H, Xu J, Warren CM, et al. Endothelial cells provide an instructive niche for the differentiation and functional polarization of M2-like macrophages. *Blood*. Oct 11 2012;120(15):3152-62. doi:10.1182/blood-2012-04-422758

83. Tinoco R, Otero DC, Takahashi AA, Bradley LM. PSGL-1: A New Player in the Immune Checkpoint Landscape. *Trends Immunol*. May 2017;38(5):323-335. doi:10.1016/j.it.2017.02.002

84. Gardin C, Ferroni L, Leo S, Tremoli E, Zavan B. Platelet-Derived Exosomes in Atherosclerosis. *Int J Mol Sci*. Oct 19 2022;23(20)doi:10.3390/ijms232012546

85. Fox R, Nhan TQ, Law GL, Morris DR, Liles WC, Schwartz SM. PSGL-1 and mTOR regulate translation of ROCK-1 and physiological functions of macrophages. *Embo j*. Jan 24 2007;26(2):505-15. doi:10.1038/sj.emboj.7601522

86. Weyrich AS, Elstad MR, McEver RP, et al. Activated platelets signal chemokine synthesis by human monocytes. *J Clin Invest*. Mar 15 1996;97(6):1525-34. doi:10.1172/jci118575

87. Weyrich AS, McIntyre TM, McEver RP, Prescott SM, Zimmerman GA. Monocyte tethering by P-selectin regulates monocyte chemotactic protein-1 and tumor necrosis factor-alpha secretion. Signal integration and NF-kappa B translocation. *J Clin Invest*. May 1995;95(5):2297-303. doi:10.1172/jci117921

88. Suzuki J, Hamada E, Shodai T, et al. Cytokine secretion from human monocytes potentiated by P-selectin-mediated cell adhesion. *Int Arch Allergy Immunol*. 2013;160(2):152-60. doi:10.1159/000339857

89. Celi A, Pellegrini G, Lorenzet R, et al. P-selectin induces the expression of tissue factor on monocytes. *Proc Natl Acad Sci U S A*. Sep 13 1994;91(19):8767-71. doi:10.1073/pnas.91.19.8767

90. Florence JM, Krupa A, Booshehri LM, Allen TC, Kurdowska AK. Metalloproteinase-9 contributes to endothelial dysfunction in atherosclerosis via protease activated receptor-1. *PLoS One*. 2017;12(2):e0171427. doi:10.1371/journal.pone.0171427

91. Yabluchanskiy A, Ma Y, Iyer RP, Hall ME, Lindsey ML. Matrix metalloproteinase-9: Many shades of function in cardiovascular disease. *Physiology (Bethesda)*. Nov 2013;28(6):391-403. doi:10.1152/physiol.00029.2013

92. Watanabe H, Nakanishi I, Yamashita K, Hayakawa T, Okada Y. Matrix metalloproteinase-9 (92 kDa gelatinase/type IV collagenase) from U937 monoblastoid cells: correlation with cellular invasion. *J Cell Sci*. Apr 1993;104 (Pt 4):991-9. doi:10.1242/jcs.104.4.991

93. Galt SW, Lindemann S, Medd D, et al. Differential regulation of matrix metalloproteinase-9 by monocytes adherent to collagen and platelets. *Circ Res*. Sep 14 2001;89(6):509-16. doi:10.1161/hh1801.096339

94. Pereira AM, Strasberg-Rieber M, Rieber M. Invasion-associated MMP-2 and MMP-9 are up-regulated intracellularly in concert with apoptosis linked to melanoma cell detachment. *Clin Exp Metastasis*. 2005;22(4):285-95. doi:10.1007/s10585-005-8672-8

95. Blom AB, Radstake TR, Holthuysen AE, et al. Increased expression of Fcgamma receptors II and III on macrophages of rheumatoid arthritis patients results in higher production

of tumor necrosis factor alpha and matrix metalloproteinase. *Arthritis Rheum*. Apr 2003;48(4):1002-14. doi:10.1002/art.10871

96. Räisänen-Sokolowski A, Glysing-Jensen T, Russell ME. Donor and recipient contributions of ICAM-1 and P-selectin in parenchymal rejection and graft arteriosclerosis: insights from double knockout mice. *J Heart Lung Transplant*. Aug 1999;18(8):735-43. doi:10.1016/s1053-2498(98)00058-8

97. Izawa A, Ueno T, Jurewicz M, et al. Importance of donor- and recipient-derived selectins in cardiac allograft rejection. *J Am Soc Nephrol*. Nov 2007;18(11):2929-36. doi:10.1681/asn.2006111261

98. Wang K, Zhou Z, Zhou X, Tarakji K, Topol EJ, Lincoff AM. Prevention of intimal hyperplasia with recombinant soluble P-selectin glycoprotein ligand-immunoglobulin in the porcine coronary artery balloon injury model. *J Am Coll Cardiol*. Aug 2001;38(2):577-82. doi:10.1016/s0735-1097(01)01347-x

99. Zhou Z, Penn MS, Forudi F, et al. Administration of recombinant P-selectin glycoprotein ligand Fc fusion protein suppresses inflammation and neointimal formation in Zucker diabetic rat model. *Arterioscler Thromb Vasc Biol*. Oct 1 2002;22(10):1598-603. doi:10.1161/01.atv.0000032676.20514.8f

100. Wu C, Zhao Y, Xiao X, et al. Graft-Infiltrating Macrophages Adopt an M2 Phenotype and Are Inhibited by Purinergic Receptor P2X7 Antagonist in Chronic Rejection. *Am J Transplant*. Sep 2016;16(9):2563-73. doi:10.1111/ajt.13808

101. Sablik KA, Jordanova ES, Pocorni N, Clahsen-van Groningen MC, Betjes MGH. Immune Cell Infiltrate in Chronic-Active Antibody-Mediated Rejection. *Front Immunol*. 2019;10:3106. doi:10.3389/fimmu.2019.03106

102. Ikezumi Y, Suzuki T, Yamada T, et al. Alternatively activated macrophages in the pathogenesis of chronic kidney allograft injury. *Pediatr Nephrol*. Jun 2015;30(6):1007-17. doi:10.1007/s00467-014-3023-0

103. Chatterjee D, Moore C, Gao B, et al. Prevalence of polyreactive innate clones among graft--infiltrating B cells in human cardiac allograft vasculopathy. *J Heart Lung Transplant*. Mar 2018;37(3):385-393. doi:10.1016/j.healun.2017.09.011

104. Huibers M, De Jonge N, Van Kuik J, et al. Intimal fibrosis in human cardiac allograft vasculopathy. *Transpl Immunol*. Sep 2011;25(2-3):124-32. doi:10.1016/j.trim.2011.07.001

105. Oviedo-Orta E, Bermudez-Fajardo A, Karanam S, Benbow U, Newby AC. Comparison of MMP-2 and MMP-9 secretion from T helper 0, 1 and 2 lymphocytes alone and in coculture with macrophages. *Immunology*. May 2008;124(1):42-50. doi:10.1111/j.1365-2567.2007.02728.x

106. Khush KK, Cherikh WS, Chambers DC, et al. The International Thoracic Organ Transplant Registry of the International Society for Heart and Lung Transplantation: Thirty-fifth Adult Heart Transplantation Report-2018; Focus Theme: Multiorgan Transplantation. *J Heart Lung Transplant*. Oct 2018;37(10):1155-1168. doi:10.1016/j.healun.2018.07.022

107. Colvin MM, Cook JL, Chang P, et al. Antibody-mediated rejection in cardiac transplantation: emerging knowledge in diagnosis and management: a scientific statement from the American Heart Association. *Circulation*. May 5 2015;131(18):1608-39. doi:10.1161/cir.0000000000000093

108. Tellides G, Pober JS. Interferon-gamma axis in graft arteriosclerosis. *Circ Res*. Mar 16 2007;100(5):622-32. doi:10.1161/01.Res.0000258861.72279.29

109. Lu X, Gong J, Dennery PA, Yao H. Endothelial-to-mesenchymal transition: Pathogenesis and therapeutic targets for chronic pulmonary and vascular diseases. *Biochem Pharmacol*. Oct 2019;168:100-107. doi:10.1016/j.bcp.2019.06.021

110. Loupy A, Duong Van Huyen JP, Hidalgo L, et al. Gene Expression Profiling for the Identification and Classification of Antibody-Mediated Heart Rejection. *Circulation*. Mar 7 2017;135(10):917-935. doi:10.1161/circulationaha.116.022907

111. Halloran PF, Potena L, Van Huyen JD, et al. Building a tissue-based molecular diagnostic system in heart transplant rejection: The heart Molecular Microscope Diagnostic (MMDx) System. *J Heart Lung Transplant*. Nov 2017;36(11):1192-1200. doi:10.1016/j.healun.2017.05.029

112. Mantell BS, Cordero H, See SB, et al. Transcriptomic heterogeneity of antibody mediated rejection after heart transplant with or without donor specific antibodies. *J Heart Lung Transplant*. Nov 2021;40(11):1472-1480. doi:10.1016/j.healun.2021.06.012

113. Langfelder P, Horvath S. WGCNA: an R package for weighted correlation network analysis. *BMC Bioinformatics*. Dec 29 2008;9:559. doi:10.1186/1471-2105-9-559

114. Danaher P, Kim Y, Nelson B, et al. Advances in mixed cell deconvolution enable quantification of cell types in spatial transcriptomic data. *Nat Commun*. Jan 19 2022;13(1):385. doi:10.1038/s41467-022-28020-5

115. Sun C, Wu MH, Guo M, Day ML, Lee ES, Yuan SY. ADAM15 regulates endothelial permeability and neutrophil migration via Src/ERK1/2 signalling. *Cardiovasc Res*. Jul 15 2010;87(2):348-55. doi:10.1093/cvr/cvq060

116. Shu B, Zhou YX, Li H, Zhang RZ, He C, Yang X. The METTL3/MALAT1/PTBP1/USP8/TAK1 axis promotes pyroptosis and M1 polarization of macrophages and contributes to liver fibrosis. *Cell Death Discov*. Nov 27 2021;7(1):368. doi:10.1038/s41420-021-00756-x

117. Su H, Na N, Zhang X, Zhao Y. The biological function and significance of CD74 in immune diseases. *Inflamm Res*. Mar 2017;66(3):209-216. doi:10.1007/s00011-016-0995-1

118. Lisowska A, Święcki P, Knapp M, et al. Insulin-like growth factor-binding protein 7 (IGFBP 7) as a new biomarker in coronary heart disease. *Adv Med Sci*. Mar 2019;64(1):195-201. doi:10.1016/j.advms.2018.08.017

119. Rossdeutsch A, Smart N, Dubé KN, Turner M, Riley PR. Essential role for thymosin β4 in regulating vascular smooth muscle cell development and vessel wall stability. *Circ Res*. Aug 3 2012;111(4):e89-102. doi:10.1161/circresaha.111.259846

120. Bandaru S, Ala C, Zhou AX, Akyürek LM. Filamin A Regulates Cardiovascular Remodeling. *Int J Mol Sci*. Jun 18 2021;22(12)doi:10.3390/ijms22126555

121. Barton PJ, Birks EJ, Felkin LE, Cullen ME, Koban MU, Yacoub MH. Increased expression of extracellular matrix regulators TIMP1 and MMP1 in deteriorating heart failure. *J Heart Lung Transplant*. Jul 2003;22(7):738-44. doi:10.1016/s1053-2498(02)00557-0

122. Smits M, Wurdinger T, van het Hof B, et al. Myc-associated zinc finger protein (MAZ) is regulated by miR-125b and mediates VEGF-induced angiogenesis in glioblastoma. *Faseb j*. Jun 2012;26(6):2639-47. doi:10.1096/fj.11-202820

123. Zhang J, Liu J, Wu J, Li W, Chen Z, Yang L. Progression of the role of CRYAB in signaling pathways and cancers. *Onco Targets Ther*. 2019;12:4129-4139. doi:10.2147/ott.S201799

124. Ruggeri ZM. The role of von Willebrand factor in thrombus formation. *Thromb Res*. 2007;120 Suppl 1(Suppl 1):S5-9. doi:10.1016/j.thromres.2007.03.011

125. Järvinen PM, Myllärniemi M, Liu H, et al. Cysteine-rich protein 1 is regulated by transforming growth factor-β1 and expressed in lung fibrosis. *J Cell Physiol*. Jun 2012;227(6):2605-12. doi:10.1002/jcp.23000

126. Elsafadi M, Manikandan M, Dawud RA, et al. Transgelin is a TGFβ-inducible gene that regulates osteoblastic and adipogenic differentiation of human skeletal stem cells through actin cytoskeleston organization. *Cell Death Dis*. Aug 4 2016;7(8):e2321. doi:10.1038/cddis.2016.196

127. Scott BJ, Qutob S, Liu QY, Ng CE. APM2 is a novel mediator of cisplatin resistance in a variety of cancer cell types regardless of p53 or MMR status. *Int J Cancer*. Sep 1 2009;125(5):1193-204. doi:10.1002/ijc.24465

128. Dong G, Huang X, Wu L, Jiang S, Tan Q, Chen S. SREBF2 triggers endoplasmic reticulum stress and Bax dysregulation to promote lipopolysaccharide-induced endothelial cell injury. *Cell Biol Toxicol*. Feb 2022;38(1):185-201. doi:10.1007/s10565-021-09593-1

129. Klein-Hessling S, Muhammad K, Klein M, et al. NFATc1 controls the cytotoxicity of CD8(+) T cells. *Nat Commun*. Sep 11 2017;8(1):511. doi:10.1038/s41467-017-00612-6

130. Wang H, Nie L, Wu L, Liu Q, Guo X. NR2F2 inhibits Smad7 expression and promotes TGF-β-dependent epithelial-mesenchymal transition of CRC via transactivation of miR-21. *Biochem Biophys Res Commun*. Mar 25 2017;485(1):181-188. doi:10.1016/j.bbrc.2017.02.049

131. Finka A, Mattoo RU, Goloubinoff P. Experimental Milestones in the Discovery of Molecular Chaperones as Polypeptide Unfolding Enzymes. *Annu Rev Biochem*. Jun 2 2016;85:715-42. doi:10.1146/annurev-biochem-060815-014124

132. Vanhooren J, Derpoorter C, Depreter B, et al. TARP as antigen in cancer immunotherapy. *Cancer Immunol Immunother*. Nov 2021;70(11):3061-3068. doi:10.1007/s00262-021-02972-x

133. Ye T, Xu J, Du L, Mo W, Liang Y, Xia J. Downregulation of UBAP2L Inhibits the Epithelial-Mesenchymal Transition via SNAIL1 Regulation in Hepatocellular Carcinoma Cells. *Cell Physiol Biochem*. 2017;41(4):1584-1595. doi:10.1159/000470824

134. Li Q, Wang W, Hu YC, Yin TT, He J. Knockdown of Ubiquitin Associated Protein 2-Like (UBAP2L) Inhibits Growth and Metastasis of Hepatocellular Carcinoma. *Med Sci Monit*. Oct 6 2018;24:7109-7118. doi:10.12659/msm.912861

135. Bhattacharyya S, Wu M, Fang F, Tourtellotte W, Feghali-Bostwick C, Varga J. Early growth response transcription factors: key mediators of fibrosis and novel targets for anti-fibrotic therapy. *Matrix Biol*. May 2011;30(4):235-42. doi:10.1016/j.matbio.2011.03.005

136. Milde-Langosch K. The Fos family of transcription factors and their role in tumourigenesis. *Eur J Cancer*. Nov 2005;41(16):2449-61. doi:10.1016/j.ejca.2005.08.008

137. Hu X, Li YQ, Li QG, Ma YL, Peng JJ, Cai SJ. Osteoglycin (OGN) reverses epithelial to mesenchymal transition and invasiveness in colorectal cancer via EGFR/Akt pathway. *J Exp Clin Cancer Res*. Mar 2 2018;37(1):41. doi:10.1186/s13046-018-0718-2

138. Angiolilli C, Leijten EFA, Bekker CPJ, et al. ZFP36 Family Members Regulate the Proinflammatory Features of Psoriatic Dermal Fibroblasts. *J Invest Dermatol*. Feb 2022;142(2):402-413. doi:10.1016/j.jid.2021.06.030

139. Kobayashi A, Takahashi T, Horita S, et al. Activation of the transcription factor c-Jun in acute cellular and antibody-mediated rejection after kidney transplantation. *Hum Pathol*. Dec 2010;41(12):1682-93. doi:10.1016/j.humpath.2010.04.016

140. Mintet E, Lavigne J, Paget V, et al. Endothelial Hey2 deletion reduces endothelial-to-mesenchymal transition and mitigates radiation proctitis in mice. *Sci Rep*. Jul 10 2017;7(1):4933. doi:10.1038/s41598-017-05389-8

141. Wang XM, Liu XM, Wang Y, Chen ZY. Activating transcription factor 3 (ATF3) regulates cell growth, apoptosis, invasion and collagen synthesis in keloid fibroblast through transforming growth factor beta (TGF-beta)/SMAD signaling pathway. *Bioengineered*. Dec 2021;12(1):117-126. doi:10.1080/21655979.2020.1860491

142. Malabanan KP, Kanellakis P, Bobik A, Khachigian LM. Activation transcription factor-4 induced by fibroblast growth factor-2 regulates vascular endothelial growth factor-A transcription in vascular smooth muscle cells and mediates intimal thickening in rat arteries following balloon injury. *Circ Res*. Aug 15 2008;103(4):378-87. doi:10.1161/circresaha.107.168682

143. Chen X, Xu J, Bao W, et al. Endothelial Foxp1 Regulates Neointimal Hyperplasia Via Matrix Metalloproteinase-9/Cyclin Dependent Kinase Inhibitor 1B Signal Pathway. *J Am Heart Assoc*. Aug 2 2022;11(15):e026378. doi:10.1161/jaha.122.026378

144. Whitmore HAB, Amarnani D, O'Hare M, et al. TNF-α signaling regulates RUNX1 function in endothelial cells. *Faseb j*. Feb 2021;35(2):e21155. doi:10.1096/fj.202001668R

145. Choy JC, McDonald PC, Suarez AC, et al. Granzyme B in atherosclerosis and transplant vascular disease: association with cell death and atherosclerotic disease severity. *Mod Pathol*. May 2003;16(5):460-70. doi:10.1097/01.Mp.0000067424.12280.Bc

146. Adachi M, Imai K. The proapoptotic BH3-only protein BAD transduces cell death signals independently of its interaction with Bcl-2. *Cell Death & Differentiation*. 2002/11/01 2002;9(11):1240-1247. doi:10.1038/sj.cdd.4401097

147. Wehner J, Morrell CN, Reynolds T, Rodriguez ER, Baldwin WM, 3rd. Antibody and complement in transplant vasculopathy. *Circ Res*. Feb 2 2007;100(2):191-203. doi:10.1161/01.Res.0000255032.33661.88

148. Huibers MM, Vink A, Kaldeway J, et al. Distinct phenotypes of cardiac allograft vasculopathy after heart transplantation: a histopathological study. *Atherosclerosis*. Oct 2014;236(2):353-9. doi:10.1016/j.atherosclerosis.2014.07.016

149. Hruban RH, Beschorner WE, Baumgartner WA, et al. Accelerated arteriosclerosis in heart transplant recipients is associated with a T-lymphocyte-mediated endothelialitis. *Am J Pathol*. Oct 1990;137(4):871-82.

150. Fu Y, Lin Q, Zhang Z, Zhang L. Therapeutic strategies for the costimulatory molecule OX40 in T-cell-mediated immunity. *Acta Pharm Sin B*. Mar 2020;10(3):414-433. doi:10.1016/j.apsb.2019.08.010

151. Tkachev V, Furlan SN, Watkins B, et al. Combined OX40L and mTOR blockade controls effector T cell activation while preserving T(reg) reconstitution after transplant. *Sci Transl Med*. Sep 20 2017;9(408)doi:10.1126/scitranslmed.aan3085

152. Morrell CN, Murata K, Swaim AM, et al. In vivo platelet-endothelial cell interactions in response to major histocompatibility complex alloantibody. *Circ Res*. Apr 11 2008;102(7):777-85. doi:10.1161/circresaha.107.170332

153. He L, Li Q, Du C, Xue Y, Yu P. Glis2 inhibits the epithelial-mesenchymal transition and apoptosis of renal tubule cells by regulating the β-catenin signalling pathway in diabetic kidney disease. *Biochem Biophys Res Commun*. Jun 4 2022;607:73-80. doi:10.1016/j.bbrc.2022.03.111

154. Amrouche L, Aubert O, Suberbielle C, et al. Long-term Outcomes of Kidney Transplantation in Patients With High Levels of Preformed DSA: The Necker High-Risk Transplant Program. *Transplantation*. Oct 2017;101(10):2440-2448. doi:10.1097/tp.0000000000001650

155. Roux A, Bendib Le Lan I, Holifanjaniaina S, et al. Antibody-Mediated Rejection in Lung Transplantation: Clinical Outcomes and Donor-Specific Antibody Characteristics. *Am J Transplant*. Apr 2016;16(4):1216-28. doi:10.1111/ajt.13589

156. Morrell MR, Pilewski JM, Gries CJ, et al. De novo donor-specific HLA antibodies are associated with early and high-grade bronchiolitis obliterans syndrome and death after lung transplantation. *J Heart Lung Transplant*. Dec 2014;33(12):1288-94. doi:10.1016/j.healun.2014.07.018

157. Tran A, Fixler D, Huang R, Meza T, Lacelle C, Das BB. Donor-specific HLA alloantibodies: Impact on cardiac allograft vasculopathy, rejection, and survival after pediatric heart transplantation. *J Heart Lung Transplant*. Jan 2016;35(1):87-91. doi:10.1016/j.healun.2015.08.008

158. Irving CA, Carter V, Gennery AR, et al. Effect of persistent versus transient donor-specific HLA antibodies on graft outcomes in pediatric cardiac transplantation. *J Heart Lung Transplant*. Oct 2015;34(10):1310-7. doi:10.1016/j.healun.2015.05.001

159. Durandy A, Kaveri SV, Kuijpers TW, et al. Intravenous immunoglobulins--understanding properties and mechanisms. *Clin Exp Immunol*. Dec 2009;158 Suppl 1(Suppl 1):2-13. doi:10.1111/j.1365-2249.2009.04022.x

160. Bingham CO, 3rd, Looney RJ, Deodhar A, et al. Immunization responses in rheumatoid arthritis patients treated with rituximab: results from a controlled clinical trial. *Arthritis Rheum*. Jan 2010;62(1):64-74. doi:10.1002/art.25034

161. Woodle ES, Shields AR, Ejaz NS, et al. Prospective iterative trial of proteasome inhibitor-based desensitization. *Am J Transplant*. Jan 2015;15(1):101-18. doi:10.1111/ajt.13050

162. Yang J, Chen J, Young JS, et al. Tracing Donor-MHC Class II Reactive B cells in Mouse Cardiac Transplantation: Delayed CTLA4-Ig Treatment Prevents Memory Alloreactive B-Cell Generation. *Transplantation*. Aug 2016;100(8):1683-91. doi:10.1097/tp.0000000000001253

163. Rostaing L, Vincenti F, Grinyó J, et al. Long-term belatacept exposure maintains efficacy and safety at 5 years: results from the long-term extension of the BENEFIT study. *Am J Transplant*. Nov 2013;13(11):2875-83. doi:10.1111/ajt.12460

164. Young JS, Chen J, Miller ML, et al. Delayed Cytotoxic T Lymphocyte-Associated Protein 4-Immunoglobulin Treatment Reverses Ongoing Alloantibody Responses and Rescues Allografts From Acute Rejection. *Am J Transplant*. Aug 2016;16(8):2312-23. doi:10.1111/ajt.13761

165. Cornell LD, Schinstock CA, Gandhi MJ, Kremers WK, Stegall MD. Positive crossmatch kidney transplant recipients treated with eculizumab: outcomes beyond 1 year. *Am J Transplant*. May 2015;15(5):1293-302. doi:10.1111/ajt.13168

166. Bentall A, Tyan DB, Sequeira F, et al. Antibody-mediated rejection despite inhibition of terminal complement. *Transpl Int*. Dec 2014;27(12):1235-43. doi:10.1111/tri.12396

167. Eisen HJ, Tuzcu EM, Dorent R, et al. Everolimus for the prevention of allograft rejection and vasculopathy in cardiac-transplant recipients. *N Engl J Med*. Aug 28 2003;349(9):847-58. doi:10.1056/NEJMoa022171

168. Arora S, Andreassen AK, Andersson B, et al. The Effect of Everolimus Initiation and Calcineurin Inhibitor Elimination on Cardiac Allograft Vasculopathy in De Novo Recipients: One-Year Results of a Scandinavian Randomized Trial. *Am J Transplant*. Jul 2015;15(7):1967-75. doi:10.1111/ajt.13214

169. Keogh A, Richardson M, Ruygrok P, et al. Sirolimus in de novo heart transplant recipients reduces acute rejection and prevents coronary artery disease at 2 years: a randomized clinical trial. *Circulation*. Oct 26 2004;110(17):2694-700. doi:10.1161/01.Cir.0000136812.90177.94

170. Kobashigawa JA, Pauly DF, Starling RC, et al. Cardiac allograft vasculopathy by intravascular ultrasound in heart transplant patients: substudy from the Everolimus versus mycophenolate mofetil randomized, multicenter trial. *JACC Heart Fail*. Oct 2013;1(5):389-99. doi:10.1016/j.jchf.2013.07.002

171. Cuadrado-Payán E, Diekmann F, Cucchiari D. Medical Aspects of mTOR Inhibition in Kidney Transplantation. *Int J Mol Sci*. Jul 12 2022;23(14)doi:10.3390/ijms23147707

172. Lonze BE, Tatapudi VS, Weldon EP, et al. IdeS (Imlifidase): A Novel Agent That Cleaves Human IgG and Permits Successful Kidney Transplantation Across High-strength Donor-specific Antibody. *Ann Surg*. Sep 2018;268(3):488-496. doi:10.1097/sla.0000000000002924

173. Nandakumar KS, Collin M, Olsén A, et al. Endoglycosidase treatment abrogates IgG arthritogenicity: importance of IgG glycosylation in arthritis. *Eur J Immunol*. Oct 2007;37(10):2973-82. doi:10.1002/eji.200737581

174. Allhorn M, Briceño JG, Baudino L, et al. The IgG-specific endoglycosidase EndoS inhibits both cellular and complement-mediated autoimmune hemolysis. *Blood*. Jun 17 2010;115(24):5080-8. doi:10.1182/blood-2009-08-239020

175. von Pawel-Rammingen U, Johansson BP, Björck L. IdeS, a novel streptococcal cysteine proteinase with unique specificity for immunoglobulin G. *Embo j*. Apr 2 2002;21(7):1607-15. doi:10.1093/emboj/21.7.1607

176. Lood C, Allhorn M, Lood R, et al. IgG glycan hydrolysis by endoglycosidase S diminishes the proinflammatory properties of immune complexes from patients with systemic lupus erythematosus: a possible new treatment? *Arthritis Rheum*. Aug 2012;64(8):2698-706. doi:10.1002/art.34454

177. Deng MC. The AlloMap™ genomic biomarker story: 10 years after. *Clin Transplant*. Mar 2017;31(3)doi:10.1111/ctr.12900

178. Moayedi Y, Foroutan F, Miller RJH, et al. Risk evaluation using gene expression screening to monitor for acute cellular rejection in heart transplant recipients. *J Heart Lung Transplant*. Jan 2019;38(1):51-58. doi:10.1016/j.healun.2018.09.004

179. Halloran PF, Madill-Thomsen KS. The Molecular Microscope Diagnostic System: Assessment of Rejection and Injury in Heart Transplant Biopsies. *Transplantation*. Jan 1 2023;107(1):27-44. doi:10.1097/tp.0000000000004323

180. Halloran PF, Madill-Thomsen K, Aliabadi-Zuckermann AZ, et al. Many heart transplant biopsies currently diagnosed as no rejection have mild molecular antibody-mediated rejection-related changes. *J Heart Lung Transplant*. Mar 2022;41(3):334-344. doi:10.1016/j.healun.2021.08.004